TUESDAY, JUNE 5, 1984

8:00–10:00 Petree Hall in the Los Angeles Convention Center

FORMAL OPENING AND PLENARY SESSION

8:15 WELCOME AND TRIBUTE TO THE FOUNDER'S GROUP;* Merle K. Loken, M.D., Ph.D., *President, Society of Nuclear Medicine*

REMARKS: B. Leonard Holman, M.D., *Chairman, Scientific Program Committee 1984*

REMARKS: Shelley D. Hartnett, CNMT, *President, Technologist Section*

REMARKS: Thomas P. Haynie III, M.D., *Chairman, Credentials and Membership Committee*

8:30 THE FIFTH ANNUAL GEORG CHARLES DE HEVESY NUCLEAR MEDICINE PIONEER AWARD PRESENTATION honoring Henry N. Wagner, Jr., M.D., The Johns Hopkins Medical Institutions: S. James Adelstein, M.D., Ph.D., *Lecturer,* Massachusetts General Hospital.

9:00 First Annual SNM Lectureship: *Imaging with Radiolabeled Antibodies.* Steven M. Larson, M.D., National Institutes of Health

10:00 Opening of the 1984 SNM Exposition

*The Founders' Group, as identified on the program of the First Annual Meeting of the Society of Nuclear Medicine, which took place May 29–30, 1954, at the Benjamin Franklin Hotel in Seattle, WA, includes (in alphabetical order): A. Kearney Atkinson, M.D.; Thomas Carlile, M.D.; Eggert T. Feldsted, M.D.; William H. Hannah, B.S.; Milo Harris, M.D.; Norman J. Holter, M.A.; Rex L. Huff, M.D.; Tyra T. Hutchens, M.D.; Robert G. Moffat, M.D.; Joseph R. Nealen, S.J.; Asa Seeds, M.D.; and Charles P. Wilson, M.D.

10:30–12:00 Room 217A

CARDIOVASCULAR I: VENTRICULAR FUNCTION— NEW TECHNIQUES AND APPLICATIONS

Moderator: H. William Strauss, M.D.
Comoderator: Jonathan M. Links, Ph.D.

CHANGES IN VENTRICULAR FUNCTION DURING EMOTIONAL STRESS AND COLD EXPOSURE. M.C. Kiess, R.A. Moore, J. Dimsdale, N.M. Alpert, C.A. Boucher, H.W. Strauss. Massachusetts General Hospital, Boston, MA.

Patients with cardiac disease freqently develop symptoms with emotional stress or cold exposure. To investigate the effects of these stresses in normal subjects, an ambulatory ventricular function monitor (VEST) (previously reported to measure EFs which correlate well with gamma camera measurements) was employed to record sequential 2 minute time activity curves from the left ventricles of 6 healthy men (ages 19-24) during a control period and during a 30 minute stress interview with a psychiatrist. Four of the subjects were also monitored in a cold room (1° C) for 20 min. In addition to the left ventricular time-activity curve, heart rate (HR), and BP (cuff) were recorded. All subjects had increases in HR, BP and EF during the stress interview. Cold, however, produced decreases in HR and EF and an increase in BP. The results (mean±SD) are tabulated below:

	HR	BP	EF
Rest	66± 2	121/80 ±13/4	51±11
Interview	76±11*	158/101± 7/7*	68±13*
Rest Pre-cold	70± 7	114/76 ±12/5	58± 7
Cold	63± 4*	141/94 ±14/5*	37± 4*

*p<.05

End-systolic and end-diastolic counts and hence volume decreased during the interview and increased during cold exposure.

These data suggest that (1) ambulatory changes in ventricular function can be measured with the VEST, and (2) significant changes in cardiovascular physiology are seen in normal subjects during a stress interview and exposure to cold.

ESTIMATION OF LEFT VENTRICULAR EJECTION FRACTION BY COMPUTERIZED SINGLE CARDIAC PROBE SYSTEM WITH ECHOCARDIOGRAM. Y. Suzuki, M. Ide, N. Kenemoto, H. Tomoda, and M. Nakamura Tokai University, School of Medicine, Isehara-city, Japan

We developed a computerized single cardiac probe system combined with echocardiogram which permits the physician to position the detector more easily and properly. With this system left ventricular ejection fraction(LVEF) can be estimated by the three different modes: first pass(FP) mode, beat-by-beat(B-B) mode and ECG multigated(MG) mode. In FP mode complex demodulation technique is applied for estimation of the background counts. The purpose of this paper is to describe the accuracy and reproducibility of the LVEF estimated by this system. In 40 patients with various heart diseases, the LVEFs estimated by this system using above-mentioned 3 modes were compared with those of obtained by gamma camera. There were good correlations between the LVEFs estimated by each of the 3 modes of this system and obtained by gamma camera. The correlation coefficient (r) between the LVEFs estimated by FP mode, B-B mode and MG mode, and those of by gamma camera was 0.938, 0.932, and 0.930, respectively. In 15 patients FP mode study was repeated continuously and LVEFs obtained in the initial and repeat studies were compared. There was good agreement between these results(r=0.953). In 12 patients positioning of the probe over the left ventricle and background area was repeated 5 times and LVEFs were estimated each time by B-B mode. There was no significant standard deviation compared to the mean LVEFs in each patient; the percent coefficient of variation was less than 8.0%. In conclusion, our results suggest that LVEF can be estimated accurately by each of the 3 modes of this system and reproducibility seems to be sufficient for clinical studies.

ETIOLOGY OF CARDIOGENIC SHOCK EARLY AFTER OPEN-HEART SURGERY: ASSESSMENT BY Tc-99m RBC WALL MOTION SCINTIGRAPHY. T Bateman, R Gray, A Chaux, M Lee, J Matloff, M Raymond, D Berman. Cedars-Sinai Medical Center, Los Angeles, CA

When life-threatening cardiogenic shock (CI 1.8 l/min/m^2, elevated right and left-side filling pressures) occurs early (0-48 hrs) after open-heart surgery, routine approaches frequently cannot distinguish between expected etiologies: (1) transient systolic failure of the LV, RV, or both, common early postoperatively (postop); (2) perioperative infarct of the LV or RV; (3) myocardial restriction due to active pericardial bleeding or to accumulated clots and fluid; (4) diminished LV reserve from aneurysmectomy; and (5) residual valvular regurgitation. Distinction is critical, because (1), (2), and (4) will be treated by optimizing preload and afterload; (3) with urgent (if active bleeding) or semi-urgent surgery; and (5) with repeat valvular surgery. In 22 pts with unexpected early postop cardiogenic shock, Tc-99m-RBC equilibrium radionuclide ventriculography revealed: global LV (3 pts)

or RV (3 pts) dysfunction, new segmental LV dysfunction (2 pts), active bleeding (5 pts) and/or accumulated pericardial fluid (8 pts) with hyperdynamic LV and RV, and a small hyperdynamic LV without effusion (1 pt), providing a specific etiologic diagnosis in all cases. In our Cardiac Surgical ICU, therapeutic decisions frequently await and depend on the results of equilibrium radionuclide ventriculography, now routinely performed in postop pts with unexpected cardiogenic shock.

A METHOD TO IDENTIFY EARLY VENTRICULAR DYSFUNCTION USING RESTING GATED BLOOD POOL SCANS (GBPS) IN PATIENTS WITH CORONARY ARTERY DISEASE (CAD). R.J. Schwarzberg, D.W. Seldin, L.L. Johnson, P.O. Alderson. Columbia University, NY.

To determine the sensitivity of regional 1st and 2nd time derivative (1DV, 2DV) images to assess ventricular function (VF) in CAD, the resting GBPS of 8 normal patients (pts) and 20 pts with CAD who had coronary angiography and contrast ventriculography (CV) were analyzed. The 1DV and 2DV of the systolic time-activity curve were determined for each left ventricular pixel in the GBPS. These values were displayed as functional images that were reviewed by three readers to determine the presence of regional abnormalities. No regional abnormalities were seen in the conventional GBPS or 1DV or 2DV images of the 8 normal pts. Regional GBPS and DV image abnormalities were seen in all 10 pts with CAD and abnormal wall motion by CV. The DV image abnormalities were in the distribution of 18/22 coronary arteries (CA) with≥50% stenoses; 2 of these regions showed normal wall motion by CV and conventional GBPS. DV images were abnormal in 2/8 CAs without significant stenoses. In addition, regional DV image abnormalities were present in 9of 10 pts with CAD who had normal wall motion and global ejection fraction by both CV and resting GBPS. These 10 pts showed regional abnormalities in the distribution of 13/15 CAs with significant stenoses and 2/15 CAs without such stenoses. The results suggest that time derivative functional images derived from resting GBPS provide a more sensitive means for detecting regional left ventricular dysfunction than several other current methods, especially in pts with mild CAD.

EFFECT OF POSITIVE PLEURAL PRESSURE ON LEFT VENTRICULAR PERFORMANCE. T.K. Natarajan, M. Karam, R. Wise, H.N. Wagner, Jr. The Johns Hopkins Medical Institutions, Baltimore MD.

A sudden increase in pleural pressure such as coughing or a valsalva maneuver causes a transient increase in left ventricular stroke volume but the mechanism is not known. To help understand this phenomenon we studied 7 normal volunteers during spontantous breathing and when breathing under positive pleural pressure. The positive pleural pressure was developed by expiring against a 24cm H2O threshold load. Radionuclide ventriculography using a double gating technique was performed. Image data were acquired during the cardiac cycles occuring during positive pleural pressure by means of a pressure transducer coupled to an EKG gate. They were compared to data acquired by EKG gating alone under quiet respiration as control. Results are shown for end diastolic (EDC), end systolic (ESC) and stroke counts (SC) and are expressed as % change from control for each parameter.

Results:	EDC	ESC	SC
pleural pressure +24 cm H2O	+25% (p<0.001)	+37% p<0.02	+23.5% (p<0.001)

We conclude that a transient increase in positive pleural pressure comparable to that reached during forceful coughing increases stroke volume and cardiac output through a combination of increased end diastolic volume with a lesser increase in end systolic volume. This effect was seen in the absence of any change in cardiac rhythm or rate.

A NEW METHOD FOR FOURIER ANALYSIS IN ECG-GATED CARDIAC BLOOD POOL EMISSION COMPUTED TOMOGRAPHY (ECT). T.Ito, H.Maeda, K.Takeda, T.Nakagawa, N. Yamaguchi, T.Konishi and T.Ichikawa. Mie Univ. School of Medicine, Tsu, Mie, Japan.

An integrated technique for Fourier analysis in multigated blood pool ECT study has been developed. Following the administration of 15-20 mCi of Tc-99m RBC, ECG-gated cardiac blood pool data were acquired using an ECT system with dual opposed gamma cameras. Fundamental studies for data acquisition showed that acquisition time of 10 sec. for each projection, 14 divisions of one cardiac cycle and angular interval of 6°(60 projections over 360°) were reasonable for clinical purpose. Total acquisition time was about 5 minutes under these conditions.

Data were processed as follows. 1) Transaxial (TA) tomographic images in every phase of cardiac cycle were reconstructed by convolution algorithm. 2) TA images were rotated to construct sagittal (SAG) and short axial (S-A) oblique-angle tomography which are respectively parallel and perpendicular to the long axis of either of the ventricles. 3) Images covering the portion other than the purposed ventricle were eliminated from the series of SAG images in every phase of the cycle. 4) Images in the same phase were summed to construct a series of SAG and S-A planar images. 5) Fourier analysis was made to construct phase and amplitude images.

The advantages of this method are that the phase and amplitude images from arbitrary directions can be obtained, that the region of interest can be selected on a three dimensional basis, eliminating the overlapping activity of the other ventricle or neighbouring tissues, that the diseased areas can be easily and accurately localized even in small inferior wall myocardial infarction and that patient study can be finished within 5 minutes.

10:30–12:00 **Room 216BC**

INSTRUMENTATION I: EMISSION COMPUTED TOMOGRAPHY

Moderator: Ronald J. Jaszczak, Ph.D.
Comoderator: James A. Sorenson, Ph.D.

THE DESIGN AND CLINICAL UTILITIES OF A FAN BEAM COLLIMATOR FOR A SPECT SYSTEM. B.M.W. Tsui, G.T. Gullberg*, E.R. Edgerton, D.R. Gilland, T. Rho, R.E. Johnston, J.R. Perry and W.H. McCartney. *The University of North Carolina, Chapel Hill, NC. General Electric Medical Systems Operations Milwaukee, WI.

A low-energy fan-beam collimator (LEFB) designed for SPECT imaging of the head was evaluated using physical measurements, phantom and clinical studies. In the transverse image plane, the collimator holes are tapered and converged to a focal point 58 cm from the collimator face. In the longitudinal image plane, the collimator holes are straight and parallel. The collimator holes are hexagonal in shape and 13 cm in length. The extended hole design allows improved clearance of the patient's shoulders during rotation such that the collimator face may be positioned 8.5 cm closer to the patient's head than is possible with conventional collimators. At the center of rotation with the closest rotational radius, the spatial resolutions for the LEGP, LEHR, and LEFB collimators are 17.0, 14.4 and 12.2 mm, respectively. The point source sensitivities are 330, 220 and 190 (at 15 cm) cpm/μCi, respectively. Line spread functions at various distances from the collimator face, both in air and in water, were measured. Reconstruction algorithms and a special attenuation correction method for the fan beam geometry were developed and various reconstruction parameters for the LEFB collimator were determined experimentally. Images of a SPECT phantom were obtained to evaluate the imaging capabilities of the LEFB collimator and the reconstruction algorithm. Clinical comparisons of SPECT bone images of the temporomandibular joints obtained with both LEGP and LEFB collimators on the same patients show superior image quality with the LEFB collimator.

PERFORMANCE TESTING ROTATING GAMMA CAMERA SPECT SYSTEMS. A. Todd-Pokropek, University College London, U.K.

A reasonably simple protocol for testing the performance of rotating gamma camera SPECT systems has been

established, which could be performed in about 10 hours. This protocol has been used to test almost all currently available systems, including GE, Siemens, Technicare, Elscint, Philips, CGR, etc. In general, several models of a given system were tested in order to give an indication of the range of results that might be obtained. Reconstructions were performed in a standard manner (Uniformity correction, Ramp filter, no attenuation correction) in order to try to eliminate the effect of differences in software. In addition to using the Jaszczak phantom as an overall test pattern, measurements were made of spatial resolution, energy resolution, contrast, variations of sensitivity and uniformity with angle, etc. Results indicated that some systems, with a high resolution collimator and after very careful setting up, could achieve a spatial resolution of the order of 11mm, with good image quality. Not all commercially available systems performed as well. Strong indication was given of the need to improve spatial resolution, even at the expense of sensitivity, confirming the results from simulated tomographic data for various design compromises. Tests were also performed varying the energy window used. It was found that only very few system were capable of producing artefact free images with other than a symmetric photopeak window. However, very significant improvement of image quality of current systems with respect to older systems was noted. This protocol has been used, in addition, to establish a routine quality assurance program for such SPECT systems.

TRIANGULAR SPECT SYSTEM FOR BRAIN AND BODY ORGAN 3-D IMAGING: DESIGN CONCEPT AND PRELIMINARY IMAGING RESULT. C. Lim S. Gottschalk, R. Schreiner, R. Walker, F. Valentino, J. Covic, A. Perusek, C. Pinkstaff, J. Janzso. Technicare Corporation, Solon, OH

The SPECT systems based on 2-D detectors for projection data collection and filtered BPJ image reconstruction have the potential for true 3-D imaging, providing contiguous slice images in any orientation. Anger camera-based SPECT systems have the natural advantage supporting planar imaging clinical procedures. However, current systems suffer from two drawbacks; poor utilization of emitted photons, and inadequate system design for SPECT. The SPECT system consisting of three rectangular cameras with radial translation would offer the cylindrical FOV of 25cm to 40cm diameter allowing close detector access to the object. This system would provide optimized imaging for both brain and body organs in terms of resolution and sensitivity. For brain imaging a tight detector triangle with fan beam collimation, matching detector UFOV to the head, allows full 2π utilization of emitted photons, resulting in >4 times sensitivity increase over the single head system. Minification of intrinsic detector resolution in fan beam collimation further improves system resolution. For body organ imaging the three detectors with parallel hole collimators, rotating in noncircular orbit, provides both improved resolution and threefold sensitivity increase. Practical challenge lies in ensuring perfect image overlap from three detectors without resolution degradation and artifact generation in order to benefit from the above improvements. An experimental system has been developed to test the above imaging concept and we have successfully demonstrated the superior image quality of the overlapped images. Imaging concept analysis will be presented with preliminary imaging results.

HIGH RESOLUTION POSITRON TOMOGRAPHY USING PCR-I. G.L. Brownell, C.A. Burnham, *B. Sandrew, D.R. Elmaleh, E. Livni and H. Kizuka. Physics Research Laboratory and *Department of Neurosurgery, Massachusetts General Hospital, Boston, MA 02114

PCR-I is a high resolution positron tomograph developed by the Physics Research Laboratory of the Massachusetts General Hospital to explore resolution limits of positron tomographs. PCR-I currently obtains images with 4.8 mm FWHM resolution at the center. Plane thickness may be varied between 5 and 10 mm. The instrument uses analog coding to obtain high resolution images without mechanical motion. This permits rapid dynamic imaging and gated cardiac imaging as well as conventional high resolution imaging.

A series of studies has been carried out to demonstrate the ability of PCR-I to image structures in small animals

F-18 in the rat skeleton is clearly defined and various structures such as the spinal processes can be clearly resolved. A sequence of images at different spacing provides a three-dimensional reconstruction of the rat skeleton.

Blood volume and palmitic acid have been imaged in the dog heart. Again, the sequence of images provides a clear delineation of the three dimensional nature of the blood pools and of the surrounding musculature.

Blood flow, blood volume and glucose metabolism have been studied in the monkey brain. Structures within the brain of the Rhesus monkey can be clearly resolved. Increased activity resulting from induced seizures in the squirrel monkey have been observed and delineated.

All of these studies indicate areas of future animal and clinical research using the high resolution tomograph, PCR-I. Supported by ROICA32873-3.

COMPARATIVE STUDY OF MYOCARDIAL PERFUSION IMAGING BY TL-201 SINGLE-PHOTON ECT AND N-13 AMMONIA POSITRON CT. N. Tamaki, Y.Yonekura, M.Senda, T.Fujita, K.Murata, S.Tanada, E.Saji, K.Torizuka. Kyoto University Medical School, Kyoto, Japan. and K. Yamamoto. Brookhaven National Laboratory, Upton, NY.

Thallium (Tl) single-photon emission CT (SPECT) has been available for three-dimensional evaluation of myocardial perfusion. To assess the value and limitation of Tl SPECT, the images were compared with N-13 ammonia positron CT(PCT) in phantom and clinical studies. SPECT was performed by gamma camera rotation over 180° after Tl 2 mCi injection. PCT was performed using 4 detector ring whole-body PCT device after N-13 ammonia 20 mCi injection. Acquisition time was 16 min for SPECT and 20 min (transmission) plus 10 min (emission) for PCT. No attenuation correction was done in SPECT, while in PCT it was accurately performed from the transmission data. Collected counts in a single slice were 100-180K by SPECT and 5-12M by PCT. The spatial resolution was about 16 mm for SPECT and 8 mm for PCT in FWHM. Because of better resolution and higher count statistics, PCT delineated fine cardiac structures, such as papillary muscles and apical thinning, while the myocardium looked thicker in SPECT due to poorer resolution. Regional distribution was comparatively evaluated by circumferential profile methods in the same plane in 5 normal cases. As compared to PCT, Tl distribution was less in the septal and posterior regions and more in the lateral region due to photon attenuation.

In conclusion, Tl SPECT provides poorer images due to inadequate count density with poor resolution, as compared to PCT. It has severe limitation for quantitative evaluation of myocardial perfusion. However, one of the advantages of SPECT is that cardiac short-axis and long-axis sections can easily be reorganized.

10:30-12:00 **Room 212B**

NMR I: CLINICAL

Moderator: William J. MacIntyre, Ph.D.
Comoderator: Mack S. Lin, M.D., Ph.D.

COMPARATIVE EVALUATION OF NMR AND NUCLEAR MEDICINE IN DISC SPACE INFECTION - A PILOT STUDY. M. Modic, D. Feiglin, D. Piraino, J.K. O'Donnell, R.T. Go, M. Weinstein, W.J. MacIntyre. Cleveland Clinic Foundation, Cleveland, Ohio.

Six patients with proven disc space infection underwent bone scanning with 975MB$_q$ Tc-99m HDP together with NMR imaging on a 0.6T superconducting magnet to obtain weighted T1 30mSec (TE .3 Sec TR) and T2 (120mSec TE 3 Sec TR) images within a 48 hr. period. All patients had plain radiographic evaluation of the areas involved. Three pts. had Ga-67 Citrate scans using 222MB$_q$ activity following the bone scan and 1 patient had CT images of the involved area.

All 6 bone scans showed increased bony uptake in at least the adjacent vertebral end plates but did not show any abnormal uptake in the region of the disc. Bony activity distribution was non-specific and could have been consistent with either degenerative or osteomyelitic change. Gallium imaging in one case supported the latter diagnosis

but did not indicate presence of disc space involvement. Two other cases showed bony involvement to the extent of the bone scan; one showing minimal uptake due to antibiotic therapy. Plain radiographs were suggestive of disc space infection in all cases. NMR in all cases revealed marked disc space and adjacent bone involvement to the extent shown on bone scans. T1 and T2 weighted images appeared highly specific for either infection or degenerative change and were unaffected by antibiotic therapy.

NMR appears to be more sensitive in evaluation of disc space infection than radionuclide studies. NMR is also able to provide significant anatomic information involving thecal sac and neural structures. Nuclear medicine studies appear equally sensitive though less specific in the evaluation of bone involvement except perhaps where antibiotic therapy has been used.

EVALUATION OF ABDOMINAL AORTIC ANEURYSMS WITH NMR IMAGING. A. Evancho, M. Osbakken, and W. Weidner. The Pennsylvania State University, Hershey Medical Center, Hershey PA.

7 patients (5 male and 2 female, age range from 50 to 88) with angiographic proven abdominal aortic aneurysms were evaluated with NMR imaging (1.5 K gauss system) of the abdomen. Images were obtained in transverse, coronal and saggital planes with three radiofrequency pulse sequences [saturation recovery (SR), inversion recovery (IR), and spin echo (SE)]. All of the aneurysms were identified as to site and relative size with NMR images. The lumen in which there was flowing blood was always dark (low intensity), whereas the aneurysmal area which contained presumed clot was brighter (high intensity) on SR images. Although the size, location and relationship to other blood vessels was best demonstrated on aortography, NMR images provided similar information in all cases. NMR images correctly demonstrated thrombus in six cases.

In conclusion, NMR imaging provides a clear delineation of the anatomy of abdominal aortic aneurysms. In addition, it can provide information concerning tissue type, i.e., it distinguished clot from moving blood. It may be possible in the future to further characterize atherosclerotic and other pathological changes in vessel architecture by using various pulse sequences and timing parameters to provide in vivo histological typing.

NMR CHARACTERIZATION OF PITUITARY TUMORS. M. Osbakken, J. Gonzales, and R. Page. The Pennsylvania State University, Hershey Medical Center, Hershey, PA.

Twelve patients (5 male, 7 female, mean age 37.9± 20) with pituitary tumors were extensively evaluated with NMR imaging using a 1.5K gauss resistive magnet. Saturation recovery (SR), inversion recovery (IR) and spin echo (SE) pulse sequences were used for qualitative characterization of the lesions. T_1 calculations were also performed for brain and pituitary. Tumor histology and endocrine status were correlated with NMR data. All tumors were large with suprasellar extension (6 with prolactin secretion, 6 without). Pituitary T_1's ranged from .2 to .64, the mean T_1 being longer than that of brain (Brain = .4 ± .04; Pit = .48 ± .14). 3 patients with histological evidence of homogeneous adenomas had long T_1's (0.58 ± .05). 3 patients with evidence of recent or old hemorrhage into the pituitary had much shorter T_1's (0.29 ± .12). There was no relationship between prolactin secretion and T_1. Qualitative T_1 and T_2 information can be obtained by using a combination of SR, IR, and SE images. Using this method in our patients, homogeneous adenomas had similar T_1's and longer T_2's compared to the brain, while patients with bleeds had shorter T_1's and T_2's. Image T_1 characteristics correlated well with the calculated T_1 values. The range of T_1 (and potentially T_2) values which occur in apparently similar lesions are most likely due to anatomical and pathophysiological variations in these lesions. It may be ultimately possible to separate different types of pathological processes based on NMR image T_1 and T_2 characteristics after careful comparative studies of NMR and histological data are completed. The combination of calculated T_1 and T_2 with image T_1 and T_2 information may also be useful in further characterization of lesions.

ECG gated NMR-CT for Cardiovascular Diseases. J.Nishikawa, K,Machida, M.Iio, N.Yoshimoto, T. Sugimoto. Tokyo Univ. Hospital, Tokyo. and H. Kawaguchi, H.Mano. Shimadzu Co. Ltd., Kyoto, Japan.

We applied NMR-CT to cardiac study with ECG gated technique to evaluate the left ventricular (LV) function and compared it with cardiovascular nuclear medicine study (NM). Our NMR-CT machine has resisitive air-core magnet with 0.15 Tesla. The saturation recovery image or inversion recovery image were obtained as 256 x 256 matrix and 15 mm in thickness. The study population was ten patients who were evaluated both by NMR image and by NM performed within one week interval. The heart muscle was able to be visualized without any contrast material nor radioisotopes in inversion recovery images, whereas saturation recovery images failed to separate heart muscle from blood pool. The wall motions of LV in both methods were well correlated except for inferior wall. The values of ejection fraction in NMR image were moderately low, but two modalities showed satisfactory correlation (r=0.85). The region of myocardial infarction was revealed as wall thinning and/or wall motion abnormality. It is still preliminary to draw a conclusion, however, it can be said that in the evaluation of LV function, method by NMR might be of equal value to those of NM. It can be certain that eventually gated NMR-CT will become more effective method for various aspects of cardiovascular evaluation.

RESPIRATORY GATING OF MAGNETIC RESONANCE IMAGES. J.A. Clanton, V.M. Runge, A.E. James, Jr. Vanderbilt University Medical Center, Nashville, Tn.

When compared to most other high resolution imaging modalities (i.e. CT), magnetic resonance (MR) requires significantly more time for data acquisition. The average MR scan time ranges from 2 to 6 minutes. Cardiac and respiratory motion cause large artifacts and significantly reduce the resolution of internal structures. Thus, a method for gating MR acquisition with the respiratory cycle was developed.

The respiratory cycle was followed via a pneumatic bellows placed around the patients chest, observing the change in pressure caused by motion of the chest with a transducer linked to the bellows by plastic tubing. The voltage output from the transducer was monitored by an electronic device which could be set to start and stop acquisition at any portion of the respiratory cycle.

We have performed studies on 5 volunteers and 23 patients gating the acquisition of data to the end-expiratory portion of the respiratory cycle. Respiratory gating eliminated the gross motion artifacts normally present at 0.5 T and markedly improved visualization of hepatic vessels. In 2 patients one with a pheochromocytoma snd one post splenic embolization, the tissue abnormalities could only be diagnosed with the use of respiratory gating.

Gating of data acquisition by chest wall motion in MR is feasible and significantly improves the diagnostic potential of MR imaging, particularly at higher field strengths where motion artifact is more severe.

STROKE, EVOLUTION OF NMR IMAGING CHARACTERISTICS. R.L. Nicholson, T. Carr, A. Kertesz, S. Black, P. Cooper, S. Stewart, St. Joseph's Research Institute, London, Canada.

This study evaluates NMR imaging characteristics of stroke and temporal evolution of these features.

Patients with acute stroke clinically had NMR imaging (prototype 0.15T resistive imager, Technicare,Inc.) acutely(n=37), at approximately 2 weeks (n=31) and 3 months (n=10). Patients with old (> 1 yr.) stroke were also imaged (n=7). Partial saturation sequences were used employing echo time (T_E) of 30, 60 and 120 msec, as well as inversion recovery (IR) sequences.

Partial saturation images displayed a homogeneous increase in signal at lesion sites in both bland and hemorrhagic infarcts, reflecting prolongation of spin-spin relaxation (T_2) due to increased tissue water content, blood

and edema being indistinguishable. IR images recovered low signal from bland infarcts due to prolongation of spin-lattice relaxation (T_1) by tissue edema, hemorrhagic lesions had short T_1 centrally (blood) with moderate or increased IR signal, and low signal peripherally (edema). On follow-up IR imaging, hematomas developed low signal centres, possibly reflecting cavitation, with short T_2 rims, possibly indicating the presence of iron-laden macrophages. In 2 patients with hemorrhagic infarcts an area of increased signal (prolonged T_2) was seen on initial partial saturation images in the homologous portion of the other hemisphere (normal by CT). This may reflect a local alteration of blood volume or velocity. In 5 patients with old infarcts, a rim of prolonged T_2 was seen at the periphery of old lesions, possibly reflecting a local chronic increase in extravascular or intravascular water, slowing of blood velocity, or a zone of neuronal dropout.

Detailed pathophysiologic correlation is required to understand the basis of these NMR findings.

10:30-12:00 **Room 217B**

NEUROLOGY I: CLINICAL

Moderator: Abass Alavi, M.D.
Comoderator: Nathaniel M. Alpert, Ph.D.

REGIONAL CEREBRAL BLOOD FLOW (RCBF) MEASUREMENTS BY SPECT ANALYSIS OF XENON-133 TRANSIT: VALIDATION OF TECHNIQUE AND CLINICAL CORRELATION. K Rezai, P Kirchner, C Armstrong, J Ehrhardt, H Damasio, H Adams, A Damasio, University of Iowa, Iowa City, IA.

The SPECT system (Tomomatic-64) developed by Lassen et al for rCBF measurements with Xe-133 was validated with phantom simulations and clinical studies.

A bi-compartmental flow phantom was developed consisting of a Xenon-133 pump connected in series to head and lung compartments. Flow rates between 0.2 and 1.4 brain volumes/min (20-140 cc/100 ml/min) were tested against Tomomatic measurements by linear regression. Correlation was excellent (r=1.0) in the range of 0.2-1.2 (20-120 cc/100 ml/min), representing flow rates which are most likely to be encountered in clinical studies. Flow rates above 1.2 (120 cc/100 ml/min) were significantly underestimated.

32 studies on 20 volunteers gave a mean normal flow of 72 (SD=12) cc/ 100g/min. Mean regional flow ranged from 62 in frontal lobes to 75 in central gray matter. Right-to-left variation was less than 5%. The lowest regional flow in a normal subject was 45 cc/100g/min.

68 studies were performed on 30 stroke patients. In 27 rCBF was less than 45 in affected brain areas for a sensitivity of 90% which improved to 97% when comparisons with contralateral brain were included.

Initial CT scans were normal or non-diagnostic in 10, but showed CVA's in regions of reduced rCBF in 17 patients. rCBF abnormalities involved greater portions of brain than CT changes, often (8/17) including distant regions, unpredicted by CT or clinical studies but known to be strongly interconnected to the area of structural damage.

SPECT estimates of rCBF appear to be a sensitive research and diagnostic tool and complement the structural information provided by CT.

KINETIC AND METABOLIC CONSIDERATIONS IN THE USE OF (I-125) HIPDM AS A TRACER FOR QUANTITATIVE MEASUREMENT OF REGIONAL CEREBRAL BLOOD FLOW. G. Lucignani, A. Nehlig, R. Blasberg, C.S. Patlak, L. Anderson, H.F. Kung, C. Fieschi, F. Fazio, and L. Sokoloff. Laboratory of Cerebral Metabolism, National Institute of Mental Health, Bethesda, MD.

The kinetics of cerebral uptake and the metabolism of radioactive iodine labeled HIPDM (N,N,N'-trimethyl-N'-(2-hydroxy-3-methyl-5-(I-125)iodobenzyl)-1,3-propanediamine) (I-125)HIPDM were studied in vivo in male adult Sprague-Dawley rats in order to evaluate the potential usefulness of this compound for quantitative measurement of regional cerebral blood flow (rCBF). The first pass extraction fraction of (I-125)HIPDM in brain was found to be about 80%. The arterial concentration of unmetabolized (I-125)HIPDM following an i.v. pulse drops rapidly and represents only 30% of the blood sample total radioactivity at 60 minutes, whereas 92% of the radioactivity in brain tissue at the same time is in unaltered (I-125)HIPDM. The rate constant for (I-125)HIPDM transport across the blood-brain barrier (BBB) was calculated on the basis of a distribution model in which bi-directional exchange of the tracer between brain tissue and vascular space is assumed. A kinetic model and an operational equation have been derived for determination of rCBF with this molecule. The model and equation take into account the three following factors: (a) incomplete first pass extraction; (b) HIPDM metabolism; (c) bi-directional flux of tracer across the BBB. Our observations suggest that this molecule might be of potential usefulness for rCBF measurements with single photon emission tomography, provided that all these factors are evaluated in man.

MEASUREMENT OF OXYGEN METABOLISM,123-I-IMP DISTRIBUTION AND rCBF-Xe IN PATIENTS WITH ISCHEMIC VASCULAR DISEASE. C. Raynaud, G. Rancurel, Y. Samson,E.Kieffer, J.C. Baron, E.Cabanis,N.A.Lassen,D.Comar,J.Rapin,J.L.Moretti,S.Askienazy,S. Ricard and M.Bourdoiseau.Serv.Hosp.F.Joliot, Dept.Biol.CEA, Orsay and Hôpital Salpêtrière, Paris, France.

To evaluate the merits of various proposed procedures before cerebral revascularization,we measured rCBF($C15O_2$),rOEF, $rCMRO_2$,by PET,continuous inhalation technique,rCBF(Xe)and 123-I-IMP by SPECT(Tomomatic 64) in six patients with occlusive disease of the carotid arteries.IMP acquisitions were made 3 different times,3-10 min(IMP 10),accepted as a CBF index,1-2 h.and 4-5 h.The same head position was used for PET and SPECT and tomographic slices were parallel to cantho-meatal line. For easy comparison of the results, the decrease or increase of each parameter was expressed in per cent of contralateral value.

Ten ischemic areas were defined on the basis of CBF. On 5 areas the decrease of rCBF was moderate, with mean values of 27%,33% and 22% for rCBF($C15O_2$),rCBF(Xe)and IMP 10; $CMRO_2$ decreased similarly by 29%; the IMP fixation improved significantly with time and the decrease of 22% found at 10 min was reduced to 9% at 5 hours.

On the other 5 areas,the rCBF decrease was larger, with mean values of 46%,40% and 37% for rCBF($C15O_2$),rCBF(Xe)and IMP 10;the 50% decrease in $CMRO_2$ was slightly higher. In these areas the IMP fixation failed to improve with time, the mean decrease values were 37% at 10 min and 39% at 5 h. In this small group of patients, a similar rCBF asymmetry was found with 3 different methods and a specific IMP kinetics was observed on areas with moderately decreased $CMRO_2$ which may indicate the persistence of underlying viable tissue. For such studies a high sensitivity SPECT system with short acquisition time is necessary.

DYNAMIC RATE CONSTANTS FOR F-18-DEOXYGLUCOSE UPTAKE IN NORMAL AND TUMORAL BRAIN TISSUE. R.A. Brooks, B. Shatzman, A. Tran, G. Di Chiro, G.H. Weiss. NIH, Bethesda, MD.

Twenty-one patients with brain tumors were studied with ^{18}F-deoxyglucose scanning. "Dynamic" scans were done at 2½ minute intervals during the first 30 minutes of uptake, and two conventional scans were done at about one and two hours, respectively, after injection. Values of the rate constants k_1-k_3 and glucose metabolic rate R were obtained by fitting the curve of tissue uptake over the first 30 minutes to the 3-compartment model, and values of k_4 were obtained by comparing the late scan with the last 3 dynamic scans and the 1 hour scan.

There was no difference in rate constants k_1-k_3 between normal cortical tissue and high or low grade gliomas. However the rate constants k_1 and k_2 obtained from the 30 minutes of dynamic scanning were 2-4 times higher than those reported by others for uptake curves measured over several hours.

There was good correlation between metabolic rates determined from the first 30 minutes and from the conventional scan, and this correlation improved slightly when the conventional determination was made using fitted rate constants, but the dynamically obtained values were 10% higher than the conventional ones. These discrepancies may be related to a non-equilibrium distribution of free tracer within the second compartment (tissue) at early times.

The k_4 values did not differ overall among high-grade tumors, low-grade tumors, and normal cortex, although for six high grade tumors k_4 was 30% lower than the cortical k_4 for those six patients. This may indicate a slight reduction in phosphatase in high grade gliomas.

CORRELATIVE STUDIES OF THE BRAIN WITH POSITRON EMISSION TOMOGRAPHY (PET), NUCLEAR MAGNETIC RESONANCE (NMR) AND X-RAY COMPUTED TOMOGRAPHY (XCT) A. Alavi, J.C. Leonard, R.A. Zimmerman, R.W. Dann, J. Chawluk, P. Bottomley, R. Regington, M. Reivich. Hospital of the University of Pennsylvania, Philadelphia, PA

Twenty-four patients with a variety of CNS disorders were examined with NMR, PET and XCT within a short period of time. NMR images were obtained using an experimental 0.12 Tesla resistive magnet. Partial saturation technique was used to acquire NMR images either as two-dimensional single axial plane or as three-dimensional volume images. PET imaging was performed following the administration of 18F-fluorodeoxyglucose. In nine patients with brain tumor all three modalities identified the neoplastic lesion. XCT provided a better differentiation of tumor from surrounding edema than NMR. PET was most accurate in determining the histologic grade of the tumor. In one patient with acute stroke NMR failed to identify the CNS abnormality. In the remaining three patients the findings on the NMR images corresponded well to those seen on the XCT. PET images demonstrated metabolic abnormalities which usually appeared more extensive. The presence of ventricular dilatation and cortical atrophy was demonstrated by both NMR and XCT, although the latter appeared more pronounced with NMR. PET studies showed pronounced reduction in posterior temporo-parietal region metabolism in patients with dementia. In patients with seizure and psychotic disorders, while PET showed certain abnormal patterns, both XCT and NMR appeared normal. These data indicate that NMR provides excellent delineation of structural changes compared to those seen by XCT. PET imaging on the other hand demonstrates regional metabolic activity which compliments anatomic findings on XCT and NMR.

SIMULTANEOUS ESTIMATIONS OF BLOOD BRAIN BARRIER (BBB) PERMEABILITY AND LOCAL CEREBRAL BLOOD VOLUME (CBV) IN HUMAN BRAIN TUMORS WITH POSITRON TOMOGRAPHY AND Ga-68 EDTA. R.A. Hawkins, M.E. Phelps, S.-C. Huang, J.A. Wapenski, P.D. Grimm, P. Greenberg, R.G. Parker, G. Juillard and D.E. Kuhl. UCLA School of Medicine, Los Angeles, CA.

Using Ga-68 EDTA and a two compartment model for diffusion across the BBB that includes a weighted subtraction term for determination of the relative CBV (compared to a normal region of brain with an intact BBB) or the absolute value of CBV (using measurements of Ga-68 concentrations in the blood: the input function), we determined values for the forward and reverse rate constants (k1 and k2) for diffusion across the BBB as well as values of CBV in 12 subjects with primary or metastatic brain tumors. Patients were studied on a NeuroECAT tomograph; imaging times were 1 to 10 minutes per scan for a total of about 2 hours. Measurements of Ga-68 concentrations were made on plasma arterial samples. Four direct measurements (in 3 subjects) of CBV using C(15-O) were also obtained. Values of k1 (the transfer constant which numerically approximates the capillary permeability surface area (PS) product) averaged 0.0030 ($\pm$ 0.0017) ml/min/gm while k2 averaged 0.0308 ($\pm$ 0.0157)/min. Linear regression analysis of the relative CBV in 7 tumor deposits in 4 paired Ga-68 EDTA/C(15-O) studies compared to normal brain tissue resulted in a correlation coefficient of 0.97 for the two methods. The estimates of k1 and k2 were insensitive to changes in the location of the control regions (although CBV estimates changed appropriately) as well as to substituting the input function for a normal brain region when determining the absolute CBV of the lesions.

10:30-12:00 **Room 216A**

RADIOASSAY

Moderator: Benjamin Rothfeld, M.D.
Comoderator: Martin L. Nusynowitz, M.D.

PERIFUSIONAL TECHNIQUES FOR SCREENING ANTIBODIES (Ab) IN LIVING TISSUE. G.L. DeNardo, A.W. Saxe, S.J. DeNardo, A. Epstein, C. Suey. UCD Medical Center, Sacramento, CA and Northwestern Univ., Chicago, IL. Supported by DOE Grant DE AT03-82, ACS Grant PDT-94F and UC Cancer Coord. Committee.

Ab of interest for radioimmunodiagnosis and therapy are often screened by assessing binding avidity in systems substantially different from that which prevails in the patient. While studies in humans are the ultimate determinant for success, these are associated with practical obstacles. We have adapted perifusional techniques to provide screening under circumstances closer to that of the patient. Normal mouse tissues, mouse and human cancers were perifused with Eagle's media into which was placed I-125 human serum albumin, cancer-specific Ab, non-specific Ab, or fibrinogen. Monoclonal Ab against human mammary cancer and Raji lymphoma were studied. The interstitial albumin space was determined and was consistent with the literature. All of this radioactivity could be washed from the tissue. In contrast, 4-10X greater specific Ab accumulated in the human tumor, and equally large amounts of fibrinogen. Almost two-thirds of these proteins could not be washed from the tumor. Accumulation of specific Ab was also 4-10 times greater in tumor than in other tissues. Non-specific Ab did not accumulate. These observations document the feasibility of screening Ab against living tissues using the perifusional technique. The technique has potential for determining the number of available binding sites under tissue conditions as well as quantifying differences between antibodies or between antibody and its fragments. An exciting application of the technique relates to its use for screening cancer removed from patients in order to determine the suitability of an antibody for diagnosis or treatment specifically in that patient.

CA19-9: A PROMISING TUMOR MARKER FOR PANCREATIC CARCINOMA. H.Sakahara, K.Endo, K.Nakajima, A.Hidaka, T.Nakashima, H.Ohta, K.Torizuka, A.Naito and T.Suzuki. Depertment of Nuclear Medicine and Surgery, Faculty of Medicine, Kyoto University, Kyoto, Japan

In order to evaluate CA19-9 as a tumor marker for pancreatic carcinoma (PC), serum levels of CA19-9 were compared with those of CEA and elastase-1 in 56 patients, consisted of 43 cases with histologically proven adenocarcinomas and 13 cases with chronic pancreatitis. Serum levels were determined by using RIA kit obtained from CIS, France (CA19-9 and CEA) and Abbot (elastase-1). The sensitivity, specificity and accuracy for the diagnosis of untreated PC are as follows.

(cut off level)	CA19-9 (>37U/ml)	CEA (>15ng/ml)	elastase-1 (>400ng/ml)
sensitivity	81%	65%	60%
specificity	85%	77%	46%
accuracy	82%	68%	57%

CA19-9 gave the highest accuracy among tumor markers we have studied and serum levels were markedly elevated over 100U/ml in 30 (70%) cases with PC, whereas none in chronic pancreatitis. CA19-9 values were closely related to the tumor size and the presence or absence of metastsis on CT findings. Small tumors of less than 3cm in diameter, although the site of tumor was limited to the head of the pancreas, showed positive results in 2 out of 5cases. Furthermore, CA19-9 was at a level of less than 22U/ml in 98 normal cotrols and was found to be elevated in only 4 (3%) out of 124 patients with benign diseases, including liver diseases, gastric ulcer, cholelithiasis, and so on.

These results indicate that CA19-9 is much better in diagnosis and management of PC than is CEA.

FIBRINOPEPTIDE A (FPA) RADIOASSAY IN THE EVALUATION OF CANCER. M.L. Nusynowitz, N.J. Hutchison. University of Texas Medical Branch, Galveston, TX.

The conversion of fibrinogen to fibrin by thrombin results in the release of FPA; the plasma concentration of FPA is a marker of the rate of conversion of fibrinogen and is an indicator of the clotting process. All coagulation processes leading to the formation of a fibrin clot will result in generation of FPA, quantifiable by radioassay. Malignant metastases are believed to function as tissue factors for the initiation of coagulation, and cancer activity should be reflected by elevation of FPA concentrations. We have used a commercially available FPA radioimmunoassay test kit to evaluate FPA concentrations in cancer patients. A normal range for FPA in our laboratory was established on 20 men and women. The distribution is log normal and the 95% confidence limits are 0.6-9.8 ng/ml plasma, with a mean of 2.4. Analysis of variance revealed a between duplicates coefficient of variation (CV) of 5.8% and a between run CV of 6.5%, both acceptable values. No significant difference was noted between duplicates. FPA and carcinoembryonic antigen (CEA) concentrations were determined in 52 patients with active cancer and 11 with presumably inactive disease. For the active cancer group, FPA alone was elevated in 27%, CEA alone was elevated in 17%, and both were high in 27%. A higher positive rate for FPA was seen in breast and lung cancer, whereas in colon cancer, CEA was more sensitive. Two patients in the presumably inactive group had positive FPA. The results indicate that FPA is more sensitive in active cancer than CEA; the two tests supplement each other as markers of disease activity. The FPA radioassay appears to be a good marker for following therapy of patients with cancer.

PLASMA L-DOPA IN THE DIAGNOSIS OF PATIENTS WITH MELANOMA. V.M. Camp, D.R. Murray, and B.A. Faraj, Departments of Radiology (Div Nuc Med) and Surgery, Emory University School of Medicine, Atlanta, GA.

Melanoma is one of a group of neoplasms that is characterized biochemically by abnormal tyrosine metabolism. The main objective of this paper is to establish whether or not the measurement of plasma L-dopa represents a specific indicator for the biochemical diagnosis of melanoma. Two groups of patients were studied: group 1 consisted of 20 patients with stage 2 and 3 disseminated melanoma, and group 2 consisted of 20 patients with non-malignant melanoma. L-dopa in plasma was measured by a radioenzymatic technique. The method was based upon the incubation (37°C, 40 min) of 50 µl of plasma in the presence of catechol-O-methyltransferase, dopa decarboxylase and S-[3H]-adenosylmethionine (5 µCi, sp. act. ci/mmol). The formed methylated decarboxylated metabolite 3H-3-O-methyldopamine was characterized by radiochromatographic analysis. The results of the study showed that plasma L-dopa was elevated significantly in patients with disseminated melanoma (av 4.9 ng/ml) as compared with non-malignant melanoma patients (av 0.9 ng/ml) and control subjects. In summary, the measurement of plasma L-dopa represents a specific marker for detection of metastatic melanoma.

IN VIVO DETERMINATION OF BONE BLOOD FLOW. M. S. Rosenthal, P. M. DeLuca, Jr., D. W. Pearson, and R. J. Nickles, Department. of Medical Physics, University of Wisconsin, Madison, WI.

Quantitative measurement of bone blood flow is vital to understand the hemodynamics of bone systems especially in the study of asceptic bone necroses. These "silent bends" result from micro-emboli in femoral arterioles from small nitrogen bubbles released from lipids during a diver's ascent. A technique to determine bone blood flow in vivo has been developed by measuring the rate of inert gas washout of Ar-41 ($t_{1/2}$ = 1.83 h, E = 1293 keV) from the bone mineral matrix.

Argon gas is formed in vivo by neutron activation of Ca-44 using 14.3 MeV neutrons, following the reaction Ca-44(n, α)Ar-41. The blood flow in the irradiated bone is determined by measuring the clearance rate of Ar-41 using gamma-ray spectroscopy. To date, measurements have been made on dead and living rats (weight 300g). The results indicate that in the no-flow situation the clearance rate is consistent with the physical half- life of Ar-41, while for the live rats the clearance rate for argon is dependent on the flow of blood in the bone. The observed clearance times correspond to flows greater than 3 ml of blood per 100 ml of argon distribution volume/min (F/pV), with the bone-blood partition coefficient for argon approximately one. In addition, measurements of the partitioning of argon and other gases with bone have been measured in order to understand blood-bone systems more fully.

Supported in part by USDOE contract DE-AC02-76EV01105 and PHS Grant 5T32 CA09206CT.

PROPOSED MECHANISMS WHEREBY THE T3U, DIALYZED FRACTION (%FT4) AND ANTIBODY EXTRACTED (AE) T4 NORMALIZE BINDING PROTEIN EFFECTS IN FREE T4 (FT4) ASSAYS DO NOT EXPLAIN THE FINDINGS IN MONTHYROIDALLY ILL (NTI) PATIENTS. L.R. Witherspoon, S.E. Shuler and S. Gilbert. Ochsner Clinic, New Orleans, LA.

Apparently falsely low FT4 results are observed in patients with NTI. FT4 estimates in NTI using some AE assays are lower than the corresponding FTI. Both are lower than equilibrium dialysis (ED) results. These three approaches to FT4 estimation are similar - the T3U, %FT4 and %AE all are inversely related to TBG concentration. A FT4 estimate may be obtained by multiplying any of these x total T4 concentration. The mass of AE T4 may be quantitated by competitive binding, either after separation of AE T4 from serum (two step) or by employing a radiolabeled T4 analog recognized by the antibody but not by TBG. We made FT4 estimates in euthyroid patients with ↑, normal or ↓ TBG concentrations; in hyper- and hypothyroid patients; and in NTI patients presumed euthyroid. Each approach produces similar results in euthyroid patients. The T3U and some AE assays display TBG dependence at TBG <10 and >50 ug/ml. In hyperthyroidism, the T3U is ↑, %FT4 normal or ↑, while the %AE is ↓. All FT4 results are ↑ in hyperthyroidism. In hypothyroidism the T3U is ↓, %FT4 normal or ↓, while the %AE is ↑. All FT4 results are ↓ in hypothyroidism. In NTI, the T3U is appropriate for the TBG concentration, %FT4 is often ↑ and %AE is ↓. Furthermore, methods for quantifying the AE mass do not agree - index results are ↓, analog results lower, such that %B/B is >100%, while the two step results are normal. The suggestion that the T3U, %FT4 and %AE all serve to normalize TBG effects in FT4 assays is inadequate. AE assays should be employed clinically with caution until the apparent anomalies, especially those seen in the analog systems, are explained.

10:30–12:00 **Room 212A**

GASTROENTEROLOGY I: HEPATOBILIARY AND ESOPHAGUS

Moderator: Heidi S. Weissmann, M.D.
Comoderator: Richard C. Reba, M.D.

CHOLECYSTOKININ (CCK) FUNCTIONAL CHOLESCINTIGRAPHY (FC) IN PATIENTS SUSPECTED OF ACALCULOUS BILIARY DISEASE (ABD). D. Fink-Bennett, P. DeRidder, W. Kolozsi, R. Gordon and J. Rapp. William Beaumont Hospital, Royal Oak, MI. and Northern Columbiana County Community Hospital, Salem OH.

To determine if CCK FC can aid in the diagnosis (Dx.) of ABD, we retrospectively analyzed the max. gallbladder (GB) ejection fraction response (EFR) to CCK in 240 patients (pts.) with persistent symptoms of biliary colic, a normal GB Ultrasound exam and/or OCG.

Each pt. (NPO after 12 A.M.) received 5 mCi of technetium (Tc)-99m Hepatolite™. After max. GB filling, .02 ug/kg CCK was administered (1-3 minutes) I.V. Back-

ground corrected GB EFs were determined q.5 min. X4 by ratioing the pre-CCK GB cts. minus post-CCK GB cts. to pre-CCK GB cts.

In 131/240 pts. the max. GBEFR was <35%; 76 had a cholecystectomy (Cx.), 2 an exploratory lap., 53 medical Rx. Of the 76 post-Cx. pts., 74 had chronic cholecystitis (CC) (67 acalculous, 7 calculous), 2 were normal. Exploratory lap. pts. had no GB disease. Clinically 69/70 (4 no followup, 1 no change) post-op CC pts. are improved. One normal GB pt. has persistent pain, the other a Sphincter of Oddi dyskinesia. Of the 53 medical Rx. pts., 23 are lost to followup, and 2 died. Twenty-four are clinically felt to have ABD, 4 are not.

In 109/240 pts. the max. GBEFR was >35%. Eleven underwent surgery, 98 medical Rx. 4/11 Cx. pts. had CAC, 7 were normal. Of the 98 medical Rx. pts., 21 lack followup, 71 are clinically felt not to have ABD;6 are felt to have ABD.

CCK FC appears to be a useful test for the detection of ABD. Its predictive value (GBEF <35%) in Cx. pts. is 97%; in all pts. (assuming medical Rx. correct), 94% (sensitivity - 91%, specificity - 93%).

SAFETY OF EXOGENOUS (CCK-8) AND ENDOGENOUS (FATTY MEAL) CHOLECYSTOKININ (CCK) INDUCED GALLBLDDER (GB) DYNAMICS IN PATIENTS WITH CHOLELITHIASIS. H. Brar and G.T. Krishnamurthy. VA Medical Center and Oregon Health Sciences University, Portland, OR.

The quantitation of biliary dynamics in patients requires induction of GB contraction and emptying by CCK. However, it is not clear how safe it is to induce GB emptying in a patient with known gallstones. This study was undertaken to document the safety of induction of GB emptying in 50 patients with gallstones and the results are compared with 55 normal subjects. After 4-6 hours of fast, each subject was given 3-5 mCi of Tc-99m-IDA. Sixty minutes later, the subject was positioned under a gamma camera and the data were acquired at 1 frame/min. for 30 min. (CCK-8) or 60 minutes (fatty meal). Saline placebo was given at 5 minutes and CCK-8 or fatty meal at 10 minutes. Onset of symptoms was recorded and correlated with GB ejection period. GB ejection fraction (EF) was calculated for 3 doses (5, 10 & 40 ng/kg) of CCK-8 and fatty meal (8 oz/70 kg).

Compared to normals, GB emptying in general was lower in patients with cholelithiasis for all 3 doses of CCK-8 and fatty meal. Five patients (10%) with cholelithiasis experienced a mild to moderate degree of nausea and intermittent abdominal pain during GB ejection and the symptoms were similar to their previous experience during an attack of cholecystitis. All symptoms abated within 10 minutes without therapy. No incidence of impaction of GB stone in the common bile duct was seen. It is concluded that the GB emptying required for quantitative biliary dynamics can be induced safely with either exogenous or endogenous CCK in patients with known cholelithiasis.

THE SONOGRAPHIC MURPHY'S SIGN: ANOTHER PERSPECTIVE. P. Colletti, P.W. Ralls, S.A. Lapin, D.C.P. Chen, M.E. Siegel, J. Halls. LAC/USC Medical Center.

Cholescintigraphy (CS) is currently the most accurate test to detect acute cholecystitis (AC). We evaluate the sonographic Murphy's sign (M) along with detection of gallstones (S) in AC.

Real time ultrasound (RT) with attention to M and S was performed in 194 patients with suspected AC. CS with Tc-99m disofenin carried out for 4 hours was done in 70 patients. Surgical and clinical results were complied. Liberal criteria for AC was used.

Of patients with the combination M and S, 94% had AC (84/89). Of patients without the M or S, 96% did not have AC (71/74). Comparison results in RT and CS are:

	ULTRASOUND				CHOLESCINTIGRAPHY	
	Stones		No Stones			
	M+	M-	M+	M-	+	-
AC+	22	6	4	3	31	4
AC-	2	3	7	23	3	32

The positive predictive value (PV) of M-S was 92% (22/24) and of CS was 91% (31/34). The negative PV of -M-S was 88% (23/26) and of CS was 88% (32/36). Only 36% (4/11) of cases with +M and -S had AC.

We conclude that the combinations +M+S or -M-S are as reliable as +CS and -CS respectively. An algorithm using RT to screen for AC is proposed in which +M+S cases are positive and -M-S cases are negative. +M-S and -M+S cases would require CS. This would rapidly triage 70% of cases with 93% accuracy. The cost of RT would need to be at least 1/3 less that CS for this to be cost effective.

DETECTION, LOCALIZATION AND QUANTITATION OF PARTIAL OBSTRUCTION OF COMMON BILE DUCT (CBD) BY SCINTIGRAPHY; CORRELATION WITH CHOLANGIOGRAM. G.T. Krishnamurthy, D. Lieberman and H. Brar. VA Medical Center and Oregon Health Sciences University, Portland, OR.

Recent literature in medical journals does not show any major role for scintigraphy in the evaluation of jaundice. A project was undertaken to test critically the role for scintigraphy in the detection, localization and quantification of partial obstruction of CBD using Tc-99m-IDA and the results are correlated with cholangiogram. After 4 to 5 hours of fast, each of 12 patients with documented CBD obstruction was given 3 to 8 mCi of Tc-99m-IDA and serial hepatobiliary images at 2 minute intervals were taken for 90 minutes using gamma camera and the data were collected on computer for quantitation. At 70 minutes 10 ng/kg of CCK-8 was infused over a 3 minute period (n=8). Liver excretion half time, GB ejection fraction (EF) and ejection rate (ER) were obtained. The results were compared with established values in normal subjects. The location of CBD obstruction was made from analogue images.

Partial CBD obstructon was charaterized in all but one by prolonged liver excretion half time, reduced GB EF and ER (less than 3.5%/min) and intrahepatic bile pooling with excellent CHD and CBD delineation proximal to obstruction thus aiding in the exact anatomic location which correlated well with cholangiogram. The degree of obstruction (ER) correlated well with dilitation of CBD on cholangiogram. These preliminary results show a promise for scintigraphy in the evaluation of CBD obstruction and offer a great potential for non-invasive quantitation of the degree of CBD obstruction.

SCINTIGRAPHIC DIFFERENTIATION OF INTRAHEPATIC TUMORS. H.Creutzig,C.Brölsch,K.Gratz,P.Neuhaus, St.Müller,O.Schober,W.Lang,H.Hundeshagen,R.Pichlmayr. Medizinische Hochschule Hannover FRG

Intrahepatic tumors in asymptomatic patients are seen with increasing frequency.Treatment is dependend of the histology:while follicular nodular hyperplasia (FNH) and hemangiomas need no further treatment, all other tumors should be resected.

In a prospective study we investigated the usefulness of two-stage scintigraphy (TSS) for the differentiation . The cholescintigraphy was started with a perfusion study, followed by a scan in the parenchymal phase and in the excretion phase.There is a typical scintigraphic pattern for FNH (hyperperfusion,normal parenchymal uptake delayed excretion) and hemangioma (hypoperfusion, no uptake), while all other tumors may have a mixed pattern. Therefore a blood pool is added to look for a hemangioma, if there is no typical pattern for FNH in the cholescintigraphy.

The TSS classified correct 21 of 23 patients with FNH, 17 of 18 with hemangiomas, all 3 with adenoma and 36 of 37 with primary malignant intrahepatic tumors. The TSS is more accurat than CT or sonography, save and inexpensive and therefore the method of first choice in the differentiation of intrahepatic tumors.

RADIONUCLIDE QUANTIFICATION OF OROPHARYNGEAL CLEARANCE WITH AND WITHOUT PHARYNGITIS. P.S. Robbins, J.A. Siegel, A.H. Maurer, B.P. Schachtel, and L.S. Malmud. Temple University Health Sciences Center, Philadelphia, PA and VICKS Research Center, Shelton, CT.

The purpose of this study was to evaluate a new radionuclide method for quantifying oropharyngeal clear-

ance (C) in 10 otherwise normal patients with and without pharyngitis (PH). Patients with objective evidence of PH initially swallowed 10 ml of water mixed with 1 mCi Tc-99m sulfur colloid and then performed a dry swallow each 15 seconds. This was repeated 1-4 weeks later when there was no evidence of pharyngitis (NP). Images were acquired using a high sensitivity collimator for 0.1 sec/image for 30 sec and 15 sec/image for an additional 270 sec. Time activity curves generated from a region of interest over the oropharynx were fit to a biexponential function, $C = Ae^{-k_1 t} + Be^{-k_2 t}$; where A and B are the percent of activity clearing with fast and slow components, k_1, and k_2, respectively, with half times $0.693/k_{1,2}$. Data, complete for 9/10 patients, yielded (mean ± SD):

	Fast Component		Slow Component	
	% A	T1/2	% B	T1/2
PH	64.4±12.4	21.4±15.5	34 ±12	289±137
NP	29.2±18.4	10.5± 4	41.3±19.2	315±138

The T1/2 for the slow component was reproducible for PH and NP. The fast component was slightly prolonged with PH, but not to statistical significance (p>.2). We conclude that a biexponential model of clearance may be used to quantify oropharyngeal function, for patients with normal and abnormal swallowing.

RADIONUCLIDE ESOPHAGEAL TRANSIT OF A LIQUID BOLUS: A REAPPRAISAL. R.H. Holloway, R.C. Lange, L. Magyar, R. Greene and R.W. McCallum. Yale University School of Medicine, New Haven, CT.

Measurement of radionuclide esophageal transit (RT) using a liquid bolus has been suggested as a screening test for esophageal motor disorders (EMD). We prospectively evaluated RT in 49 patients referred for esophageal manometry. Ten subjects with normal manometry served as controls. RT was performed using two 10 ml boluses of water labeled with 250 uCi ^{99m}Tc-sulfur colloid. Patients were studied supine and the swallow sequences framed in 1 second intervals. Transit time was measured from the time of entry to the time of exit from the esophagus. Mean transit time in normal subjects was 9.1±2.1 (SD) sec. The test was abnormal if the transit time was prolonged (>15 sec) in at least 1 of 2 swallows. RT agreed with manometry in 36/49 patients (75%), including 9/9 achalasics, 3/3 diffuse esophageal spasm, 3/7 'nutcracker esophagus' and 7/8 non-specific motor disorders (NSMD). 4/18 patients with normal manometry had abnormal RT. 9/31 patients with abnormal manometry had normal RT, including 4/7 nutcracker esophagus, 3/3 hypertrensive LES, 1/1 scleroderma and 1/8 NSMD. Sensitivity of RT was 70% and specificity 77%. The false positive rate was 15% and the false negative rate 39%. Conclusions: 1) RT identifies patients with absent or impaired peristalsis; 2) There is substantial incidence of false negatives among patients with manometric disorders but normal peristalsis; 3) Abnormal RT did occur in some patients with normal manometry. RT using a liquid bolus may not be sensitive enough as a screening test for EMD, but it may be an important adjunct to manometry.

SCINTIGRAPHIC ASSESSMENT OF BARRETT'S ESOPHAGUS. J.A. Kotler, R.E. Sampliner, F.J. Kogan, R.E. Henry, B.F. Mason. University of Arizona and VAMC Tucson, Arizona.

Barrett's (B) esophagus is defined by the presence of columnar epithelium above the gastroesophageal junction. Patients with 5cm histologically proven B were evaluated for mucosal labeling (ML), esophageal motility (EM), gastroesophageal reflux (GER), and gastric emptying (GE) of solids and liquids with and without iv metaclopramide (MCP). ML, after premedication with cimetidine, was evaluated 20 and 40 min after injection of Tc-99m04 with ANT and RAO views. Eight of 11 B and 0 of 2 controls (C) labeled esophageal mucosa. EM was assessed in the supine position over one min after a 15ml swallow of Tc-99mSc-H20. The normal pattern shows sequential, aboral, discreet peaks with no retrograde movement over one min in three computer derived regions over the esophagus. Five of 16 B and 1 of 6 C demonstrated abnormal pattern. GER was assessed in the supine position by serially increasing extrinsic binder pressures from 0 to 100 Torr after ingestion of 300ml of Tc-99mSc-orange juice (OJ). GER was present in 13 of 15 B and 0 of 11 C. Reflux ranged from 5.1% to 30% at 100 Torr. Hiatal hernia (HH) was identified in 14 of 16 B by endoscopy and in 10 of 16 by scintigraphy. GE was evaluated after a liquid meal of 300ml Tc-99mSc-OJ and a solid meal of Tc-99mSc-egg salad sandwich. The supine subject was imaged anteriorly for 30 min (liquid) or 60 min (solid). GE was assessed an additional 10 min after MCP. Clearance time (50%) for solid GE was calculated from extrapolated linear fits of decay corrected data. There was no significant difference in liquid or solid GE between B and C. We conclude; 1)ML detects B with lower sensitivity than previously reported. 2)EM disorders are frequently found in B. 3)GER is frequently identified in B. 4)HH can be identified by nuclear technique. 5)B shows normal GE and responds to MCP.

1:30-3:00 **Room 217A**

CARDIOVASCULAR II: RADIONUCLIDE ANGIOCARDIOGRAPHY IN CORONARY ARTERY DISEASE

Moderator: Harvey J. Berger, M.D.
Comoderator: Robert H. Jones, M.D.

PREOPERATIVE DETERMINATION OF REVERSIBILITY OF WALL MOTION ABNORMALITIES USING F-18 FLUORODEOXYGLUCOSE AND N-13 AMMONIA POSITRON TOMOGRAPHY. R. Brunken, J. Tillisch, R. Marshall, H. Schelbert, S. Huang and M. Phelps. UCLA Center for the Health Sciences, Los Angeles, CA.

We postulated that positron emission tomography (PET) with F-18 fluorodeoxyglucose (FDG) and N-13 ammonia (NH3) performed preoperatively could predict recovery of segmental ventricular function following revascularization in patients with ischemic heart disease and resting wall motion abnormalities. The ventricle was divided into anterior, lateral, inferoposterior and septal regions and wall motion abnormalities were determined in blind fashion from angiogram, radionuclide ventriculogram and 2-D echo. Using criteria previously established in this lab, regional infarction was defined as reduction in both NH3 and FDG counts, while ischemia was identified by an increase in FDG counts relative to NH3 counts. Infarcted regions were expected to show little or no improvement in wall motion while normal or ischemic regions were expected to show improved function following revascularization.

Abnormal wall motion was identified in 28 regions in 12 patients; in 10 of these patients (13 regions) there was evidence clinically of prior transmural infarction. Of the 15 regions which were either ischemic or normal tomographically, 14 had improved function postoperatively, including 5 with clinical evidence of prior infarction. Of the 13 regions classified as infarct, none showed improved function postoperatively including 8 with no prior clinical evidence of infarct.

Thus, PET with FDG and NH3 can reliably predict recovery of segmental function following revascularization in patients with resting wall motion abnormalities.

SPECIFICATION LV REGIONAL WALL MOTION ABNORMALITIES (RWMA) IN CAD AND NON-CAD PATIENTS BY PHASE ANALYSIS OF RADIONUCLIDE VENTRICULOGRAMS (RNV).

E.Henze, D. Müller, C. Delagardelle, F. Bitter, M. Stauch, W.E. Adam, University of Ulm, Germany

RWMA are thought to be highly specific for CAD although they have been described in aortic regurgitation (AR) and in pts on daunorubicin (DAU) as well. In an attempt to further specify non-CAD RWMA, consecutive exercise RNV of 17 pts with proven severe CAD were compared with resting RNV of 24 pts with transmural myocardial infarction (MI), 28 pts on a critical dose of DAU and 25 AR pts. RWMA were defined objectively from parametric images by a decreased sectorial amplitude of more than 2 standard deviations of normal. In 15/17 CAD pts (88%) and in 19/24 MI pts (79%) a significantly decreased regional amplitude was found. Importantly, in all abnormal CAD and MI amplitude scans (100%) a significantly abnormal phase shift in the same

region could be noted. In 6/28 pts on DAU (21%) an apical hypokinesis could be verified. In contrast to CAD, however, the phase distribution was normal in all these DAU pts. The pts with AR demonstrated a very inhomogenious pattern. A normal image was seen in 5 pts, 6 pts had an infarct-like pattern with regionally decreased amplitudes and phase shifting, 7 pts showed a normal amplitude image with yet regional phasic delay, and the remainder 7 pts had an apical hypokinesis with normal phase distribution. In conclusion, standardized phase analysis of RNV data provides a powerful tool for specifying RWMA. It allows a highly specific separation of RWMA between CAD and DAU pts. The inhomogenious pattern in AR pts can in part be explained by increased wall stress and/or incomplete left bundle conduction abnormalities and awaits further evaluation.

RADIONUCLIDE FOURIER AMPLITUDE ANALYSIS TO PREDICT POST-ANEURYSMECTOMY EJECTION FRACTION. D.M. McCarthy, J.P. Kleaveland, P.T. Makler, Jr., A. Alavi. University of Pennsylvania, Philadelphia, PA

Post-operative LV ejection fraction (EF) is an important determinant of outcome following aneurysmectomy but is difficult to predict noninvasively. First harmonic Fourier analysis of radionuclide angiography (RNA) in patients with aneurysms gives characteristic phase and amplitude images which delineate contractile and dyskinetic regions. Since pixel amplitude is proportional to stroke counts, the summed amplitude values from the contractile region (CR) and the aneurysm should reflect regional stroke volumes. A predicted post-operative LVEF may be determined from the pre-operative global LVEF and the proportion of the total amplitude located in the CR.

We studied 19 patients undergoing LV aneurysmectomy with pre- and post-operative RNA. Three patients were excluded for technical reasons, leaving 16 patients for analysis. There were 13 males, and the mean age was 56.8 yrs (range 45-78). All patients had a history of anterior myocardial infarction and were undergoing surgery for recurrent sustained ventricular tachycardia. The global LVEF increased from 0.25±.13 (sd) pre-operatively to 0.38±.11 following surgery ($p<.001$). The predicted post-operative LVEF (from amplitude analysis of the pre-operative RNA) averaged 0.35±.13 and correlated significantly with the actual post-operative LVEF ($r=0.87$, SEE=.06, $p<.01$).

The results suggest that the LVEF following aneurysmectomy can be predicted from Fourier amplitude analysis of the pre-operative RNA.

COMPARISON OF EJECTION FRACTION AND PULMONARY BLOOD VOLUME RATIO AS MARKERS OF LEFT VENTRICULAR DYSFUNCTION WITH SINGLE VESSEL CORONARY DISEASE BEFORE AND AFTER PTCA. P. Liu, M. Kiess, R.D. Okada, C.A. Boucher, H.W. Strauss Massachusetts General Hospital, Boston, MA

Exercise induced increases in pulmonary blood volume (PBV) have been shown to correlate with transient exercised-induced increase in left ventricular (LV) filling pressure. To analyze the impact of single vessel disease on LV function, ejection fraction (EF) and PBV were measured by serial supine exercise gated scans (GBPS) on 53 patients with left anterior descending artery disease undergoing coronary angioplasty (PTCA). EF was defined by standard methods. The PBV ratio was taken as the exercise to rest counts from the lung regions of interest as previously reported. Regional wall motion (WM) was quantified by averaging the results of 5-point score system in each region from 3 observers. Normal was defined as: rest EF $\geq$ .50 and increase in EF with exercise, PBV $\leq$ 1.06 and no deterioration in WM on exercise. Of the 53 patients, 54% were found to be abnormal by EF, but 83% by PBV ($p<.01$). Abnormal PBV ratio was also highly associated with exercise induced deterioration in WM on GBPS ($p<.05$). After PTCA, the proportion of patients with abnormal EF remained unchanged (50%), whereas those with abnormal PBV ratio decreased significantly (to 38%, $p<0.01$).

We conclude: (1) PBV ratio (filling pressures) is more frequently abnormal than EF (systolic function) in single vessel disease; (2) There is a significant improvement of PBV ratio after PTCA; (3) This discordance of parameters of systolic and diastolic function suggests that PBV (and hence diastolic function) is a more sensitive indicator of changes in ventricular function following an intervention than EF.

EXERCISE RADIONUCLIDE VENTRICULOGRAPHY TO DETECT RESTENOSIS FOLLOWING CORONARY ANGIOPLASTY
EG DePuey, LL Leatherman, WE Dear, RD Leachman, EK Massin, VS Mathur, and JA Burdine. Baylor College of Medicine, St. Luke's Episcopal Hospital, The Texas Heart Institute, Houston, TX

Forty one patients (pts) underwent semiupright exercise gated radionuclide ventriculography (EGRNV) before, within 3 d after single vessel transluminal coronary angioplasty (TCA), and 4 to 12 mos later, at which time follow-up cardiac catheterization was also performed. Prior to TCA 76% of pts had abnormal EGRNV, as defined by a failure to increase ejection fraction (EF) by 5 points or the development of a new regional wall motion abnormality. Stenosis was reduced from 90 ± 7% to 18 ± 17%. Early after TCA, exercise duration and maximum double product increased ($p's<.005$). Resting EF was unchanged (56.5 ± 10.5 vs 56.7 ± 9.8), but exercise EF increased from 58.3 ± 11.9 to 65.3 ± 11.5 ($p<.001$). EGRNV normalized in 61% of pts with abnormal pre-TCA studies ($p<.001$).

Pts were subgrouped according to the percent increase in stenosis demonstrated angiographically at 4-12 mos {Group I (n=23): ≤20%; Group II (n=10): >20% but <50%; Group III (n=8): ≥50%}. Pts with abnormal EGRNV early after TCA were demonstrated to have a greater percent increase in stenosis at late follow-up than pts with normal EGRNV (41 ± 30% vs 19 ± 25%, $p<.001$). Early after TCA EGRNV was abnormal in 5% of Group I pts vs 75% in Group III ($p<.01$), and EF increased to a greater degree during exercise in Group I pts (+11.3 ± 7.5 vs +3.5 ± 6.5 points, $p<.01$). At 4-12 mos EGRNV was abnormal in 27% of Group I vs 88% of Group III ($p<.01$), and during exercise EF increased in Group I pts (+11.8 ± 7.8 points) but decreased in Group III (-1.9 ± 8.7 points) ($p<.0005$). The accuracy of abnormal EGRNV in predicting >50% restenosis was 73% early post-TCA and 77% at 4-12 mos. We conclude that EGRNV is a valuable test to verify the success of TCA and to detect subsequent restenosis.

ATRIAL PACING AS AN ALTERNATIVE TO SUPINE EXERCISE (SE) IN RADIONUCLIDE VENTRICULOGRAPHY (RNV). V. LeGrand, S. Wells, W.W. O'Neil, J. Jenkins, M.D. Gross, R. Vogel, University of Michigan and the VA Medical Centers, Ann Arbor, MI 48105.

Stress RNV is at times of limited value as many patients cannot achieve a sufficient pressure rate product (PRP). Atrial pacing is a noninvasive alternative to SE by bicycle ergometry. A swallowable electrode attached to a flexible wire is positioned in a retroatrial position in the esophagus and when connected to a variable output stimulator, variable rate (120,140,160 beats/min) atrial pacing ventriculography (APV) can be performed. RNV is performed in the sitting position at rest and at each pacing stage. APV was compared to SE RNV in 4 patients with coronary artery disease (CAD) and 3 normal volunteers (N). Tolerance to APV was excellent with adequate pacing. All subjects reported a minor sensation of chest burning. No arrhythmias occured. At maximal APV mean PRP was 174 ± 26.

		EF	Diastolic Volume	Systolic Volume
N	APV	58±7 → 60±3	144±35 → 90±13	62±23 → 37±7
	SE	58±1 → 71±3	139±16 → 136±11	58±7 → 41±16
CAD	APV	49±14 → 43±19	162±62 → 138±64	90±62 → 90±70
	SE	46±13 → 48±10	163±77 → 181±55	97±73 → 99±51

The diastolic volumes in APV fell in all patients. Systolic volumes fell in N but not in CAD to APV. A flat EF response to APV was seen in both N and CAD patients. APV is an alternative to SE RNV although PRP remains low. Volume changes in APV are different than in SE RNV and in the interpretation of the results of APV in CAD, changes in systolic and diastolic volumes may be more important than the response of EF.

1:30–3:00 **Room 216BC**

COMPUTERS AND DATA ANALYSIS I: SPECT

Moderator: Guy H. Simmons, Ph.D.
Comoderator: Jon H. Erickson, Ph.D.

TWO-DIMENSIONAL FILTERING OF SPECT IMAGES USING THE METZ AND WIENER FILTERS. M.A. King, R.B. Schwinger, B.C. Penney, and P.W. Doherty. University of Massachusetts Medical Center, Worcester, MA.

Presently, single photon emission computed tomographic (SPECT) images are usually reconstructed by arbitrarily selecting a one-dimensional "window" function for use in reconstruction. A better method would be to automatically choose among a family of two-dimensional image restoration filters in such a way as to produce "optimum" image quality. Two-dimensional image processing techniques offer the advantages of a larger statistical sampling of the data for better noise reduction, and two-dimensional image deconvolution to correct for blurring during acquisition. An investigation of two such "optimal" digital image restoration techniques (the count-dependent Metz filter and the Wiener filter) was made. They were applied both as two-dimensional "window" functions for preprocessing SPECT images, and for filtering reconstructed images. Their performance was compared by measuring image contrast and per cent fractional standard deviation (% FSD) in multiple acquisitions of the Jaszczak SPECT phantom at two different count levels. A statistically significant increase in image contrast and decrease in % FSD was observed with these techniques when compared to the results of reconstruction with a ramp filter. The adaptability of the techniques was manifested in a lesser % reduction in % FSD at the high count level coupled with a greater enhancement in image contrast. Using an array processor, processing time was 0.2 sec per image for the Metz filter and 3 sec for the Wiener filter. It is concluded that two-dimensional digital image restoration with these techniques can produce a significant increase in SPECT image quality.

CHARACTERIZATION OF COMPTON SCATTERING IN EMISSION TOMOGRAPHY. M.F. Bruno, R.H. Huesman, S.E. Derenzo and T.F. Budinger. Donner Laboratory, University of California, Berkeley, CA

Characterization of the scatter background in positron emission tomography and in single photon emission tomography is necessary for the development of scatter correction algorithms and for the optimization of tomograph design parameters. Computer programs using Monte Carlo methods have been used to obtain event distributions which conform to the scattering cross sections of Klein and Nishina. Scattering is simulated in an attenuating medium of arbitrary complexity and the number of scatters undergone by each photon is not artificially limited.

Early work has emphasized the simulation and detection of positron-anihilation photons. The results from these simulations agree very closely with results from scattering experiments using the Donner 280-Crystal Positron Tomograph. A large number of simulations have been performed to determine the scatter impulse response as a function of source position, attenuator size, photo-peak energy discrimination, and shielding geometry. Although the shape of the scatter background depends on the position of the source, these simulations show that it is only a very weak function of attenuator radius. They also show that the amplitude, but not the spatial extent of the scatter background can be effectively reduced with a reduction in shielding gap, and that a photo-peak energy discrimination of two percent or better is required to reduce the FWHM of the scatter point-spread function to less than 10 cm.

AN OBJECT INDEPENDENT ATTENUATION CORRECTION IN SPECT: ELIMINATING THE EFFECTS OF SCATTER AND COLLIMATOR PSF. A. Todd-Pokropek, R. Marsh, M.C. Gilardi, P. Gerundini, and F. Fazio. University College London U.K. and University of Milan,Italy.

An important aim in SPECT, for example in the measurement of cerebral function using labelled amines such as IMP and HIPDM is to quantitate regional uptake in terms of activity concentration. However a major requirement for such systems is to be able to perform an accurate attenuation correction independent of object activity distribution. This is clearly not the case with most commercially available software packages which only work with circularly symmetrical objects and an artificial attenuation coefficient. A technique has been developed for scatter correction by collecting tomograms for multiple energy windows and then performing a weighted subtraction,

$$P'(x,\text{theta}) = \sum_j P_j(x,\text{theta}) \otimes FILT_j(x)$$

where $P_j(x,\text{theta})$ is the projection for the jth energy window, and $FILT_j$ is an appropriate convolving filter, determined from physical measurements and by Monte Carlo simulation. This can eliminate up to 80% of scattered events. In addition the effect of the collimator PSF as a function of distance is deconvolved. An attenuation coefficient of ~0.144 may then be used. It is also essential that artefact free images are obtainable at other energies than for a symmetrical photopeak window. This technique has been tested on a specially designed head phantom, and also used on patient data. A significant increase in contrast, can be achieved, for small objects of the order of 50%. Variations in contrast as a function of position are considerably reduced.

IMPROVEMENT OF SPECT IMAGING FOR MYOCARDIAL PERFUSION STUDIES USING A MEDIAN FILTER PREPROCESSING TECHNIQUE. U. Raff, T.R. Nelson, E.R. Ritenour, Department of Radiology, University of Colorado Health Sciences Center, Denver, CO.

Single photon emission computed tomography (SPECT) with Tl-201 has been shown to provide a valuable contribution to the diagnostic process of myocardial injuries. However, the quality and quantitation of clinical tomographic data are severely limited by the statistics present in the raw data. For Tl-201 imaging low-pass filtering before backprojection results in a substantial loss of resolution in the tomographic planes. This study evaluates the effect of preprocessing low count density Tl-201 raw data (max counts per pixel 40-50) with median filters prior to the application of a standard filtered backprojection (FBP) algorithm. To simulate clinical Tl-201 data, the IOWA heart phantom has been loaded with an apparent 2:1 ratio in activity with a 45° infarct area (same activity level as background). The statistics used matched those of a clinical setting. Before reconstruction raw data were filtered with 1) 3 x 3 box, 2) 3 x 3 "+", 3) 5 x 5 box and 4) 5 x 5 "+" median filters and the tomographic planes were compared to the results obtained by using non preprocessed raw images. Reconstruction using FBP was performed using 1) Ramp, 2) Hanning, and 3) Butterworth filters with a cut-off frequency equal to the Nyquist frequency. Our results show that preprocessing of Tl-201 raw data prior to reconstruction: 1) improves the reconstruction quality, 2) reduces considerably the background noise level and 3) does not degrade image resolution with respect to conventional methods. Optimal median filters were found to be a 3 x 3 "+" for small objects and a 5 x 5 "+" for larger objects while applying a Butterworth weighted ramp filter during reconstruction.

IDEAL FLOOD FIELD IMAGES FOR SPECT UNIFORMITY CORRECTION. B.E. Oppenheim and C.R. Appledorn, Indiana University School of Medicine, Indianapolis, IN

Since as little as 2.5% camera non-uniformity can cause disturbing artifacts in SPECT imaging, the ideal flood field images for uniformity correction would be made with the collimator in place using a perfectly uniform sheet source. While such a source is not realizable the equivalent images can be generated by mapping the activity distribution of a Co-57 sheet source and correcting subsequent images of the source with this mapping.

Mapping is accomplished by analyzing equal-time images of the source made in multiple precisely determined positions. The ratio of counts detected in the same region of two images is a measure of the ratio of the activities of the two portions of the source imaged in that region. The activity distribution in the sheet source is determined from a set of such ratios. The more source positions imaged in a given time, the more accurate the source mapping, according to results of a computer simulation.

A 1.9 mCi Co-57 sheet source was shifted by 12 mm increments along the horizontal and vertical axes of the camera face to 9 positions on each axis. The source was imaged for 20 min in each position and 214 million total counts were accumulated. The activity distribution of the source, relative to the center pixel, was determined for a 31 x 31 array. The integral uniformity was found to be 2.8%. The

RMS error for such a mapping was determined by computer simulation to be 0.46%.

The activity distribution was used to correct a high count flood field image for non-uniformities attributable to the Co-57 source. Such a corrected image represents camera plus collimator response to an almost perfectly uniform sheet source.

A PROMISING HYBRID APPROACH TO SPECT ATTENUATION CORRECTION. M.H. Lewis, T.L. Faber, J.R. Corbett, E.M. Stokely. U. Texas Health Sci Ctr, Dallas, TX.

Most methods for attenuation compensation in SPECT either rely on the assumption of uniform attenuation, or use slow iteration to achieve accuracy. However, hybrid methods that combine iteration with simple multiplicative correction can accomodate nonuniform attenuation, and such methods converge faster than other iterative techniques. We evaluated two such methods, which differ in use of a damping factor to control convergence. Both uniform and nonuniform attenuation were modeled, using simulated and phantom data for a rotating gamma camera. For simulations done with 360° data and the correct attenuation map, activity levels were reconstructed to within 5% of the correct values after one iteration. Using 180° data, reconstructed levels in regions representing lesion and background were within 5% of the correct values in three iterations; however, further iterations were needed to eliminate the characteristic streak artifacts. The damping factor had little effect on 360° reconstruction, but was needed for convergence with 180° data. For both cold- and hot-lesion models, image contrast was better from the hybrid methods than from the simpler geometric-mean corrector. Results from the hybrid methods were comparable to those obtained using the conjugate-gradient iterative method, but required 50-100% less reconstruction time. The relative speed of the hybrid methods, and their accuracy in reconstructing photon activity in the presence of nonuniform attenuation, make them promising tools for quantitative SPECT reconstruction.

1:30-3:00 **Room 214BC**

RADIOPHARMACEUTICAL CHEMISTRY I: Tc-99m

Moderator: Michael D. Loberg, Ph.D.
Comoderator: Maria P. Litelpo, Ph.D.

MYOCARDIAL KINETICS OF HEXAKIS(TRIMETHYLPHOSPHITE) TECHNETIUM-99m (I) CHLORIDE (Tc-TMP) IN RATS, RABBITS, DOGS, CATS AND PIGS. M.S. Robbins and M.D. Adams, Mallinckrodt, Inc., St. Louis, MO

Tc-TMP is readily taken up by the myocardium following intravenous administration to rats and dogs. In order to assess its potential as a myocardial perfusion imaging agent, the biodistribution and pharmacokinetics of Tc-TMP were evaluated following intravenous administration to rats, rabbits, dogs, cats and miniature pigs. Rats and rabbits were killed at several time points within a 24 hr period after treatment and tissue samples were assayed for radioactivity. In rats, estimated heart, liver and lung half-lives were 14.4 hr, 24 min and 40 min, respectively. In rabbits, 0.6% dose/g was observed in the heart at 30 min. Corresponding heart/blood, heart/liver and heart/lung ratios were 39.1, 10.7 and 5.1. Gamma camera imaging experiments were conducted in rabbits, dogs, cats and pigs over a 1-2 hr period following administration of Tc-TMP. All species exhibited myocardial uptake resulting in sustained visualization, although myocardial image intensity was less pronounced in the pig compared to the other species. Regions of interest were selected over the heart, liver and background, and time-activity curves were generated. Minimal myocardial clearance was observed in all species during the imaging time course. Hepatic activity was rapidly cleared in rabbits and pigs ($t_{\frac{1}{2}}$ < 1.0 hr) resulting in improved heart/liver ratios at later time intervals. The myocardial accumulation and retention of Tc-TMP, demonstrated in five species, supports clinical evaluation as a myocardial imaging agent.

SYNTHESIS, CHARACTERIZATION AND IDENTIFICATION OF THE HEXAKIS(TRIMETHYLPHOSPHITE)[Tc-99m]TECHNETIUM(I) CATION AS A MYOCARDIAL IMAGING AGENT. R.T. Dean, M.D. Adams, F.W. Miller, M.S. Robbins, D.W. Wester and D.H. White. Mallinckrodt, Inc., St. Louis, MO.

Hexakis(trimethylphosphite)[Tc-99m]technetium(I), a monocationic complex, was synthesized for evaluation as a myocardial imaging agent. The above product was synthesized by reacting a methanolic solution of $NaTcO_4$ with trimethyl phosphite in an inert atmosphere at 100° for 30 min. Using the Tc-99 isotope, mg quantities were isolated for full characterization by precipitation from the reaction mixture using sodium tetraphenylborate. Recrystallization from methanol gave crystals of the tetraphenylborate salt. Elemental analyses, Tc-99 and P-31 NMR, mass spectra, X-ray photoelectron spectra, ir and X-ray crystal structure were all consistent with a hexacoordinate octahedral structure of the proposed monocation. The products formed from the Tc-99 isotope and the Tc-99m isotope were shown to be identical by HPLC using simultaneous radiometric and UV detection. The myocardial imaging properties of the title compound were evaluated by rat biodistribution and dog imaging. Five minutes after intravenous administration in rats, 3% dose/gm was in the heart with tissue ratios of heart/blood of 30, heart/liver of 4, heart/lung of 2. These compare to Tl-201 values of 6% dose/gm in the heart with tissue ratios of heart/blood of 24, heart/liver of 6, heart/lung of 1. Imaging in an anesthetized dog revealed excellent myocardial uptake with persistent images through a 60 minute period. From these data the hexakis(trimethylphosphite)[Tc-99m]technetium(I) cation was identified as a myocardial imaging agent suitable for further evaluation.

PHARMACOLOGICAL CHARACTERIZATION OF Tc-99m(CN-t-butyl)$_6^+$: A POTENTIAL HEART AGENT. D.B. Pendleton, M.L. Delano, H. Sands, B.M. Gallagher, M.P. Liteplo, L.L. Camin and V. Subramanyam. New England Nuclear Corp., Billerica, MA

We have investigated the pharmacological behavior of hexakis(t-butylisonitrile)Tc(I) (Jones, et al., J. Nucl. Med. 23: 16, 1982) and evaluated it as a potential myocardial perfusion radiopharmaceutical. This complex produces good to excellent heart images in rats, guinea pigs, rabbits, cats, dogs, pigs and baboons. Good heart uptake in guinea pigs, cats and pigs may be predictive of good myocardial imaging in man, since the hearts of these three species extract Tl-201, but not Tc-99m(dmpe)$_2$-Cl$_2^+$ (similar to man, but unlike other animal species). Biodistribution studies reveal initial heart uptake of 1.3 to 2.2% of the injected activity. Imaging and biodistribution show significant initial lung activity which clears substantially during the first hour after injection. Little or no myocardial washout is observed.

In rabbits with ischemia induced by coronary artery ligation, the complex distributes as a function of blood flow. Simultaneous injection of Tl-201 and Tc-99m(CN-t-butyl)$_6^+$ with subsequent dual isotope imaging shows that their initial distribution is similar.

The complex is extracted 100% by isolated rabbit and guinea pig hearts perfused with buffer. When human blood is mixed and co-injected with the complex, myocardial extraction is reduced, but remains high (73-75%). Uptake of the complex by rat myocytes in culture is not inhibited by either ouabain or K^+.

These results suggest that this complex may be a promising myocardial perfusion agent and should be tested in man.

EFFECTS OF LIGAND STRUCTURE ON THE LIPOPHILICITY AND BIODISTRIBUTION OF Tc-99m-AMINE OXIME CHELATES. W.A. Volkert, E. McKenzie*, T.J. Hoffman*, D.E. Troutner†, and R.A. Holmes. Departments of Radiology and Chemistry†, University of Missouri and Nuclear Medicine and Research Services*, Veterans Administration Hospital, Columbia, MO.

Propylene amine oxime (PnAO) or 3,3'-(1-3-propanediyl-diimino) bis(3-methyl-2-butanone) dioxime, forms a neutral-lipid soluble Tc-99m-chelate in aqueous solutions. When injected it efficiently crosses the intact normal blood-brain-barrier (BBB) with approximately 80% extracted on first transit in baboon brain at normal cerebral blood flow (50 ml/min/100g). In this study we evaluated the effects of altered ligand structure (backbone) on the physical properties and biodistribution of several different Tc-99m amine oxime chelates in rodents. Three analogues of PnAO were evaluated: ethyleneamine oxime (EnAO), butylene-amine (BnAO), and amine oxime (AO). Each formed a neutral Tc-99m complex, determined by electrophoresis. Their octanal/saline partition coefficients were distinctly different with Tc-99m-BnAO (0.49±0.09) and Tc-99m-AO (0.07±0.02) being significantly less than Tc-99m-PnAO (44.3±4.9). It was not possible to prepare Tc-99m-EnAO in aqueous solution as a single chemical species but when the complex was injected into rats it localized in normal brain almost identical to Tc-99m-PnAO. Both Tc-99m-AO and Tc-99m-BnAO failed to exhibit any detectable brain uptake and were both rapidly excreted through the kidneys and liver. These results show that slight structural modifications of the ligand backbone can significantly alter chelate lipid solubility and brain extraction. This infers that Tc-99m-AO and -BnAO have complex structures that are distinctly different from Tc-99m-PnAO and -EnAO.

NEW Tc-99m BRAIN IMAGING AGENTS. HF Kung, CC Yu, J Billings M Molnar, R Wicks and M Blau*. SUNY/Buffalo and VA Medical Center, Buffalo, NY, *Harvard Medical School, Boston, MA

In developing new Tc-99m brain perfusion imaging agents for SPECT, a series of BAT (bis-aminoethanethiol) derivatives was prepared. These N_2S_2 ligands formed stable and neutral complexes with reduced Tc-99m, either by Sn(II)-PPi or sodium borohydride reduction. The purity of the Tc-99m complexes was >95% (HPLC reverse-phase column, acetonitrile: pH 7.0 buffer, 85:15). The biodistribution in rats was evaluated using I-125 iodoantipyrine (IAP), a free diffusible tracer, as the internal reference. Compounds with a free hydroxyl group (I and IV) showed lower brain uptake, inspite of high P.C.; this may be related to in vivo instability of the complexes. High initial brain uptake was observed for three compounds (II, III and V), however, only compound V (P.C.=384) showed significant brain retention. Planar imaging with compound V in a monkey demonstrated that the compound localized in brain and the retention time was $T_{1/2}$=35 min. Compounds of this type may be useful as brain imaging agent in themself or as a basis for further structural modification to improve brain uptake and retention.

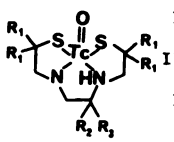

	R_1	R_2	R_3	P.C.+	2 Min*	15 Min*
I	CH_3	H	CH_2OH	64	0.4(0.3)	0.2(0.5)
II	CH_3	H	CH_2NH_2	47	1.3(1.0)	0.3(0.5)
III	CH_3	H		260	2.3(1.7)	0.3(0.7)
IV	CH_3	H		197	0.4(0.3)	0.2(0.4)
V	C_2H_5			384	2.2(1.1)	0.7(1.2)

*Total % brain uptake(ratio of Tc-99mBAT/I-125IAP in brain)
+Partition coefficient (1-octanol: pH 7.0 buffer)

SYNTHESIS AND EVALUATION OF N_2S_2 COMPLEXES OF Tc-99m AS RENAL FUNCTION AGENTS. A.R. Fritzberg, S. Kasina, D. Eshima and D.L Johnson, University of Utah, Salt Lake City UT; A.G. Jones and J. Lister-James, Harvard Medical School, Boston MA; and A.Davison and J.W.Brodack, MIT, Boston MA

Complexes of Technetium-99m based on derivatives of the diamide disulfur ligand, N,N'-bis(mercaptoacetyl)ethylenediamine (DADS) have shown promise in clinical studies as a Tc-99m replacement for I-131 hippuran for renal function studies (JNM 23:377,1982; 24: P80, 1983). However, problems of specificity, rate of renal excretion, and differences in behavior based on stereochemistry have caused them to be biologically inferior to hippuran. New ligands have been synthesized with the objectives of overcoming these disadvantages. In many cases stereoisomers resulted which were separated by HPLC and individually studied in animals. The parent Tc-99m DADS and amide carbonyl positional isomers including oxalyl and asymmetric showed that excretion rates and specificity were sensitive to these changes. Insertion of a hydroxymethylene group in the center ring gave chelate ring stereoisomers, but both were rapidly excreted with high specificity. Methyl group addition to the center ring gave isomers that showed increased renal retention; 29% and 12% were found in the kidneys of mice at 10 min for the two products. Carboxylate group addition gave isomeric products with differences between isomers greater for center ring compared to side ring substitution. Extension of the carboxylate group to acetate as well as amide and glycine conjugation reduced isomer differences, but increased hepatobiliary excretion. Based on studies in mice and other species, several ligands appear promising and testing in humans is underway.

1:30-3:00 **Room 212A**

ONCOLOGY I: CLINICAL RADIOIMMUNOIMAGING

Moderator: E. Edmund Kim, M.D.
Comoderator: Samuel E. Halpern, M.D.

QUANTITATION OF IMAGING WITH I-131-F(ab')$_2$ FRAGMENTS OF MONOCLONAL ANTIBODY IN PATIENTS. P.J. Moldofsky, N.D. Hammond, C.B. Mulhern, Jr. Fox Chase Cancer Center and Jeanes Hospital, Philadelphia, PA.

Iodine-131 labeled F(ab')$_2$ fragments of monoclonal antibody (IgG_{2a} immunoglobulin with specificity for a cell surface antigen of colon carcinoma) have been used for quantitative imaging of tumor in 27 patients. Activity of I-131 F(ab')$_2$ fragments localized in tumor and in liver was quantitated using a modification of the method of Thomas SR (Radiology 1977;122:731-737), employing computer-acquired conjugate views (i.e. 180 opposed) to eliminate need for tumor or organ depth and tissue attenuation. The method was validated with an abdominal imaging phantom showing accuracy of +/- 10%. Quantitation indicates that activity reaches a peak in tumor at 48-72 hours and the ratio of activity in hepatic metastases to activity in liver peaks at approximately 72 hours. Mean activity in tumor was less than 0.01% of the administered dose per gram of tumor at any imaging time from 24 to 168 hours, while mean activity in surrounding liver was less than .002% of administered dose per gram of liver at any imaging time. Liver activity decreased monotonically with time, showing no peak activity. This non-invasive method of quantitating the distribution of F(ab')$_2$ fragments of monoclonal antibody in patients has proven accurate by comparison with phantom simulation. This type of quantitation is necessary for evaluating optimal imaging times, comparing relative utility of various antibodies and has use for therapeutic applications of monoclonal antibody fragments.

IN-111 CHELATE CONJUGATES OF HUMAN TRANSFERRIN (HTr) AND MOUSE MONOCLONAL ANTI HUMAN TRANSFERRIN RECEPTOR ANTIBODY (αHTrR MoAb)* FOR TUMOR IMAGING. D.A. Goodwin[1], C.F. Meares[2], C.I. Diamanti[1], M. McCall[2], M. McTigue[1], F. Torti[3], and B. Martin[3]. VA Med. Ctr. Palo Alto[1]; Divisions of Nuc. Med.[1] and Oncology[3], Stanford Univ. School of Med.; and Dept. of Chem.[2], U.C. Davis, Davis, CA.

At least one of the major pathways of uptake of the commonly used tumor scanning agent Ga-67 is via the transferrin receptor. This suggested the use of stably radio-labeled HTr, and αHTrR MoAb for tumor imaging in humans. HTr and mouse αHTrR MoAb* were alkylated with 1-(parabromacetamidobenzyl)-EDTA. The mM Alkylproteins, ≤1 chelate/molecule were labeled with 1-3 mCi In-111 citrate pH$_5$ (Sp Act ≈ 100-300 Ci/m mole). Images were made 24 hours after 1 mCi IV and in some patients blood levels, urine excretion and digitized whole body scans were obtained at 1, 24, 48 and 96 hours post injection. Ten patients with biopsy proven prostate cancer were studied with In-111 HTr, and four with In-111 αHTrR MoAb; all had positive mets on bone scan. In-111 HTr persisted in the circulation with a

T1/2 of ≈ four days, ≈ 5%/day being excreted in the urine, to a total of ≈ 60% in 21 days. Nine of ten scans were false negative due to the high blood background. In-111 αHTrR disappeared rapidly from the blood; with most in the bone marrow at 24 hours. ROI analysis of three patients showed whole body 94% at 24 hours, 89% at 48 hours, and 82% at 96 hours (T1/2 = 10.7 days); liver 19% at 1 hour, 25% at 24 hours, and 21% at 96 hours; spleen 3% at 1 hour, 8% at 24 hours, 7.3% at 48 hours, and 3% at 96 hours. The high bone marrow background allowed only a few of the bone mets seen on bone scan to be visualized. Other tumor types not located in bone may be more easily seen.

* Hybritech Inc., San Diego, CA, 92121

FACTORS INFLUENCING THE UPTAKE OF A NEW MONOCLONAL ANTIBODY (LICR-LON-M8) IN SKELETAL METASTASES FROM BREAST CARCINOMA. **N. Slack, R.M. Rainsbury, J.H. Westwood, R.C. Coombes, A.M. Neville, R.J. Ott, T.S. Kalirai, V.R. McCready, J.-C. Gazet. Ludwig Institute for Cancer Research (London Branch) and the Royal Marsden Hospital, Sutton, Surrey, U.K.**

Preliminary studies with an In 111 labelled monoclonal antibody to Human Milk Fat Globule Membrane (LICR-LON-M8) showed successful localisation of breast carcinoma bone metastases without the necessity of blood background subtraction (1). A further 18 patients with breast carcinoma have been investigated to elucidate in more detail the factors influencing the uptake of antibody. All patients had serial bone scintigrams and X-rays in addition to the antibody scintigrams at 18-48 hours after injection. The M8 was labelled with In 111 DTPA.

Thirteen sites were positive on the antibody scintigrams alone. In X-ray positive lesions (25) antibody scintigrams were more often positive in lytic (15) than sclerotic (5) or mixed (5) lesions. In nine cases the focal disease was smaller than 2 cm but five larger focal lesions were negative. Correlative studies showed that positive antibody scintigrams were found in new lesions or progressive disease preceding X-ray or positive bone scintigrams. In a few patients, negative antibody scintigrams were found with positive X-ray or bone scintigrams following successful therapy. The study was particularly valuable in two patients differentiating malignant disease from other causes of positive bone scintigrams or X-rays.

(1) Location of metastatic breast carcinoma by a monoclonal antibody chelate labelled with Indium-111. R.M. Rainsbury, J.H. Westwood, R.C. Coombes, A.M. Neville, R.J. Ott, T.S. Kalirai, V.R. McCready, J.-C. Gazet. The Lancet, 934-938, 1983.

BIOKINETICS OF A RADIOIODINATED ANTIBREAST CARCINOMA MONOCLONAL ANTIBODY AND FRAGMENT IN HUMANS. M.R. Zalutsky, M. Noska, W.D. Kaplan, D. Hayes, D. Colcher, J. Schlom, and D. Kufe. Harvard Medical School, Boston, MA and The National Cancer Institute, Bethesda, MD.

Monoclonal antibody B6.2 is promising for the detection of breast cancers; it binds to >80% of human breast carcinoma (hbc) lines, its antigen is not seen in serum, and it localizes selectively in hbc xenografts in nude mice. We have studied the biokinetics of I-131 activity following injection of I-131-IgG and $F(ab')_2$ each in 4 patients (pts). The antibody was labeled using iodogen and tested for specific binding to hbc membrane extracts prior to injection. Pts received 0.6-1.1 mCi of I-131 and 50-100 µg of protein. Blood clearance of I-131 activity was biphasic with half times of 2 and 15.4 hrs for IgG; 1 and 30 hrs for $F(ab')_2$. Dehalogenation was noted: by 72 hrs post-injection, 22% (IgG) and 21% [$F(ab')_2$] of the injected dose of I-131 was found in the urine. In 2 pts receiving I-131 IgG, stomach uptake was 7-10% at 24 hrs. Protein associated activity in the blood was >90% for the first 8 hrs and gradually decreased to 79% (IgG) and 58% [$F(ab')_2$] at 48 hrs. High liver uptake, reported with other antibody systems, was not observed; <20% of the activity was seen in the liver at all time points for both proteins. In 1/4 pts receiving IgG and 4/4 receiving $F(ab')_2$, bone marrow uptake was clearly noted. In these pts, >20% of the activity present in blood was cell associated. This is not inconsistent with the observation that B6.2 binds to granulocytes in vitro. Increased binding to cells in the blood for $F(ab')_2$ probably accounts for the anomolously longer blood clearance half times observed for $F(ab')_2$ vs IgG and low liver accumulation most likely reflects the absence of hepatic or circulating B6.2 antigen.

SPECT WITH I-123 LABELED $F(AB')_2$ FRAGMENTS FROM MONOCLONAL ANTI-CEA ANTIBODIES IN COLON CARCINOMA. B.Delaloye, A. Bischof-Delaloye, J.Ph.Grob, F.Buchegger, S.Halpern, V.von Fliedner, J.P.Mach. Ludwig Inst. for Cancer Research, Div. of Nucl. Medicine and Inst. of Biochemistry, Lausanne, CH.

11 patients with colorectal carcinoma were studied, 4 with primary, 7 with recurrent (1) or metastatic lesions. After injection of 1,5mg of $F(ab')_2$ of monoclonal anti-CEA antibodies No 35 (n=9) or 202 (n=2) labeled with I-123 (p,5n) (3-4mCi) whole body distribution was measured on anterior and posterior views at 1,6,24,48 h. SPECT was performed with a dual head device at 6,24,48 h. $F(ab')_2$ No 202 showed relatively high bone marrow uptake and high urinary activity (74% of injected activity in 3 days), but low liver activity (≈ 14% of whole body activity at 24 h). With $F(ab')_2$ No 35 bone marrow activity was lower, mean relative liver uptake 17% and mean urinary activity 24%. In 2 surgical specimens tumor to normal tissue ratios were measured at day 5 post injection and found to be 6,8,15,9 for one, 3,5,7,2 for the other in comparison with mucosa, serosa, fat and blood respectively. All 5 localized carcinoma were detected by ECT, the best images being obtained at 24 h. On the 6 h scans 4 patients with liver metastases showed cold lesions which became positive on the 24 h ECT in 2 of them whereas the 2 others remained doubtful. 2 patients with liver involvement showed no uptake. In 1 patient under therapy 2 small lung metastases were not detected. 2/2 bone metastases showed tracer uptake 1 of them was previously unknown. High quality images can be obtained with this method already at 24 h but the detection of metastases especially in the liver is sometimes difficult.

IN VIVO DETECTION OF PROSTATIC CARCINOMA WITH ANTIBODIES AGAINST PROSTATIC ACID PHOSPHATASE. F.H. DeLand and D.M. Goldenberg, Univ Kentucky and V.A. Medical Centers, Lexington, KY and Center for Molecular Medicine and Immunology, Newark, NJ.

Serum prostatic acid phosphatase (PAP) immunoassay is used to evaluate patients with prostatic carcinoma; however, as with other tumor markers, the enzyme levels do not necessarily reflect the presence or extent of tumor. We investigated the use of radiolabeled PAP antibodies for the in vivo detection of prostatic carcinoma by external scintillation imaging. Nine patients with prostatic carcinoma were entered into the study. Each received from 2.0 to 2.5 mCi of I-131 labeled antibody to PAP, administered i.v. The immunogen (PAP) was purified from normal human seminal fluid. Antiserum was prepared in rabbits by injecting the purified PAP. The antibodies were labeled with I-131 by chloramine-T method (10 to 20 Ci/g of IgG). Total body images were obtained at 24 and 48 hrs following administration of the labeled antibody. Nontarget I-131 activity was diminished by computer processing. Tumor sites detected by I-131 antibodies were correlated with other diagnostic procedures. In 7 of 9 patients primary and metastatic sites of cancer were detected by antibody imaging, however, no bone lesions were detected (6 cases). In 3 patients with concomitant pulmonary tumors, one was identified as of prostate origin. The serum PAP was normal in 4 patients; however, the primary tumor was identified in 3 of these. These findings suggest that the localization of prostatic carcinoma by means of in-vivo imaging of labeled antibodies to PAP is feasible and offers diagnostic opportunities based upon the functional characteristics.

1:30–3:00 **Room 217B**

PULMONARY I

Moderator: Harold L. Atkins, M.D.
Comoderator: Rashid A. Fawwaz, M.D.

AEROSOL DELIVERED RADIOLABELED ANTIBODIES TO ECTOPIC LUNG CARCINOMA ANTIGENS IN SCINTIGRAPHIC TUMOUR DETECTION. M.P. Best, Dunedin Hospital, Dunedin, New Zealand.

Biologically specific antibodies offer increased specificity of inhalation scintigraphy in pulmonary malignancy at present limited to detection of airways obstruction. Polypeptide ectopic antigens produced by epithelial lung tumours provide a targeting focus for radiolabeled antibodies. Image resolution using the intravenous route is poor due to the small proportion of the dose targeting to the tumour site and ineffective clearance of the background. The inhalation route minimizes non-specific distribution and utilizes mucociliary clearance as a contrast enhancement mechanism. Mucociliary deposition is cleared more effectively than alveolar deposition. Submicronic aerosol droplets produced by airjet nebulisers ensure peripheral airways penetration and deposition. Affinity purified polyclonal goat antibodies against calcitonin labeled with 150MBq of Tc-99m are delivered to the lungs to produce dynamic images over 24 hours. Pure synthetic human calcitonin ensures production of monospecific antibodies that can be affinity purified. Labeling with Tc-99m by stannous chloride reduction is effected on the solid phase Sepharose beads. An antibody-antigen concentration gradient over a small distance can be provided with radiolabeled antibodies from aerosol deposition. Histologically neoplastic cells are typically separated from the mucous layer by bronchial mucosa and a thin uninvolved lamina. A localised high concentration of labile antigen is present in extracellular spaces at the tumour site. A study is progressing to determine if specific antibody-antigen agglutination contributes towards localised impairment of mucociliary clearance at tumour sites creating contrast.

RESTORATION OF PERFUSION AFTER STREPTOKINASE OR HEPARIN THERAPY IN PATIENTS WITH PULMONARY EMBOLI. D.C.P. Chen, P.L. Chandeysson, E.P. Miranda, H. Chen, H.M. Goodgold, N.G. Nolan, H.N. Wagner Jr. Washington Hospital Center, Washington, DC and Johns Hopkins Hospital, Baltimore, M.D.

Stretokinase (SK) has been used as a potent thrombolytic drug for treating pulmonary emboli. The restoration of pulmonary perfusion after SK therapy was evaluated by comparing to heparin treatment with serial lung perfusion scans for periods of 2 days to 9 months. Total of 206 lung scans were performed in 17 pts (10 M, 7 F, mean age 64.5) treated with SK and 86 pts (50 M, 36 F, mean age 62.6) treated with HP. All lung scans were obtained in 6 projections after IV injection of 3 mCi Tc-99m MAA. Perfusion defects were expressed by the unit of segment (SG).

The initial perfusion defects were much larger in pts treated with SK than those with HP treatment (7.9 ± 3.1 vs. 5.3 ± 2.5 SG, $P < .001$). There were significant restoration of perfusion after the therapy in both SK and HP groups (7.9 ± 3.1 to 3.3 ± 3.7 SG, $P < .001$); 5.3 ± 2.5 to 3.2 ± 2.5 SG, $P < .01$). In comparison with the degree of perfusion recovery in the HP group (51.5 ± 33.7% of initial perfusion defect), marked improvement was noted in the SK group (73.6 ± 30.7%, $P < .05$). Of 12 pts with massive emboli (> 6 segments), 64% of the defects were restored after SK therapy which was significantly better than those receiving HP treatment (44%, $P < .05$). However, 4/11 (36%) pts older than age 60 had poor degree of perfusion recovery even with SK therapy.

We concluded that pts who received SK therapy had significant scan improvement of perfusion recovery compared to the HP treatment. SK should be considered when treating pts with massive emboli.

COMPARISON OF Tc-99m DTPA AEROSOL WITH RADIOACTIVE GAS VENTILATION IMAGING IN PATIENTS (PTS) WITH SUSPECTED PULMONARY EMBOLISM (PE). P.O. Alderson, S.A. Kroop, D.R. Biello, B.A. Siegel, A. Gottschalk, P.B. Hoffer, L. Ramanna, A.D. Waxman. Multi-Institutional Aerosol Study Group, New York, NY, St. Louis, MO, New Haven, CT, Los Angeles, CA.

The utility of Tc-99m labeled DTPA aerosol (A) as a ventilation agent was compared to that of Xe-133 (Xe) or Kr-81m (Kr) gases in a series of 100 pts (age range 20-83, 53% women) undergoing ventilation-perfusion (V-P) imaging for suspected PE. The majority of pts had A and Xe studies in conjunction with P scans; 26 had A and Kr studies. All A studies were comprised of multiple 100K ct views performed prior to P scanning. Conventional Xe or Kr studies were then performed in conjunction with a multiview P scan. The studies were later reviewed by four independent readers who evaluated 100 V-P studies (100 A-P pairs, 100 gas-P pairs) and the accompanying chest radiographs and determined the probability of PE as none, low, high, or nondiagnostic (NDX). The A scans showed central hot spots in 27% of pts, but poor peripheral penetration in only 5%. Prominent lower lobe deposition was seen in 19 of the 66 pts who inhaled A upright, but in none who inhaled in the supine position. The A-P and gas-P scans were either both diagnostic or both NDX 82% of the time. There was 77% agreement between probability categories for A-P and Kr-P studies, and 74% agreement with Xe-P. These results were better than the interobserver agreement for gas-P studies alone. Angiography revealed that 3 A-P studies were true negatives, 3 were true positives (pos), and one was a false pos (also pos by gas-P). The results suggest that commercially available DTPA aerosols provide comparable results to gas-P studies in pts with suspected PE.

A PHARMACOKINETIC APPROACH TO THE EVALUATION OF AEROSOL SOLUTES FOR LUNG PERMEABILITY STUDIES. D.L. Waldman and D.A. Weber. University of Rochester School of Medicine and Dentistry, Rochester, NY.

The distribution and clearance of inhaled radioactive aerosols prepared from five Tc-99m labelled derivatives of HIDA, Tc-99m DTPA and Tc-99m O4- were evaluated in Beagle dogs. The investigation was designed to develop new aerosol solutes and to obtain information on molecular transport across the alveolar capillary membrane by evaluating molecular structure versus biological activity relationships. Aerosols with an aerodynamic mean diameter of .48 microns (σg=1.50), produced in a jet nebulizer, were administered to anesthetized dogs through an endotrachial tube. Aerosols were evaluated twice in each of five dogs for three HIDA derivatives, pertechnetate, and DTPA. Two other HIDA derivatives were evaluated twice in one animal. Sixty min. quantatative gamma camera studies were obtained.

ROI processing and functional mapping of images showed distribution and clearance of identically sized aerosols to have a strong dependance on chemical properties. Dimethyl HIDA, trimethylbromo HIDA, and DISIDA with capacity factors (k') of -0.24, 0.63, and 0.65 respectively gave mean lung clearance $t_{½}$ times of 76.6, 206.7, and 97.3 min. 4-bromo HIDA and 3,5-dichloro HIDA were administered to one animal; $t_{½}$ times were 80.0 and 330 min. Two hydrophilic compounds, Tc-99m DTPA and Tc-99m O4-, were examined; $t_{½}$ times were 49.6 min. and 21.2 min. respectively. A trend is seen where $t_{½}$ values increase with lipophilicity; this suggests that structure activity relationships could be built on lipophilicity. These studies support the contention that molecular transport in the lung is an intercellular mechanism.

CLEARANCE OF AEROSOLIZED Tc-99m DTPA FROM NORMAL VS. ACUTELY SMOKE-INJURED DOG LUNGS. Z.D. Grossman, W.R. Clark, Jr., C. Ritter-Hrncirik, F.J. Warner, F.D. Thomas, J.G. McAfee and L. Witanowski. Upstate Medical Center, SUNY, Syracuse, NY.

Acute cigarette smoke exposure is known to reversibly increase the clearance rate of aerosolized DTPA from human lungs. We studied DTPA clearance after acute severe plywood smoke exposure, on the order of that experienced by burn victims, since current diagnostic methods (Xe-133 and radiographs) for major inhalation injury are insensitive and/or non-specific.

Smoke generated from burning plywood sawdust and kerosene was delivered via endotracheal tube at 37° C. Skin burns were not inflicted (so the pulmonary consequences of thermal injury were not factors). Chest radiographs and Xe-133 studies were obtained before and after smoke injury but before DTPA aerosol delivery.

Six normal and 7 smoke-exposed anesthetized mongrel dogs were studied with 3 mCi of Tc-99m DTPA delivered by aerosol for 5 minutes (Cadema Aerosol Inc.). Pulmonary Tc-99m DTPA activity was quantitated by computer. Data were acquired over the lungs at 1 frame per 10 secs. for 16 minutes, and the $t_{1/2}$ of DTPA washout from the lungs was calculated. The mean $t_{1/2}$ of 6 normal dogs was 36.52

min. (S.D. 17.73), while the $t_{1/2}$ of 7 smoke-injured dogs was 6.08 min. (S.D. 1.99). The longest $t_{1/2}$ of an injured lung (9.68 min.) was slightly more than half of the shortest $t_{1/2}$ of a normal lung (15.36 min). Thus, acutely smoke-injured dog lungs clear Tc-99m DTPA much faster than normal lungs, consistent with an increase in lung epithelial permeability. This technique may be promising clinically, since early diagnosis of inhalation injury is important for optimal therapy.

ABILITY OF CHEST RADIOGRAPHY TO PREDICT WIDESPREAD SCINTIGRAPHIC VENTILATION ABNORMALITIES IN PATIENTS WITH SUSPECTED PULMONARY EMBOLISM (PE). R. Smith, K. Ellis, P.O. Alderson, Columbia University, New York, NY.

The false negative rate of ventilation-perfusion (V-P) scintigraphy for PE increases in the presence of widespread obstructive pulmonary disease (OPD) because diffuse V abnormalities conceal potential V-P mismatches. To determine whether this situation could be predicted accurately by a pre-scintigraphy chest x-ray (CXR), a double-blind evaluation of 55 CXRs and V-P scans in 53 patients (pts) was performed. Multiview Kr-81m (Kr) scans were done in 38 cases and pre-perfusion Xe-133 (Xe) studies including washout in 17. All CXRs were obtained within 24 hrs of the scans and none showed infiltrates that would otherwise render the V-P scan nondiagnostic (NDX). All V-P scans showing V abnormalities in ≥67% of the lung fields were considered NDX, and those showing V abnormalities in 50-67% of the lungs were considered "borderline" for interpretation. CXRs were classified as showing diffuse OPD, focal OPD, or as no evidence for OPD. All V and all P scans were abnormal; 7 cases were read as high probability for PE, 29 as low probability and the remainder as NDX. Eleven of 13 (85%) pts with diffuse OPD by CXR had NDX scans (8/9 Kr, 3/4 Xe) and two were considered borderline. However, none of 10 pts with focal OPD by CXR had NDX scans and only 2 were considered borderline. The CXR showed no OPD in 32 cases, but 8 (25%) had enough V abnormalities to be classified NDX (2 of 21 Kr scans, 6 of 11 Xe scans) and 2 others (both Kr scans) were considered borderline. The findings confirm that V scintigraphy with either Kr or Xe is more sensitive than the CXR in detecting airways disease, but indicate that V-P scintigraphy is likely to be NDX for PE in pts whose CXRs demonstrate diffuse OPD.

1:30-3:00 **Room 212B**

ENDOCRINE I

Moderator: Harry R. Maxon III, M.D.
Comoderator: I. Ross McDougall, M.D.

EXPERIENCE WITH TECHNETIUM-THALLIUM SUBTRACTION IMAGING OF PARATHYROID LESIONS. W.R. Ferguson, J.D. Laird, C.F.J. Russell, Royal Victoria Hospital, BELFAST, N.Ireland, U.K.

During the period April, 1982-December,1983, a group of patients with biochemical evidence of hyperparathyroidism was studied, using a modification of the technique described by Ferlin et al.

A gamma camera, with dual isotope acquisition and an on-line computer, was fitted with a low energy, parallel hole collimator. Two analyzer windows were used, one for Tc-99m (140 KeV 20%), the other for Tl-201 (80 KeV 30%). Thirty minutes after IV administration of 1 mCi pertectnetate, a pair of 5 min. supine images of the neck and upper mediastinum was acquired. Without patient-movement, 2 mCi Tl-201 were given IV and a further five pairs of 5 min. images were recorded. Analysis required correction of the Tl-201 images for the down-scatter of Tc-99m, and subsequent subtraction of the corresponding, normalized Tc-99m images to delineate the uptake of Tl-201 not attributable to functioning thyroid.

Of the 42 examinations to date, 20 were considered positive and, of the these, 11 have had surgery. Correlation of findings yielded 10 true-positives (all were adenomas of 620 mgm. or over). There was one false-positive study. Seven patients who had negative scans have also had surgery. Three had four gland hyperplasia, and four had anenomas of less than 620 mgm.

Based on the results to date, this examination can be expected to show all large adenomas. A negative scan does not exclude four gland hyperplasia or the presence of a small adenoma.

IS THERE A ROLE FOR DUAL TRACER IMAGING IN DETECTION OF PARATHYROID DISEASE? K.A. McKusick, E.L. Palmer, J. Hergenrother, H.W. Strauss. Massachusetts General Hospital, Boston, MA.

Avidity of Tl 201 (Tl) for pathological thyroid tissue could compromise the specificity of dual tracer imaging for parathyroid (PT) adenoma or hyperplasia. Within 24 hours of scheduled PT surgery, 17 patients were imaged with 5 mm pinhole collimator and gamma camera, and digital data acquired for sequential 5 min intervals as follows: initial image 4 hours after 100uCi I^{123} (12 pts) or 15 min after iv 450uCi Tc^{99m} (5 pts), followed by background image in Tl 80 KeV 20% window, followed by 3 additional images immediately after iv 2.0mCi Tl. The collimator was 6 cm from anterior surface of neck. Ultrasound (U/S) was done in 13 pts. Criteria for abnormal dual tracer test indicative of PT hyperplasia or adenoma was any definable mismatched Tl uptake compared to I^{123} or Tc image, or eccentric or extrathyroidal Tl uptake. Under optimal circumstances, knowing results of U/S and surgery, 2 observers analyzed data from computer display. Fifty-two PT glands were examined by surgery; Tl detected 12/13 adenomas, 6/11 hyperplasia; however, there was abnormal Tl uptake in the region of 16/28 normal PT glands. Thyroid disease was demonstrated in 13/16 of these at surgery or U/S.

False positive uptake was more common in pts with abnormal thyroid image (8/13) than in pts with normal appearing thyroid (1/4). Even using the most stringent criteria, false positive uptake was misleading with respect to the presence or site of PT adenoma in 6 pts. More PT adenoma were positive on dual Tl study (12/13) than on U/S (9/12); however, the low specificity of the dual tracer study indicates that as a prospective test the tracer technique should not be the primary or sole imaging modality for detection of PT disease.

HIGH SENSITIVITY LOCALIZATION OF PARATHYROID TUMORS BY NUCLEAR IMAGING IN 50 PROVEN CASES. M.D. Okerlund, K. Sheldon, S. Corpuz, W. O'Connell, D. Faulkner, M. Galante, and O. Clark. University of California Medical Center, San Francisco, CA.

50 patients with surgically and biochemically proven hyperparathyroidism had imaging studies of the neck performed with Thallium-201 chloride (2-3mCi) and Tc-99m pertechnetate, a gamma camera and pinhole collimator, and acquired and processed with a DEC PDP-11 computer with color coding for differences in localization of Tl-201 (in thyroid and parathyroid tumor) compared with pertechnetate (in the thyroid alone.)

38 of 43 single parathyroid adenomas (88%) were successfully localized, 6 of 9 multiple adenomas in 3 such patients, and 11 of 12 hyperplastic glands in 3 patients with secondary hyperparathyroidism, and 1 of 1 with cancer. With regard to tumor size, 92% of tumors 1.0 cm. or larger were found, but only 50% of those smaller than 0.7 cm. One substernal adenoma 0.6 cm. in size was missed, but 5 of 6 adenomas previously missed at surgery were found successfully. No normal or functionally suppressed glands were identified, and no false positive studies were seen, even in patients with abnormal thyroid glands.

Nuclear imaging studies with computerized comparison are the most efficacious single method for preoperative localization of parathyroid tumors yet reported, and distinguish single versus multiple disease with high reliability. All 3 intrathyroidal parathyroid adenomas were identified as to site with this method. Advantages of preoperative localization of parathyroid tumors include planning of surgical approach, shortening of operations, and localization of thyroidotomy for intrathyroid tumors.

PARATHYROID SCANS AND THYROID UPTAKE OF THALLIUM 201 OF SUBJECTS IN CHRONIC HEMODIALYSIS. M.L. Maayan, J.E. Rubin, G. Berlyne, E.M. Volpert, R. Sellitto, S. Schor, D. Braun-

stein, R. Johnson, E.Z. Wallace, R.N. Bitton, J. Watkins and P. McCann. Veterans Administration Medical Center and SUNY Downstate Medical Center, Brooklyn, N.Y.

Patients in chronic hemodialysis were injected i.v. 1mCi each Thallium Chloride 201 (TlCl) and Technetium 99m pertechnetate (Tc99m) and imagings of the thyroid and parathyroid glands were taken after 30, 60 and 90'. Parathyroid scans were obtained by computerized subtraction of the Tc99m from the TlCl image. The percentage uptake of TlCl and Tc99m was measured at 1 and 3 hrs in normal, hemodialyzed and thyroxine treated subjects as well as in untreated and thyroxine treated mice. Thyroid tests and serum electrolytes were routinely determined.

Enlarged parathyroid glands were visualized in 5 out of 6 patients on hemodialysis. TlCl uptake was greatly decreased and thyroid imagings poor in patients in renal failure. This was parallel in all cases with a high serum K^+. Tc99m uptake and scans were unaffected by renal status. Administration of L-thyroxine greatly reduced the thyroidal uptake and accompanying scans after both Tc99m and TlCl in human subjects as well as in experimental animals.

CONCLUSIONS: a) TlCl - Tc99m subtraction scans enabled visualization of hyperplastic parathyroid glands in patients in chronic hemodialysis. b) Thyroid uptake of TlCl was inversely related to the serum K^+ level. c) Both Tc99m and TlCl thyroidal uptake were inhibited by administration of L-thyroxine, hence TSH dependent.

QUANTITATION OF BONE MINERAL BY DUAL PHOTON ABSORPTIOMETRY (DPA): EVALUATION OF INSTRUMENT PERFORMANCE. W.L. Dunn, A.O'Duffy, H.W. Wahner, Mayo Clinic, Mayo Foundation, Rochester, MN.

Quantitation of bone mineral is used with increasing frequency for clinical studies. This paper will detail the principle of DPA and present an evaluation of the technique.

DPA measurements were performed with a scanning dual photon system constructed at this institution and modeled after the device developed at the University of Wisconsin (Invest. Radiol. 12:180, 1977). The components are a rectilinear scanner frame, 1.5 Ci Gd-153 source, NaI(TL) detector and a PDP 11/03 computer. Dual discriminator windows are set on the 44 and 100 keV photon energies of Gd-153.

Instrument linearity, accuracy and reproducbility were evaluated with ashed bone standards and simulated tissue covering. In these experiments computed and actual bone mineral have a correlation coefficient of 1.0 and a SEE of approximately 1.0% (Linear regression analysis). Precision and accuracy of a standard were studied over a period of two years. Mean error between actual and measured bone mineral was 0.28%. In vivo precision in six subjects averaged 2.3% (CV) for lumbar spine measurements. The effect of soft tissue compositional change was studied with ashed bone standards and human cadaver spine specimens. Intraosseous fat changes of 50% produced an average bone mineral measurement error of 1.4%. A 20% change in fat thickness produced a 2.5% error. In situ and in vitro scans of 9 cadaver spines were performed to study the effect of extraosseous fat. The mean percent difference between the two measurements was 0.7% (SEE=3.2%).

CLINICAL APPLICATION OF DUAL PHOTON ABSORPTIOMETRY (DPA) AT THE LUMBAR SPINE (LS) IN THE DIAGNOSIS OF OSTEOPOROSIS. H.W.Wahner, W.L.Dunn, B.L. Riggs, Mayo Clinic, Mayo Foundation, Rochester, MN.

This study evaluates the effectiveness of DPA to seperate patients with osteoprosis (greater than 2 spinal fractures, normal Ca, P, absence of drugs, and metabolic bone disease) from a normal population. Performance criteria for the instrument have been described previously (Radiology 136:485,1980). Data was obtained from a propspective study of 105 normal women, 75 patients with osteoporosis and a retrospective study of 300 patients with osteoporosis seen in 1982/83.

Results: (1) Area density (gm/cm2) was found superior to mass (gm) due to the occasional problem to clearly identify the boundaries of L1-4. (2) Seperation of the two populations was best when L1-L4,L2-L4,L3 alone or 10 paths over the mid lumbar area were used. One pass was not acceptable. (3) Compression fractures (CF) in the LS showed an increase in area density intially but area density may be undistinguishable from intact vertebrae later. To correct for this loss of bone area a factor predicting the area of lumbar vertebrae and based on patients actual height and weight was introduced and tested. (4) In the retrospective study a negative correlation was found between number of thoracic spine CF and bone mineral values in the LS. (5) A fracture threshold value of BM defined as the level below which 95% of all patients with CF were found was determined to be 0.98 g/cm2.

Summary: 65% of patients with two or more spinal CF could be seperated from the normal population (outside 2SD). By using a correction factor for height loss this could be further increased to about 70%. CF in the LS may falsely elevate bone mineral values.

WEDNESDAY, JUNE 6, 1984

10:30–12:00 **Room 217A**

CARDIOVASCULAR III: RADIONUCLIDE IMAGING IN ACUTE MYOCARDIAL INFARCTION

Moderator: Samuel E. Lewis, M.D.
Comoderator: Denny D. Watson, Ph.D.

PREDICTION OF INFARCT VOLUME IN PATIENTS UNDERGOING REPERFUSION THERAPY BY Tc-99m ANTIMYOSIN SPECT. T. Yasuda, R.C. Leinbach, B.A. Khaw, H.K. Gold, H.W. Strauss. Massachusetts General Hospital, Boston, MA.

The predictability of infarct volume by Tc-99m antimyosin SPECT was evaluated within 24 hours of chest pain and this was compared to the length of akinesis (AK) from the pre-discharge left ventriculogram (LVgram). Ten patients (pts) with acute myocardial infarction who underwent streptokinase thrombolytic therapy (success 8, failure 2) were subjects of this investigation. None had previous infarction.

Average reperfusion time was within 4.5 hours and 20mCi of Tc-99m antimyosin was given intravenously within 8 hours after chest pain; SPECT imaging was performed within 18 hours after injection. Infarct volume was calculated from SPECT and expressed as grams of myocardial infarction (GMI).

Ten days later, a 30°RAO contrast LVgram was recorded and the length of AK (corrected for magnification) was measured along the LV border at the end-diastolic phase and expressed as cm of AK.

GMI and AK were measured independently without knowledge of each other. Results are shown below:

Pts	1	2	3	4	5	6	7	8	9	10
GMI (gm)	93	71	72	26	49	33	44	48	15	64
AK (cm)	15.3	9.4	12.5	9	10.4	5.4	6.9	11	1.3	10.3

GMI (gm) = 5.21 x AK (cm) + 3.79 ($r=0.85$, $p<0.002$)

These data demonstrate a good correlation of GMI and AK. Infarct volume can be measured by antimyosin SPECT within 24 hours of chest pain and predict residual LV dysfunction in pts undergoing reperfusion therapy.

DOES REGIONAL LEFT VENTRICULAR DYSFUNCTION OCCUR DISTANT FROM THE INFARCT ZONE IN INITIAL ACUTE TRANSMURAL MYOCARDIAL INFARCTION? J.L.Meizlish, M.Plankey, B.L.Zaret and H.J. Berger, Yale University, New Haven, CT

To test the hypothesis that myocardial infarction (MI) in one coronary vascular bed may be associated with ischemia in another, the incidence of regional wall motion (RWM) abnormalities distant from the ECG-localized MI was studied in 86 patients (pts) with initial acute transmural MI but without post-MI angina. Multigated cardiac blood pool imaging was performed in 4 views

within 24±16 hours (mean ±SD) of chest pain. By ECG, 46 pts had anterior (ANT) MI, and 40 pts had inferior (INF) MI. The left ventricle (LV) was divided into 10 contiguous segments (5 ANT, 2 apical, and 4 INF) and graded on a 5-point scale from dyskinetic to normal (nl). In INF MI, no pt had abnl RWM in any of the 5 ANT segments, and all RWM abnormalities were contiguous. In ANT MI, INF segments were abnl only in 8/46 pts; in only 1 of these 8 pts was the INF RWM abnormality separated from the primary ANT abnormality by interposed nl RWM. In the other 7 pts, the INF RWM abnormalities were contiguous with extensive ANT dysfunction and resulted in LV ejection fractions $\leq$27% in all cases (mean, 15%). The apex frequently was abnl both in ANT MI (46/46) and INF MI (18/40), but never was discontiguous from other areas of abnl RWM.

Thus, in initial acute transmural MI without post-MI angina, RWM abnormalities are contiguous and do not occur distant from the MI zone. This suggests that separate RWM abnormalities are rare in the absence of clinical ischemia and probably are due to multiple areas of MI.

EARLY ANEURYSM FORMATION FOLLOWING ANTERIOR MYCARDIAL INFARCTION: A BETTER PREDICTOR OF MORTALITY THAN LEFT VENTRICULAR EJECTION FRACTION. J.L.Meizlish, M.Plankey, H.Berger, and B. Zaret, Yale University, New Haven, CT

To compare the prognostic effect of aneurysmal infarct expansion (AN) to ejection fraction (EF), 52 consecutive high risk patients (pts) with initial anterior transmural myocardial infarction (MI) underwent 4-view bedside multigated cardiac blood pool imaging within 48 hours of chest pain and prehospital discharge. AN was strictly defined as an akinetic or diskinetic portion of the left ventricle which had diastolic deformity and was adjacent to areas with normal motion. EF $<$35% was found to be the best EF cut-off for testing prediction of mortality. One year follow-up was performed by telephone interview (14 months, range 6-21).

AN developed in 18/52 pts (35%), 9 developed by 48 hours and 9 further predischarge. 35/52 patients (69%) had EF $<$35%. One year mortality was 27% (14/52). AN was highly predictive of death: 11/18 pts with AN died, while only 3/34 without AN died (χ^2=16.35, p$<$.001). This was independent of EF: EF did not differ between pts with and without AN (27.5±8.8 vs 31.5±11.2, p NS). In contrast EF $<$ 35% was not as useful in predicting mortality; 12/35 pts with EF $<$ 35% died while 2/17 with EF $\geq$35% died (χ^2=2.95, p NS). The presence of AN was equally sensitive (79% vs. 86%) and far more specific (82% vs. 39%) than EF for the prediction of mortality.

We conclude, AN occurs frequently early following anterior MI and is an important and specific marker for mortality. It is superior to EF as a prognostic indicator in this high risk subset of pts and therefore may be a useful parameter in stratification of pts in trials designed to reduce mortality.

RIGHT AND LEFT VENTRICULAR EJECTION FRACTION AFTER AN ACUTE INFERIOR WALL MYOCARDIAL INFARCTION AND THE VALUE OF V4R TO PREDICT THE SITE OF OBSTRUCTION. S.H. Braat, P. Brugada, K. den Dulk, H.J.J. Wellens. Dept. of Cardiology, University of Limburg, Annadal Hospital, Maastricht, The Netherlands.

This study was undertaken to compare the right (RVEF) and left ventricular ejection fraction (LVEF) after an acute inferior wall myocardial infarction (MI) caused by an obstruction in the right coronary artery (RCA) or circumflex coronary artery (CX) and to evaluate the value of lead V4R to predict the site of stenosis which caused the MI.

In 42 consecutive patients (pts) admitted with an acute inferior wall MI a standard ECG and V4R were recorded. A nuclear angiogram was made one week after the acute MI and the RVEF and LVEF were calculated. Ten to 14 days (mean 12.7) after the acute MI a coronary angiogram was performed to determine the site of occlusion, which had caused the acute MI. According to the site of occlusion the pts were divided in three groups: Group A: the stenosis which had caused the MI was located in the RCA above the first branch to the right ventricle (RV); Group B: the stenosis was below the first branch to the RV in the RCA and Group C: the stenosis was located in the CX. The RVEF and LVEF in these groups were as follows:

No. of patients	Group	LVEF	RVEF
17	A	55±7%	29±9%
14	B	56±7%	43±5%
11	C	53±9%	44±3%

Nineteen pts had ST-segment elevation $\geq$ 1 mm in V_4R and 17 of these pts had an obstruction above the first branch to the RV in the RCA. There is statistically no significant difference between the LVEF in the three different groups while the RVEF is significantly lower in group A. These pts can be identified by recording V4R.

THE FREQUENCY, ETIOLOGY, AND SIGNIFICANCE OF SEPTAL INVOLVEMENT IN ACUTE INFERIOR MYOCARDIAL INFARCTION. A Lew, T Weiss, J Maddahi, PK Shah, I Geft, HJC Swan, W Ganz, D Berman. Cedars-Sinai Med Ctr, Los Angeles, CA

Involvement of the interventricular septum (IVS) in acute myocardial infarction is usually attributable to proximal left anterior descending artery (pLAD) occlusion; however, the IVS is also supplied by the posterior descending branch of the right coronary artery (RCA). Therefore we investigated the frequency and significance of IVS involvement in acute inferior myocardial infarction (IMI) in 34 consecutive patients with IMI using thallium-201 scintigraphy (Tl-201), radionuclide ventriculography (RNV) and coronary angiography. Tl-201 perfusion defects of the IVS were found in 16 pts (Group 1), 11 of whom also had an IVS wall motion (WM) abnormality. In all 18 patients with normal IVS Tl-201 uptake (Group 2), IVS WM was also normal. IMI was due to RCA thrombosis in all 16 (100%) pts in Group 1 but in only 11 (61%) of the pts in Group 2; the remaining 7 had circumflex thrombosis. The frequencies of multiple-vessel disease and pLAD stenosis were similar in Group 1 and in Group 2 (81% vs 78% and 31% vs 33%, respectively). The table summarizes the data for left ventricular (LV) ejection fraction (EF) and right ventricular (RV) EF in pts with RCA thrombosis (T) in Groups 1 and 2:

		Mean LVEF	Mean RVEF*	RVEF 35%
Group 1	(n=16)	53%	32%	8 pts
Group 2 with RCA T	(n=11)	53%	45%	0 pts

*p$<$0.05. We conclude that IVS involvement in acute IMI 1) is frequent (47%), 2) appears to result from RCA thrombosis and cannot be attributed to pLAD disease, and 3) is associated with greater RV dysfunction.

REVERSE THALLIUM-201 REDISTRIBUTION PATTERN IN STREPTOKINASE REPERFUSED MYOCARDIUM: A SIGN OF REESTABLISHED FLOW TO A PARTIALLY VIABLE MYOCARDIUM. T Weiss, J Maddahi, A Lew, PK Shah, I Geft, HJC Swan, D Berman, W Ganz. Cedars-Sinai Medical Center, Los Angeles, CA

We have noted that the pattern of reverse redistribution (RR) on rest-redistribution Tl-201 scintigrams is a common finding in patients who have undergone streptokinase therapy (SKT) in evolving myocardial infarction. Thus we studied the significance of RR pattern in 70 patients who underwent SKT as well as rest-redistribution Tl-201 study (7-10 days after SKT), coronary arteriography and resting radionuclide ventriculography. Tl-201 images were visually interpreted by consensus of three experienced observers with a 4-point scoring system (0=nl, 3=severe defect), and RR was defined as decrease by at least 1 score between rest and 4-hr studies. Fifty of 70 patients (Group I) showed RR pattern and the remaining 20 (Group II) did not. On angiography, coronary arteries supplying the myocardial segments with RR were patent, suggesting that coronary flow has been reestablished to these regions. In 23 patients Tl-201 % washout rate was quantitated and showed significantly higher ($p < .001$) values in the regions demonstrating RR pattern compared to the adjacent normal regions (49±15% vs. 24±15%). Normal or near-normal wall motion was observed in 80% of myocardial segments with marked RR (2 score change) and 54% of those with mild RR (1 score change). We conclude that in patients who have undergone streptokinase therapy, reverse Tl-201 redistribution is common in previously jeopardized myocardial segments with subsequent successful reperfusion and partial myocardial salvage. The reverse redistribution phenomenon may indicate higher than normal flow rates to the salvaged epicardial regions resulting in faster washout of Tl-201.

10:30-12:00 **Room 216BC**

INSTRUMENTATION II: PLANAR IMAGING

Moderator: L. Stephen Graham, Ph.D.
Comoderator: Mark W. Groch, M.S.

EFFECTS OF ASYMMETRIC PHOTOPEAK WINDOWS ON FLOOD FIELD UNIFORMITY AND SPATIAL RESOLUTION FOR SCINTILLATION CAMERAS. R. LaFontaine, L.S. Graham, and M.A. Stein, UCLA School of Medicine, Los Angeles, CA and V.A.M.C., Sepulveda, CA.

The use of asymmetric high windows is known to reduce the amount of scatter that is present in an image. In this study intrinsic and extrinsic flood field uniformity and line spread functions were used to quantitate the effects of window asymmetry, using energy and renormalization maps based on Tc-99m. Five different windows with settings of intrinsic symmetric, 5, 10, 20, and 30% asymmetric (defined as count loss relative to the symmetric window) were used. Extrinsic measurements were obtained with several combinations of forward and backscatter. Uniformity was expressed in terms of the Uniformity Index and NEMA parameters. Spatial resolution was evaluated from FWHM, FWTM, and MTF values. For Tc and Tl-201, flood field uniformity showed a generally linear decrease as a function of asymmetry. Although intrinsic field uniformity for Tc was better than for Tl at each setting, in the presence of scatter Tc values deteriorated more rapidly with increasing window asymmetry and in some conditions were inferior to those of Tl. I-131 uniformity indices were poorer than those of Tc and Tl for all settings. FWHMs and FWTMs showed improvement with window asymmetry only in the presence of scatter, FWTMs for Tc decreased by 15% at 10% asymmetry but only reached 20% at 30% asymmetry. By comparison, Tl values decreased by 17% at 10% asymmetry and exhibited no further change upto 30%. Cold sphere lesion contrast followed a similar pattern for Tc and Tl. These results demonstrate that improvement in spatial resolution and contrast can be achieved with the use of asymmetrical windows, but potential benefit in terms of lesion detectability must be considered from the perspective of decreased field uniformity.

EFFECT OF ENERGY WINDOW ON LV EJECTION FRACTION USING ECG-GATED ENERGY SPECTROSCOPY. S.L. Bacharach, M.V. Green, S. Findley, R.O. Bonow, S.M. Larson. NIH, Bethesda, MD.

Changes in volume and shape of the left ventricle (LV) may significantly effect the shape of the LV energy spectrum observed during a gated equilibrium, cardiac study. We tested this supposition by creating a gamma ray energy spectrum at each moment in time during the cardiac cycle. Each spectrum was created at progressive 50 msec increments during a cardiac cycle by gating for 300 beats. Two sets of spectra were obtained from each of 10 subjects studied at rest: one from an LV region of interest (ROI), one from a background (BKG) ROI. Multiple LV time activity curves (TAC's) were obtained using multiple energy windows placed over the energy spectra. Both raw and BKG corrected TAC's were produced. BKG correction was performed using the same energy (E) window. BKG TAC's were flat over the photopeak and time variant at lower E's (single and multiple scatter region). Ejection fraction (EF) was found to be strongly dependent on the exact position of the energy window used. Moving a narrow (4KeV) window over the photopeak in 4 KeV steps produced a (roughly) linear increase in EF with energy, maximum EF occurring at the highest window measured (155-158 KeV). Comparing the two halves of the photopeak (126-140 KeV and 140-154 KeV), the EF's obtained differed significantly (high E window exceeded low E by 25%±5%). Similarly, progressive movement of a 20% window across the photopeak produced a change in EF of 10%/10KeV change in window position. Increasing the width of a narrow window centered about the photopeak, however, produced no measureable change in EF for windows up to 25%. Thus placement or changes in the position of an asymmetric photopeak window may alter ejection fraction significantly.

SCINTICOR: ™ A NEW DIGITAL GAMMA CAMERA. * D.W. Heyda†, R.H. Jones††, Baird Corporation, Bedford, MA†. and Duke University, Durham, N.C.††

A new mobile gamma camera, Scinticor,™ has been developed with major improvements in design and performance.

The instrument has a new scintillation detector which is a block of NaI (Tl), (8x8x1") optically divided into (20x20) elements with 115 photomultiplier tubes (PMT's) coupled to the scintillation exit glass of the crystal. Integrated hybrid circuits on each PMT transform the signal to a digital pulse which is the input to the digital positioning logic and dual window pulse height analyzer. Detector reliability is enhanced by automatic electronic tuning of each PMT. A new high sensitivity collimator provides 70% greater sensitivity than the present multi crystal collimator with same FWHM. The detector's special purpose array processor performs in real time (up to 100 frames/sec): ECG digitization, creation of first pass cardiac functional images and corrections for field uniformity, deadtime, radioactive decay, and environmental background. Data transmission to the mobile data processing console is via a 10Mb/s fiber optic link.

Initial results(Fig.1)indicate a major advance in collimated detector sensitivity and count rate with saturation over 1,000,000 cps. Energy resolution is 25% FWHM at 122 keV, Dynamic Edge Resolution is 3mm, Static Resolution is 10mm. Initial clinical studies indicate this instrument is suitable for a wide range of dynamic studies.
* Patents applied for.

SPATIAL RESOLUTION IN IMAGING SYSTEMS: EQUIVALENT WIDTH A REALISTIC MEASURE TO REPLACE FWHM. B. Knoop, K. Jordan, R. Judas, O. Schober. Medical School Hannover, West-Germany

It was the purpose of the study to discuss and recommend a realistic measure for the spatial resolution in nuclear medicine imaging systems.

If the assumption of a gaussian line spread function is fullfilled, the resolution index FWHM describes the associated frequency transfer function as well. In the case of septal penetration and scattering this basic assumption is no longer valid. So FWHM has no relevance with respect to transfer characteristics. Therefore equivalent width (EW)

$$EW = \int_{-\infty}^{\infty} LSF(x)dx/LSF(0)$$ and autocorrelation width (AW)

$$AW = \int_{-\infty}^{\infty} [LSF(x) \circledast LSF(x)]dx/[LSF(x) \circledast LSF(x)]_{x=0}$$

well known parameters in signal theory, are examined concerning a realistic measure of spatial resolution. These parameters are connected to line spread functions (LSF) and modulation transfer functions (MTF) regardless of its analytical form.

Two cold spheres (20mm & 30mm Ø) in a Tc-99m filled disc phantom were imaged with a gamma camera (LEAP collimator) in a 20 cm source collimator distance, with air and water as a scattering medium. Resolution indices and image contrast, C: = (non target-target)/non target, are summarized.

Scatter	FWHM(mm)	EW(mm)	AW(mm)	C(20)	C(30)
Air	16,5	17,5	24	40%	70%
Water	18,5	32	72	20%	40%

We conclude: Contrast changes caused by scatter are much better reflected by changes of EW than FWHM. Therefore we recommend EW as a realistic resolution index for imaging quality in nuclear medicine. AW seems by its definition suitable for quantitation purposes.

ATTENUATION COEFFICIENTS FOR Tc-99m PHOTONS IN WATER-FILLED PHANTOMS, DETERMINED WITH A GAMMA CAMERA: VARIATION WITH ENERGY WINDOW. C.C. Harris, K.L. Greer, C.E. Floyd, R.J. Jaszczak, E.C. Fearnow and R.E. Coleman. Duke University Medical Center, Durham, NC.

Values of the linear attenuation coefficient, μ, near 0.12 cm^{-1} used in attenuation compensation of Tc-99m ECT scans of uniform cylindrical phantoms give better results than use of 0.15 cm^{-1}. The latter value is theoretical, and does not take into account recoil photons from Compton scattering, but continues to be used in new SPECT software development and other quantitative imaging situations.

To investigate the influence of Compton scattering on the effective linear attenuation coefficient, a gamma camera and a multichannel pulse height analyzer were used

to determine values of μ for photons in water as a function of energy window, using the entire camera field as a region of interest. Two cylindrical water-filled phantoms, circular (22 cm O.D.) and elliptical (22.5 X 30.5 cm O.D.) were used with point sources of Tc-99m at depths up to 21 cm. Energy spectrum data were integrated over: top half of photopeak, 10%, 20% and 30% centered windows and bottom half of photopeak.

Almost all attenuation plots were exponential, with highest values of μ (0.122 to 0.128 cm^{-1}) at top half of photopeak, and with μ decreasing as the energy threshold was lowered (0.117-0.116, 0.108-0.106, 0.105-0.097, and 0.100-0.091 cm^{-1} for windows noted above, for circular and elliptical (short axis) phantoms, respectively).

This variation with energy window suggests that there is within the "photopeak" a distribution of scattered photons the magnitude of which increases with decreasing energy, and accounts for improved attenuation corrections with values of μ less than the theoretical 0.15 cm^{-1}.

VARIATIONS IN ATTENUATION COEFFICIENTS FOR Tc-99m PHOTONS WITH SOURCE DEPTH AND REGION-OF-INTEREST SIZE. E.C. Fearnow, J.A. Stanfield, R.J. Jaszczak, C.C. Harris and R.E. Coleman. Duke University Medical Center, Durham, NC.

A theoretical attenuation coefficient ($\mu = 0.15\ cm^{-1}$) and an empirically determined coefficient (μ') have been used in count-based determinations of ventricular volumes. The value μ' is influenced by scatter conditions. We have investigated the effect of source depth and region-of-interest (ROI) size on μ' using a water phantom.

A Tc-99m point source positioned in the phantom at depths from 4 to 25 cm and in air at 2.5 cm was imaged with a gamma camera with a 20% window. The empirical μ' was equal to $\ln(A/B)/C$, where A = background corrected count rate of source in air and B = background corrected count rate at source depth C. A 96 cc Tc-99m-filled sphere was imaged in a water phantom at a depth of 9 cm and 1 cc of this sample was imaged in air. Fourteen ROIs ranging from 180 to 1600 pixels (1 pixel = 0.174 cm^2) were drawn around the image of the sphere. The value of μ' was equal to $\ln(96D/E)/F$, where D = background corrected count rate for 1 cc source and E = background corrected count rate for the sphere ROI at depth F (9 cm).

For the point source at increasing depths the value of μ' increased from 0.086 to 0.13 cm^{-1} approximately linearly. With increasing ROI size the value of μ' decreased nonlinearly from 0.113 to 0.087 cm^{-1} with the decrements becoming smaller with larger ROIs.

The empirically determined attenuation coefficient μ' is influenced by source depth and ROI size. Use of such a coefficient should include consideration of these factors.

10:30–12:00 **Room 214BC**

RADIOPHARMACEUTICAL CHEMISTRY II: GENERAL

Moderator: Kenneth A. Krohn, Ph.D.
Comoderator: Michael R. Kilbourn, Ph.D.

COMPARISON OF RADIOLABELED BROMOMISONIDAZOLE AND MISONIDAZOLE AS PROBES FOR HYPOXIC TISSUE. J.S. Rasey, K.A. Krohn, N. Nelson, and Z. Grunbaum, University of Washington, Seattle, WA 98195.

Misonidazole and related nitroimidazoles may be useful for diagnostic detection of hypoxic cells in tumor, stroke, or myocardial infarct due to binding by metabolic reactions which are limited to cells with low oxygen tension. 4-Bromomisonidazole has been synthesized from misonidazole. If labeled with a gamma emitting bromine isotope, it may be useful in nuclear imaging of hypoxic tissue. It has been compared to misonidazole in radiolabeled form as a probe for hypoxic cells in an in vitro tumor model, the multicellular tumor spheroids. This system is useful for screening nuclear imaging agents. These "pseudo tumors" have cell-cell contact, three dimensional growth, and development of central necrosis similar to in vivo tumors, but lack the complications of a vascular system and host physiological influences.

EMT-6 tumor cell spheroids with necrotic, hypoxic cores were incubated with 50 μm C-14-bromomisonidazole or C-14-misonidazole. Maximum levels of C-14-bromomisonidazole (approx 5 fold medium levels) were attained by 10 hrs while C-14-misonidazole uptake reached a similar maximum level only after 23 hrs. In autoradiographs, essentially no label from bromomisonidazole or misonidazole accumulated in oxic cells at the periphery of the spheroid while cells presumed to be hypoxic but viable adjacent to the necrotic center were heavily labeled at incubation times $\geq$ 5 hrs. HPLC techniques can separate C-14-misonidazole from C-14-bromomisonidazole and will allow us to determine if bromine remains attached to stably bound C-14 labeled compounds after spheroids have metabolized C-14-bromomisonidazole. (Supported by grant #CA34570, NIH).

SYNTHESIS OF A FLUORINE-18 LABELED HYPOXIC CELL SENSITIZER. P.A. Jerabek, D.D. Dischino, M.R. Kilbourn, and M.J. Welch. Washington University School of Medicine, St. Louis, MO

The objective of this work was to synthesize a positron emitting radiosensitizing agent as a potential in vivo marker of hypoxic regions within tumors, and ischemic areas of the heart and brain. The method involved radiochemical synthesis of fluorine-18 labeled 1-(2-nitro-1-imidazolyl)-3-fluoro-2-propanol via nucleophilic ring opening of 1-(2,3-epoxypropyl)-2-nitroimidazole by fluorine-18 labeled tetrabutylammonium fluoride (TBAF). Fluorine-18 TBAF was prepared by the exchange reaction of TBAF with aqueous fluorine-18 produced by proton bombardment of enriched oxygen-18 water. The aqueous solution was evaporated carefully by azeotropic distillation with acetonitrile. The fluorine-18 labeled TBAF was taken up in N,N-dimethylacetamide or dimethylsulfoxide, then reacted with the epoxide at 60C for 30 minutes. Separation and identification of the fluorine-18 labeled products by high performance liquid chromatography showed a radioactive peak with a retention time identical to that of 1-(2-nitro-1-imidazolyl)-3-fluoro-2-propanol and a second radioactive peak with a retention time three minutes longer in addition to unreacted fluorine-18 labeled TBAF. The second radioactive peak may represent fluorine-18 labeled 1-(2-nitro-1-imidazolyl)-2-fluoro-3-propanol. The average radiochemical yield from reactions run in N,N-dimethylacetamide using 20 micromoles of TBAF and 1-2 mg of the epoxide was 17% in a synthesis time of about 40 minutes. The synthesis of fluorohydrins by the reaction of fluorine-18 labeled TBAF on epoxides represents a new method for the preparation of fluorine-18 labeled fluorohydrins.

[F-18]N-FLUORO-N-ALKYLSULFONAMIDES: NOVEL REAGENTS FOR RADIOFLUORINATION. N. Satyamurthy, G.T. Bida, J.R. Barrio, and M.E. Phelps. UCLA School of Medicine, Los Angeles, CA.

We report here a new regioselective method for radiofluorination which involves the use of organometallic compounds as substrates. [F-18]N-Fluoro-N-alkylsulfonamides, prepared by fluorination of N-alkylsulfonamides with [F-18]fluorine, react readily with aryllithium or arylGrignard reagents to give [F-18]fluoroaryl derivatives.

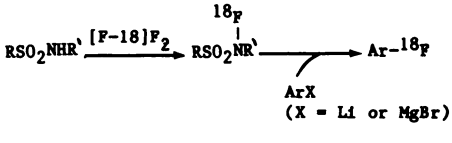

As a typical example, [F-18]fluorine gas (50 microMol) diluted in neon (0.2%, v/v) prepared using the Ne-20 (d, α) nuclear reaction, is reacted with N-endo-norbornyl (p-tolyl)sulfonamide at room temperature and the product, [F-18]N-fluoro-N-endo-norbornyl(p-tolyl)sulfonamide, is then treated with phenyllithium or phenylmagnesium bromide to produce [F-18]fluorobenzene in 60-70% radiochemical yields. This reaction represents a novel, general route to [F-18]arylfluorides of moderate specific activity (1-10 Ci/mmole), and is potentially valuable for the synthesis of a variety of radiotracers, including radiolabeled enzyme inhibitors and neurotransmitter ligands for application in positron emission tomography.

QUANTITATIVE AUTORADIOGRAPHIC MEASUREMENT OF REGIONAL MYOCARDIAL SUBSTRATE UPTAKE IN HYPERTENSIVE RATS. Y. Yonekura, N.Tamaki, K.Torizuka, Kyoto Univ, Kyoto, Japan, A.B.Brill, P.Som, K.Yamamoto, S.Srivastava, J.Iwai, BNL, Upton, NY, D.R.Elmaleh, E.Livni, H.W.Strauss, MGH, Boston, MA, M.M.Goodman, F.F.Knapp,Jr., ORNL, Oak Ridge, TN.

Quantitative double tracer autoradiographic technique permits to study the distribution of two tracers in the same section of small animals with high spatial resolution. We have applied this technique to measure regional myocardial perfusion and substrate uptake in hypertensive rats. To compare regional myocardial uptake of fatty acid and glucose analogs with regional myocardial perfusion, three different double tracer experiments were conducted utilizing the difference of physical half-lives as follows: i) (C-14)3-methyl-heptadecanoic acid (BMHDA) and Tl-201 (TL), ii) (C-14)2-deoxy-D-glucose (DG) and TL, iii) (F-18) 2-fluoro-2-deoxy-D-glucose (FDG) and BMHDA. DG (or FDG), BMHDA and TL were administered to rats 45 min, 15 min and 5 min prior to sacrifice, respectively. The autoradiograms were digitized and quantitated using a videodensitometry film analysis system.

Myocardial perfusion as indicated by TL distribution was homogenous in both normotensive and hypertensive rats. However, hypertensive myocardium showed decreased uptake of BMHDA in the endocardial and septal regions, where DG showed markedly increased uptake. Double tracer experiment with BMHDA and FDG clearly demonstrated this complementary relation in the same section. These data indicate that hypertensive myocardium has abnormal substrate utilization although regional myocardial perfusion is not impaired. Moreover, (C-11)BMHDA and (F-18)FDG may be used to measure regional myocardial substrate utilization in humans with positron emission tomography.

CHARACTERIZING POTENTIAL HEART AGENTS WITH AN ISOLATED PERFUSED HEART SYSTEM. D.B. Pendleton, H. Sands, B.M. Gallagher, and L. L. Camin. New England Nuclear Corp., Billerica, MA

We have used an isolated perfused heart system for characterizing potential myocardial perfusion radiopharmaceuticals. Rabbit or guinea pig (GP) hearts are removed and perfused through the aorta with a blood-free buffer. Heart rate and ventricular pressure are monitored as indices of viability. Tc-99m-MAA is 96-100% retained in these hearts, and Tc-99m human serum albumin shows less than 5% extraction. Tl-201 is 30-40% extracted.

It is known that in-vivo, Tc-99m$(dmpe)_2Cl_2^+$ is taken up by rabbit heart but not by GP or human heart. Analogous results are obtained with the isolated perfused heart model, where the complex is extracted well by the isolated rabbit heart (24%) but not by the GP heart (<5%). Values are unchanged if human, rabbit or GP blood is mixed and co-injected with the complex.

Tc-99m$(dmpe)_3^+$ is also taken up by rabbit but not by GP hearts in-vivo. However, isolated perfused hearts of both species extract this complex well (45-52%). Heart uptake is diminished to <7% if the complex is pre-equilibrated with human blood. GP blood produces a moderate inhibition (in GP hearts only) and rabbit blood has no effect. This suggests that a human or GP blood factor may have a significant effect on heart uptake of this complex.

Tc-99m$(CN\text{-}t\text{-}butyl)_6^+$ is taken up well by both rabbit and GP hearts in-vivo, and is extracted 100% by both isolated perfused hearts. Heart retention remains high (73-75%) in the presence of human blood.

IN VIVO TUMOR LOCALIZATION OF TECHNETIUM-LABELED METALOTHIONEIN/MONOCLONAL ANTIBODY CONJUGATES G.L. Tolman, R.J. Hadjian, M.M. Morelock, P.L. Jones, W. Neacy, F.A. Liberatore, H.Sands, B.M. Gallagher, New England Nuclear Corp., Immunopharmaceutical R&D Department, No. Billerica, MA 01862

The use of radioiodinated monoclonal antibodies (MAb) directed against tumor associated antigens for imaging has reinforced the need for additional labeling methods to permit the use of other medically relevant radionuclides. The low molecular weight metal binding protein, metallothionein (MT) has a high avidity for several radionuclides including Tc-99m. The conjugation of a Zn-MT to MAb B6.2 directed against human breast carcinoma was studied using glutaraldehyde as the bifunctional cross-linker. The Zn-MT-B6.2 conjugate was labeled with Tc-99m to form a Tc-99m labeled MT-B6.2 conjugate. Radiolabeled conjugates were shown to retain high immunoreactivity compared to radioiodinated B6.2 in a direct cell binding assay on target MCF7 breast carcinoma cells and a low non-specific binding to antigen negative melanoma cells. These conjugates were evaluated in athymic mice bearing subcutaneous Clouser breast or A375 nonspecific melanoma tumors. The specificity of uptake in the target tumor to nonspecific tumor was equivalent to that of the radioiodinated antibody over the first 24 hours in vivo. The blood clearance was more rapid for the Tc-99m MT conjugates and this enhanced clearance permitted superior images to be obtained within 24 hours. This labeling methodology produces stable Tc-99m labeled antibodies, retaining high immunoreactivity and demonstrating good localization and imaging in this model system. (Patent pending.)

10:30–12:00 **Room 212B**

BONE AND JOINT I

Moderator: Hee-Myung Park, M.D.
Comoderator: Lawrence E. Holder, M.D.

THE MDP SKULL UPTAKE TEST: A NEW DIAGNOSTIC TOOL. P.J.Ell, P.H. Jarritt, I. Cullum and D.Lui. The Middlesex Hospital Medical School, London, UK.

An original approach to the measurement of bone turnover is presented. With SPET, we have measured in pgr/ml, the uptake of MDP by the skull in man. The Cleon 710 scanner, ring phantoms and bone biopsies were used for ultimate in vivo/in vitro count recovery correlation and calibration.

A normal range for 24 patients was found: 8.5 to 19.5 pgr/ml with a mean of 14. For patients with bony metastases (12), the values were: 22.5 to 50,mean of 30. For 5 patients with osteomalacia, the values were 46 to 68, mean of 62: for 12 patients with hyperparathyroidism, the values were 37 to 48.5, mean of 43. In 3 patients with Pagets disease, the values were 58.5 to 75, with a mean of 65.

In 76 patients with metastatic disease to bone, the conventional wholebody bone scan was investigated against the following: 24h wholebody retention of MDP (WBR), skull uptake as described and GFR by Cr-51-DTPA. There is a correlation between GFR and WBR - r=0.67. There is a lesser correlation between GFR and skull uptake - r=0.3. There is no correlation between skull uptake and WBR - r=0.1.

The comparison of skull uptake data with normal whole body bone scans leads to a significant proportion of cancer patients with positive skull uptake data. Monostotic disease (especially if metabolic in nature) expresses itself by abnormal skull uptake even if the clinical site of abnormality lies outside the skull.

This new technique is ideal as a tool to investigate phosphonate concentration in bone. With it, we have shown the effect of specific activity of label on skull uptake, which increases as the specific activity of labelled MDP decreases.

EVALUATION OF EXTREMITY PAIN IN CHILDREN USING TECHNETIUM-99m MDP BONE SCAN - A GENERAL HOSPITAL EXPERIENCE. H.M. Park, P.A. Rothschild, C.B. Kernek, Indiana University Medical Center, Indianapolis, IN.

This study was undertaken to evaluate the efficacy of three-phase bone scan in detection of significant pathology i.e., osteomyelitis (OM), septic joint, cellulitis, etc., in children with symptoms of extremity pain. A total of 100 consecutive patients (age 9 days - 16 yrs, 63 boys and 37 girls) were studied. We reviewed their scans, x-rays and hospital records. The final diagnoses were based on the findings of needle aspiration, surgical drainage, biopsy, culture, and on the therapeutic response. In 87%, sufficiently long clinical follow-up was available to confirm the final diagnoses. In the remaining 13%, the symptoms resolved quickly and follow-up was not felt necessary.

TABLE. FINAL DIAGNOSES AND SCAN RESULTS

Final Dx	No.	Dx by Scan	Sensitivity	Specificity
Acute OM	20	17	85%	97%
Cellulitis	15	14	94%	100%
Septic Joint	15	15	100%	100%

The scan was essential in pinpointing the lesions in pts with referred or nonlocalizing extremity pain. The +ve and -ve predictive values of the scan for OM were 89% and 96% respectively. One spiral fracture was misinterpreted as diffuse OM. One "Subacute epiphyseal OM" was not detected. In two cases, cellulitis and septic joint obscured underlying OM. Prior antibotic therapy resulted in one equivocal scan. Although less sensitive (29%) in early OM, radiographs play an important complimentary role.

In summary, bone scans detected underlying pathology for extremity pain in 61% of all pts studied.

SUBCLINICAL CLUBBING OF FINGERS AND TOES ON BONE SCINTIGRAPH - W.M. Sy & I.S. Seo, The Brooklyn Hospital, Brooklyn, NY

A total of 1258 hands/feet images obtained with routine bone scintigraphs in 687 adults were reviewed for evidence of increased activity along the tips of the digits (RNC). Sixty-five adults (96 images) showed such features. Fifty-seven had images of both hands and feet, while 8 had hand images only. In 17/57 only increased distal toe activity was observed, in 3/57 only the tips of the fingers, and in 37/57 all distal phalanges showed RNC. Where both fingers and toes showed RNC, toe activity was greater in 24, comparable in 11 and less in 2. Only nine of 65 patients showed overt image and clinical features of hypertrophic pulmonary osteoarthropathy (HPO). Only 8 of 65 patients had clinical clubbing of the fingers, so that in 57 no corresponding clinical clubbing was demonstrable.

The majority, 52/65, primary lung malignancy was the underlying associated condition of the RNC, and the remaining 13 were associated with other causes. The incidence of RNC associated with lung malignancy was comparable in both sexes but HPO was greater (6:1) in women. In some cases RNC was the first clue to an underlying lung malignancy.

Conclusions: RNC on bone image probably represents subclinical clubbing. The tips of the toes, possibly because of their more dependent position, manifested RNC more consistently and more intensely.

DETECTION OF AVASCULAR NECROSIS IN ADULTS BY SINGLE PHOTON EMISSION COMPUTED TOMOGRAPHY. B.D. Collier, R.P. Johnson, G. Carrera, A.T. Isitman, R.S. Hellman, and J.S. Zielonka. Medical College of Wisconsin, Milwaukee, WI

Twenty-one adult patients with the clinical diagnosis of avascular necrosis (AVN) of the femoral head were examined with planar bone scintigraphy (high resolution collimator) and single photon emission computed tomography (SPECT). The duration of hip pain ranged from 1 day to 18 months. Risk factors (including steroids, renal transplantation, alcoholism, and trauma) were present in 17 cases. A final diagnosis of AVN (20 hips), osteochondral facture (1), or stress fracture (1) was established for 17 patients. The 4 remaining patients, who were radiographically normal and did not complain of pain 3 months later, were thought to have no significant bone pathology. SPECT and planar bone scintigraphy were reported as positive for AVN only if a photopenic bony defect could be identified. In particular, uniformly increased activity throughout the femoral head was not considered to be diagnostic of AVN.

	Sensitivity (Hips with AVN)	Specificity
SPECT	0.85	1.00
Planar	0.55	1.00

	Sensitivity (Patients with AVN)	Specificity
SPECT	0.80	1.00
Planar	0.53	1.00

We conclude that by identifying a photopenic defect which is not evident on planar bone scintigraphy, SPECT can contribute to accurate diagnosis of AVN.

STEROID OSTEOPATHY. J.J. Conway and S.C. Weiss. The Children's Memorial Hospital, Chicago, IL.

Patients receiving steroids or having disease processes which increase natural steroid production often demonstrate "the classic x-ray changes" of avascular necrosis of bone. Bone scintigraphy in these patients most frequently demonstrates an increased radionuclide localization. The literature suggests that the increased activity is related to healing of the avascular process. In a recent study of Legg-Calve-Perthes Disease (LCPD), 37 of the children had multiple studies and increased activity within the epiphysis during revascularization was extremely rare. Not only are the scintigraphic findings in steroid osteopathy dissimilar to that in healing LCPD, but the time interval for healing is much to short for that of avascular necrosis and no patients demonstrated an avascular phase on bone scintigraphy.

Of 15 children with renal transplants on steroid therapy, 9 demonstrated x-ray and clinical findings of osteopathy. In 8 of 9 instances, bone scintigraphy showed increased localization of radionuclide in the affected bone. Improvement or a return to normal occurred in those patients in whom steroids were discontinued.

The following is a proposed mechanism for steroid osteopathy. Steroids affect the osteoblastic and osteoclastic activity of bone and weaken its internal structure. Ordinary stress produces microtrabecular fractures. Fractures characteristically stimulate reactive hyperemia and increase bone metabolism. The result is increased bone radiopharmaceutical localization. The importance of recognizing this concept is that steroid osteopathy is preventable by reducing the administered steroid dose. As opposed to avascular necrosis, bone changes are reversible.

SCINTIGRAPHIC EVALUATION OF SOFT TISSUE TUMORS WITH TECHNETIUM(V)-99m DIMERCAPTOSUCCINIC ACID, A NEW TUMOR SEEKING RADIOPHRMACEUTICAL. H. Ohta, M. Yoshizumi. Tamatsu Hospital, Kobe, Japan; K. Endo, K. Torizuka, A. Yokoyama, Kyoto University, Faculty of Medicine and Pharmaceutical Sciences, Kyoto, Japan; K. Yamamoto Brookhaven National Lab, Upton, NY

Recently, a very promising tumor seeking agent, a Tc(V)-99m dimercaptosuccinic acid (Tc(V)-DMS), which was labelled under optimal pH 8 and very low $SnCl_2$ concentrations, has been developed. An equilibrium between a stable form and a dissociated form of anion TcO_4^{3-}, structual similarity to PO_4^{3-}, postulated for tumor uptake. And we have previously reported that Tc(V)-DMS scintigram would be useful in the diagnosis of medullary thyroid carcinoma.

In our interest to widen its applicability, the scintigraphic examinations of soft tissue tumors with Tc(V)-DMS and comparative study with Ga-67 citrate were performed in 58 patients. Scintigrams were made 60-120 min after i.v. administration of 10 mCi Tc(V)-DMS using a conventional gamma camera. Tc(V)-DMS was found to have superior sensitivity of 90% for malignant tumors (including aggressive fibromatosis) to that with Ga-67 citrate of 56%, but inferior specificity of 71% to that with Ga-67 citrate of 80%. And the accuracy of the scan in soft tissue tumors with Tc(V)-DMS and Ga-67 citrate was 78% and 71%, respectively. Although the accumulation of Tc(V)-DMS has been detected in some benign soft tissue tumors and the exact mechanism of Tc(V)-DMS accumulation remains to be elucidated, these data indicated that Tc(V)-DMS scintigraphy would be of great use in the detection of extension or location of malignant soft tissue tumors.

10:30-12:00 **Room 217B**

HEMATOLOGY I: LEUKOCYTES

Moderator: David A. Goodwin, M.D.
Comoderator: George N. Sfakianakis, M.D.

MONOCLONAL ANTIBODIES AND COUPLING REAGENTS TO CELL MEMBRANE PROTEINS FOR LEUKOCYTE LABELING. J.G. McAfee, G. Gagne, G. Subramanian, R.F. Schneider. Upstate Medical Center, SUNY, Syracuse, NY.

Current gamma-emitting agents for tagging leukocytes, In-111 oxine or tropolone, label all cell types indiscriminantly, and nuclear localization in lymphocytes results in radiation damage. Coupling reagents and murine monoclonal antibodies (Mab) specific for cell surface antigens of human leukocytes were tried as cell labeling agents to avoid nuclear localization.

10^8 mixed human leukocytes in Hepes buffer were added to tubes coated with 5 mg of dry cyclic dianhydride of DTPA for 15 minutes at room temperature. After washing, 0.1 ml of In-111 Cl in ACD (pH 6.8) was added. After 30 minutes, a cell labeling yield of 23% was obtained. Washing the cells in an elutriation centrifuge showed that this label was irreversible.

Mab for cell surface antigens of human granulocytes were labeled with 300 µCi of I-125 using the Iodobead technic and unbound activity was removed by gel column chromatography. 1-10 µg were added to 10^8 mixed leukocytes in 0.5 ml plasma or saline for 1 hr. With Mab anti-leu M4 (clone G7 E11), an IgM, the cell labeling yield was 21%, irreversible, and specific for granulocytes. With anti-human leukocyte Mab NEI-042 (clone 9.4), an IgG2a, and anti-granulocyte Mab MAS-065 (clone FMC11) an IgG1, the cell labeling was relatively unstable.

Labeling of leukocyte subpopulations with Mab is feasible, and the binding of multivalent IgM is stronger than that of other immunoglobulins. DTPA cyclic anhydride is firmly bound to cell membranes, but the labeling is non-specific.

THE USE OF RADIOLABELED MONOCLONAL ANTIBODIES FOR CELL LABELING IN VIVO. P. W. Doherty, B. Woda, D. J.Hnatowich. University of Massachusetts Medical Center, Worcester, MA.

We have evaluated the potential of in vivo cell surface labeling using radiolabeled monoclonal antibodies (MoAbs) directed against their surface antigens. Two MoAbs, a specific antibody (anti-Thy-1 OX7) and a nonspecific control antibody (anti-CEA) were coupled with DTPA, labeled with ^{111}In and evaluated against rat thymocytes, marrow cells, and lymphoma cells (all known to be Thy-1 positive) both in vitro and in vivo. Enumeration of the cells which bound the radiolabeled MoAb was done by detecting the antibody on the cell surface with a Fl-F(ab')$_2$ goat anti-mouse IgG and analyzing fluorescence (Fl) in a flow cytometer (FACS). The thymocytes, which could be labeled in whole blood, showed a labeling efficiency of 80-100%. The labeling, which could be inhibited by cold antibody, was stable up to 72 hours and did not interfere with either cell viability or functional integrity. Following IV injection of the MoAbs in normal rats, there was very good visualization of the bone marrow not seen with the control. Analysis of the marrow cells on the FACS showed that at two hours over 60% of the marrow cells were specifically labeled as against 2% for the control. Within 15 minutes of injecting ^{111}In-OX7 into rats with lymphoma, 70% of the activity in blood was bound to circulating lymphoma cells. The ability to stably label, rapidly target, and image specific cell populations in vivo has wide ranging diagnostic and therapeutic implications.

LEUKEMIC CELL LABELING WITH INDIUM-111-OXINE. T. Uchida, Y. Takagi, S. Matsuda, T. Yui, T. Ishibashi, H. Kimura, and S. Kariyone. Fukushima Medical college, Fukushima, Japan.

Leukemic cells were labeled with In-111-oxine in patients with acute leukemia. In vitro labeling studies revealed that labeling efficiency reached maxinum 80.8 ± 3.6 % (mean ± 1SD) by 2 times washes after 20 minutes incubation time. Cell viability was assessed by trypan blue exclusion test and in vitro culture of leukemic cells, which showed no cellular damage during labeling procedure. Elution of In-111 from the labeled cells was 10.0 ± 1.2% at 12 hours after labeling. For in vivo leukemic cell kinetic studies, more than 10^8 leukemic cells separated from Ficoll-Hypacque sedimentation were labeled by 30 minutes of In-111-oxine incubation and two times washes at 37°C. In vivo studies were performed in 7 patients with acute myeloblastic, lymphoblastic leukemia and blastic crisis of chronic myelocytic leukemia. Labeled leukemic cells disappeared in single exponential fashion with half life of 9.6 to 31.8 hours. Total leukemic cell pool in peripheral circulation was calculated, which correlated well with peripheral leukemic cell counts (r=0.99). No relationship was observed between total leukemic cell pool and leukemic cell turnover rate. Migration patterns of labeled leukemic cells showed that pulmonary uptake was evident within 15 minutes after the infusion and returned to base-line. Splenic and hepatic uptake showed gradual increase up to 24 hours. Bone marrow accumulation was shown only in 2 cases. Nowadays, we have no suitable radionuclides for leukemic cell labeling. In-111-oxine labeled leukemic cells would overcome this difficulty.

KINETICS OF INDIUM-111-LABELED LEUKEMIC CELLS IN PATIENTS WITH ACUTE NON-LYMPHOCYTIC LEUKEMIA. Y.Suzuki and K. Yamauchi. Tokai University, School of Medicine, Isehara-city, Japan.

The kinetics of autologous leukemic cells labeled with In-111 oxine were studied in 5 patients with acute myeloblastic leukemia(AML) and one patient with acute premyelocytic leukemia(APL), and kinetics of OKM1 monoclonal antibody-treated leukemic cells were studied in one patient with acute monoblastic leukemia(AMoL). Recoveries of 33.7 ±23.3%(range, 22.0 to 48.1%) were achieved at 10min after injection of In-111 oxine labeled leukemic cells in AML and APL patients. However, in a patient with AMoL recovery of 12.3% was only achieved at 10min after injection of OKM1-treated leukemic cells. Clearance of the activity from blood was rapid up to one in all patients. The clearance curve of the activity in 5 AML patients showed a hump or a plateau from one to 5hr after injection of labeled leukemic cells. In APL patient and AMoL patient, however, this hump or plateau was not noted. In AML and APL patients the activity over the spleen was higher than that of over the liverat from 30min to 3hr after and showed a plateau or gradual rising thereafter. In a patient with AMoL, the hepatic activity was higher than the splenic activity at 30min after, but thereafter the latter became higher than the former. Liver activity curves showed transient fall at 3hr after and then gradual uprising in all patients. In a patient with APL, high activity was noted over the kidneys. This rose to a maximum after 3hr and then decreased rapidly. Since In-111 oxine stays firmly attached to the cells in spite of the possibility of radiation damage in a long-term survey, it seems an ideal label for studying leukemic cell kinetics.

IN-111 TROPOLONE COMPLEX FOR STUDY OF LYMPHOCYTE KINETICS: EVIDENCE FOR AN INDUCED DEFECT IN STRUCTURE, FUNCTION AND VIABILITY. E. Balaban, T.R. Simon, P. Kulkarni, J. White, M. Newton, E. Frenkel, Dallas VA Med. Ctr., Dallas, TX.

The lipid soluble In-111 and tropolone complex (In-T) has been proposed as a desirable cell labeling moiety for in vivo studies. Its advantages over In-111 complexed to oxy- or acetylacetonate are water solubility and efficient cell labeling in plasma. We examined the effect of In-T on lymphocyte integrity and function in preparation for studies of lymphocyte kinetics in traffic. At equal concentrations, both normal and lymphocytes from patients with chronic lymphocytic leukemia had cellular In-T uptake consistently 20% greater than that achieved with In-111 oxine. This desirable uptake led to studies of function and viability. Lymphocyte mitogenmediated blastogenic capability (an intrinsic lymphocyte function) was measured in vitro in ficoll-hypaque isolated normal lymphocytes with varying concentrations and intervals of exposure of In-T. Marked impairment of lymphocyte blastogenic responsiveness was seen with 3 different mitogens (concanavalin A, phytohemagglutinin P, and pokeweed mitogen). Severe functional impairment was seen when cells were exposed to a In-T concentration of 10 ul/ml for 20 minutes; and a lesser effect was noted even at 10-minute incubation exposure. Cell viability, evaluated by trypan blue exclusion, was normal immediately following cell labeling, but rapidly and progressively failed to exclude (i.e. effective viability). Scanning electron microscopy demonstrated loss of the normal surface villous architecture within 36 hours of in vit-

ro incubation following a 20-minute exposure. Thus, although In-T has attractive features, its effect on lymphocyte structure, function and viability eliminate it for in vivo studies in traffic kinetics.

SCINTIGRAPHIC FOLLOW UP OF AUTOLOGOUS SPLENIC GRAFTS - AN EXPERIMENTAL AND CLINICAL STUDY. H.Reilmann,H.Creutzig,R.Pabst,D.Kamran,Medizinische Hochschule Hannover, West Germany

The risk of overwhelming sepsis in splenectomized patients is well known and autotransplantation of splenic tissue might be considered as a prophylactic approach.Little is known,however, of the success of grafting in man.

In six patients with autologous grafts after emergency splenectomy the "trapping function" (TF) was measured by sequential scintigraphy with heat damaged red cells every third month.

To correlate TF with blood flow and histology, different experiments were done in pigs: ligation of the splenic artery or partial splenectomy or total splenectomy with grafting of fragments either subfascially or in the greater omentum.TF, blood flow with Rb-86 and immune response was measured at different times after surgery.

Remnants left at the main vessels did not grow, while splenic tissue left at smaller vessels increased in size. There were great differences in blood flow per gram splenic tissue, but a significant correlation between TF and blood flow. All experimental grafts showed a normal function both of the white and the red pulp. In patients there was a growth of grafts in four, while in two no TF could be measured.
TF is an indicator of relative blood flow to splenic grafts and therefore useful in the follow up of grafted patients

10:30–12:00 **Room 212A**

GASTROENTEROLOGY II: GASTRIC

Moderator: Leon S. Malmud, M.D.
Comoderator: Naomi P. Alazraki, M.D.

GASTRIC ULCER LOCALIZATION: POTENTIAL USE OF IN VIVO LABELING. A. Pera and H. Rose, Chicago Osteopathic Medical Center, R. Seevers, C. Bekerman, and S. Pinsky, Michael Reese Hospital and Medical Center, Chicago, IL.

The work of Braunstein et al. suggests that sucralfate labeled by binding to Tc-99m HSA permits the visualization of gastric ulcers. Potential problems with this technique are: 1) decreased binding of sucralfate to ulcer sites due to the labeling method of binding to exogenous protein (HSA); 2) overlying activity that may obscure identification of the ulcer. Because of these problems we have examined the possibility of direct in vivo Tc-99m labeling of sucralfate after it has already bound to the ulcer.

In vitro studies were done to determine the binding of Tc-99m pertechnetate to sucralfate in the presence of tin in HCl solution at pHs comparable to those found in the stomach. Rapid and efficient labeling was achieved with 75-95% of the label bound to sucralfate at 30 minutes.

In vivo studies were performed in rabbits with aspirin induced ulcers and in ulcer free human volunteers. The animal studies confirm that orally administered Tc-99m pertechnetate will bind to previously ingested sucralfate and that the labeled material will bind to the ulcers. Tc-99m pertechnetate was also shown to bind well to previously ingested sucralfate in humans.

Our results suggest that it is possible to label sucralfate in vivo. This method would offer the following advantages: 1) a simpler labeling procedure; 2) the potential of increased sensitivity by delaying the labeling until much of the sucralfate not bound to ulcer has passed, and thus decreasing the activity that remains in the stomach; and also by leaving the protein binding sites of the sucralfate free to interact with the ulcer since no exogenous protein is involved in labeling.

TECHNETIUM-99M COLLOIDAL BISMUTH SUBCITRATE: A NOVEL METHOD FOR THE EVALUATION OF PEPTIC ULCER DISEASE. T.E. Vasquez, K.P. Lyons, M. Raiszadeh, M. Fardi, and P. Snider. Veterans Administration Medical Center, Long Beach, CA.

The therapeutic agent colloidal bismuth subcitrate (CBS) selectively binds to peptic ulcers. We have developed a method for labeling this agent with Tc-99m. Chromatographic quality control studies of the agent on silica gel coated strips (ITLC-SG) showed that more than 97% of Tc-99m was bound to CBS. During in-vitro stability testing, the radiolabel was stable for a minimum of 6 hours. The chromatographic findings are in agreement with the in-vivo distribution of the agent which showed no significant radioactivity in thyroid, kidneys,liver, or bladder. The resulting Tc-99m-CBS solution is administered orally in drinking water. Preliminary animal studies have been conducted on 5 adult 3 kg New Zealand rabbits sedated with 50 mg Ketamine I.M. The rabbits were intubated with I.V. tubing advanced to the stomach. They were given a gastric erosive suspension of 600-1000 mg/kg of pulverized ASA in 10 cc tap water. Four hours later they were given 3-4 mCi of the radiotracer in a 5 cc volume of water. Serial in-vivo images were obtained for 2 hours which included thyroid, abdomen, and urinary bladder. Next the stomachs were excised, opened along the greater curvature, imaged, vigorously washed and reimaged.

All 5 rabbits showed avid localized binding of radiotracer which remained fixed even with vigorous washing. Areas of normal appearing mucosa were relatively devoid of radiotracer.

This new compound may have significant clinical usefulness in the detection of peptic ulcer disease. In addition, such a non-invasive technique, carrying none of the risks or discomfort of endoscopy could also find application in the evaluation of the response to therapy.

ASSESSMENT OF GASTRIC EMPTYING IN NORMAL SUBJECTS WITH SUCRALFATE (CARAFATE) AND AMPHOJEL. A.R. Marano, E.K. Prokop, V.J. Caride, R. Mc Callum. Hospital of St. Raphael and Yale Medical School, New Haven, CT.

Aluminum-containing antacids (e.g Amphojel) and aluminum-containing compounds such as sucralfate (Carafate) have been shown in animal and human studies to delay gastric emptying, and are one proposed mechanism of action for healing of duodenal ulcers. Therefore, we designed a study to study the effects of Carafate and Amphojel on gastric emptying.

Ten normal volunteers of mean age 27 years with no previous history of upper gastrointestinal diseases were studied. For each test the subject ingested a meal composed of 30gm of cooked chicken liver injected with 1mCi of 99m-Tc-S-C, mixed with 7.5 oz. of beef stew, and eaten with 4 oz. of water labeled with 100uCi of 111-In-DTPA. Immediately after ingestion of the meal, the subject was placed supine under a gamma camera. Gastric emptying (GE) was expressed as percent emptyed. On separate days the subject was given either 1gm of Carafate (190mg Al/gm) or placebo in a double blind fashion one hour prior to the test meal. On the third day, each subject was given 30cc of Amphojel (105mg Al/5cc) followed 30 minutes later by the test meal. GE at 2 hours for the solid meal was 60%, 69%, and 54% and 79%, 86%, and 68% at 3 hours for placebo, Carafate, and Amphojel respectively. A small but not significant difference in gastric emptying between Amphojel and placebo was seen from 2 to 3 hours. For the liquid meal approximately 90% emptying was present at 1 hour for all three studies. Further studies will be needed to determine whether these medications administered in the standard doses given here may affect gastric emptying in duodenal ulcer patients.

HISTAMINE DELAYS GASTRIC EMPTYING OF SOLID FOOD IN MAN THROUGH HISTAMINE, RECEPTORS. K. Sridhar, R. Lange, and R.W. McCallum, Yale University, New Haven, Connecticut.

We have shown that histamine (H) contracts the cat

pylorus and duodenum through H_1 receptor mechanisms (J Clin Invest 68:582, 1981). We investigated the effect of H infusion on gastric emptying (GE) and the role of H_1 and H_2 receptor blockade in healthy volunteers. Radionuclide GE studies were performed using chicken liver labeled in vivo with ^{99m}Technetium-sulfur colloid as a marker of solid food. Study days were as follows: a baseline GE study (Day 1); H infused continously IV at a rate of 40 ug/kg/hr during the GE study (Day 2); an IV bolus of 50 mg of diphenhydramine (Day 3), or 300 mg cimetidine (Day 4) given just prior to the continuous infusion of H; a final day when cimetidine was given alone (Day 5). GE was monitored for 2 hours on each day. The results of Days 1, 2 and 3 are summarized below (†p<0.05 vs baseline or Day 1).

	% ISOTOPE REMAINING IN THE STOMACH (MEAN±SEM)			
Study Day				
1	87.5±5.6	71.6±7.5	56.3±5.0	44.5±4.5
2	98.9±1.1	93.4±2.7†	77.1±4.0†	†60.6±1.4
3	82.3±4.8	65.0±5.4	53.2±6.8	42.7±6.5

Pretreatment with cimetidine (Day 4) augmented the delay in GE induced by H infusion, while cimetidine without H (Day 5) had no effect on GE. We conclude that: 1) H given at a dose which elicits maximal acid secretory response in man significantly delays GE; and 2) H_1 receptor blockade but not H_2 blockade prevented this effect. Histamine may play a modulatory role in human gastric emptying through an H_1 receptor mechanism.

VARIABILITY OF GASTRIC EMPTYING TIME USING STANDARDIZED RADIOLABELED MEALS. P.E. Christian, C.M. Brophy, M.J. Egger, A. Taylor, J.G. Moore. University of Utah School of Medicine, Salt Lake City UT

To define the range of inter- and intra-subject variability on gastric emptying measurements, eight healthy male subjects (ages 19-40) received meals on four separate occasions. The meal consisted of 150 g of beef stew labeled with Tc-99m SC labeled liver (600 uCi) and 150 g of orange juice containing In-111 DTPA (100 uCi) as the solid- and liquid-phase markers respectively. Images of the solid and liquid phases were obtained at 20 min intervals immediately after meal ingestion. The stomach region was selected from digital images and data were corrected for radionuclide interference, radioactive decay and the geometric mean of anterior and posterior counts.

More absolute variability was seen with the solid than the liquid marker emptying for the group. The mean solid half-emptying time was 58 ± 17 min (range 29-92) while the mean liquid half-emptying time was 24 ± 8 min (range 12-37). A nested random effects analysis of variance showed moderate intra-subject variability for solid half-emptying times (rho = 0.4594), and high intra-subject variability was implied by a low correlation (rho = 0.2084) for liquid half-emptying. The average inter-subject differences were 58.3% of the total variance for solids (p = 0.0017). For liquids, the inter-subject variability was 69.1% of the total variance, but was only suggestive of statistical significance (p = 0.0666).

The normal half emptying time for gastric emptying of liquids and solids is a variable phenomenon in healthy subjects and has great inter- and intra-individual day-to-day differences.

DO CALORIES OR OSMOLALITY DETERMINE GASTRIC EMPTYING. R.B. Shafer, A.S. Levine, J.M. Marlette, and J.E. Morley. VA Medical Center, Minneapolis, MN.

Recent animal studies suggest that gastric emptying is dependent on the caloric and osmotic content of the ingested food. These studies have involved intubation with infusion of liquid meals into the stomach. Scintigraphic methods, which are non-invasive and do not alter normal physiology, are now available for precise quantitation of gastric emptying. To study the role of calories and osmolality on gastric emptying, we employed a standardized ^{99m}Tc-scrambled egg meal washed with 50 cc tap water in 10 normal human volunteers. A variety of simple and complex sugars, non-absorbable complex carbohydrate (polycose), medium chain fatty acid (MCFA) and gluten were dissolved in water and ingested with the test meal. Each subject acted as his own control. Coefficient of variation in control tests in each subject 12 weeks apart was 9.9%. Results showed that incremental glucose (25-66 gm) produced a linear increase in gastric emptying (T/2 control 50 ± 3, 25 gm 60 ± 3, 50 gm 79 ± 3 and 66 gm 102 ± 3 minutes). 25 gm fructose (T/2 59 ± 3 minutes) and 25 gm polycose (T/2 59 ± 3 minutes) had similar effects to glucose. 25 gm sucrose and 25 gm gluten did not significantly differ from controls. MCFA had an effect similar to 50 gm glucose -- suggesting that calories are important in gastric emptying. However, 25 gm xylose markedly prolonged gastric emptying to 80 ± 5 minutes. The rank order for osmolality for substances tested MCFA = gluten < polycose < fructose < sucrose = glucose < xylose defined no relationship to gastric emptying. Our results suggest that neither calories nor osmolality alone determine gastric emptying. A specific food does not necessarily have the same effect on gastric emptying in different individuals.

1:30-3:00 **Room 217A**

CARDIOVASCULAR IV: MYOCARDIAL BLOOD FLOW

Moderator: Donald H. Schmidt, M.D.
Comoderator: Frans J. Wackers, M.D.

DUAL LABEL SINGLE PHOTON EMISSION TOMOGRAPHY: A NEW METHOD TO ASSESS REDISTRIBUTION IN REGIONAL CORONARY BLOOD FLOW AFTER NITROGLYCERIN. P. Liu, S. Houle, B. Kimball, R.J. Burns, D. Gilday, R.D. Weisel, A. Warbick-Cerone, L. Johnston, and P.R. McLaughlin, Toronto, Canada

We have developed a new method to quantitate changes in coronary blood flow (CBF) by single photon emission tomography (SPECT) of dual-labelled intracoronary human albumin microspheres (HAM) before and after an intervention. After initial validation in pigs, we studied 20 pts in the cath lab with 10 pts receiving saline to serve as controls, and 10 pts receiving nitroglycerin (NTG). Thermodilution coronary sinus flow (CSF) measurements were made at rest and after each intervention. After pacing to mild angina, serial injections of Tc-99m HAM, 40 µg of NTG or saline, and In-111 HAM were made in the left main coronary artery. After routine coronary arteriography, the pt underwent dual-peak SPECT with the image slices reconstructed along the longitudinal axis of the heart. Quantitative circumferential profiles were made for each slice by plotting the average count per pixel in each 18° segment of the left ventricle. After correction for absolute coronary blood flow, the difference between the pre- and post-NTG profile was obtained, and a significant change took place if it exceeded 2 S.D. from control. The segments were classified into normal, mildly, moderately or severely compromised territories according to upstream coronary anatomy. Results were as follows:

Perfusion Class	% Stenosis	% segment with increase in flow	Total % increase in flow
Normal	<50	67	24
Ischemic: Mild	50-75	71	33 *
Moderate	75-90	77 *	44 *
Severe	>95	52 *	17 *

(* p<.05 as compared to normal)

We conclude: (1) SPECT of intracoronary HAM combined with CSF measurement represents a powerful tool in assessing changes in regional CBF after an intervention; (2) By this method, NTG gave preferential redistribution of CBF to the mild and moderately ischemic zones of the heart.

THE RELATIONSHIP OF CORONARY FLOW RESERVE (CFR) TO STRESS THALLIUM-201 MYOCARDIAL PERFUSION (Tl) AND RADIONUCLIDE VENTRICULOGRAPHY (RNV). V. LeGrand, R. Vogel, M.D. Gross, J. Mancini, VA Medical Center, Ann Arbor, MI 48105.

Coronary arteriography (CA) can be used to delineate the abnormal anatomy in coronary artery disease (CAD), but the degree of the impairment of coronary blood flow (CBF) cannot be predicted precisely by CA. As a reduction in maximal hyperemic blood flow (MHBF) characterizes a functionally significant coronary lesion, the ratio of contrast-induced MHBF to basal CBF: the coronary flow reserve (CFR) reflects the physiologic significance of a coronary lesion. Recent developments in digital coronary angiography allow CFR to be measured at CA. To assess the relationship of CFR to other noninvasive tests of myocardial perfusion and

function the results of stress Tl and RNV were compared to those of CA and CFR for the distribution of 48 arteries in 20 patients. Seven patients had normal CA without spasm: 3 with abnormal CFR had a discrete Tl defect or global RNV dysfunction. The remaining 4 had normal CFR, Tl and RNV. Thirteen had CAD without prior infarction. Segmental Tl and RNV were compared to CA and CFR (table).

	CA (% Stenosis)		CFR	
	< 50%	> 50%	Normal	Abnormal
Tl	0 / 19	10 / 12	0 / 21	10 / 10
RNV	0 / 19	6 / 12	1 / 21	6 / 10

Normal CFR was seen in patients with both normal Tl and RNV; while Tl was best associated with abnormal CFR in CAD and may be the preferable noninvasive modality to identify physiologically significant, abnormal CBF in suspected cases of CAD.

ASSESSMENT OF STENOSIS SEVERITY: CORRELATION OF ANGIOGRAPHY, T1-201 SCINTIGRAPHY, AND INTRACORONARY PRESSURE GRADIENTS. T Bateman, M Raymond, L Czer, A Chaux, R Kass, J Matloff, D Berman, R Gray. Cedars-Sinai Medical Center, Los Angeles, CA

To clarify the relationship between angiographic and hemodynamic stenosis severity and the appearance during stress-redistribution myocardial Tl-201 scintigraphy (Ex-Tl) of a visual (V) or quantitative (Q) perfusion defect (PD) or washout (WO) abnormality, 24 pts with CAD underwent intracoronary pressure gradient study at bypass surgery (CABG). All had pre-CABG Ex-Tl without interval deterioration. The mean diastolic pressure gradient (MDG) measured at reproducible hyperemic flow rates was determined for 34 stenoses (13 LAD, 7 LCX, 14 RCA) and compared with the results of Ex-Tl in subtended myocardial regions (LAD=anterior; LCX=posterolateral; RCA=inferior). Fourteen stenoses (50-99% diameter narrowing) were unassociated with VPD despite maximal exercise: MDG was 9±5mmHg, with MDG/mean aortic diastolic pressure (ADP) ratio of 0.12±0.07. QPD and QWO analysis detected 8 of these. Thirteen stenoses (90-100% severity) led to reversible VPD: MDG was 36±11 mm Hg, MDG/ADP ratio was 0.52±0.17, and Q analysis was abnormal in 12/13. Seven stenoses (90-100% severity) subtended infarcted myocardium: MDG was 42±21 mm Hg, MDG/ADP ratio was 0.52±0.18, and V and Q analyses were abnormal in all. Conclusions: 1) Ex-Tl correlates better with hemodynamic severity of stenoses than does angiography; 2) V abnormalities identify stenoses of major angiographic and hemodynamic severity, while Q analysis detects some (57% in this study) stenoses of lesser severity; 3) stenoses causing reversible Ex-Tl abnormalities present similar hemodynamic impediments to those causing myocardial infarcts.

EFFECT OF PERCUTANEOUS TRANSLUMINAL CORONARY ANGIOPLASTY ON CORONARY RESERVE. T. Lassar, L. Hendrix, G. Ray, and D. Schmidt. University of Wisconsin Medical School-Mount Sinai Medical Center, Milwaukee, WI.

This study was done to assess the effect of percutaneous transluminal coronary angioplasty (PTCA) on regional myocardial perfusion (RMP) in the region distal to a stenosis in 48 patients. Quantitative RMP in ml/100g/min was measured from the washout of Xe-133 following selective injection into the involved coronary artery. After successful dilatation, determined by a reduction in %stenosis to a ≤ 50% lesion and in pressure gradient across the lesion, the RMP measurement was repeated. In these patients, mean %stenosis was 85% pre PTCA and 29% post PTCA with mean pressure gradient of 60 mm Hg pre PTCA and 21 mm Hg post PTCA. 21 of these 48 patients also had RMP measured after isoproterenol (ISO) both pre and post PTCA to increase myocardial oxygen demand to assess coronary reserve. Heart rate (HR) and systolic blood pressure (SBP) were constant pre and post PTCA which allowed a valid comparison. The results were as follows:

	Control (n=48)		ISO (n=11)	
	Pre	Post	Pre	Post
RMP	71±18	84±22*	119±23	144±35*
HR	75±11	71±12^{ns}	103±18	105±21^{ns}
SBP	136±20	133±21^{ns}	138±30	137±32^{ns}

Compared to pre: *p<.05, ns=not significant

A group of 13 patients with normal coronary arteries and ventricular function showed a mean control RMP of 78±15 and a mean ISO RMP of 140±26. The data demonstrate that following successful PTCA quantitative RMP improves both at rest and with an ISO challenge and is similar to RMP in normal coronary arteries.

REGIONAL HETEROGENEITY OF MYOCARDIAL BLOOD FLOW DETECTED AND QUANTIFIED BY XENON-133 WASHOUT ANALYSIS IN PATIENTS WITH CORONARY ARTERY DISEASE. S. Port, T. Lassar, and D.H. Schmidt. University of Wisconsin Medical School, Mount Sinai Medical Center, Milwaukee, WI.

The Xenon-133 washout technique has been used to measure myocardial blood flow (MBF). However, controversy exists regarding the ability of the method to detect regional heterogeneity of MBF. We measured MBF (ml/100gm/min) in the circumflex and anterior descending arteries after injection of 12-15 mCi Xenon-133 in saline into the left coronary of 12 patients. Each patient had one diseased branch (≥75% stenosis) and one normal branch (0-30% stenosis) of the left coronary. Control flow (C-MBF) was measured and flow was remeasured after 0.15 mg/kg/min x 4 min. intravenous dipyridamole (D-MBF). Coronary resistance (Res) was calculated as mean aortic pressure/MBF.

	0-30% Stenosis	≥75% Stenosis
C-MBF	67±13	61±14
D-MBF	208±43	134±41*
D/C MBF	3.2±0.7	2.2±0.6*
C-Res	1.5±0.3	1.8±0.4*
D-Res	.5±0.1	0.8±0.2*

*p<.03 compared to 0-30% stenosis group

After dipyridamole, significant regional heterogeneity of tracer uptake was seen on the Xenon images. As shown above, MBF in the diseased artery was markedly lower and resistance higher compared to the normal artery. The ratio of D-MBF in the diseased vessel to D-MBF in the normal vessel was 0.64±.13.

These data provide unequivocal evidence that this technique can detect and quantitate regional heterogeneity of coronary flow even when low flow areas are contiguous with high flow areas.

COMPARISON OF THE ANGIOGRAPHIC AND SCINTIGRAPHIC EVALUATION OF THE SUCCESS OF PERCUTANEOUS TRANSLUMINAL CORONARY ANGIOPLASTY. V. LeGrand, F. Wueron, W.W. O'Neil, J. Juni, M.D. Gross, R. Vogel, University of Michigan and the VA Medical Centers, Ann Arbor, MI 48105.

The hemodynamic effects of percutaneous transluminal coronary angioplasty (PTCA) are difficult to assess as the change in the degree of arterial stenosis (AS) or transluminal pressure gradients (TPG) do not portray the functional result of this procedure. Diminished maximal hyperemic blood flow (MHBF) characterizes a functionally significant coronary lesion and the ratio of MHBF to basal coronary blood flow: the coronary flow reserve (CFR), which now can be estimated at the time of coronary angiography (CA), is an alternative approach to determining the physiologic significance of a lesion. CFR was obtained in 5 patients with single vessel coronary artery disease (CAD) and compared to stress Thallium-201 myocardial scintigraphy (Tl), ejection fraction (EF) and ventricular wall motion (WM) by radionuclide ventriculography (RNV) and the results of CA (AS and TPG) before and after PTCA.

	Before PTCA	After PTCA
Δ EF(< 5%)	4/4	1/4
WM assynergy:	4/4	0/4
Tl defect:	5/5	0/5
AS (%):	60 to 99	20 to 40
TPG (mmHg):	30 to 65	10 to 25
CFR abnormal:	5/5	0/5

Despite the persistence of moderate AS and/or a TPG, Tl and WM returned to normal when CFR was normalized. Thus, Tl and RNV are reliable, noninvasive indicators of the functional results of PTCA and can be used to assess its hemodynamic effects.

1:30-3:00 Room 216BC

COMPUTERS AND DATA ANALYSIS II: CARDIAC

Moderator: David A. Weber, Ph.D.
Comoderator: Thomas K. Lewellen, Ph.D.

VALIDATION OF FACTORIAL ANALYSIS IN A SIMULATION STUDY AND IN SEQUENTIAL CARDIAC FIRST-PASS ACQUISITIONS. J.C. Maublant and I. Mena, UCLA School of Medicine, Harbor-UCLA Medical Center, Torrance, CA.

This study was designed to assess the accuracy and reproducibility of factorial analysis. Assuming that a dynamic acquisition visualizes several overlapping compartments (cpts) having different time-activity curves (TACs) then factorial analysis is supposed to isolate the TACs of these different cpts. Its accuracy was tested with a computer simulated 16-frame dynamic acquisition representing two cpts partly or completely overlapping and having different TACs. The reproducibility was assessed in seven patients who underwent six consecutive left ventricular first-pass radionuclide angiographies, three in the right and three in the left anterior oblique projections. Because of the short half-life of the tracer (gold-195m, T 1/2 = 30.5 sec) all the acquisitions could be performed in similar conditions of background. A series of 16 frames representing a composite cardiac cycle was reconstructed with four beats and submitted to factorial analysis. In the simulation data a perfect accuracy was found in any situation of partially overlapping cpts. For the totally overlapping cpts differing in size, the TAC of the small cpt was often distorted while the TAC of the large cpt was always correctly identified. In the patients the time of maximum and minimum of the TACs was reproducible in all projections. The coefficient of correlation of the amplitude was 0.74 between the RAO and LAO projections. By comparison it was 0.73 for the TACs obtained from a left ventricular region of interest. In conclusion factorial analysis provides sufficiently accurate and reproducible results in cardiac first-pass study to envision its clinical applications.

A COMPUTER MODEL LEADING TO QUANTIFICATION OF FIRST PASS RADIONUCLIDE IMAGING IN VENOUS OBSTRUCTION. P.W. Barr and T.R. Simon. Dallas V.A. Medical Center, Dallas, TX.

Superior vena cava (SVC) syndrome may develop gradually, denying necessary emergency radiation therapy because of delayed recognition. Conventional interpretation of dynamic radionuclide SVC-grams typically miss 50% of clinically asymptomatic patients. We hypothesized that a numerical model describing radio-labeled blood flow in the vicinity of vascular obstruction would improve sensitivity without compromising specificity and allow quantitation of the test.

This fluid dynamic model assumes steady-state incompressible flow in a rigid pipe. The model examines intermixing of labeled and unlabeled confluent branches, as well as flexible acquisition geometries, timing, and radionuclide bolus characteristics. Computer generated time-activity curves (TAC's) were analyzed using procedures which maximize sensitivity to the magnitude of obstruction while minimizing the effects of bolus and acquisition variations. We demonstrated that the integral of the TAC over any vessel segment represents a local relative mean velocity, given a bolus which completely traverses the region of interest. Thus, from a calculated local relative velocity, a local relative vessel diameter may be inferred. A simple data reduction process, which lends itself to digital data processing equipment commonly found in nuclear imaging laboratories, was developped. Advantages of the technique include quantitation of the obstruction, and the facility to summarize the dynamic study as a single velocity image.

So far, these predictions aided in diagnosing 8 patients with suspected SVC obstruction and 2 normal controls. We found good agreement between conventional contrast angiography (when available) and the modeled velocity radioangiogram for determining obstruction sites and magnitudes. Furthermore, the improved sensitivity of the technique allowed detection of obstructions far smaller than those detected by conventional dynamic radioangiography.

We conclude that this model provides clinically significant quantitation that improves the detection rate for SVC obstruction.

UNDERESTIMATION OF CARDIAC DIASTOLIC PARAMETERS USING HIGH PHASE RECONSTRUCTION S.L. Bacharach, M.V. Green, P.J. Parentesis, A.M. Sindelar, R.O. Bonow, H.O. Ostrow, S.M. Larson. NIH, Bethesda, MD

High phase (HP) mode cardiac gating capabilities have recently become available on commercial computer systems. The assumption is made in the HP method that fluctuations in beat length cause uniform compression or expansion of events in the cardiac cycle. The HP method thus alters the time per frame from beat to beat, so that all beats precisely fit into a fixed number of frames, eliminating count fall-off in late diastole. The assumptions made in the HP method differ from those of the usual, fixed time per frame high temporal (HT) resolution method. We applied both techniques to the same list mode data from 25 subjects in normal sinus rythm (NSR) studied at rest. HP always used 40 frames, while HT used a time/frame for each subject equal to the same mean duration (1/2 msec) as HP. A clinically irrelevant (<1%) difference in left ventricular (LV) ejection fraction (EF) was found between HT and HP. LV Peak ejection rate (PER) was higher with HT than HP (P>0.95) by 4% on average, and peak filling rate (PFR) was 14% higher on average with HT than HP (P>0.999). Times to PER and PFR did not differ significantly. Theoretical calculations and simulations (varying beat length by both cycle truncation and "stretching") showed that if a violation of the assumptions of either the HP or HT models occurs, that model will produce reduced values of EF, PER and PFR, the reduction being most apparent for diastolic parameters. Our data suggest therefore that the assumptions underlying the HP method are less valid than those of the HT method in resting subjects in NSR. We conclude that for systolic parameters these inter-method differences are negligible. Diastolic parameters may be significantly underestimated using the HP method

FAST AND RELIABLE AUTOMATED VENTRICULOGRAPHY FOR GATED BLOOD-POOL STUDIES. M.G. Lima. Technicare Corp, Solon, OH

A set of algorithms, requiring only one single operator-interaction and minimal running time, has been generated to analyze left-ventricular function from cardiac gated Tc-99m Blood-pool Nuclear Medicine scintigrams (CBPS).

The process depends mainly on an optimal edge enhancement filter derived in the frequency domain and applied to the study via FFT. The bandpass filter is based on Prolate Spheroidal wave functions and was described by Shanmugam et al in 1979. It maximizes output in the vicinity of edges, and is adapted here to enhance the ventricular region of interest (ROI) yielding images with sharp edges and good signal-to-noise ratio (SNR). This procedure does not require previous background subtraction from initial images in order to adequately define left-ventricular contours. A filter format has been chosen which will allow successful performance of the technique over a wide range of CBPS.

The filtered image is then scanned and, on the original frame edges around ROI are marked and counts within ROI are defined. It will automatically run for any allowed number or size of frames. Processing time averages less than one minute when employing an Array Processor for a set of 32 64x64 pixel frames.

Nuclear Medicine image processing applications of such filter have not been reported to date. This process has been tested on variable rate, variable ejection fraction, known volume Vanderbilt cardiac phantom; with maximum deviation of 3.5% and estimated standard diviation (SD) of 1.7%.

When compared to other processes currently available, this technique is clearly more reliable due to its accuracy, speed and simplicity. It has also been used to determine ventricular volumes from gated SPECT images, with a respectable SD of 2.8%.

EFFECTS OF 180° ACQUISITION ON TOMOGRAPHIC IMAGE QUALITY. R.L. Eisner, G.T. Gullberg, J.A. Malko and D.J. Nowak, General Electric Medical Systems Group, Milwaukee, WI and Emory University, School of Medicine, Atlanta, GA.

A computer simulation study was performed to isolate the effects of various parameters on tomographic image quality derived from view data acquired over 180°. The shape of the tomographic point spread function is found to depend on the exact 180° of view data used to perform the reconstruction. Distortions arise because of the view-to-view variation of the planar point

spread function caused by changes in the distance between the point source and the camera-collimator system and the associated effects due to attenuation and scatter. Quantitative tomographic studies can thus be compromised by the nature of the 180° view data used for reconstruction. Circumferential profile analysis of simulated myocardium reconstructions in simple attenutators, for example, shows that regional uptake becomes progressively more incorrect as the 180° acquisition becomes more asymmetric about the planar view of maximum cardiac counts. Moreover, for routine 180° tomographic acquisitions, distortion in object shape should be expected for non-symmetric data acquisition. For objects close to the collimator surface, 180° acquisition does provide a significant improvement in tomographic resolution compared to a 360° acquisition.

PHARMACOKINETICS OF I-123 METAIODOBENZYLGUANIDINE (MIBG). WHY AND WHEN PHEOCHROMOCYTOMAS (PHEO) ARE IMAGED. J. Glowniak, J. Sisson, B. Shapiro, T. Mangner, L. Myers, D. Wieland, W. Beierwaltes. University of Michigan Medical Center; Ann Arbor, MI

I-131 MIBG detects PHEO but tumors have been found to visualize scintigraphically at different times after injection of the agent. Although most tumors are seen best at 48 hours and later, some are seen better or only at 24 hours after injection. Early release of I-131 MIBG by some tumors may contribute to the 10% false negative rate of this procedure. Compared with I-131, I-123 has better imaging characteristics and can be given in larger doses, thus lending I-123 MIBG to quantification and assessment of pharmacokinetics. Six patients with PHEO (1 bilateral, adrenal, 1 extra-adrenal, 4 malignant) were studied after injection of 6-10 mCi of I-123 MIBG. Images obtained at 17-24 hours invariably portrayed the PHEO better and detected more of the malignant tumors than those at 2-3 hrs. The extra-adrenal PHEO was seen only at 17 hours with I-123 MIBG and only at 24 hours in the longer I-131 MIBG studies.

The ratio of net biologic retentions of I-123 MIBG after background subtraction and correction for physical decay in the tumors at different times (~20 hr/~2 hr) varied widely: 0.54-1.59, including ratios in tumors within the same patient. Ratios of retentions in the peri-tumor backgrounds were 0.38-0.86.

In conclusion: (1) superior imaging characteristics of I-123 permit pharmacokinetic studies of I-123 MIBG of PHEO, (2) visualization was better at ~ 20 than at ~ 2 hrs because I-123 MIBG decreased more rapidly from background than from tumors and probably because the I-123 MIBG concentration increased in some tumors.

1:30–3:00 **Room 214BC**

RADIOPHARMACEUTICAL CHEMISTRY III: HALOGENS

Moderator: Daniel S. Wilbur, Ph.D.
Comoderator: Donald M. Wieland, Ph.D.

RADIOSYNTHESIS AND PHARMACOKINETICS OF HIGH SPECIFIC ACTIVITY ^{75,77}Br-BROMPERIDOL, A POTENT BUTYROPHENONE NEUROLEPTIC. S.M. Moerlein and G. Stöcklin. Institut für Chemie 1 (Nuklearchemie), Kernforschungsanlage Jülich, Fed.Rep.Germany

Bromperidol, 4-[4-(4-bromophenyl)-4-hydroxypiperidino]-4'-fluorobutyrophenone, is a potent neuroleptic which has found clinical use in the treatment of schizophrenia. Of the major dopaminergic receptor-binding ligands, bromperidol has the greatest specificity for binding to cerebral dopamine receptors (K_i = 3.7 nM) relative to competitive cerebral serotonin (K_i = 26 nM), α-adrenergic (K_i = 100 nM) or histamine (K_i = 700 nM) receptors. We have therefore prepared bromperidol labelled with no-carrier-added (n.c.a.) ^{75}Br ($t_{1/2}$ = 1.6 hr β^+) or ^{77}Br ($t_{1/2}$ = 52 hr EC) for evaluation as a radiopharmaceutical for mapping cerebral dopamine receptor areas with PECT technology, as well as for non-invasive pharmacodynamic studies in man with conventional nuclear medicine equipment.

4-[4-(4-trimethylstannylphenyl)-4-hydroxypiperidino]-4'-fluorobutyrophenone, TMSn-P, was synthesized in 40% chemical yield by reaction of trimethylstannyl sodium with bromperidol. TMSn-P was purified by preparative HPLC and characterized by ^{1}H-NMR and GC-MS. TMSn-P was radiobrominated in methanol using n.c.a. $^{75}Br^-$ or $^{77}Br^-$ and dichloramine-T as oxidizing agent. Product ^{75,77}Br-bromperidol was separated from impurities, including chlorinated side-product haloperidol, using HPLC (RP-18; MeOH/H_2O/Et_3N = 70/30/0.3). For a reaction time of 5 minutes, and an overall radiopharmaceutical production time of 30 minutes, ^{75,77}Br-bromperidol was obtained in physiological saline solution with 40% radiochemical yield and a specific activity > 10,000 Ci/mmole. The pharmacokinetics in rodents and PECT studies in primates using ^{75,77}Br-bromperidol will be compared with that of previously-reported ^{75,77}Br-brombenperidol.

MODIFICATION OF LYPOPHILIC GROUPS AND REPLACEMENT OF PHOSPHORUS BY ARSENIC TO STUDY THE EFFECT ON MYOCARDIAL SPECIFICITY OF RADIOIODINATED PHOSPHONIUM CATIONS. P. C. Srivastava, B. A. Owen, and F. F. Knapp, Jr., Nuclear Medicine Group, Oak Ridge National Laboratory, Oak Ridge, TN.

The organic cation, (E-1-iodo-1-penten-5-yl)triphenylphosphonium iodide (I), shows attractive myocardial uptake and retention in rats and dogs. The effect of modification of lypophilic groups attached to phosphorus and replacement of phosphorus by arsenic on myocardial specificity and retention of radioiodinated cations has now been evaluated. Triphenylarsonium (II, M=As), dicyclohexylphenylphosphonium (III, M=P) and dimethyl-n-octylphosphonium (IV, M=P) cations ($[R_3M^+$-$(CH_2)_3$-CH=CH*I$]I^-$) attached to the E-1-[^{125}I]iodo-1-pentenyl group were prepared via NaI-chloramine T iodination of the corresponding vinylboronic acid cation substrates. Compounds I-IV and the respective precursors were analyzed (TLC, NMR, and C&H) and ^{125}I analogs I-IV were evaluated in rats (5/group). All four agents showed good uptake and retention demonstrating that these structural alterations do not greatly affect the myocardial specificity of these interesting new agents.

^{125}I Compound	Range in heart, % dose/gm (mean heart:blood)		
	5 min	30 min	60 min
I	3.7-4.7 (22)	3.4-5.3 (38)	3.8-4.5 (50)
II	1.7-3.6 (11)	2.6-4.3 (13)	3.7-3.7 (18)
III	2.8-3.8 (9)	2.7-3.7 (16)	3.2-3.9 (21)
IV	2.2-2.9 (6)	1.4-2.4 (8)	1.9-3.6 (19)

Research sponsored by the Office of Health and Environmental Research, U.S. Department of Energy, under contract W-7405-eng-26 with the Union Carbide Corporation.

COMPARATIVE DUAL TRACER STUDIES OF β-METHYL-(1-C-14)HEPTA DECANOIC ACID (BMHDA) AND 15-p-(I-131)-IODOPHENYL-β-METHYL PENTADECANOIC ACID (BMPDA) IN HYPERTENSIVE RATS. K. Yamamoto, P. Som, A. B. Brill, Y. Yonekura, M. M. Goodman, F. F. Knapp, Jr., D. R. Elmaleh and H. W. Strauss. Brookhaven National Laboratory, Upton, NY, Oak Ridge National Laboratory, Oak Ridge, TN, and Massachusetts General Hospital, Boston, MA.

C-11 labeled BMHDA, a branched chain fatty acid, has been reported to be a potential myocardial metabolic tracer for positron emission tomography (PET).

We have studied the distribution of C-14 BMHDA and I-131 BMPDA in hypertensive rat hearts, using quantitative dual isotope autoradiographic (ARG) techniques.

Dahl stain rats (blood pressure: 214±8 mmHg) were injected with 10 μCi of C-14 BMHDA and 170 μCi of I-131 BMPDA. Just after sacrifice, hearts and lungs were removed and processed for ARG. The tissue sections (20 μm thick) were placed on x-ray film for 1 day to reveal the distribution of I-131. The 2nd exposure for C-14 was performed 3 months later to permit the decay of I-131. Selected pairs of ARG images were digitized and quantitated using a videodensitometric system.

C-14 BMHDA showed very heterogenous distribution in the hypertensive myocardium. Decreased uptake was seen in the endocardial region. I-131 BMPDA showed the same uneven distribution as C-14 BMHDA. The correlation coefficients

of these two tracers distribution calculated from paired quantitative images were excellent (0.91-0.96).

Our data suggest that I-123 labeled BMPDA could be used as a biochemical marker to measure fatty acid derangement for single photon emission tomography, and may have wider application than C-11 BMHDA which is limited due to availability of PET devices.

DOE Cont. No. DE-AC02-76CH00016 (BNL); W7405-eng-26 (ORNL)

RADIOIODINATED FENETYLLINE (CAPTAGON) - A NEW POTENTIAL BRAIN IMAGING AGENT ? H.J.Biersack, H.Klünenberg, H.P. Breuel, S.-N.Reske, K.Reichmann, C.Winkler, Inst.Nuclear Medicine, University of Bonn and Amersham Buchler,Braunschweig

Since about 2 years ^{123}I-labeled iodoamphetamines (IMP) and diamines (HIPDM) have been used for scintigraphic brain investigations. As another possibly useful brain imaging agent we studied radioiodine labeled Fenetylline which is metabolized into Amphetamin. Thirty wistar rats were injected 5 µCi ^{125}I-IMP and 2 µCi ^{131}I-Fenetylline each simultaneously. The animals were sacrificed 5,10,15,30,60, and 120 min. p.i.. The radioactivity content of tissue specimens (brain, cerebellum, liver, kidney, lung, myocardium, muscle) was measured in a well-counter (% dose/g tissue). In 2 dogs sequential cerebral scintigraphy was performed following the injection of 0.5 mCi ^{131}I-Fenetylline. Three patients underwent brain SPECT after injection of 6.5 mCi ^{123}I-Fenetylline.

The results can be summarized as follows: after 5 / 10 min. p.i. Fenetylline-uptake in the brain of rats was 1.0/1.3 % compared to 1.3/1.9 % (IMP). A fast decrease of cerebral Fenetylline concentration was established after 30 (0.2 %) and 60 (0.5 %) min.. The canine and human sequential scintigraphy revealed a rapid cerebral uptake (maximum after 2-10 min.) suggesting that Fenetylline is concentrated in the brain as a function of cerebral blood flow. From our first clinical findings it appears to be likely that the combined use of ^{123}I labeled IMP and Fenetylline for SPECT may lead to a more differentiated evaluation of cerebral blood flow and metabolism.

SYNTHESIS AND EVALUATION OF p-IODOPHENTERMINE (IP) AS A BRAIN PERFUSION IMAGING AGENT. D.R. Elmaleh, H. Kizuka, J. Garpeau, G.L. Brownell, M. Keiss, M. B-Kovach, R.N. Hanson* and H.W. Strauss. Massachusetts General Hospital and *Section of Medicinal Chemistry, Northeastern University, Boston, MA 02114

Recently N-isopropyl-p-[^{123}I]-iodoamphetamine (IMP) has been reported as a potential cerebral perfusion imaging agent for single-photon emission tomography (SPECT). Since addition of a methyl group in the alpha position of amphetamine results in increased lipophilicity and prolonged residence time of the compound in the brain, we synthesized and evaluated the biological behavior of p-Iodo phenteramine (IP). IP was prepared by diazotization of p-aminophentermine followed by decomposition of the diazonium salt with KI. Radioiodinated analog was prepared either by the solid-phase isotopic exchange reaction of Mangner et al or by decomposition of the piperidinotrazine derivative with a radiochemical yield of 40-60%.

Biodistribution in rats showed that the brain concentration of ^{131}I-IP was 1.69±0.53, 1.70±0.23 and 1.72±0.11 % injected dose/g tissue at 5, 30 and 60 min respectively, after IV injection. The lung uptake was 10.82 % ID/g at 5 min and decreased to 7.7% ID/g at 60 min. The thyroid activity was low during the first hour of the study indicating minimal deiodination on the aryl ring. Sequential images of the brains of three dogs after intracarotid injection of ^{123}I-IP showed localization of activity to one hemisphere of the brain, and clearance of <15% at one hour. In addition, SPECT images revealed more intense localization in the region of gray matter then white matter in the brain. This work is supported by R01CA26371-5, DOEAC0-2-76EV04115.

ENRICHED XENON-124 FOR THE PRODUCTION OF HIGH PURITY IODINE-123 USING A CP-42 CYCLOTRON. D. Graham, I.C. Trevena, B. Webster, D. Williams. Atomic Energy of Canada Limited, Vancouver, Canada.

The preferred production route for I-123 is that employing the I-127 (p,5n) reaction. This reaction requires energies beyond the capabilities of compact industrial cyclotrons. The possibility of using the reactions

Xe-124 (p,2n) Cs-123 → Xe-123 → I-123
Xe-124 (p,pn) Xe-123 → I-123

was investigated using xenon containing 50% Xe-124.

Three xenon gas targets were evaluated on an external beamline of the CP-42 cyclotron installed at TRIUMF in Vancouver. Two of these targets performed routinely with beam currents of 75µA and one of these has been tested satisfactorily with natural xenon with a beam current of 150µA. The targets have been relatively thin, about 1-2 MeV, with an incident proton energy of 24-26 MeV. The maximum production from a single run has been 1.1Ci I-123 at the end of chemical processing. I-125 is formed from Xe-126 present in the target gas. Because the half life of Xe-125 is 17h compared with 2h for Xe-123, the I-125 content is dependant upon the length of the irradiation and time that the target gas is allowed to decay prior to processing. With optimum timing, the I-125 content is less than 0.2% at the end of processing. I-123 is washed from the target with dilute base. Since 50% Xe-124 costs about U.S.$130/ml, processing procedures and equipment design must ensure negligible losses. This demonstration of a route for the production of I-123 will enable those with access to a compact cyclotron with an external beamline to produce "(p,5n)" quality I-123 using a Xe-124 gas target.

1:30-3:00 **Room 217B**

NEUROLOGY II: QUANTITATIVE METHODS

Moderator: Martin Reivich, M.D.
Comoderator: Alfred P. Wolf, Ph.D.

THE EVALUATION OF THE LUMPED CONSTANT FOR DEOXYGLUCOSE AND FLUORODEOXYGLUCOSE IN MAN. M. Reivich, J.H. Greenberg, A. Wolf, J. Fowler, C. Arnett, R. Ferrieri, H. Atkins, R. Dann A. Alavi. University of Pennsylvania and Brookhaven National Laboratory, Philadelphia, PA and Upton, Long Island, NY

The use of glucose analogues to measure local cerebral glucose metabolism (LCMRgl) is an established and powerful technique. Quantification of LCMRgl in man requires knowledge of the value of the lumped constant (LC) which describes the relationship between the uptake of the glucose analogue by the tissue to the uptake of glucose. We have directly measured the LC of both deoxyglucose (DG) and fluorodeoxyglucose (FDG) in 14 male volunteers using C-11 2-deoxy-D-glucose (n=6) and 18-F 2-fluoro-2-deoxy-D-glucose (n=8) respectively. In each subject the internal jugular vein and a radial artery were catheterized so that cerebral venous and arterial blood samples could be obtained. The radionuclide was infused intravenously over 50-60 minutes using an infusion schedule to produce a step change in arterial plasma radionuclide concentration and blood samples were drawn and analyzed for the determination of the extraction fraction of the tracer and of glucose. The lumped constants for deoxyglucose and fluorodeoxyglucose in man are 0.56 ± .043 (SEM) and 0.52 ± .028 (SEM) respectively. LCMRgl was determined in a series of 12 young normal volunteers using C-11 DG (n=6) and 18-F FDG (n=6) and the values of the respective LC. Average whole brain glucose consumption was determined to be 4.99 ± 0.23 mg/100 gm/min and 5.66 ± 0.37 mg/100 gm/min using C-11 DG and 18-F FDG respectively. There is no significant difference between these measurements (t=1.56, df=10) and they both agree well with reported values in the literature using the Kety-Schmidt technique.

PET MEASUREMENT OF GLUCOSE MEMBRANE TRANSPORT USING LABELED ANALOGS: DISTINCTION OF TRANSPORT FROM METABOLIC PROCESSES. J.E. Holden, R.A. Koeppe, S.J. Gatley, Medical Physics Department, University of Wisconsin, Madison, WI

Carrier mediated glucose transport rates across brain capillary and myocardial cell membranes are many times

higher than those expected for simple diffusion, and transport regulation can be an important determinant of tissue metabolic status. We have investigated the use of glucose analogs and dynamic positron tomography for the non-invasive measurement of unidirectional membrane transport rates. If analog extraction is sufficiently low, transport rates can be inferred directly from fitted kinetic rate constants. Fitting calculations were seen to be sensitive to the difficult to measure rapid components of the arterial input curves, to contributions from blood-borne label in the early data points, and to interference from other chemical forms in cases of significant phosphorylation. This last uncertainty was studied using serial scans of normal brain after venous injection of the well-transported but poorly phosphorylated analog 3-deoxy-3-fluoroglucose. Transport rate constants derived from 4-parameter fits of three hours of data were compared to those derived from 2-parameter fits of the first 12-20 minutes of data. Errors due to trapped label were absorbed primarily into the apparent distribution volume, allowing accurate estimation of transport rate constants from a brief data acquisition period. Our study of the distinction of transport from phosphorylation also bears on the important question of the significance of the individual rate constants in the four-parameter fitting of brief dynamic scan sequences in studies of metabolic rate using 2-deoxy-2-fluoroglucose.

THE TEST-RETEST PETT EXPERIMENT PARADIGM: THE SUBJECT AS HIS OWN REFERENCE. J.A.G. Russell and A.P. Wolf. Brookhaven National Laboratory, Upton, NY

Using the radiotracer carbon-11 deoxyglucose, and the PETT we measured the regional glucose metabolic rates in the brains of 20 normal resting male subjects twice within an interval of less than 3 hours. For each of 12 cerebral regions the mean percentage change in metabolic rate between the two measurements were computed for the group. The measurement errors were propagated through all of the calculations from the PETT data acquisition to the mean of the ratios. Typical group mean changes for regions usually involved in cognitive activities were 6% (SD 3%) and for the cerebellum and thalamus 2% (SD 1%). To test the sensitivity of the paradigm we compared the regional changes between a resting condition and a hand-clasping task in 5 normal subjects and found typical task-related increases of 14% (SD 5%) in regions associated with volitive motor activity. When compared statistically to the changes measured in the resting group, the task-related changes were significant at the 5% level or smaller in 10 of the 12 regions. We will describe the Test-Retest methodology, the quantitative image comparison techniques, and the propagation of errors through the entire PETT method to yield a quantitative intervention-related effect measure.

REPRODUCIBILITY STUDY OF A NON-INVASIVE POSITRON CT (PCT) TECHNIQUE USING O-15 WATER FOR SCREENING RELATIVE CEREBRAL BLOOD FLOW RESPONSES DUE TO NEUROBEHAVIOR INTERVENTIONS. SC Huang, JC Mazziotta, RE Carson, N MacDonald, ME Phelps, UCLA School of Medicine, Los Angeles, California

The noninvasive PCT technique that uses O-15 water but without arterial blood sampling is rapid and can provide relative cerebral blood flows. The technique is potentially useful for screening cerebral responses due to neurobehavior tasks. To characterize the accuracy of the technique, we have studied the reproducibility of the technique in 5 normal subjects under the control condition of eyes closed and ears open. Four repeated studies (10 min. apart) were done on each subject. In each study, a bolus of O-15 water (30 mCi) was injected intravenously. A single 60-second PCT scan was initiated concurrent with the injection. No arterial blood samples were taken. The PCT images were reconstructed and normalized individually relative to the mean radioactivity concentration of the brain slice. The normalized radioactivities in various cortical and subcortical regions were obtained and their fluctuations among the repeated studies evaluated. The results show the PCT images of the repeated studies are visually indistinguishable from each other. The standard deviations of the normalized regional radioactivities were in the range of 2-4% with an average SD of 2.98% in all the regions (27/subject) of the five subjects. It is concluded that the noninvasive PCT technique using O-15 water is useful for screening relative cerebral blood flow changes of 5% or more.

A NEW QUANTITATIVE METHOD FOR MEASURING OXYGEN EXTRACTION FRACTION: HUMAN STUDIES. S. Takagi, K. Ehara, M.D. Ginsberg, P.J. Kenny, R.D. Finn, and A.J. Gilson. Mount Sinai Medical Center, Miami Beach, FL.

The purpose of this presentation is to apply a newly developed equation for oxygen extraction fraction (OEF) (Int. Symposium on CBF & Metab. Measurement, Heidelberg, 1983) to human studies using PET scanning. Previous simulation studies indicate advantages of this method include: stability of calculated OEF to the error in flow values as well as to the time shift effect between the head and the arterial curves. Three studies were done in each of 7 patients; (1) 100-130 mCi of O-15 bolus inhalation, (2) intravenous injection of 20-40 mCi of O-15 labeled water, (3) bolus inhalation of 20-30 mCi of C-11 labeled carbon monoxide. After the administrations of radioactive oxygen and water, serial 16 second scans in 7 slices were obtained for at least 2 minutes. Arterial samples were obtained from the radial artery, and recirculated water of metabolism was also measured.

OEF values in 28 regions of interest were calculated by our method (OEF(T)) as well as by the already established method by Mintun et al. (OEF(M)) with the measurement times (MT) of 39 sec (30.5-47.5 sec), 56 (47.5-64.5), 73 (64.5-81.5) and 90 (81.5-98.5). Mean OEF(T) calculated with MT of 90 sec was 0.37 $\pm$ 0.12. There was no significant difference between OEF(T) from different MTs.

Highly significant correlation of r = 0.998 was observed between OEF(T) (y) and OEF(M) (x) with a regression line of y = 1.04 x - 0.002 (MT of 90 sec). If the recirculated water of metabolism was not corrected, OEF(T) (90 sec) was overestimated by 0.043 $\pm$ 0.018 (11.6 $\pm$ 4.9%).

From these data, it is concluded that our new equation gives accurate OEF values in human studies.

POSITRON COMPUTED TOMOGRAPHY STUDIES OF CEREBRAL METABOLIC RESPONSES TO COMPLEX MOTOR TASKS. M.E. Phelps, J.C. Mazziotta. UCLA School of Medicine, Los Angeles, CA.

Human motor system organization was explored in 8 right-handed male subjects using ^{18}F-fluorodeoxyglucose and positron computed tomography to measure cerebral glucose metabolism. Five subjects had triple studies (eyes closed) including: control (hold pen in right hand without moving), normal size writing (subject repeatedly writes name) and large (10-15 X normal) name writing. In these studies normal and large size writing had a similar distribution of metabolic responses when compared to control studies. Activations (percent change from control) were in the range of 12-20% and occurred in the striatum bilaterally > contralateral Rolandic cortex > contralateral thalamus. No significant activations were observed in the ipsilateral thalamus, Rolandic cortex or cerebellum (supplementary motor cortex was not examined). The magnitude of the metabolic response in the striatum was greater with the large versus normal sized writing. This differential response may be due to an increased number and topographic distribution of neurons responding with the same average activity between tasks or an increase in the functional activity of the same neuronal population between the two tasks (present spatial resolution inadequate to differentiate). When subjects (N=3) performed novel sequential finger movements, the maximal metabolic response was in the contralateral Rolandic cortex > striatum. Such studies provide a means of exploring human motor system organization, motor learning and provide a basis for examining patients with motor system disorders.

1:30-3:00 Room 212B

NMR III: CLINICAL/INSTRUMENTATION

Moderator: James W. Feltcher, M.D.
Comoderator: Barbara Y. Croft, Ph.D.

COMPARISON OF I-123 IMP UPTAKE AND NMR SPECTROSCOPY IN THE BRAIN FOLLOWING EXPERIMENTAL CAROTID OCCLUSION.
B.L. Holman, F. Jolesz, J.F. Polak, J. Kronauge and D.F. Adams. Harvard Medical School and Brigham and Women's Hospital, Boston, MA.

Both I-123 IMP scintigraphy and NMR have been suggested as sensitive detectors of changes shortly after acute cerebral infarction. We compared the uptake of N-isopropyl I-123 p-iodoamphetamine (IMP) and NMR spectroscopy of the brain after internal carotid artery ligation. Thirteen gerbils were lightly anesthetized with ether. After neck dissection, an internal carotid artery was occluded. After 2.8 hours, 100 μCi I-123 IMP was injected intravenously into the 13 experimental animals plus 3 controls. Seven gerbils remained asymptomatic while 6 developed hemiparesis. At 3 hours after ligation, the animals were killed. The brains were bisected and T_1 and T_2 relaxation times were determined for the right and left hemispheres by NMR spectroscopy immediately after dissection. I-123 IMP uptake was then determined in the samples. Interhemispheric differences in uptake for I-123 IMP uptake was 2.2% ± 0.5% in the control, 33.5% ± 9.6% in the asymptomatic and 54.6% ± 9.7% in the symptomatic animals. Significant differences were seen with I-123 IMP in 6/7 asymptomatic and 6/6 symptomatic animals. Significant differences in T_1 and T_2 were seen in 2/7 of the asymptomatic and 5/6 of the symptomatic animals. In conclusion, I-123 is more sensitive than T_1 or T_2 for the detection of cerebral perfusion abnormalities while T_1 and T_2 more accurately separate symptomatic from asymptomatic animals.

EARLY IN VIVO DETECTION OF ACUTE CANINE MYOCARDIAL ISCHEMIA BY NMR. P.W. Pflugfelder, G. Wisenberg, F.S. Prato, S.E. Carroll, K.L. Turner. St. Joseph's Hospital, London, CANADA.

To determine the ability of proton nuclear magnetic resonance imaging (NMRI) to detect early myocardial ischemic injury, a ligature was placed around the anterior descending(3) or circumflex(3) artery in 6 dogs. In vivo imaging was done at end diastole using a .15T (6.25MHz) resistive NMR unit prior to and for 4-6 hours after coronary artery occlusion. Image acquisition was by spin echo (SE) (TE 30 msec TR<1sec, TE 30 msec TR>1sec, TE 60 msec TR>1sec) and inversion recovery (IR) pulse sequences. Compared to normal surrounding myocardium, NMR signal increased within the ischemic zone as follows:

IMAGING SEQUENCE	% INCREASE SIGNAL (±SD) POST OCCLUSION 0-60min.	61-120min.	121-180min.	181-240min.
TE30TR<1	29±20*	31±14*	41±24*	34±31*
TE30TR>1	28±15*	30±23*	42±27*	42±30
TE60TR>1	93±26	151±60*	171±86*	144±96
IR	-2±8	16±13	-5±3	12±9

*denotes p<.05

Changes of evolving infarction by microscopic examination of the excised heart correlated well with the extent of NMR changes. Excellent visualization of the ischemic zone was obtained using the SE technique, particularly the TE 60 msec SE sequence. IR imaging did not demonstrate ischemia. T2 of ischemic myocardium was increased 50±3% above normal myocardium in the first hour and 78±27% in the third hour post occlusion (p<.05). In conclusion, NMRI can detect early myocardial ischemic injury, best with the TE 60 msec SE sequence, thus providing a potential tool for evaluating the efficacy of interventions to limit myocardial infarct size.

CORRELATION BETWEEN THE MALIGNANT PHENOTYPE OF VIRUS TRANSFORMED CELLS AND DECREASED PROTON RELAXATION TIMES.
J.W. Fletcher, L.R. Hendershott, J.A. Fernandez-Pol. St. Louis University and St. Louis VA Medical Center, St.Louis, MO.

The Nuclear Magnetic Resonance (NMR) properties of normal rat kidney (NRK) cells and their cloned transformed derivatives (CTD), Kirsten sarcoma-(K) and Simian virus 40-(SV) NRK cells were studied. Cells were cultured in DME media containing 10% (v/v) calf serum. After washing, cells were harvested, counted, volume determined and viability established. NMR measurements were made on cell pellets with a permanent magnet system operating at 10 MHz and 37°C utilizing a Hahn spin-echo sequence.

The proton T_1 for NRK cells was 1332±78msec (± 1 SD). In contrast, the T_1 of both CTD was reduced: T_1 for SV-NRK cells was 1053±108msec and for K-NRK was 912±53msec. Parallel decreases in T_2 relaxation times were also found in both CTD in comparison with the NRK cells. Shortened T_1 and T_2 values were also found when cells were maintained in various media during NMR measurements.

The results indicate that there is a correlation between the malignant phenotype and the shortened T_1 and T_2 values of the SV-NRK and K-NRK cell lines in culture. This relationship was strengthened by the finding that similar results were observed when the cells were maintained in a variety of media during the NMR determinations. The shortened NMR proton relaxation times may be due to the position of the SV-NRK and K-NRK cells in the cell cycle as a significant proportion of the CTD are in the S or M phases of the cell cycle in comparison to NRK cells.

VALIDATION OF T1 RELAXATION TIMES ON AN NMR IMAGING SYSTEM: CAN IT BE DONE? P.T. Cahill, R.J.R. Knowles, and J.B. Kneeland. The New York Hospital-Cornell Medical Center, New York, N.Y.

Validation of T1 values determined on an NMR imaging system requires a careful assessment of the methodology of data acquisition and of computational techniques. In our study on 0.5T Teslacon imaging system, we have investigated various combinations of pulse sequences and have concluded that repeated spin echoes with different repetition times provide the most practical basis for simultaneous imaging and calculation of T1 values. Samples of various dilutions of propylene glycol with T1 values ranging from 0.2 to 2.0 sec (measured on NMR spectrometer at 0.5T) were studied in the following configurations: isolated both in the center and at the periphery of the rf coil, outside and inside an inhomogeneous phantom, and on the outside and inside of a canine. These studies were repeated at different values of the 180-degree rf tip angles. Statistical error analysis included background corrections and propagation of errors for the various cases. Our method for calculation of T1 values gives an average accuracy of better than 10% for T1 values up to 1.2 seconds. For samples placed on canines, respiration artifacts were found to contribute significantly greater errors.

QUANTITATION OF LUNG WATER BY NMR IMAGING: A PRELIMINARY STUDY. R.L. Nicholson, F.S. Prato, R. Wexler, L. Carey, S. Vinitski, T. Carr., St. Joseph's Research Institute and University Hospital, London, Canada.

This study investigates the relation of the NMR spin-lattice relaxation time (T_1) to tissue wetness in an animal model of pulmonary edema.

Imaging was performed with a whole-body resistive magnet prototype NMR imager (Technicare, Inc.) operating at 0.15T. Following control NMR imaging, mongrel dogs (n=4) were anesthetized and subjected to saline pulmonary lavage (15 ml/kg) while in a lateral position, repeated 2-5 times to produce mild to severe edema and hypoxemia (prelavage, on 100%, P_aO_2 > 300 mm Hg; post lavage P_aO_2 65-85 mm Hg). The animals were maintained on positive pressure ventilation with halothane/O_2. Model P_aO_2 stability was 15%/hr. Axial NMR images were obtained at the level of the carina. Partial saturation pulse sequences (90°-180°-spin echo) were used in which the T_2 parameter was held constant (time to echo, T_E) at 30 msec, while the T_1 parameter (repetition rate, T_R) varied in multiple steps from 500-4500 msec, allowing production of a parametric image of T_1 distribution. Following sacrifice, two 1-cm thick transverse sections were removed from the lungs at the level of the carina. One set of transverse sections was

analyzed intact and from the adjacent section four samples (approx. 5 cm^2) were excised. Gravimetric measurement of dry and wet weights was done, and comparison made to T_1 measurements found by in vivo imaging.

Tissue wetness bore a linear relation to T_1 both when lung samples (n=12, r=0.7, $p < 0.02$) and whole slices (n=8, r=0.66, $p = 0.05$) were used. As well, the data corresponds well to previous data determined in vitro at a different field strength, using a different animal model. Thus, T_1 calculation may allow quantitation of lung water.

NUCLEAR MAGNETIC RESONANCE (NMR) BLOOD FLOW IMAGING. R.R. Price, J.A. Patton, M.D. Kulkarni, D.R. Pickens, J.J. Erickson, W.H. Stephens, C.L. Partain and A.E. James, Jr., Vanderbilt University School of Medicine, Nashville, TN.

Picture element values in NMR images are dependent not only upon T_1 and T_2 relaxation times but also on the local density and velocity of hydrogen nuclei moving through the region being imaged. In 1959 Singer demonstrated the potential of non-imaging NMR for measuring blood flow. Recently several investigators have proposed methods for combining NMR imaging with NMR blood flow measurements. We have investigated the relationships between various radio-frequency pulse sequences and flow rate and their effects on image intensity using a constant flow pump and a 0.5 Tesla Technicare Teslacon NMR imager. Dilute mixtures of ethylene glycol were used to simulate blood. Flow measurements were made in Tygon tubing (12 mm) at variable velocities ranging from 0-35 cm/sec. The flow phantom was used to calibrate several pulse sequences relating image intensity and vascular flow velocity. Representative patient studies demonstrating blood-flow have been performed. The calibration is being extended to pulsatile flow systems.

1:30-3:00 **Room 212A**

RENAL, ELECTROLYTE, HYPERTENSION I

Moderator: Andrew T. Taylor, M.D.
Comoderator: Harold L. Atkins, M.D.

PREDICTING THE EFFECTS OF DIETARY MANIPULATION IN CHRONIC RENAL DISEASE. A.M. El Nahas, S.A. Brady, A.Masters-Thomas V. Wilkinson, A.J.W. Hilson, and J.F. Moorhead. Royal Free Hospital, London, England.

It has been suggested that the progressive fall in renal function in some patients with CRF is due to hyperperfusion of the remnant nephrons in response to the relatively high protein diet of modern life. We attempted to assess this and to see what was the shortest time in which any effect could be demonstrated. In the first phase, 39 patients with CRF had their renal function followed for 6 months on their normal diet and 6 months on a low-protein diet (LPD). The patients on LPD all showed an improvement in the rate of fall of renal function. This was marked in patients with mainly tubular disease, and poor in those with glomerular and vascular disease. In the second phase, 11 of these patients (and 1 other) were started on a high protein diet (HPD) for two weeks, and then switched back to a LPD for 2 weeks. There was no change in GFR during this period, but there were marked changes in ERPF, which correlated well with the changes in renal function in the first phase ($r = 0.76$, $p < 0.01$); 4/4 patients with tubular disease showed a rise in ERPF on HPD and a fall on LPD, while only 4/8 with glomerular or vascular disease responded. In the third phase, we assessed the effect of a single high-protein meal in normal volunteers. This showed that there are major changes in hemodynamics following a meal, such that it is not possible to make any statement about renal function using the single-shot methods. We conclude that a 2-week period of HPD followed by LPD allows prediction of the possible beneficial response to diet in CRF; that this is best monitored by ERPF; and that a single meal may invalidate renal function measurement.

^{99m}Tc-APROTININ: A NEW TRACER FOR KIDNEY MORPHOLOGY AND FUNCTION. C.Bianchi, C.Donadio, G.Tramonti, P.Lorusso, L. Bellitto, F.Lunghi. Cattedra di Nefrologia Medica, Clinica Medica 2, Istituto di Fisiologia Clinica CNR, Istituto di Patologia Medica 1, University of Pisa, SORIN Biomedica, Saluggia, Italy.

Aprotinin (Ap), a low molecular weight polypeptide (6500 dalton), is a protease inhibitor which is electively and stably accumulated in the kidney. In 112 adult patients, with either uni- or bilateral renal disease with different degrees of renal impairment (from normal GFR to advanced renal failure), renal scans were performed by means of Ap labelled with ^{99m}Tc. Highly satisfactory renal scans were obtained in all patients. In 20 patients with renal failure (serum creatinine 1.8-8.5 mg/dl, mean 4.7) a comparison was made of the renal scans obtained with ^{99m}Tc-Ap and with ^{99m}Tc-DMSA. ^{99m}Tc-Ap was slightly better than ^{99m}Tc-DMSA, especially in patients with far advanced renal failure. Some aspects of the pharmacokinetics of ^{99m}Tc-Ap were studied in 72 cases. In 22 of these patients plasma clearance of ^{99m}Tc-Ap was determined by the single injection method using a two-compartment model. In patients with GFR>90 ml/min plasma cl of ^{99m}Tc-Ap was 67.6±8.4 SD ml/min. A good correlation was observed between plasma clearance of ^{99m}Tc-Ap and GFR (r=0.74). After i.v. injection ^{99m}Tc-Ap was stably fixed by the kidney. Renal radioactivity remained stable between the 2nd and the 8th hour after the injection. Urinary excretion of radioactivity measured in 35 patients in the first and in the second 2-hour interval after i.v. injection of ^{99m}Tc-Ap was negligible in all patients (2.7±1.5 SD percent of the dose in the first 2 hours; 2.8±1.4 SD between the 2nd and the 4th hour).
Conclusions. ^{99m}Tc-Ap is an excellent agent for renal imaging. It also seems promising for renal function studies.

THE EFFECT OF MALEATE INDUCED PROXIMAL TUBULAR DYSFUNCTION ON THE RENAL HANDLING OF Tc-99m DMSA IN THE RAT. A.P. Provoost and M. Van Aken. Dept. Ped. Surgery, Erasmus University, Rotterdam, The Netherlands.

In the healthy kidney Tc-99m DMSA accumulates in the proximal tubular cells. Consequently, impairment of the reabsorptive function of these cells may alter the renal handling of this static renal imaging agent.

We investigated in rats the effects of a sodiummaleate (Ma) (2mmol/kg iv) induced proximal tubular dysfunction on the renal accumulation and excretion of Tc-99m DMSA. Such a treatment results in a moderate fall of the glomerular filtration rate, glycosuria, aminoaciduria and a tubular proteinuria. In 7 adult male Wistar rats, Tc-99m DMSA scans were taken before Ma, on the day of treatment, and 1 week thereafter. The accumulation of Tc-99m DMSA in kidneys (Ki) and bladder (Bl) was determined at 1, 2, 4, and 24 hours after i.v. injection. The results, expressed as a percentage of the injected dose are presented below:

day	Ki 1hr	Bl	Ki 2hr	Bl	Ki 4hr	Ki 24hr	
C -7	37±3	12±2	40±2	15±2	45±3	49±3	(mean ± SD)
Ma 0	8±2	34±11	6±2	38±9	8±4	15±2	
Ma 7	35±4	17±2	39±5	20±6	40±3	47±4	

These findings show that a reversible Ma induced impairment of the proximal reabsorptive capacity severely alters the renal tubular handling of Tc-99m DMSA. In contrast to the control situation, only a small fraction of the DMSA is retained in the kidney and the majority is transported directly to the urinary bladder. When similar alterations are observed in clinical Tc-99m DMSA scans, this may be an indication of an impairment of the proximal tubular function.

THE EFFECT OF RADIOPHARMACEUTICAL CHOICE ON THE DETERMINATION OF RELATIVE RENAL FUNCTION IN RATS WITH UNILATERAL RENAL OBSTRUCTION. A. Taylor and R. Lallone. University of Utah and VA Medical Center, Salt Lake City UT

A significant divergence of GFR and ERPF within a single kidney could lead to different estimates of relative renal

function depending on which radiopharmaceutical is administered. To address this question, we studied adult male Sprague-Dawley rats with unilateral ureteral obstruction by giving each animal an intravenous injection of 10 uCi of I-125 iothalamate (GFR), I-131 hippurate (ERPF), and Tc-99m DMSA and measuring the 30 minute clearance (renal uptake and urine excretion) of each agent. Normal control animals were sham operated; 25 experimental animals were subjected to permanent unilateral ureteral occlusion and studied at 6 hours, 1, 3, 7 and 14 days. Acute ureteral obstruction impaired the clearance of iothalamate to a much greater degree than OIH or DMSA at 6 hours and 1 day ($p<.005$) and 3 days ($p<.05$). The decline in DMSA clearance reflected ERPF more closely than GFR .

PERCENT RENAL FUNCTION OF THE OBSTRUCTED KIDNEY
() shows % injected dose cleared by obstructed kidney

	Hippurate	DMSA	Iothalamate
Control	51.6 (37.9)	49.4 (22.4)	48.2 (31.4)
6 hours	35.6 (24.6)	36.4 (15.3)	21.4 (9.7)
1 day	25.6 (16.8)	25.6 (10.6)	15.8 (7.8)
3 days	18.8 (12.0)	13.6 (5.7)	10.0 (4.4)
7 days	22.8 (15.6)	14.0 (5.8)	12.0 (7.0)
14 days	13.3 (9.0)	9.3 (3.4)	6.3 (2.7)

In evaluating renal disease, one should consider the functional parameter reflected by the radiopharmaceutical as well as the underlying disease state.

RENAL FUNCTION IN PATIENTS WITH RENOVASCULAR HYPERTENSION FOLLOWING INHIBITION OF ANGIOTENSIN CONVERTING ENZYME. H. Drew, N. LaFrance, W. Bender, G. Walker, H. Wagner, Jr. The Johns Hopkins Medical Institutions, Baltimore, MD.

Effective renal plasma flow (ERPF) after a single injection of I-131 iodohippuran was measured using an open 2-compartmental system, described by Sapirstein, and using the single blood sample method described by Tauxe. Three patients (pts) had bilateral and 6 had unilateral renal artery stenosis, 2 received renal transplants and 1 had normal renal arteries. Pts. were studied the day prior (baseline) to receiving MK-421, an angiotensin converting enzyme inhibitor, 4 hrs after (acute) the initial oral dose and 3 to 4 days (chronic) following continued therapy. Glomerular filtration rate studies were performed from a single injection of Tc-99m DTPA along with each ERPF study and filtration fractions (FF) calculated.

Using the 2-compartmental method for ERPF in pts with unilateral disease the FF of 0.29 decreased to 0.22 acutely and remained depressed after 3-4 days. Using the single plasma method for ERPF the FF decreased from 0.30 to 0.20 acutely and chronically. In bilateral disease and renal transplant pts there were similar decreases in FF that persisted. Although the 2 methods of calculating ERPF showed some variation in individual pts, both methods indicated that FF fell in pts receiving the drug, indicating disruption of glomerular autoregulation. Both methods were clearly effective in detecting changes in renal function of this order of magnitude.

CAPTOPRIL INDUCED RENOGRAPHIC ALTERATION IN UNILATERAL RENAL ARTERY STENOSIS. H.Y. Oei, G.G. Geyskes, E.J. Dorhout Mees, C.B.A.J. Puijlaert. University Hospital Utrecht, The Netherlands.

In patients with unilateral renal artery stenosis (URAS) captopril administration will deteriorate glomerular filtration in the affected kidney by interruption of autoregulatory mechanisms. This effect might be detectable on renography and could be useful for the diagnosis of renovascular hypertension.

After discontinuation of all medication, Tc-99m diethylene triamine pentaacetic acid (DTPA) gammacamera renography, followed by I-131 orthoiodohippurate (OIH) renography were performed in 15 hypertensive patients who were poorly controlled with medical therapy. This double examination was repeated some days later after administration of 25 mg captopril one hour prior to the examination. After this, angiography was done and patients with stenosis of the renal artery were treated by percutaneous transluminal dilatation (PTD). Five patients were excluded due to bilateral or segmental stenosis of the renal artery.

Four URAS-patients, in whom the bloodpressure improved after PTD, showed after administration of captopril a striking renographic alteration in the affected kidney. The DTPA-renogram which initially had an upslope phase, showed a blooddisappearance curve and the OIH-renogram, which still had an upslope phase, showed a slower excretion. These renographic alteration did not occur in the other 2 URAS-patients, who had no benefit of the PTD and in the 4 remaining patients without stenosis.

These findings suggest that captopril induced renographic alterations may be important for the diagnosis of hemodynamic significant URAS. For this purpose either DTPA or OIH can be used.

3:30–5:00 **Room 217A**

CARDIOVASCULAR V: VALVULAR HEART DISEASE/ RIGHT VENTRICULAR FUNCTION

Moderator: Elias H. Botvinick, M.D.
Comoderator: P. Todd Mackler, M.D.

ATRIAL CORRECTED FOURIER AMPLITUDE RATIOS FOR THE SCINTIGRAPHIC QUANTITATION OF VALVAR REGURGITATION. M.W. Dae, E.H. Botvinick, J.W. O'Connell, D.F. Faulkner, C.D. Porter, N. Schechtmann. University of California, San Francisco, CA.

Current scintigraphic methods commonly overestimate the degree of valvar regurgitation (VR), and displace normal ratios from unity, owing largely to RA contamination of the RV region of interest in the "best septal" LAO projection. We developed a method to correct for this overlap, using the Fourier amplitude (AMP) ratio. Amplitude is first "weighted" for phase angle using a vectorial sum, to improve assessment in patients (PTS) with contraction abnormalities. RV AMP is then corrected for underestimation by adding the product of mean LAO RA AMP times the difference between RA areas in anterior and LAO projections to the calculated RV AMP. In 15 PTS with aortic or mitral VR, corrected AMP ratios (CAR) were compared to ratios assessed angiographically and in 12 PTS without VR were compared to uncorrected AMP ratios (UAR), and to stroke volume ratios (SVR) from SV images (SVI), and ED and ES counts data (CT).

	REGURGITANT RATIO (Mean±SD)			
	CAR	UAR	SVR(SVI)	SVR(CT)
No VR	1.09±.23	1.48±.29*	1.50±.38*	1.19±.48
VR	2.16±.73	(*$p<0.05$ vs CAR)		

CAR interobserver agreement was high ($R=.97$). When VR PTS ranked by CAR as mild (1.3-1.8), moderate (1.9-2.5), or severe (>2.5) were compared to similar catheterization based ranks, there were no significant differences using the Mann-Whitney test for ordinal data.

CAR is a simple, objective and reproducible method of quantitating VR. It reduces the error in those without VR, allows sensitive identification of mild VR, and maintains accurate assessment of severe VR.

THE AORTIC EJECTION FRACTION: A NEW TECHNIQUE FOR DIAGNOSING AORTIC INSUFFICIENCY. J.C. Kantor, M.E. Siegel, P. Colletti, C. McKay, K. Lee, J. Halls, L. Jacobs, D. Yamauchi, S. Rahimtoola. USC School of Medicine, Los Angeles, CA.

Pulsations of the ascending aorta during fluoroscopy in patients (pts) with aortic insufficiency (AI) have been described. We observed a similar phenomenon in pts undergoing scintiangiography who have documented AI. This paper describes a technique to validate and quantitate this observation.

We studied 17 patients with AI documented by cardiac catheterization and 14 subjects of a demographically matched control group with no evidence of AI. First pass studies were acquired in the RAO 15° projection after a bolus of 20 mCi of Tc-99m pertechnetate. After framing, identical ROI's were placed over the proximal aorta during systole and diastole excluding activity of the pulmonary arteries and/or atria. An aortic ejection fraction (AEF) was determined. The calculated AEF data was correlated

with the presence or absence of AI.

The mean AEF from the group of 17 patients was 26.9 ± 7.0, while the mean for the non AI group was 12.0 ± 6.5. These are statistically different at the P < .01 level. An AEF of 18 optimally separates the 2 groups with a sensitivity, specificity, and accuracy of 88%, 86%, and 87% respectively. Preliminary data demonstrates a mean reduction in AEF of 14.6 units in the AI patients who, to date, have undergone aortic valve replacement.

Our initial data suggests that this technique, using the AEF, may be able to identify patients with AI without the task of isolating the right ventricle.

CAPTOPRIL-INDUCED REDUCTION OF REGURGITATION FRACTION IN AORTIC INSUFFICENCY. J.Kropp*, S.N.Reske*, H.J.Biersack*, I.Heck**, H.Mattern**, C.Winkler*. Inst. Clin.Exp.Nucl.Med., **Med.Polikl., University of Bonn/FRG

Stimulated Renin-Angiotensin System (RAS) in aortic insufficency (AI) leads to increased afterload and consequently to augmented aortic regurgitation (R). Therefore Captopril (C)-mediated RAS-inhibition should diminish systemic vascular resistance and thus reduce R. In 9 patients (pts) with pure severe AI regurgitation fraction (RF) and left ventricular ejection fraction (LVEF) were determined before and 1 hr after i.v. injection of 25 mg C by gated radionuclide ventriculographie (RNV), using red blood cells labeled in vivo with 15 mCi Tc-99m. Enddiastolic and endsystolic frames were derived from the left ventricular volume curve. ROI's were selected over both ventricles. Ventricular boundaries were defined by a fourier phase image overlay. RF was calculated by the background corrected count rate ratio of left and right ventricular ROI. Arterial blood pressure(BP), heart rate (HR), plasma levels of angiotensin I, II (A1,A2), and the activity of angiotensin converting enzyme (ACE) were determined before and 1 hr after C-injection. Before C-medication mean RF was 54 % (range 34 % - 67 %), after C mean RF decreased to 37 % (17 % - 59 % range, p≪.05). Mean LVEF increased not significantly from 60 % (range 51%-70 %) to 66 % (range 56 % - 77 %, p≈0.55). C did not significantly change HR or BP (HR: p≈0.9, BP: p≈0.6). A2 and ACE activity decreased to 40% and 50% of control values (p≪.01), respectively. A1 increased excessively.

In conclusion: inhibition of ACE reduces significantly aortic regurgitation in patients with AI and has thus a beneficial effect on left ventricular performance.

REST AND EXERCISE RIGHT VENTRICULAR FUNCTION FROM GATED XENON SCANS. .A.C. Tweddel, W. Martin, A.I. McGhie, J.H. McKillop and I. Hutton, Royal Infirmary, Glasgow, Scotland.

Right ventricular function is of considerable clinical interest in acute myocardial infarction involving the right ventricular wall and in the patient with obstructive airways disease. The aim of this study was to assess the use of Xe-133 to evaluate right ventricular ejection fraction (RVEF), as both standard first pass and gated blood pool techniques present methodological problems.

400 MBq of Xe-133 were injected intravenously over 20-25 seconds and listmode data acquired using a mobile gamma camera with an ultra high sensitivity parallel collimator. A 15° left anterior oblique projection was used, acquisition being initiated when right ventricular activity becomes apparent and terminated as this leaves the ventricle. With the rapid excretion of Xenon, scans can be repeated after 5 minutes.

In 10 healthy volunteers, RVEF ranged from 40-55%, compared to a range 8-38% in 10 patients with acute myocardial infarction involving right ventricular wall. In 5 patients with scans repeated at 10 minutes a mean difference of 2% in RVEF was obtained. The analysis of RVEF was only subject to small inter-observer (3%), and inter-observer (2.5%) variation. In comparison with gated blood pool scintigrams good correlation of resting RVEF was obtained (r=.91, n=15). In volunteers resting RVEF increased from a mean of 43% ∓ 4 to 49% ∓ 7 during peak maximal supine exercise. In 10 patients with chronic obstructive airways disease, where resting RVEF was above 30%, exercise RVEF tended to increase, whereas, below 30% on peak exercise RVEF was further impaired.

Gated Xenon scans offer a simple, reliable assessment of RVEF in various clinical situations with interventions.

VALIDATION OF NORMAL AND PATHOLOGIC RIGHT VENTRICULAR FUNCTION USING ULTRA-SHORT-LIVED KRYPTON-81m
C. Nienaber, R. Spielmann, B. Wasmus, D. Mathey, R. Montz, W. Bleifeld
University Hospital Eppendorf, Department of Cardiology and Nuclear-Medicine

Measurement of right ventricular ejection fraction (RVEF) using conventional count-based, non-geometry dependent first-pass radionuclide techniques and technetium labelled compounds (T/2 = 6 hours) implies unnecessary whole body radiation and repeated injections of isotope for sequential RVEF estimate.
Kr-81m (T/2 = 13 secs) continuously eluted in 5 % glucose from a bed-side rubidium-81 generator is intravenously infused providing high count density and high photon flux for rapid imaging of the right-side chambers in ECG-gated equilibrium acquisition mode. A variable right anterior oblique projection is adjusted for optimal right atrio-ventricular separation. Left-sided heart and lung background is minimized by rapid decay and efficiant exhalation of Kr-81m, requiring no algorithm for background correction. RV septal and free wall contours are aligned by a semiautomatic edge detection program; tricuspid and pulmonary valve planes are defined from phase images using variable ROIs to compensate for systolic valve plane motion. Both, inter- and intra-observer variability are≤5 %. Kr-81m studies are validated by biplane cine-angiographic assessment of RVEF based on Simpson's rule. To cover a wide range of RVEF (13 %-63 %) both methods were compared in 10 normals, 11 patients (pts) with pulmonary hypertension (PH), 4 pts with RV outflow tract obstruction (RVOT-OB) and 4 pts with RV infarction (RV-MI) at rest (R) and during dynamic exercise (E). Correlation of all data points is good: r = 0.89; Rest: r = 0.92; exercise: r = 0.84. Kr-81m RVEF x̄ ± SD:

	normals	PH	RVOT-OB	RV-MI
R	49 ± 6	40 ± 8	46 ± 9	36 ± 8
E	60 ± 7*	36 ± 7*	53 ± 11	37 ± 9

* p≪0.05

Conclusion: Equilibrium RV imaging using Kr-81m is an accurate and reproducible method with potential for serial assessment of RVEF in a variety of RV abnormalities both at R and during E. Advantages of this method include: extremly low radiation to patients, high photon flux for rapid imaging and clear atrio-ventricular separation without background.

ASSESSMENT OF RIGHT VENTRICULAR FUNCTION BY INTRAVENOUS INFUSION OF KRYPTON-81m. R.P.Spielmann, C.Nienaber , G.Wasmus, P.Stritzke, R. Montz,and D.G.Mathey. Dept. of Nuclear Medicine and Dept. of Cardiology , Univ. Hospital, Hamburg, West Germany.

Kr-81m equilibrium ventriculography was used to assess right ventricular (RV) function at rest (R) and during submaximal bicycle exercise (E) in patients (pts) with different cardiopulmonary disorders. Kr-81 was continously eluted in 5% dextrose from a portable Rb-81 generator and infused through a peripheral vein. Due to the short half-life (13s) and the free diffusibility of Kr-81 through the alveolar membrane, activity in the left side of the heart is neglible. This allows imaging in a RAO position which provides the best seperation between the right atrium and the RV. Determination of RV ejection fraction (RVEF) involved the definition of an endiastolic and an endsystolic region of interest by a semi-automatic computer algorithm. The standard deviation of RVEF determinations by two independent observers was 0.047. Kr-81 RVEF was related to X-ray angiographic (XA) RVEF and hemodynamic measurements. The correlation coefficient between Kr-81 and XA RVEF was 0.82(n=25). When all pts were divided into two groups according to their mean pulmonary artery pressure, significant differences in the RVEF during E between these groups were found with both Kr-81 and XA ventriculography. The correspondence between Kr-81 and XA data underlines the potential of Kr-81 as a reliable noninvasive tool in assessing RV function.

3:30–5:00 **Room 217B**

CARDIOVASCULAR VI: MYOCARDIAL METABOLISM

Moderator: Heinrich R. Schelbert, M.D.
Comoderator: Nizar Mullani, Ph.D.

RECOVERY OF GLUCOSE METABOLISM IN REPERFUSED CANINE MYOCARDIUM DEMONSTRATED BY POSITRON-CT (PCT). M. Schwaiger, M.D., H. Sochor, M.D., O. Parodi, M.D., M.

Grover, M.D., H.W. Hansen, C. Selin, H.R. Schelbert, M.D., UCLA School of Medicine, Los Angeles, CA.

We previously examined with PCT in chronic dogs the long-term metabolic recovery during reperfusion after a 3 hr ischemic insult. Increased regional glucose utilization at 24 hrs of R accurately identified reversible tissue injury documented by late improvement in segmental function by ultrasonic crystals. To define the early metabolic events after a 3 hr LAD balloon occlusion, regional blood flow and glucose utilization was studied in 8 dogs with PCT, N-13 ammonia (NA) and F-18 deoxyglucose (FDG) at 2 hrs and at 24 hrs after R. The dogs were then thoracotomized and MBF by microspheres, arterio-venous differences for glucose, lactate and O_2 across the reperfused segment (LAD vein) and the left ventricle (coronary sinus) measured. Immediately after reperfusion, MBF and FDG uptake were 27±24% and 21±48% lower in the reperfused territory (RT) than in control myocardium (C). At 24 hrs, MBF by microspheres was 22±25% lower and FDG uptake 175±73% higher in RT than in C. In the RT, consumption of glucose (by Fick method) was 202±107% higher, of lactate 96±85% lower and of O_2 42±26% lower than in the entire LV. PCT measured FDG uptake correlated with glucose consumption (r=0.94) and confirmed that the segmentally increased FDG uptake at 24 hrs reflected increased glucose utilization that, as indicated by the reduced lactate consumption, was partly anaerobic. We conclude that initially after R, glucose metabolism is depressed but increases above C within 24 hrs, a time course that now can be determined noninvasively with PCT and is useful for predicting functional recovery.

METABOLIC BORDERZONE IN ACUTELY ISCHEMIC CANINE MYOCARDIUM DEMONSTRATED BY POSITRON-CT (PCT). M. Schwaiger, H. Hansen, C. Selin, S. Wittmer, J. Barrio and H.R. Schelbert. UCLA School of Medicine, Los Angeles, CA.

Acute coronary ligation in dogs results in an area of myocardial dysfunction that exceeds the area of subsequent necrosis suggesting the existence of an ischemic "borderzone" of reversibly injured myocardium. We tested this hypothesis in 9 closed chest dogs with C-11 palmitate (CPA) and serial PCT imaging after an LAD occlusion. Using a blood flow (MBF) image obtained with iv N-13 ammonia prior to CPA, regions of interest were assigned on the serial CPA cross-sectional images to the center (IC) and border (IB) of the ischemic segment and to control myocardium (CO). CPA uptake was closely related to MBF (r=0.88) implicating flow as a major determinant of CPA uptake. Clearance halftimes (T 1/2) and relative sizes (RS) of the early rapid phase on the C-11 tissue time activity curves were determined for IC, IB and CO and were:

	MBF (%)	CPA (%)	T 1/2 (min)	RS(%)
IC	33±12.1*	36.0 ±11.4*	45.5 ± 31.9*	22.5±15.7*
IB	85±20.1	87.6 ±11.5	19.4 ± 8.1*	41.8±14.1*
CO	100	100	10.6 ± 3.6	61.9± 8.7

* = $p<0.05$; % = percent of CO.

In IC, MBF, RS and T 1/2 were markedly depressed indicating impaired CPA utilization and oxidation. In IB, MBF was less than in CO though only insignificantly, while RS and T 1/2 were highly abnormal. We conclude that FFA metabolism in areas adjacent to ischemic segments but without significant MBF decreases is abnormal, presenting evidence for a metabolic borderzone which now can be identified noninvasively with positron emission tomography.

ASSESSMENT OF MYOCARDIAL INJURY AFTER REPERFUSION WITH Tl-201, Tc-99m PYROPHOSPHATE (PPi) AND F-18 DEOXYGLUCOSE (FDG). H. Sochor, M. Schwaiger, H.W. Hansen, O. Parodi, C. Selin, S.C. Huang, D. Ellison, M. Grover, H.R. Schelbert. UCLA School of Medicine, Los Angeles, CA.

We previously demonstrated that enhanced glucose utilization assessed by FDG and Positron-CT in reperfused myocardium predicts functional recovery. This study compared segmental uptake of FDG with Tl-201 and PPi as conventional indicators of tissue viability in 5 dogs, submitted to a 3 hr LAD occlusion followed by 24 hrs of reperfusion (R). Myocardial blood flow (MBF) was then determined by microspheres and Tl-201, PPi and FDG administered i.v. Regional tracer concentrations were determined by well counting of tissue samples and grouped according to MBF (% of control):

MBF	Tc-PPi (R/C)	Tl-201	FDG
<30%: 12±8%	5.6±3.8	13±7%	44±33%
<30-60%: 48±6%	13.4±4.2	51±4%	108±42%
>60%: 76±15%	10.7±4.1	96±21%	212±86%

Severe flow reductions were associated with PPi uptake increase, Tl-201 decrease and depressed glucose utilization representing mainly irreversible injury. Moderately reduced MBF areas showed the highest PPi uptake with Tl-201 similar to MBF, but preserved FDG uptake not different from control, indicating partially viable tissue. Areas with MBF >60% had significantly increased PPi despite normal Tl-201 uptake and enhanced glucose utilization and thus, preserved viability. Thus, assessment of tissue injury by conventional tracers such as Tl-201 and PPi is limited. By contrast, quantification of residual glucose metabolism by PCT appears more accurate for evaluating myocardial viability and predicting potential functional recovery.

ON THE USE OF 16-IODOHEXADECANOIC ACID (IHDA) AS A PROBE FOR MYOCARDIAL BETA-OXIDATION OF FATTY ACIDS. T.R. DeGrado, S.J. Gatley, C.K. Ng, J.E. Holden, D.R. Bernstein. Dept. of Medical Physics, University of Wisconsin, Madison, WI

The rate of myocardial clearance of label from IHDA was compared with the beta-oxidation rate by coinjection of 125-IHDA and 3-H-Palmitic Acid (THDA) into isolated rat hearts. I-125 residue curves and efflux I-125 and H-3 curves were obtained. Three groups of hearts were studied, control, ischemic and those from rats previously treated with the beta-oxidation inhibitor Ethyl 2(5(4-chlorophenyl)pentyl)-oxiran-2-carboxylate (POCA). Both labels were found to exit ischemic and POCA treated hearts more slowly than controls. In all cases, the clearance of label from IHDA was significantly slower than that of the labelled water from beta-oxidation of THDA, consistent with previous work indicating the efflux of iodide from the mitochondria to be rate-limiting. Assay of heart homogenates showed 60% of the extracted label to be iodide at 1 minute. Thus, iodide is pooled within the mitochondria and diffuses out with a characteristic rate governed by electrochemical and lemmal properties. By assuming parallel utilization of IHDA and THDA and transient clearance of both labelled metabolites from the cytosol, the H-3 curves were interpreted as equivalent with the production of free iodide in the mitochondria. A rate constant describing the flux of iodide across the mitochondrial membrane was calculated by fitting the I-125 curve (I^- output) to the H-3 curve (I^- input) convolved with a single exponential. The rate constant (k_I=2.25±.35x10^{-3} s^{-1} for normals) was similar to the largest rate constant from fitted residue curves (k=2.08±.05x10^{-3} s^{-1}).

EFFECTS OF ANOXIA, PYRUVATE, AND LACTATE ON DISTRIBUTION OF N-13 GLUTAMATE IN MYOCARDIUM. J. Krivokapich, R.E. Keen, J.R. Barrio, A. Douglas, C.R. Watanabe, S. Wittmer, K.I. Shine and M.E. Phelps. UCLA School of Medicine, Los Angeles, CA.

The primary purpose of this study was to determine the effect of anoxia on the fate of N-13 labeled glutamate (glu) in myocardial tissue. Boluses of N-13-glu were injected arterially into isolated, arterially perfused rabbit interventricular septa under control conditions, during anoxia, and during perfusion with 2 mM pyruvate or lactate. In one set of experiments, time-activity curves were generated after the boluses. In another set of experiments, ~0.1g of tissue was cut from the septum at 6 minutes after each injection. These samples were analyzed by reverse-phase HPLC. Under control conditions, glu accounted for 58% of the total N-13 radioactivity present in the sample and aspartate (asp), alanine (ala) and glutamine (gln) accounting for 20%, 16%, and 4%, respectively. During anoxia, the dominant change was an increase in ala to 40% of the N-13 radioactivity with an accompanying decrease in glu to 35%. Pyruvate perfusion produced a decrease in glu and increase in ala similar to the changes induced by

anoxia. The changes due to lactate were in the same direction but less profound. Analysis of the time-activity curves revealed 2 components. The fraction of N-13 in the residual fraction was not different during anoxia as compared to control conditions. The t 1/2 of this fraction, however, became much shorter. In conclusion, anoxia induces an increase in ala secondary to increased pyruvate availability. This is reflected in the time-activity curves as a faster washout of N-13 from the septa.

ASSESSMENT OF THE METABOLIC EFFECTS OF THE IONOPHORE GRISORIXIN ON MYOCARDIAL CELLS IN CULTURE WITH 14-C-LABELLED SUBSTRATES. J.C. Maublant, P. Gachon, M.R. Ross, W.D. Davidson, I. Mena. Harbor-UCLA Medical Center, Torrance, CA, and INSERM U195, Clermont-Fd, France and University of Southern California, Los Angeles, CA.

Cultures of myocardial cells were utilized to verify the hypothesis that the ionophore grisorixin could facilitate the anaerobic and impair the aerobic metabolism in the myocardium. This was suggested by previous experiments in which we found an increase in the cardiac work without increase in the oxygen consumption, while the myocardial uptake of 123-Iodo-hexadecenoic acid was decreased. Tissue cultures were prepared by trypsinization of the myocardium of two to four-day old newborn mice. The cultures were incubated with 14-C-glucose (n=10), 14-C-octanoate (n=14) or 14-C-acetate (n=12). Except for the controls (n=19), they also received 1 µg/ml of an alcoholic solution of grisorixin or 200 µl of 60% alcohol. The cultures were then placed in a circuit with a closed circulation of air which passed through a vibrating reed electrometer for detection of the beta radiations of the 14-CO_2 liberated by the 14-C-labelled substrates. The activity was permanently recorded for measurements of the rate of consumption of these substrates. Compared to the control values, the metabolic rate with grisorixin was significantly decreased for octanoate (77±22 vs 169±62 p mole/min/mg prot, $p<0.01$) and acetate(2.7±1.0 vs 6.0±1.3 p mole/min/mg prot, $p<0.01$). The results for glucose were 1.05±0.24 vs 0.88±0.24 n mole/min/mg prot, ($p<0.10$). Alcohol alone produced no significant effect except on the octanoate consumption. These results provide direct evidence that grisorixin favors the anaerobic pathway in the metabolism of the myocardial cells.

3:30-5:00 **Room 214BC**

DOSIMETRY/RADIOBIOLOGY

Moderator: Raleigh F. Johnson, Ph.D.
Comoderator: A. Bertrand Brill, M.D.

RADIATION DOSE ESTIMATES FOR A NEW MYOCARDIAL PERFUSION AGENT: (E-1-[^{123}I]IODO-1-PENTEN-5-YL)TRIPHENYLPHOSPHONIUM IODIDE. M.G. Stabin, E.E. Watson, J.L. Coffey, Oak Ridge Associated Universities (ORAU), Oak Ridge, TN, P.C. Srivastava, F.F. Knapp, Jr., Oak Ridge National Laboratory (ORNL), Oak Ridge, TN.

Phosphonium cations labeled with gamma-emitting radionuclides have been suggested as myocardial perfusion agents, since these cations penetrate the hydrophobic core of the myocardial cell membrane. A model agent, (E-1-Iodo-1-Penten-5-yl) triphenylphosphonium iodide labeled with ^{123}I in the 1 position, shows rapid myocardial extraction and high heart:blood and heart:liver ratios in female Fischer rats. Detailed distribution studies were performed for the purpose of extrapolating radiation dose estimates for humans. Myocardial uptake in humans, estimated from rat data, would be about 4.5% of the injected activity and would have a biological half-time of 52 hours. The doses to the heart and total body would be 0.027 mGy/MBq (0.10 rad/mCi) and 0.011 mGy/MBq (0.041 rad/mCi), respectively. The doses to the kidneys and thyroid would be 0.027 mGy/MBq (0.10 rad/mCi) and 0.37 mGy/MBq (1.4 rad/mCi), respectively. The doses to other organs, including the ovaries, would not exceed 0.012 mGy/MBq (0.043 rad/mCi). These estimates indicate that the radiation doses for this new agent are within acceptable limits for human use.

ORAU is operated under contract No. DE-AC05-760R00033 with the U.S. Department of Energy. This work was performed under Interagency Agreement No. FDA 224-75-3016, DOE 40-286-71. ORNL is operated by Union Carbide under contract No. W-7405-eng-26 with DOE.

MICRODOSIMETRIC TLD MEASUREMENTS FOR TUMOR ASSOCIATED ANTIBODY THERAPY. B.W. Wessels, P. Bacha and S.M. Quadri. George Washington University, Washington, DC.

Currently, radiation dose in experimental tumored animals undergoing radioimmunotherapy trials is computed indirectly by assessing serial time-dependent biodistribution data, mean residence times and cummulated activities. These data are then used to calculate organ doses through the standard MIRD formalism. Substantial uncertainty in the absorbed organ doses are a result of model dependent assumptions regarding geometrical and radiation attenuation factors for heterogeneous tissue equivalent medium.

We have developed a method for the direct verification of absorbed radiation dose through the use of teflon-imbedded, Teledyne $CaSO_4$:Dy thermoluminescent dosimeters (TLD) which have been modified to fit inside a 20 gauge needle. Typical TLD dimensions are in a rod-shape configuration of 0.2x0.5x5mm. These sterilized dosimeters may then be directly implanted into a variety of animal organs in which dosimetric information is desired. Recovery of the dosimeters may be obtained upon sacrifice of the animal or by surgical removal. These dosimeters have been cross-calibrated with 4 MV x-rays and in solution with I-131-NaI for a period of time ranging from 2 minutes to several weeks. Dose linearity (±5%) from 0.1 to 2000 rads has been obtained for beta emitters of minimum particle energy of 20 keV.

For animal dose measurements, 50µCi of affinity purified, I-131 labeled, p96.5 melanoma monoclonal antibody (IgG2a) was injected with carrier HSA into 6-week-old tumor bearing (Brown 2169) athymic mice. Micro TL dosimeters were then inserted with a needle plunger into at least four anatomical sites per animal. Substantial increase in TLD dose was seen in the liver and GI tract relative to the outlying muscle and tumor as expected for slow clearing intact IgG. The comparison of time-dependent, averaged percent dose/gram (N=6) and associated MIRD dose calculations with TLD dose data indicates reasonable first-order agreement between the two methods.

BETA PARTICLE DOSE TO THE MAJOR AIRWAYS FROM INHALED GAS. G. Powell, C. Reft, R. Schucard, P.V. Harper, and K.A. Lathrop. The University of Chicago, Chicago, IL.

Little attention has been given to the radiation absorbed dose to the tracheobronchial tree from inhaled beta emitters such as Xe-133 and O-15. Since the calculation of beta dose in heterogeneous media is still largely empirical, direct measurements were carried out using 20-micron thick LiF TLD dosimeters placed on the surface of a Lucite tracheal model; a hemicyclinder 10 cm long, .96 cm in radius. The dosimeter thickness in mg per centimeter squared corresponded to that of the 50-micron normal tracheal mucosa. Measurements made with O-15 and Xe-133 gave respectively 3.3 and 5.0 rads per hour for concentrations of 1 microcurie per milliliter. An additional observation in human subjects was that O-15 labeled CO2 strongly absorbed on the tracheal surface. This occurred both during breathing a constant gas concentration and during breath holding. Comparative studies with O-15 molecular oxygen revealed no such localization. The presence of water vapor in the gas which might have given similar results was eliminated by passing the gas through calcium sulfate and by confirming the absence of water vapor with gas chromatography. The localization of O-15-CO2 was determined in human subjects by comparing positron images of the trachea for O-15-O2 and O-15-CO2 after correction for attenuation scatter, uniformity, dead time and background. With the same average concentration of activity in the gas, the tracheal activity at equilibrium was ~15 times greater for O-15-CO2. The radiation absorbed dose estimate from O-15-CO2 to the tracheal mucosa was 26 rads/µCi/ml for a 30 minute study assuming that the dose from activity localized in the tracheal wall is equivalent to activity in the gas. This effect extends significantly into the pulmonary bronchial tree.

RADIATION DOSIMETRY FOR ZINC-63 FOR IV, ORAL AND JEJUNAL TUBE ADMINISTRATION USING A COMPARTMENT MODEL. RE Bigler, G Sgouros. Memorial Sloan-Kettering Cancer Center, NY, NY.

A multicompartment zinc model was used to calculate cumulated activities for zinc-63 ($T_{\frac{1}{2}}$=38.1 m) and zinc-65 ($T_{\frac{1}{2}}$= 244.1 d) given by intravenous (IV), oral and jejunum (enteral tube) administration routes. The model dramatically facilitates such calculations since only the initial conditions are changed. The cumulated activities were obtained for 8 anatomically defined regions by appropriate combinations of model compartments. Because the ovaries are especially important for risk assessment and were not resolved by the model, the 11 day liver-to-ovary ratio and the model derived total-body kinetics were assumed. The power of a model approach to radiation dosimetry is brought out very clearly by inspection of the Zn-63 results for stomach wall which show variations for route of administration from 1 to 3 mrads/mCi Zn-63 for IV or tube administration to 2.7 rads for oral administration. The dose to the liver drops from 500 mrads for IV administration to 140 mrads by tube and 100 mrads orally. Gonad (24-31 mrads) and average body doses (26 mrads) are similar to each other and as would be expected show little variation with route of administration. Our ability to estimate radiation doses to the region of the jejunum prior to any such experiments is illustrated by this work.

Zinc-63 Radiation Doses (mrads/mCi)

Target Organ	IV	Oral	Jejunum
Liver	490	104	138
Small Intestine	9.6	414	790
Muscle	1.3	1.1	1.4
Stomach Wall	1.1	2700	2.6
Jejunum (inject. site)	--	--	4100
Total Body	27	26	26

DOSIMETRIC IMPLICATIONS OF THE INFILTRATED INJECTION: F.P. Castronovo, K.A. McKusick, H.W. Strauss. Massachusetts General Hospital, Boston, MA.

Following inadvertent infiltration of a radiopharmaceutical, there is variable and uncertain uptake in target tissue. Concomitantly, there is also a concern for the radiation dose to the infiltrated site. This investigation determined the clearance and radiation burdens from various radiopharmaceutical infiltrates in a rat model. Nine separate sites were studied for: Tc-99m microspheres; Tc-99m MDP; Ga-67 citrate; and Tl-201 chloride. Following sc injection on the shaven posteriors of anesthetized adult male Sprague-Dawley rats, gamma camera and computer data were collected up to 24 hours. The resulting data were expressed semilogarithmically as the mean (N=9) of the "% retained at site" as a f(time) after injection. Nonparticulate agents showed a tri-exponential release pattern from each site, whereas the microspheres remained for an extended period of time. Using these pharmacokinetic curves, the % remaining at each site for various times, and rems/mCi per lcc infiltrate was determined:

Agent	% Retained at Site 30 min	60 min	240 min	Total rems/mCi
Tc-99m microspheres	100	100	100	360
Tc-99m MDP	23.1	14.3	6.8	49.3
Ga-67 citrate	47.6	33.6	18.4	37.8
Tl-201 chloride	70.1	63.9	47.2	1121.6

In addition, the dose 1 cm from the edge of an infiltrate would be reduced substantially.

DESIGN AND CONSTRUCTION OF EQUIPMENT FOR POINT-SOURCE, LOW ENERGY ELECTRON MICRODOSIMETRY MEASUREMENTS. C.I. Zanelli, J.A. Jungerman, C.D. Goodart, M.C. Lagunas-Solar, G.L. DeNardo, S.J. DeNardo. University of California, Davis, CA. Supported by DOE Grant DE AT03-82.

Actual measurements of dose as a function of distance for point-source, discrete energy spectra are essential to the selection of radionuclides for radioimmunotherapy, as the present theoretical basis provides extrapolations into the low energy region where assumptions about the energy-loss mechanisms are believed to break down.

We present a discussion of design criteria for an apparatus aimed at measuring dose in gases for low energy (10 to 100 keV) electron sources, as well as description of the equipment that emerged from this analysis. Given the short ranges involved, an almost-wall-less ionization chamber with cylindrical symmetry was selected. The chamber is fixed in position and a radioactive point-source is moved along its axis by remote control, preventing air disturbances in the chamber while obtaining ionization current measurements. A laser-aided positioning mechanism maintains alignment of the axis within 0.5 mm, and chamber-to-source distance is known within 0.3 mm. Special attention was given to the open-air ionization chamber design, and two different models were built. Guarding, grounding, and insulating schemes are proposed. The apparatus can be easily modified for use with gases other than air.

This equipment is presently being used to provide data for validation of, or corrections to, available theoretical calculations.

3:30-5:00 **Room 212A**

ONCOLOGY II: LYMPHOSCINTIGRAPHY AND ARTERIAL INFUSION

Moderator: Alan D. Waxman, M.D.
Comoderator: Henry H. Wellman, M.D.

QUANTITATIVE COMPARISON OF TWO RADIOCOLLOIDS FOR LYMPHOSCINTIGRAPHY. W.D. Kaplan, C.W. Piez, R.S. Gelman, S.M. Laffin, E.M. Rosenbaum, C.A. Jennings, and C.A. McCormick. Dana-Farber Cancer Institute, Boston, MA.

Recent qualitative studies suggest that a micro Tc-99m sulfur colloid (μSC) offers clinically acceptable images of the lymphatic system following intradermal injection. We have prospectively compared μSC to Tc-99m antimony colloid (SbS), the current agent of choice, in patients (pts) undergoing internal mammary lymphoscintigraphy. Twenty-eight consecutive females from 32-76 yrs of age were studied; 14 received SbS and 14 received μSC, (1.0 mCi, subcostal in posterior rectus sheath). Images (gamma camera and computer) of the injection site, anterior thorax and a Co-57 standard at the sternal notch were obtained at time 0 and 3 hrs after injection.

	Results at 3 Hrs $\bar{X}$ no. nodes	Migration (%pts) to SN†	$\bar{X}$ % node uptake	$\bar{X}$ % at inj. site	Ratio* node/Co-57
SbS	6.5	64	.45[.073-2.2]	83	.98
μSC	7.1	79	.25[.016-.53]	76	1.03††

$\bar{X}$ = mean
†SN = sternal notch
[ ] = range
*cts in most cephalad node/cts in Co-57 marker at SN
†† = 13 pts

The difference in $\bar{X}$% lymph node uptake was not statistically significant for the two groups. The clinical information obtained with the two radiocolloids was similar with respect to number of nodes seen, migration and relative "brightness" (ratio-node/Co-57). Additional patient studies will be needed to confirm this observation.

LYMPHOSCINTIGRAPHY IN MELANOMA PATIENTS USING Tc-99m DEXTRAN. D. Marciano, H. Padgett, E. Henze, C. Carlson, L. R. Bennett. UCLA School of Medicine, Los Angeles, CA.

Surgical removal of regional lymph nodes draining the site of a melanoma is a generally practiced procedure. It is often difficult in many cases of truncal melanomas near the midline or near the waistline to determine which group or groups of nodes to remove. Colloidal Au-198, Tc-99m sulfur colloid, and Tc-99m antimony sulfur colloid have all been used and have given useful clinical information. Objections, however, have been raised to the local radiation dose with these compounds. To reduce this problem while

obtaining greater information on lymph flow, we have studied dextran, a macromolecule commonly used as plasma substitute. Dextran (average mol. wt. 72,000) labeled with Tc-99m has been used to study lymph drainage from the site of truncal melanoma in 29 patients. Serial images in the first hour following intradermal injection clearly demonstrate tracer in efferent lymphatics within 5 to 10 minutes, and brief pooling in the regional lymph nodes between 20 and 60 minutes. When compared with particulate tracers such as micro Tc-99m sulfur colloid, the Tc-99m dextran appears to move much faster through the lymphatics. Overall distribution of the Tc-99m dextran to lymph nodes is very similar to our previous findings with micro Tc-99m sulfur colloid. Dextran drainage to more than one group of regional nodes was seen in 12/29 patients as compared with 17/50 patients using micro Tc-99m sulfur colloid. The superior images with Tc-99m dextran appear to make it the agent of choice.

THE DETECTION AND CLINICAL SIGNIFICANCE OF EXTRAHEPATIC ABDOMINAL PERFUSION (EHP) USING Tc-99m MAA HEPATIC ARTERIAL PERFUSION SCINTIGRAPHY (HAPS). H.A. Ziessman, R.L. Wahl, D. Lahti, J.E. Juni, J.H. Thrall, J.W. Keyes. University of Michigan Medical Center, Ann Arbor, MI.

HAPS has proven useful in the clinical management of pts receiving intraarterial chemotherapy for liver cancer. This therapy can be successful when the entire tumor-bearing liver is perfused, however abdominal EHP may reduce tumor exposure and increase systemic toxicity. EHP can be difficult to determine or be overlooked particularly when the stomach overlaps an enlarged left lobe of the liver. This study reports the frequency and clinical significance of EHP and evaluates the use of SPECT and EZ Gas (NaHCO3) to localize it. EHP was seen in 14% of 147 pts with surgically placed catheters, but was significantly more frequent, 53%, in 57 pts with percutaneously placed caths (p <.005). Significantly more pts with EHP (70%) had symptoms of drug toxicity compared to 19% without EHP (p <.005). Review of 73 HAPS studies using SPECT in addition to planar images showed EHP in 7. SPECT was very helpful in evaluating EHP suspected on planar images in 6 cases, confirming in 4, and excluding in 2. Two planar studies with likely EHP were confirmed by SPECT and 1 was inconclusive. EZ Gas effervescent granules have also been found useful in defining gastric EHP in 20 planar HAPS studies. These "air-contrast" views were helpful in confirming or excluding EHP in 80% of the studies and the initial impression was changed in 20%. Results were corroborated by oral Tc-DPTA and angiography. This study demonstrates that EHP is frequent and has important clinical significance but can be difficult to determine on HAPS. SPECT, EZ Gas and Tc-DPTA are very helpful in confirming or excluding suspected EHP.

DUAL ISOTOPE TECHNIQUE FOR IN VIVO QUANTITATIVE ASSESSMENT OF INTRA-ARTERIAL(IA) DRUG DELIVERY TO HEPATIC METASTASES. B.R. Line, G. Harper, M. Armstrong, J. Ruckdeschel. Albany Medical Center, Albany, NY.

Qualitative Tc-99m macro-aggregated albumin (MAA) scans can evaluate both IA catheter placement and regional hepatic perfusion. We report a new, dual isotope technique for the quantitative assessment of IA drug delivery to hepatic metastases (mets). Four patients (pts) with colon cancer metastatic to liver were treated for two week cycles with continuous IA 5-fluoro-2'-deoxyuridine (FUDR) infusion via an implantable pump (INFUSAID) at a dose of 0.1 to 0.3 mg/kg/d. At four week intervals each patient had quantitative hepatic imaging studies with Tc-99m SC to estimate met volume followed immediately by Tc-99m MAA through the pump to map drug distribution. MAA was distinguished from SC by computer subtraction and a distribution index (DI) expressed as the ratio of MAA in tumor vs normal tissues was determined. The lesion volume and DI were used to calculate the amount of FUDR delivered to tumor during treatment. Marked variability was found in the DI and chemotherapy delivered to tumor tissue between and within different pts. Pretreatment DIs were estimated to be 54%, 20%, 15%, and 1%. One pt demonstrated a drop in relative blood flow from a pretreatment DI of 54% to 49% at 4 weeks, and 37% at 8 weeks. The pt with the least DI (1.1%-5.0%) had the largest tumor burden (900 gm) and the smallest FUDR tumor delivery (0.2-1.1 ng/gm/min). The pt with the smallest tumor burden (80 gm) had the greatest FUDR delivery (14.8-22.1 ng/gm/min). This imaging technique provides quantitative estimates of tumor size and relative perfusion which can evaluate drug delivery to tumor and refine the assessment of both antitumor drug activity and toxicity of IA hepatic chemotherapy.

PULSATILE VERSUS STEADY INFUSIONS FOR HEPATIC ARTERY CHEMOTHERAPY. E.F. Kim, T.P. Haynie, K.C. Wright, C. Chaynsangavej, C. Gianturco, L. Lamki, and S. Wallace. The University of Texas System Cancer Center, M.D. Anderson Hospital and Tumor Institute, Houston, Texas.

Hepatic artery chemotherapy for unresectable liver tumors requires an even distribution of the drugs in the tumor vascular bed. This cannot be determined angiographically because the drugs are infused at a much lower rate than the contrast media. It is easy, however, to determine the quality of the perfusion by injecting a small volume of Tc-99m MAA in one of the side ports while chemotherapeutic agent is being infused at the same rate. Usually this shows a uniform, satisfactory distribution of isotope. Occasionally, however, some areas fail to receive Tc-99m inspite of what appears to be a good position of the catheter tip.

Since "streaming" of the infused drugs has been blamed for their uneven distribution, we decided to compare the usual steady flow infusions with infusions made pulsatile by the addition of a pulsing device (Gianturco Pump) attached to the infusion tubing.

Eighty-three patients were studied with steady as well as pulsatile infusions. In 16 of these patients the perfusion pattern was definitely changed by the pulsatile infusion. In one patient the pulsatile mode resulted in an unwanted gastric perfusion. In 5 patients the distribution was improved in one hepatic lobe and in 10 patients it was improved in both lobes.

These results show that hepatic artery perfusions can occasionally be improved by pulsing the infusate. However, pulsing can produce the unwanted perfusion of extrahepatic areas.

HEPATOBILIARY SCINTIGRAPHY IN PATIENTS RECEIVING HEPATIC ARTERY INFUSION CHEMOTHERAPY. D.F. Housholder, H.E. Hynes, S.R. Dakhil, and J.H. Marymont, Jr. St. Francis Regional Medical Center, Wesley Medical Center, and the University of Kansas School of Medicine-Wichita, Wichita, KS.

Two patients receiving hepatic artery infusion chemotherapy (HAIC) required cholecystectomy for both acute and chronic cholecystitis with cholelithiasis suggesting chemical cholecystitis. To evaluate the incidence of gallbladder dysfunction in patients receiving HAIC, we performed hepatobiliary scintigraphy using Tc-99m DISIDA or PIPIDA on eight patients receiving HAIC through an indwelling hepatic artery catheter and Infusaid® pump.

In 7 of 8 patients, there was non-visualization of the gallbladder throughout the hepatobiliary study. In the eighth patient, the gallbladder visualized at 2 hr. One patient with non-visualization of the gallbladder at 4 hr developed acute symptoms requiring cholecystectomy which showed acute and chronic cholecystitis with cholelithiasis. There was prominent sclerosis which was thought to be due to chemical cholecystitis as well as cholelithiasis.

In all 10 patients, no evidence of cholecystitis had been observed during the surgical placement of the hepatic artery catheter and Infusaid® pump. The hepatobiliary scintigraphic finding of gallbladder dysfunction in all eight patients studied is most likely due to chemical cholecystitis from HAIC. This series suggests that chemical cholecystitis is common during HAIC and can be identified by hepatobiliary scintigraphy.

We currently consider elective cholecystectomy during the operative placement of the hepatic artery catheter and Infusaid® pump.

3:30-5:00 **Room 216BC**

INFECTIOUS DISEASE

Moderator: William H. McCartney, M.D.
Comoderator: Russell Blinder, M.D.

CLINICAL UTILITY OF Ga-67 PULMONARY SCANS IN THE DIAGNOSIS AND TREATMENT OF P. CARINII PNEUMONITIS IN THE SETTING OF ACQUIRED IMMUNODEFICIENCY. R.S. Hattner, R.A. Sollitto, J.A. Golden and M.D. Okerlund. University of California, San Francisco, San Francisco, CA.

Acquired immunodeficiency syndrome (AIDS) is a severe disorder of cellular immunity of obscure etiology. Since its original recognition in 1981 the incidence of AIDS has doubled in each of the succeeding six months. The most common causes of death in AIDS are Kaposi's sarcoma and p. carinii pneumonia (PCP). The latter is treatable if diagnosed early, and AIDS patients (pts) may suffer recurrent episodes of PCP. Since the invasive technique of fiberoptic bronchoscopy with transbronchial biopsy, brushing, and bronchialveolar lavage are necessary for diagnosis and follow-up a noninvasive method of categorizing which AIDS pts require this procedure would be most welcome.

Fourteen symptomatic pts with AIDS were found to have PCP by the microscopic observation of the organism obtained from washings during fiberoptic bronchoscopy. Three had normal chest roentgenograms. Ga-67 scans of the thorax activity performed in each and pulmonary was graded 1-4 by three experienced observers (1, less than or equal to adjacent soft tissues; 2, greater than adjacent soft tissues, but less than liver; 3, equal to liver; 4, greater than liver). All scans were grades 3 or 4. After appropriate treatment 10 scans reverted to grades 1 or 2, corresponding with bronchoscopic resolution of PCP. Two pts with persistent grade 4 scans had persistent PCP at repeat bronchoscopy. Two pts died. These findings suggest that serial graded Ga scans may supplant bronchoscopy in the follow-up of treated PCP in AIDS and identify those AIDS pts with PCP resistant to conventional therapy requiring alternate therapy.

MONOCLONAL RADIOIMMUNOIMAGING OF HUMAN MELANOMA IN NUDE MICE. B.L. Engelstad, J.P. Huberty, R.S. Hattner, R.P. Triglia, H.M. Lee, D.F. Faulkner, L.E. Spitler. University of California, San Francisco, CA

To evaluate the efficacy of monoclonal radioimmunoimaging, murine specific (S) and non-specific (N) whole antibodies (W) and F(ab')2 fragments (F) that react with a non-p97 melanoma-associated antigen were radiolabeled with indium-111 (cyclic DTPA dianhydride bifunctional chelation). The products were administered in varying doses (60-250 ugm protein, 200-800 uCi) to nude mice bearing human melanomas (average 9 x 11 mm) and serially imaged scintigraphically (5.0 cm below 1.5 mm pinhole collimator). Tissue distribution was similiar over a wide protein dose range (0.1-100 ugm). Scintigraphic localization was quantitated by applying regions-of-interest to tumor (T), adjacent background (B), liver (L) and kidney (K). Qualitative scintigraphic findings included excellent tumor visualization with SW, fair tumor visualization with SF, poor or no tumor visualization with NW or NF, intense renal activity with SF or NF and moderate hepatic activity with all products. Quantitative scintigraphic findings included T/B and T/L ratios significantly higher with SW compared to NW, T/B and T/L ratios significantly higher with SW compared to SF, T/K ratios significantly higher with SF compared to NF and T/B, T/L, and T/K ratios tending to increase over time. The findings support the use of the SW product in controlled clinical trials.

THE BIODISTRIBUTION OF RADIOLABELED ANTI-LYMPHOCYTE MONOCLONAL ANTIBODY IN THE RAT. R.A. Fawwaz, T. Wang, J. Rosen, S. Srivastava, C. Iga, M. Hardy, and P.O. Alderson. Columbia University, New York.

Modulation of the immune response with anti-lymphocyte (L) monoclonal antibody (Ab) is a promising method for prevention of rejection. We examined the biodistribution of various types of anti L Abs in order to better define their mode of action. Mouse Ab against (1) all T Ls (Pan-T-Ab) and (2) helper T Ls (HT-Ab) were labeled with I-131 or In-111-DTPA. The Abs were injected separately into rats and their distribution compared with Ls prelabeled in vitro with In-111-oxine or In-111-DTPA-Ab. The biodistribution of Pan-T-Ab labeled with I-131 and In-111 was similar. At 2 hrs the mean% Id/g in spleen was 8.1±0.3%, in lymph nodes 3.5±0.4%, and in bone marrow (BM) 3.0±0.1%. Localization in the thymus was low (0.1±0.0%). At 24 hrs there was a rise in BM activity to 10.0±0.9%. The distribution of L labeled with In-111-DTPA-Ab differed from that of L labeled with In-111-oxine in that with the latter lymphoid localization was higher and BM activity decreased with time. The biodistribution of HT-Ab labeled with I-131 and In-111 also was similar but differed from that of labeled Pan-T-Ab in that there was less concentration in lymphoid organs and little activity in the body by 24 hrs, a pattern previously observed to occur with cytolysis. These results suggest that (1) HT-Ab is toxic to Ls and can be used for selective HT-L depletion; (2) Pan-T-Ab is not toxic to L but could be useful in selective lymphoid ablation if labeled with a beta-emitter; and (3) the thymus is unaffected by anti L Abs and thymectomy may be necessary to achieve optimal anti rejection treatment with anti L Abs.

DIFFERENT MIGRATORY PATTERNS OF BLOOD, SPLENIC, THYMIC LYMPHOCYTES, T AND NK CELLS LABELED WITH In-111 TROPOLONE IN RATS. G. Gagne, A.M. Garcia, J.G. McAfee. Upstate Medical Center, Syracuse, NY.

Labeled cells harvested from different lymphoid organs have been used to study lymphocyte migration in experimental animals, but the influence of the source organ on their biodistribution is largely unknown. We harvested peripheral blood cells (88% lymphocytes), splenic cells, splenic T cells after elimination of B cells by nylon wool column, thymic cells and natural killer (NK) enriched cells. For the last preparation, spleen cells were obtained from neonatal thymectomized rats, nylon wool column filtered, and centrifuged on Percoll, to obtain 27% NK cells. These 5 different cell preparations were labeled with (In-111 tropolone (<10 μCi/10^8 cells) and their blood clearance and localization were compared in Wistar rats.

Peripheral blood cells maintained a high blood level up to 24 hr. (27%), similar to previous studies in humans. They reached a high concentration in lymph nodes (25%), with comparatively low levels in the spleen and liver. In contrast, cells of splenic or thymic origin disappeared rapidly from the blood and sequestered temporarily in the lungs. Thymic cells were sequestered in the liver, and concentrated poorly in lymph nodes. Splenic T cells had a relatively high concentration in lymph nodes and marrow. NK enriched cells maintained a relatively high level in the blood, a low concentration in lymph nodes, and sequestered chiefly in the liver.

These results indicate that the source organ from which lymphocytes are extracted is a major determinant in their localization.

IN-111 WBC SCINTIGRAPHY IN ADULT OSTEOMYELITIS. L. Ehrlich, R.H. Martin, J. Saliken. Victoria General Hospital, Halifax, NS.

Unlike pediatric bone infections, adult osteomyelitis is commonly related to trauma, surgery, or direct extension from an overlying soft tissue infection. Because of this, the findings on Tc-99m MDP bone scintigraphy tend to be nonspecific. Therefore the value of In-111 WBC scintigraphy in the diagnosis of adult osteomyelitis was evaluated.

52 scans were obtained on 51 adult patients who were consecutively referred to our department with this provisional diagnosis. The diagnosis was confirmed by at least two of the following: positive culture, surgery, x-rays, laboratory results, and clinical response to antibiotics. Of the 52 scans studied the sensitivity was 84%, specificity was 82%, and the accuracy was 83%. False positive results occurred most frequently in patients with inflammatory arthritis. False negative examinations occurred in patients who had In-111 WBC concentration in overlying soft tissue

obscuring the bony abnormality. Neither the chronicity of the infection, nor prior treatment with antibiotics created difficulty in scan interpretation. It was concluded that although somewhat less sensitive than TcMDP bone scanning, In-111 WBC scintigraphy is more specific than previously studied radiopharmaceuticals in the assessment of bone infections in the adult population.

NO DIFFERENCE IN SENSITIVITY FOR OCCULT INFECTION BETWEEN OXINE AND TROPOLONE LABELED In-111 LEUKOCYTES WHEN IMAGED EARLY. F. Datz, W. Baker, A. Taylor, N. Alazraki. University of Utah School of Medicine and VA Medical Center, Salt Lake City UT.

There is an ongoing debate whether oxine or tropolone is the best labeling agent for indium leukocytes. Recent studies have given conflicting results concerning leukocyte viability, chemotaxis, and the ability to detect abscesses early with the two materials. We have undertaken a long-term prospective study to see which material gives the best clinical results early, 1-4 hours following injection.

To date, 55 patients have been studied. The first 35 patient's leukocytes were autologously labeled with oxine; the next 20 with tropolone. Imaging was performed 1-4 hours post injection (mean 3) and repeated at 24 hours. The diagnosis was confirmed by clinical course, x-ray studies, surgery, and necropsy studies.

Oxine: 19 of 35 (54%) patient studies had a clinical site of infection. The early images had a sensitivity of only 44% (7 of 16) whereas the delayed images were 95% sensitive. Of the cases positive both early and at 24 hours, 70% had more intense uptake at 24 hours.

Tropolone: 8 of 20 (40%) patient studies had a clinical site of infection. The early images had a sensitivity of 50% (4 of 8) whereas the delayed images picked up all sites of infection. Thirty-three percent of the cases positive both early and at 24 hours had more intense uptake at 24 hours.

There was no statistical difference in the sensitivities between oxine and tropolone labeled white cells.

At present, we find no difference in the early sensitivity at 1-4 hours between oxine and tropolone labeled leukocytes.

SENSITIVITY AND SPECIFICITY OF Ga-67 PULMONARY SCANS FOR THE DETECTION OF P. CARINII PNEUMONITIS IN PATIENTS WITH THE ACQUIRED IMMUNODEFICIENCY SYNDROME AND PULMONARY SYMPTOMS. R.S. Hattner, R.A. Sollitto, J.A. Golden, D.L. Coleman and M.D. Okerlund. University of California, San Francisco, San Francisco, CA.

Acquired immunodeficiency syndrome (AIDS) is a severe disorder of cellular immunity of obscure etiology. Since its original recognition in 1981 the incidence of AIDS has doubled in each of the succeeding six months. The most common causes of death in AIDS are Kaposi's sarcoma and p. carinii pneumonia (PCP). The latter is treatable if diagnosed early, and AIDS patients (pts) may suffer recurrent episodes of PCP. Since the invasive technique of fiberoptic bronchoscopy with transbronchial biopsy, brushing, and bronchialveolar lavage are necessary for diagnosis and follow-up a noninvasive method of categorizing which AIDS pts require this procedure would be most welcome.

Twenty-one pts with the syndrome of AIDS and pulmonary symptoms underwent Ga-67 scans of the thoracic region, and fibroptic bronchoscopy with washings, and brush and transbronchial biopsy. Pulmonary activity was graded in a blinded fashion by three experienced observers as follows: 1, less than, or equal to adjacent soft tissues; 2, greater than adjacent soft tissues, but less than liver; 3, equal to liver; 4, greater than liver. Eleven pts had documented PCP, and the remaining ten had non-specific pulmonary inflammation, or other, in some cases, putative, infections. The sensitivity and specificity of Ga-67 scans $\geq$ grade 3 was 100% and 90% respectively. These results suggests a useful role for graded Ga-67 scans in AIDS pts with pulmonary symptoms, permitting selection of pts with a high risk of PCP for further mandatory invasive investigation of this otherwise usually fatal disease.

3:30-5:00 **Room 212B**

CORRELATIVE IMAGING

Moderator: David A. Turner, M.D.
Comoderator: Joe C. Leonard, M.D.

HEPATIC CANCER - CORRELATIVE IMAGING WITH RADIOIMMUNODETECTION, NMR, AND TCT. F.H. DeLand, A. Lieber, M.D. Ram, Univ Kentucky and V.A. Medical Centers, Lexington, KY and D.M. Goldenberg, Center for Molecular Medicine and Immunology, Newark, NJ.

The purpose of this study was to compare the sensitivity of radioimmunodetection (RAID) imaging and nuclear magnetic resonance imaging in the detection of hepatic tumors. Twelve consecutive patients with metastatic (11) or primary (1) carcinoma of the liver were imaged concurrently with labeled antibodies-to-tumor antigens and by nuclear magnetic resonance. Evidence of hepatic tumors was correlated with other diagnostic procedures including TCT. Eleven patients were imaged with I-131 labeled antibodies to CEA, CSAP and one with I-131 labeled antibodies to AFP. Polyclonal, monoclonal, and Fab'_2 antibodies were used. The preparation and labeling of the antibodies have been described previously. Each patient received 2-3 mCi of labeled antibodies and was imaged at 24 to 48 hrs. Nontarget radioactivity was diminished by other radionuclides simulating nontumor distribution using a computer subtraction technique. NMR images were obtained with a 0.15T resistive instrument. In all twelve patients hepatic tumor was diagnosed by RAID. Nine of the hepatic tumors were confirmed by other methods. NMR demonstrated four positive findings in these nine. Computerized tomography detected tumors in three of the nine patients at the time of the first RAID examination, and subsequently in one more patient when RAID and NMR examinations were performed concurrently. In this series of patients the detection of hepatic cancer by RAID showed twice the sensitivity of NMR or TCT.

CORRELATION OF DIAGNOSTIC ULTRASOUND AND RADIONUCLIDE IMAGING IN SCROTAL DISEASE. D.C.P. Chen, L.E. Holder and G.N. Kaplan. The Union Memorial Hospital and The Johns Hopkins Hospital, Baltimore, MD.

A retrospective study was performed to evaluate the usefulness of scrotal ultrasound imaging (SU) and radionuclide scrotal imaging (RSI) in 43 patients (pts), age: 16-75. Twenty-two of them complained of scrotal pain; 18 had a scrotal mass; and 4 had a history of trauma. The final diagnoses were conformed by surgery (n = 21) and long-term follow-up (n = 22) and included 4 late phase and 1 early testicular torsion (TT), 11 acute epididymitis (AE), 4 subacute epididymitis (SE), 5 malignant tumors, 3 testicular atrophy, 2 intratesticular hematomas, 10 hydroceles or other cystic lesions, and miscellaneous.

In pts with scrotal pain, 3/4 with late phase TT were correctly diagnosed, while one pt with early TT and 11/15 with AE or SE were not diagnosed by SU. All of them were correctly diagnosed with RSI except one with scrotal cyst. SU was able to separate cystic masses (n = 10) from solid masses (n = 6), but cannot separate malignant from benign lesions. RSI has difficulty in separating cystic from solid lesions. SU was excellent in detecting 19 hydroceles and 2 intratesticular hematomas, while 3 lesions < 1 cm. were not seen in RSI.

We concluded that SU is useful in pts with scrotal mass to separate solid from cystic lesions. However, SU is unable to differentiate the acute epididymitis from early testicular torsion. In pts with acute scrotal pain, SU is not helpful and RSI should still be the first study performed.

VARICOCELESCINTIGRAPHY VERSUS X-RAY PHLEBOGRAPHY. H.Y. Oei, J.W. Arndt, W.P.Th. Mali, B.L.R.A. Coolsaet, J. Kremer. University Hospital Utrecht, The Netherlands.

In this study varicocelescintigraphy (VS) is compared to X-ray phlebography(XP). In 104 patients(pts) suspected for varicocele on physical examination, VS was performed using a large field camera and 5 mCi Tc-99m in-vivo labeled erythrocytes. This was done (without Valsalva) in upright position after taping penis to the abdomen, marking the penisbase and covering the thighs with lead. Twenty 5-sec dynamic images (DY) and 5-min static image (ST) were made. Varicocele-size was quantitated by bloodpoolvalue (BPV)using digital image of ST. BPV is the ratio of mean counts/pixel in varicocele and right iliac vessels calculated from adjacent pixels with maximum counts. On XP varicocele was diagnosed if the testicular vein was visualized after contrast injection given during Valsalva in the renal vein.

In 85 pts varicocele was confirmed on XP. In 67 of them this was recognized easily on both DY and ST; the DY shows activity in the varicocele 10-35 sec later than the iliac artery and the ST shows pooling of activity below the penisbase. In 11 pts the varicocele was only seen on ST and in other 5 pts only on DY. In the remaining 2 pts both DY and ST were false negative. The BPV in 72 pts with abnormal DY and in 11 pts with normal DY varied between 0.4-2.2(0.89$\pm$0.38) resp. 0.4-1.0(0.61$\pm$0.19). In 16 of the 19 pts who showed no varicocele on XP, VS also was negative; their BPV varied between 0.2-0.4(0.30$\pm$0.08). However, in 3 pts who initially had a normal XP, varicocele was diagnosed on both DY and ST, which was confirmed when XP was repeated.

Diagnosis of varicocele by physical examination is not accurate. VS is suitable for screeningsprocedure when both DY and ST are obtained. Pts with abnormal DY have larger varicocele than pts with normal DY.

GATED SINGLE PHOTON EMISSION TOMOGRAPHY (GSPECT) AS A MEANS OF QUANTITATIVE ASSESSMENT OF LEFT VENTRICULAR WALL MOTION.
J.L. Barat, A.J. Brendel, J.P. Colle, V. Magimel-Pelonnier, J. Ohayon, F. Leccia, P. Besse, and D. Ducassou. Hôpital Universitaire Haut-Lévêque, Bordeaux-Pessac (France).

Evaluating left ventricular (LV) function, planar radionuclide ventriculography is limited by background and counts from different depths, but GSPECT is not. Its ability to describe wall motion accurately is presented, with reference to angiographic data. 61 patients with chest pain had GSPECT 1h before left catherisation. GSPECT examined an 12 mm thick sagittal slice along the LV major axis, and contrast ventriculography (CV) analysed a 30° RAO view. Wall motion was evaluated in 10 sectors centered on a fixed point (following the Stanford group) giving 10 ejection fractions from GSPECT and 10 mean radius shortening %s for CV. The sectorial data (GSPECT vs. CV) were analyzed by linear regression.

Segment	Inferior			Apical			Anterior		
r	0.6	0.6	0.7	0.7	0.8	0.7	0.7	0.7	0.6
SEE	12	16	18	17	17	17	18	17	15

Inter and intraobserver reproducibilities were better for GSPECT than for CV.

Also a comparison was made of the diagnostic value of this method of quantification applied to the two imaging techniques using ROC analysis. The values of sensitivities at two operating points were :

Specificity	GSPECT	CV	Sign Test
90 %	75 %	90 %	p = 0.004
80 %	90 %	96 %	N.S.

We conclude that GSPECT correlates with CV and allows accurate non invasive quantitative study of all ventricular segments.

COMPARISON OF THALLIUM-201 SUBTRACTION SCINTIGRAPHY WITH SONOGRAPHY AND X-RAY CT IN THE LOCALIZATION OF PARATHYROID ADENOMA.
N. Hayashi, N. Tamaki, Y. Yonekura, M. Senda, K. Yamamoto, R. Morita, K. Torizuka. Kyoto University Medical School, Kyoto, Japan.

Precise preoperative localization of parathyroid adenoma (PTA) is helpful for surgical therapy. The role of radionuclide imaging (RN) of PTA was studied in comparison with sonography (US) and X-ray computed tomography (CT). RN was performed by subtracting I-123 images from Tl-201 images on the same position. Definite remnant uptake on this subtraction image on computer display was considered abnormal. US was performed using real-time linear array units with 5MHz transducer. CT was performed both with and without contrast media.

Their diagnostic accuracy was as follows;

	Sensitivity	Specificity	Accuracy
RN	18/30(60%)	26/27(96%)	44/57(77%)
US	14/20(70%)	25/28(89%)	39/48(81%)
CT	37/41(90%)	37/42(93%)	76/83(92%)

Sensitivity of RN was worst among these three methods. However, in two cases both US and CT mistook thyroid adenoma for PTA, while RN could diagnose PTA correctly. RN could detect four PTAs which US could not detect. All of them were apart from the thyroid, including one in the mediastinum. On the other hand, US detected three PTAs which RN failed to find. All of them were covered by the thyroid. CT showed an excellent result, but problems of ionized radiation and side effects to contrast media remained. Because RN and US have complementary roles to each other, to use both of them together seems to be pertinent for screening of PTA.

EFFICACY OF 67 GALLIUM ECT IMAGING IN LYMPHOMA, INFECTION, AND LUNG CARCINOMA: A COMPARISON WITH PLANAR IMAGING.
S.J. Harwood, M.W. Anderson, R.C. Klein, B.I. Friedman, and R.G. Carroll, Bay Pines VAMC, St. Petersburg, FL.

Emission computed tomography (ECT) studies were performed on a GE 400 A/T camera and ADAC computers (system 3 and system 3300). Thirty-three sets of ECT and planar images were obtained in 20 patients over a six month period. Imaging was performed 48 hours after the intravenous administration of 5 mc of Gallium 67 citrate. No bowel preparation was employed. Comparison is made of the initial nuclear medicine report derived from planar and ECT imaging aided by clinical knowledge versus the consensus opinion of two nuclear medicine physicians reading the planar images along with minimal clinical information.

The lymphoma series consists of 18 scans in 10 patients. There were 5 scans in which a false negative planar interpretation was changed to a true positive ECT interpretation. Sensitivity of planar imaging for lymphoma was 58% which rose to 100% with addition of ECT information. There were no false positives by either technique. There were 5 sets of scans in 5 lung carcinoma patients. Sensitivity of the planar images was 60% because of 2 false negative results. Sensitivity of the ECT technique was 100%. There were no false positives. The infection series consists of 10 scans in 5 patients. Sensitivity of ECT was 100%, sensitivity of planar was 66%. There was 1 false positive planar. For the total series the accuracy of planar imaging was 69% and the predictive value of a negative planar interpretation was 44%. Corresponding values for ECT imaging were 100%.

Our experience demonstrates significant increase in sensitivity without loss of specificity resulting from the use of Emission Computed Tomography in both chest and abdomen in patients with lymphoma, infection, and lung cancer.

THURSDAY, JUNE 7, 1984

1:30-3:00 **Room 217A**

CARDIOVASCULAR VII: DIASTOLIC LEFT VENTRICULAR FUNCTION

Moderator: Michael V. Green, M.S.
Comoderator: Tom R. Miller, M.D.

DETERMINANTS OF GLOBAL LEFT VENTRICULAR PEAK DIASTOLIC FILLING RATE DURING REST AND EXERCISE IN NORMAL VOLUNTEERS.
A.W. Filiberti, J.A. Bianco, S.P. Baker, P.W. Doherty, L.A. Nalivaika, M.A. King, J.S. Alpert, University of Massachusetts, Worcester, MA.

Early peak diastolic filling rate (PFR) of the left ventricle (LV) is said to be a sensitive index of LV dysfunction in patients with coronary disease, hypertension and hypertrophic cardiomyopathy. Radionuclide (RN) multigated PFR was measured in 20 normal volunteers (13 males, 7 females, mean age 31 yrs., range 20-43) at rest and

during supine bicycle exercise conducted to a symptomatic end-point. At rest, RN PFR was 3.4 ± SD 0.4 end-diastolic vols./sec (range 3.1 - 3.6). During exercise all normal volunteers had a progressive and numerically and statistically significant increase in PFR. Stepwise multiple linear regression (BMPD2R) was applied to the rest and exercise PFR data to develop a linear model describing the main determinants of the RN PFR. The potential independent variables which were included in the model were heart rate (HR), ejection fraction (EF), systolic arterial pressure, systolic ejection rate and exercise stage. Ranking of variables for prediction of RN PFR, and exclusion of less important variables, was done by F value criteria. The final multivariate equation was: LVPFR = -3.84437 + 0.03834 HR + 0.07537 LVEF. The model fit was highly significant ($p < 0.001$), and accounted for 89 per cent of variability in the PFR.

In summary, the left ventricular peak filling rate is critically determined by heart rate and by ejection fraction at rest and during exercise.

COMPARISON OF PEAK FILLING RATE OF LEFT VENTRICLE PRE AND POST CORONARY BYPASS GRAFT IN PATIENTS WITH AND WITHOUT MYOCARDIAL INFARCTION. M. Hourani, A. Gentili, H. Bolooki, L. Clarke, F. Ashkar, G. Sfakianakis, A. Serafini. University of Miami, Miami, FL.

The study was undertaken to evaluate improvement in diastolic function by measuring peak filling rate (PFR) of left ventricle in 57 patients (pts) undergoing coronary artery bypass graft (CABG). Twenty seven patients had coronary artery disease (CAD) but no history of myocardial infarction (MI) (Group 1). Twenty three patients had documented (MI) but no aneurysms (Group 2). Group 3 had 7 patients with CAD and aneurysms. The pre and post operative ejection fraction (EF) and PFR were calculated from the time activity curve of resting gated cardiac studies performed so that the time per frame was 0.03 sec.

	Group 1 n = 27	Group 2 n = 23	Group 3 n = 7
EF Preop. ± 1SD	58.5 ± 11.9	51.0 ± 14.5	38 ± 12.4
EF Postop. ± 1SD	58.5 ± 13.3	50.5 ± 16.8	42 ± 5.6
P	NS	NS	NS
PFR Preop. ± 1SD	2.14 ± 0.50	2.08 ± 0.62	1.56 ± 0.50
PFR Postop. ± 1SD	2.94 ± 0.83	2.69 ± 0.93	2.83 ± 0.69
P	<0.001	<0.001	= 0.008

We conclude that PFR is a more sensitive index than EF in evaluating the post-operative improvement in ventricular function in patients undergoing CABG especially in patients with normal wall motion and normal ejection fraction and will be a useful index to use for the follow-up of these patients. Improvement in PFR correlated well with the post-operative course of the patients. All patients who decreased thin PFR had a complicated post-op-course.

EVALUATION OF PATIENTS WITH CHEST PAIN BY RADIONUCLIDE VENTRICULOGRAPHY: COMPARISON OF PHASE AND 2-HARMONIC ANALYSIS. G. A. Hurwitz, T. R. Miller and D. R. Biello. Mallinckrodt Institute of Radiology, Washington University, St. Louis, MO.

Fourier-series analysis (FSA) of time activity curves has been used to enhance the detection of regional abnormalities in function of the left ventricle (LV) on radionuclide ventriculograms (RVGs). Phase, or first harmonic analysis, does not permit separate determination of systolic and diastolic function. The retention of 2 harmonics (2-H) in the FSA allows definition of both systolic and diastolic parameters, including time to peak ejection rate (TPER) and time to peak filling rate (TPFR).

We compared regional phase and 2-H analysis in 42 patients with normal LV function by conventional analysis of resting RVGs. All patients had ejection fraction greater than 50% and normal regional wall motion. Diagnoses, established by cardiac catheterization, included coronary artery disease (CAD) and chest pain but normal coronary arteries (NCA). Normal homogeneity of LV function was established in 12 normal volunteers by computing the standard deviation of the distribution of LV pixels for TPER, TPFR and phase angle on the 35° LAO views.

Diagnosis	Total	Number Abnormal		
		Phase	TPER	TPFR
CAD	20	3	1	14
NCA	22	1	0	2

Thus, in patients with CAD but normal conventional analysis of RVGs, 2-H analysis detected abnormal diastolic filling in 70% whereas phase analysis was abnormal in only 15%. In patients with NCA, abnormalities by either phase or 2-H analysis were infrequent. These data suggest that 2-H analysis may be of value in the investigation of patients with chest pain but normal LV function.

ASSESMENT OF ASYNCHRONOUS RELAXATION IN HYPERTROPHIC CARDIOMYOPATHY AND ISCHEMIC HEART DISEASE. S. Kodama, N. Tamaki, M. Senda, Y. Yonekura, Y. Suzuki, R. Nohara, S. Tamaki, H. Kambara, C. Kawai, and K. Torizuka. Kyoto University Medical School, Kyoto, Japan. and T. Mukai. The Johns Hopkins Medical Institutions, Baltimore, MD.

This study is undertaken to assess cardiac performance in relation to left ventricular(LV) asynchronous wall motion. Multigated blood-pool study was performed in 67 cases, including 14 normals(N), 16 with hypertrophic cardiomyopathy(HCM), and 37 with ischemic heart disease (IHD). IHD was further divided into 2 groups: IHD(I)(EF ≥ 50%), and IHD(II)(EF < 50%). Regional(pixel-by-pixel) volume curve was simulated by second order harmonics of Fourier series. Then, functional images of the following indexes were made: EF, TES(time to end-systole), PER(peak ejection rate), TPE(time to PER), PFR(peak filling rate), and TPF(time to PFR). The left ventricular phase distribution histograms of TES, TPE, and TPF were made to calculate the standard deviation(SD) as an asynchronous parameter of each phase.

TES(SD) was higher only in IHD(II)(11.3±5.2 deg) than N(4.8±2.5 deg). TPF(SD) was higher in HCM(11.7±9.7 deg) and IHD(15.1±11.3 deg) than N(5.3±3.7 deg), suggesting asynchronous relaxation. In the study of global LV performance, LVEF was not significantly different in HCM(64±9%) and IHD(I)(58±5%) from N(60±6%). However, PFR was lower in IHD(I)(2.3±0.6 EDV/sec) and IHD(II) (1.6±0.5 EDV/sec) than N(3.3±1.0 EDV/sec). PFR/PER was lower in HCM(0.7±0.2), IHD(I)(0.8±0.2), and IHD(II)(0.7±0.3) than N(1.0±0.2). Besides, TPF(SD) was inversely correlated with LVEF(r=-0.43), PFR (r=-0.45), and PFR/PER(r=-0.51). Thus, asynchronous relaxation is often seen in HCM and IHD, and it may be related to the disturbance of LV filling.

FIRST THIRD FILLING PARAMETERS OF LEFT VENTRICLE ASSESSED FROM GATED EQUILIBRIUM STUDIES IN PATIENTS WITH VARIOUS HEART DISEASES. M.H. Adatepe, K. Nichols, O.M. Powell and G.H. Isaacs. Allegheny General Hospital, Pittsburgh, PA.

We determined the first third filling fraction (1/3 FF), the maximum filling rate (1/3 FR) and the mean filling rate (1/3 MFR) for the first third diastolic filling period of the left ventricle in patients with coronary artery disease (CAD), valvular heart disease (VHD), pericardial effusion (PE), cardiomyopathies (CM), chronic obstructive lung disease (COPD) and in 5 normals—all from resting gated equilibrium studies. Parameters are calculated from the third order Fourier fit to the LV volume curve and its derivative. 1/3 FF% = 1/3 diastolic count - end systolic count ÷ 1/3 diastolic count x 100. Patients with CAD are divided into two groups: Group I with normal ejection fraction (EF) and wall motion (WM); Group II with abnormal EF and WM. Results are shown in the table. Abnormal filling parameters are found not only in CAD but in VHD, PE and CM.

TABLE

	N	EF%	1/3 FF%	1/3 MFR sec^{-1}	1/3 FR sec^{-1}
Normal	5	69±7	59±5	2.35±.6	3.36±.15
Gr. I CAD	21	63±8	34±8	1.33±.34	2.04±.45
Gr. II CAD	39	37±10	19±8	0.99±.4	1.50±.6
VHD	20	60±15	36±11	1.45±.35	2.08±.53
COPD	6	78±5	57±5	1.93±.34	2.93±.68
PE	3	65±27	29±17	1.57±1.1	1.12±.65
CM	3	26±17	13±.09	0.51±.57	1.07±.92

We conclude that the first third LV filling parameters are sensitive but non-specific indicators of filling abnormalities caused by diverse etiologic factors. Abnormal first third filling parameters may occur in the presence of a normal resting EF and WM in CAD.

NEW DIASTOLIC FILLING PARAMETERS FOR EVALUATION OF LEFT VENTRICULAR HYPERTROPHIES BY EQUILIBRIUM GATED STUDIES. D.G. Pavel, P. Briandet, J. Sychra, R. Fang, S. Boonyaprapa

G. Kondos, S. Rich, J. Shanes, S. Virupannavar, R. Pietras. University of Illinois, Chicago, Il.

Detection of abnormal ventricular compliance is of clinical importance and is most commonly found in left ventricular hypertrophy (LVH). The use of peak filling rate alone provides a very poor separation of patients (Pts) with LVH. We have studied 13 normal (Nl) and 50 Pts with LVH of various etiologies. All had ejection fraction > 55%, and 23 had cardiac catheterization. Method: LV time activity curve was replaced by weighted sum of 7 Fourier harmonics, expanded to 512 points. Rates normalized and expressed as % stroke volume/sec. Parameters (PAR): (A) Peak Filling Rate; (B) Duration from nadir of curve to (A); (C) Average Early Filling Rate within early 1/4 of diastole (normalized to heart rate); (D) same as (C) but within early 1/5; (E) linear discriminant function (df) containing values of (C) and (D) (df = (D + .59 x C)/100). Specificity kept by study design at 100%.

Results: Averages (Nl vs LVH ± SD): (A) 545 ± 61 vs 527 ± 172 NS; (B) 148 ± 11 vs 264 ± 120 p<.001; (C) 293 ± 36 vs 153 ± 56 p<.001; (D) 235 ± 35 vs 121 ± 45 p<.001; (E) 4.08 ± 0.55 vs 2.12 ± .076 p<.001; Sensitivity: A=48%; B=88%; C=98%; D=96%; E=98%. Ranking based on Fisher's discriminant measure, indicates top ranking for E (1.77) then C (1.72), D (1.44), B (.88). Besides parameter (E) no other combination of two PAR was found to be superior to single PAR (C). Conclusion: Average early filling rates within normalized early diastolic intervals are simple (can be used even as single PAR) and very sensitive for the evaluation of compliance abnormality in LVH.

1:30-3:00 **Room 216BC**

INSTRUMENTATION III: ECT—POSITRON

Moderator: Michael E. Phelps, Ph.D.
Comoderator: Nathaniel M. Alpert, Ph.D.

HIGH RESOLUTION POSITRON EMISSION TOMOGRAPHY USING 3 MM WIDE BISMUTH GERMANATE CRYSTALS. S.E. Derenzo, R.H. Huesman, T.F. Budinger, J.L. Cahoon, and T. Vuletich. Donner Laboratory and Lawrence Berkeley Laboratory, University of California, Berkeley, CA.

To determine the spatial resolution that can be achieved using 3 mm wide bismuth germanate (BGO) crystals, we set up a test gantry with opposing groups of 40 BGO crystals and a rotating phantom. The motion of one group of crystals, the rotation of the phantom, and data acquisition were under computer control. The system emulated a complete ring of 536 crystals on a diameter of 60 cm, with a center-to-center spacing of 3.5 mm. Coincident data were acquired only between the central 8 detectors, so that photon side penetration of the crystals for off-axis sources would be accurately simulated. Clamshell sampling was used to reduce the lateral sampling distance to 0.9 mm. The lead shielding had a 1 cm gap, an inner diameter of 30 cm, and an outer diameter of 60 cm. Each crystal had a front face 3 mm x 10 mm, a depth of 30 mm, and was coupled to its own 14 mm diameter phototube. Because the phototubes were coupled to 3 sides of the crystal array, this coupling scheme is only applicable to a single layer tomograph.

At the center of the gantry, a 0.35 mm diameter line source of Na-22 had a reconstructed point spread function (PSF) that was circular with a full-width at half-maximum (FWHM) of 2.6 mm. At a distance of 8 cm from the center of the gantry, the PSF was elliptical with a radial FWHM of 4.1 mm and a tangential FWHM of 2.7 mm. These results show that small BGO crystals can improve the spatial resolution in positron tomography by a substantial factor.

HEADTOME III: A HIGH QUANTITATION AND HIGH RESOLUTION BRAIN POSITRON EMISSION TOMOGRAPH. I.Kanno, S.Miura, M.Murakami, K.Uemura, Y.Hirose, and S.Takahashi, Research Institute of Brain and Blood Vessels-AKITA, Akita, and Shimadzu Corp., Kyoto, JAPAN

HEADTOME III, a high quantitation and high resolution positron emission tomograph (PET) has been developed. HEADTOME III was basically designed as a brain PET of 3 rings 5 planes. Each ring (75 cm diam) consists of 160 BGOs (13.4x25x40 mm). Shadow masks and septa can be used independently, corresponding to low (LR) and high resolution mode (HR), and low (LQ) and high quantitation mode (HQ), respectively. Planar resolutions at the center of the field of view (FOV) were 8.2 and 6.5 mm FWHM in LR and HR, respectively. Deterioration of resolution at 8 cm radius were 0.6 and 0.8 mm in FWHM. Slice thicknesses were 12.8 and 9.1 mm FWHM at the center of FOV with LQ and HQ, respectively, its deviation being 1.1 and 0.8 mm over FOV with each, and 0.1 mm difference between direct and cross planes in LQ mode. Sensitivities, true events for Ga-68 20 cm diam cylinder, were 32(68), 17(33), 18 and 9 kcps/(μCi/ml) with the direct (cross) planes of LRLQ, direct (cross) planes of HRLQ, direct planes of LRHQ and HRHQ, respectively. Count rates were declined 10 % at 30 kcps true events per plane but recovered up to 100 kcps within 5 % error by software correction using random coincidence events. Scattered fraction after corrected by subtracting a mean of outside the FOV in sinogram was 10 and 3 % in the reconstructed images in LQ and HQ, respectively. Long term stability evaluated cross calibration factor checked weekly in the last half year was 1.9 % COV as an average of 5 planes and 2.2 % at maximum plane. These data imply that HEADTOME III permits an accurate analysis of tracer kinetics.

PHYSICAL CHARACTERIZATION OF A TIME-OF-FLIGHT POSITRON EMISSION TOMOGRAPHY SYSTEM FOR WHOLE-BODY QUANTITATIVE STUDIES. F. Soussaline, R. Campagnolo*, B. Verrey, B. Bendriem, A. Bouvier*, J.L. Lecomte* and D. Comar. S.H.F.J., CEA, Depart. Biol., Orsay and *LETI, CEA, Grenoble, France.

The design of a first PET system using the time of flight (TOF) information, is aimed at whole-body, quantitative, dynamic, 3D studies. It comprises 3 rings of 96 CsF probes and a ring of 96 BaF_2 probes. The physical performance was measured : spatial transverse and longitudinal resolution for a reconstructed source (13 - 9 mm FWHM and 12 mm FWHM), sensitivity (12000 events/sec/axial cm), time resolution (480 psec $\pm$ 28 psec for CsF and 380 psec $\pm$28 psec for BaF_2), interplane (< 5% for the means difference for a uniform ring source) and intraplane uniformity (< 4% RMS uncertainty). Calibration in absolute concentration was performed with a precision of 2%. Special attention was directed to the specific advantages of the use of fast crystal - PM tubes for TOF measurements : -very fast count rate studies, -elimination of random events, -and improvement of the S/N ratio. Counts rates up to a million counts per sec for each detector are feasible, without loss due to pile up. Actually, the maximum count rate is 450000 events/sec due to the transfert time to magnetic disc in list mode (30 μCi/cc). At these rates, the random fraction is 30 % of the true coincidences rate, while it is less than 3 % for concentration of 1 μCi/cc. The sensitivity gain was measured as a function of the object size : 2 for the head and 4.8 the wholebody. Other advantages of TOF as Compton events reduction and the accuracy of attenuation correction coefficients are evaluated for thoracic studies.

PERFORMANCE CHARACTERISTICS OF THE UNIVERSITY OF TEXAS TOFPET-I PET CAMERA. W.H. Wong, N.A. Mullani, E.A. Philippe, R.K. Hartz, D. Bristow, K. Yerian, J.M. Gaeta, N. Ketharnavaz, University of Texas Health Science Center, Houston, TX.

The performance of the University of Texas TOFPET-I PET camera has been characterized. The camera has 720 fast cesium fluoride scintillators arranged in 5 rings to produce 9 slices images. The spatial resolution FWHM is found to be 9.0 mm, 11.0 mm and 12.0 at the center, 9 cm and 18 cm off center radius respectively. The time-of-flight resolution is about 9 cm. The true coincidence sensitivity for the outer and inner slices are about 8500 cps/μCi/cc and 22,000 cps/μCi/cc respectively for a 20 cm uniform source. The axial field-of-view spans 10.5 cm and allows the whole heart to be imaged at one time and a 3-D

surface model of the heart to be displayed. The 3-D image is found to be more useful than the conventional slice image for interpretation and is being used for normal operation. Human studies has been carrying out for both normal and MI subjects with ^{82}Rb. Fast 4 seconds dynamic images with 50% cardiac gating has been obtained.

PERFORMANCE OF A POSITION-SENSITIVE BAR DETECTOR. J.S. Karp and G. Muehllehner, Hospital of the University of Pennsylvania, Philadelphia, PA.

The spatial resolution of a NaI(Tl) 25-mm thick bar detector has been studied. The position along the detector is determined from the centroid of the light distribution measured with ten 50-mm diameter phototubes. Delay line pulse shortening is used to increase the countrate capability. A whole-body positron camera (1) consists of six such detectors.

Measurements were taken with a collimated source of 511 keV gamma rays incident at 90° to the face of the detector. The preamplifier bias threshold was optimized for spatial resolution by effectively reducing the width (FWHM) of the light distribution to about 50 mm. The average resolution obtained near the center of the detector with delay line pulse shortening is 7.5 mm (FWHM). With the delay line out and integrating all of the light, the spatial resolution is 6 mm.

A Monte Carlo computer simulation of the gamma ray detection process was performed to identify the factors contributing to the intrinsic resolution. The major factors include multiple scattering in the 25-mm thick crystal, broadening of the light distribution due to reflections in the crystal and statistical fluctuations in the number of photoelectrons released in the phototubes. Predicted resolutions are 6.5 and 4.5 mm for delay line in and out, respectively. The differences between these values and the measured values are mainly due to electronic noise and experimental finite slit width. Using the simulation to test a proposed detector modification, we predict an improvement in resolution of 1-2 mm by cutting narrow grooves in the front face of the crystal.

(1) G. Muehllehner, et al: IEEE, NS-30, 652-660, 1983.

PET ATTENUATION CORRECTION USING REPROJECTION OF MEASURED TRANSMISSION DATA. K.J. Kearfott*, L.P. Carroll+, and P. Kretz+. *Memorial Sloan-Kettering Cancer Center, New York, NY, and +The Cyclotron Corporation, Berkeley, CA.

Meaningful quantitative positron emission tomographic (PET) measurements require accurate corrections for tissue attenuation. Although the analytic method of attenuation correction (AAC) is simple and does not contribute any statistical noise to the reconstructed emission image, it is subject to error when the object under study is of non-uniform density. Direct object/air transmission ratios obtained using an external 511 keV source are advantageous for studies which include the oral and nasal cavities or bony structures. The major problem with conventional experimental attenuation correction (CEAC) is the statistical uncertainty in the transmission measurement.

A method has been developed for reducing the variance in the emission image introduced by experimental attenuation correction: transmission data are first reconstructed to form a CT image, i.e., a map of tissue attenuation for 511 keV photons, and correction coefficients are derived by reprojecting through the transmission CT image. The attenuation correction coefficients derived using this reprojected attenuation correction (RAC) are both theoretically and experimentally "less noisy" than those derived from CEAC. This is apparent in sinogram displays of the attenuation correction coefficients from phantom and patient studies. The effect of attenuation correction on the final, corrected emission image is dependent upon correlations in the data, the transmission properties of the object, the statistics of the emission and transmission measurements and reconstruction filter. The quantitative advantage derived from the use of RAC compared with CEA and AAC will depend upon these factors.

1:30-3:00 **Room 214BC**

PERIPHERAL VASCULAR DISEASE

Moderator: Michael E. Siegel, M.D.
Comoderator: Robert F. Henry, M.D.

RADIONUCLIDE ANGIOGRAPHY AND BLOOD POOL IMAGING TO ASSESS SKIN ULCER HEALING PROGNOSIS IN PATIENTS WITH PERIPHERAL VASCULAR DISEASE. N Alazraki, P F Lawrence, J B Syverud. Departments of Radiology/Nuclear Medicine and Surgery, VA Medical Center, Salt Lake City, UT and University of Utah School of Medicine.

Several non-invasive diagnostic techniques including segmental limb blood pressures, skin fluoresence, and photo plethysmography, have been evaluated as predictors of skin ulcer healing in patients with peripheral vascular disease, but none are widely used.

Using 20mCi of Tc-99m phosphate compounds, four phase bone scans were obtained, including (1) radionuclide angiogram (2) blood pool image (3) 2 hour and 4-6 hour static images and (4) 24 hour static delayed images. The first two phases were used to assess vascularity to the region of distal extremity ulceration; the last two phases evaluated presence or absence of osteomyelitis.

Studies were performed in 30 patients with non-healing ulcers of the lower extremities. Perfusion to the regions of ulceration on images was graded as normal, increased, or reduced with respect to the opposite (presumed normal) limb or some other normal reference area. Hypervascular response was interpreted as good prognosis for healing unless osteomyelitis was present.

Clinicians followed patients for 14 days to assess limb healing with optimum care. If there was no improvement, angiography and/or surgery (reconstructive surgery, sympathectomy, or amputation) was done. Results showed: sensitivity for predicting ulcer healing was 94%, specificity 89%. Patients who failed to heal their ulcers showed reduced perfusion, no hypervascular response, or osteomyelitis. Microcirculatory adequacy for ulcer healing appears predictable by this technique.

BONE AND GALLIUM SCANNING IN THE PRE-OP EVALUATION OF THE INFECTED DYSVASCULAR FOOT. C. Stewart, I. Sakimura, A. Dillon, and M.E. Siegel. Rancho Los Amigos Hospital-USC School of Medicine, Los Angeles, California.

The purpose of this study is to determine the value of bone and gallium scans in predicting healing levels in the dysvascular foot with an infection requiring amputation. Healing requires amputation at a level both free of infection and with adequate blood flow.

Forty-one such patients had bone and gallium scans and Doppler studies prior to amputation at a level selected by the surgeon. Eight patients required multiple surgeries before healing was obtained. Bone and soft tissue infections were determined from scans and healing levels predicted (SPHL) as the most distal amputation level free from infection: toectomy, Reye's, transmetatarsal, calcanectomy, Syme's, below knee. Doppler healing levels (DPHL) were predicted using a standard ischemic index.

Doppler alone predicted the final healing level (FHL) in 41% with 59% needing more proximal amputation. Scans alone predicted FHL in 64% with 26% needing more proximal amputation. Ten percent were distal to the SPHL and all healed. These scans showed infection at transition sites between amputation levels, and the more proximal level had been predicted. Using the more proximal of the DPHL and SPHL the FHL was predicted in 78% with another 12% having more proximal amputation for nursing reasons. In 10% amputation was performed between DPHL and SPHL or at the more distal level. In no case was successful surgery performed distal to the more distal SPHL or DPHL.

Bone and gallium scans used with Doppler studies are useful in optimizing the choice of amputation level in the infected, dysvascular foot.

STEADY STATE VENOGRAPHY USING 195m-GOLD. D.J. Dowsett, J.T. Ennis, C. Collum, and R.B.J. De Jong. Mater Hospital, Dublin, Ireland and Byk-Mallinckrodt, Petten, Holland.

The introduction of 195m-Au has provided a useful non-diffusible, short $T\frac{1}{2}$ isotope (30 seconds) for cardiac and vascular work. We have investigated its use as an imaging agent for the deep venous circulation of the legs comparing its results with conventional contrast venography and a routine radioisotope method using 99mTc-MAA.

The 195m-Au Generator is steadily eluted using a constant perfusion pump at 10cc/minute. The eluant was delivered into a superficial leg vein using a catheter (1.5mm Cook PVC) and 19G butterfly needle. Bilateral venograms were performed using a "Y" divider. Owing to the very short $T\frac{1}{2}$ recirculation activity was not seen and the images gave a clean picture of the lower limb venous circulation extending up to the inferior vena cava. Image density at any point (x) obeyed the formula:

$$P/V \cdot e^{-\lambda x/V}$$

Where P is the 195m-Au perfusion rate; V the blood velocity and λ the decay constant. A rapidly diminishing image density was apparent in the veins having poor flow rates. Useful steady state images of the deep leg veins up to and including the inferior vena cava were readily obtained. Unlike other venographic methods flow states were indicated.

The generator's useful 3-4 day life allows a large number of patients to be investigated. The morbidity and patient discomfort seen with contrast media is absent and its low radiation dose make it an ideal screening procedure. Twenty-four patients had venography performed using this method and were compared with contrast and 99mTc-MAA venography.

a) Flow can be measured accurately, b) abnormal collaterals are well seen, c) the vena cava is optimally imaged, d) difficulty exists with non-occlusive thrombi.

UTILIZATION OF A SYMPATHECTOMY: THE PERIPHERAL PERFUSION SCAN AS AN OBJECTIVE PROGNOSTIC INDICATOR. M.E. Siegel, C.A. Stewart, A.E. Yellin. LAC/USC Medical Center, Los Angeles, CA.

It is quite difficult to determine what effect on perfusion or clinical outcome a lumbar sympathectomy may have in patients with peripheral vascular disease (PVD). The purpose of this paper is to describe our initial results utilizing the Tl-201 peripheral vascular perfusion study at rest and during lumbar sympathetic block (LSB), as a prognostic indicator of a patient's response to sympathectomy.

Twenty-two patients with PVD scheduled to have a therapeutic lumbar sympathectomy were studied. A rest scan is performed after a 1.5 mCi IV administration of Tl-201. One week later immediately after an LSB, a second Tl-201 scan is performed. Prior to scanning, point counting is performed over the thighs, knees, calves, ankles, and clinically ischemic region (CIR) to quantify the distribution of perfusion. All patients underwent sympathectomy. The patients have been followed up to nine months.

Sixteen patients had increased perfusion to the CIR with LSB, and 13/16 (81%) have improved clinically. Six patients had decreased perfusion to the CIR with LSB, and 4/6 (67%) had clinical deterioration. Two had no change in perfusion, one clinically deteriorated further, and one had no change. No patient with decreased perfusion with LSB improved clinically. Overall accuracy was 86%.

Our initial results suggest that a Tl-201 peripheral perfusion study performed during LSB may provide useful, objective data in predicting the effect of a lumbar sympathectomy and, thus, aid in the objective decision of whether to attempt a therapeutic sympathectomy.

RADIONUCLIDE FISTULOGRAM (RnF) IN HEMODIALYSIS PATIENTS: I. S. Seo, W. M. Sy, W. Heneghan, A. Manoli, and M. Gozum, The Brooklyn Hospital, Brooklyn, NY

Prosthetic graft A-V fistulae (AVf) (10 adults) and internal AVf (14 adults) as avenues of hemodialysis were created surgically in the limbs of 24 renal failure patients. AVf can malfunction or become obstructed and to date only contrast fistulography (CnF) is used to document such problems. Thirty-three RnF's were performed in 24 patients and CnF's in seven patients.

Eleven had clinical features of AVf malfunction and 13 were asymptomatic. 99mTc compounds, TcO_4^- or MDP (20 mCi) were injected into the AVf through a 19-gauge butterfly. 2 sec. dynamic images (qualitative data) and simultaneous computer acquisition in 64 x 64 byte mode with 0.5 sec/frame for 120 frames (quantitative data) were obtained. Normal qualitative and quantitative criteria were established. 10/11 symptomatic and 2/13 asymptomatic patients showed abnormal scintigraphic features and time activity curves indicating AVf malfunction. All 12 patients demonstrated abnormal collateral formation; 8/12 had stenosis, 3/12 showed equivocal stenosis and in 1/12 no stenosis was shown. In these 12 patients the S_2 (second circulation)/S_1 (initial circulation) ratio was below 10%. In 5/12 whose S_2/S_1 ratio was less than 1%, the CnF and surgical repair confirmed the presence of stenosis. RnF appears to be a simple, benign, and accurate imaging procedure in the evaluation of AVf malfunction.

IMPROVED SENSITIVITY IN DIAGNOSING SUPERIOR VENA CAVAL FLOW COMPROMISE THROUGH RADIONUCLIDE "PHASE" IMAGING. T.R. Simon, R.A. Middleton, H.N. Lee, W. Solis. Dallas VA Medical Center, Dallas, TX.

Usual scintiangiography for venous obstruction ignores the quantitative advantages of nuclear medicine. This failing denies patients timely therapy in such cases as gradual evolution of superior vena cava obstruction.

This study prospectively examined venous flow in 116 patients using bilateral injections of Tc-99m pertechnetate. A gamma camera collected 60 images for 3 seconds each. The data was digitized, processed and displayed. A first harmonic Fourier "phase" image was generated for each study with a single cycle extending from the appearance of tracer in the axillary veins to its emergence from the right ventricle. Three sets of criteria were used: strict, requiring interrupted or collateral venous flow; sensitive, recognizing distortion or narrowing of venous channels; and phase. The latter used the colors in the phase image to encode the relative time when activity reached any given level. Abrupt color changes were interpreted as flow abnormalities.

Angiography, performed on 25 patients, showed the best sensitivity (SENS) with phase criteria (100%). Phase criteria maintained the highest SENS when the venous obstruction was diagnosed by radiography alone or by radiography and clinical follow-up. The accuracy (ACC) of the phase criteria (64-78%) was almost equal to that of the strict (SENS, 36-40%; specificity (SPEC), 93-100%; ACC 64-89%) and sensitive (SEN 85-93%, SPEC 30-67%, ACC 66-76%) criteria.

Quantitative radioangiography is recommended to sensitively and non-invasively screen patients with right upper lobe tumors to identify those who might benefit from timely therapeutic intervention for compromised venous flow.

1:30-3:00 **Room 217B**

NEUROLOGY III: QUANTITATIVE METHODS

Moderator: Henry Huang, D.Sc.
Comoderator: Joel Greenberg, M.D.

ERRORS DUE TO INSTABILITY OF THE INPUT IN THE PET CONTINUOUS INHALATION METHOD FOR CBF AND $CMRO_2$ DETERMINATION. J.A. Correia, N.M. Alpert, R.H. Ackerman, J.M. Taveras. Massachusetts General Hospital, Boston, MA.

The simple models used to compute the physiological parameters from the equilibrium inhalation method require that the arterial level of radioactivity be kept constant during the breathup and imaging periods. Drifts in the input of labeled gas or in breathing dynamics can cause drifts in these input concentrations. In order to characterize the effects of such drifts we have carried out

a computer simulation study under the following assumptions: 1. drifts are such that the various arterial blood concentrations have the form: $C(t)=C_0+mt$. This is the first term of a Taylor expansion in t and hence is representative of all slowly varying drifts; 2. drift begins after initial equilibrium is established and continues to the end of the study.

Studies were carried out for three different cases: 1. effects of drift on flow measurements; 2. Effects on OEF and $CMRO_2$ of a drift in flow measurement, and 3. Effects on OEF and $CMRO_2$ of a drift in O_2 measurement.

Systematic errors in flow tend to be minimum at zero flow and increase slowly with flow. Systematic errors in OEF and $CMRO_2$ increase rapidly as these parameters become small and tend to level off to constant values as they increase. For very large drift rates (10%/min), errors in flow vary from 3-30% depending on duration of drift. For more moderate drift rates (eg, 2%/min) errors range up to 7% for the longest drift times. For relatively stable operation errors in OEF and $CMRO_2$ are less than 15% for E> 0.2 and increase rapidly for lower values of E.

STATISITICAL ERROR IN THE MEASUREMENT OF OXYGEN UTILIZATION WITH THE ^{15}O-EQUILIBRIUM METHOD. N.M. Alpert, J.A. Correia, R.H. Ackerman, and J.M. Taveras. Massachusetts General Hospital, Boston, MA.

The propagation of statistical error in the measurement of cerebral blood flow by the ^{15}O-equilibrium method has been studied previously. This report extends the analysis to include propagation of statistical error in local oxygen extraction fraction (E) and oxygen utilization rate (U). Our calculations provide estimates of the coefficient of variation of E and U, CV(E) and CV(U). Precision calculations, based on standard error propagation methods, were carried out as a function of CBF and E. Local tissue concentrations, measured by PET, were assumed to be the only source of random fluctuation. The correlation of the estimates of CBF and E was included in the calculation of CV(U). Fig R(ight) and L(eft) are examples typical of the results of our study.

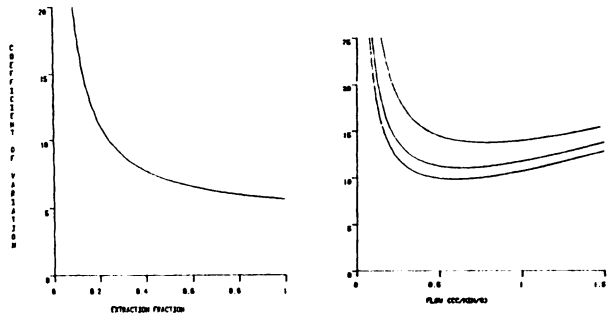

Fig L shows CV(E) vs E. CV(E) has an essentially hyperbolic shape, and for E>0.3 CV(E)<0.1. Fig R shows CV(U) vs CBF for E=0.2,0.4 and 0.6. CV(U) also has an essentially hyperbolic shape, with CV(U) approximately 0.12 for CBF > 0.4 ml/min/g and E=0.4. We conclude that the propagation of statistical error in E and U can be kept on the order of 10% with PET.

WHAT IS THE CORRECT VALUE FOR THE BRAIN:BLOOD PARTITION COEFFICIENT FOR WATER? P. Herscovitch and M.E. Raichle, Washington University School of Medicine, St. Louis, MO.

A knowledge of the brain:blood partition coefficient (λ) for water is usually required for the measurement of cerebral blood flow (CBF) with positron emission tomography (PET) and O-15 labelled water. The correct calculation of this important parameter from the ratio of brain and blood water contents will be reviewed, and the effect of physiological variations in these water contents on λ will be demonstrated.

The currently accepted value for whole brain λ is 0.95-0.96 ml/g, calculated from brain and blood water contents of 77g/100g and 80.5g/100g, respectively. However, this value for λ is incorrect, because in the calculation the blood water content value was not adjusted for the density of blood. The correct value is 0.91 ml/g. Variations in brain or blood water content affect λ. Over an hematocrit range of 25% to 55%, λ varies from 0.86 to 0.93 ml/g, due to a decrease in blood water content. λ changes with age, and varies regionally in the brain, as brain water content is inversely related to lipid and myelin content. The λ of the human newborn brain, 1.10 ml/g, is considerably higher than in the adult. Differences in λ between gray and white matter are well known. However, because of variations in water content, the λ's of thalamus (0.88 ml/g) and caudate nucleus (0.96 ml/g) are less than that of cerebral cortex (0.99 ml/g), while the λ of corpus callosum (0.89 ml/g) is greater than that of centrum semiovale (0.83 ml/g). These regional variations in λ will assume more importance as PET resolution improves. The impact of using an incorrect λ will depend upon the sensitivity of the particular CBF measurement technique to errors in λ.

POSITRON IMAGING OF INTRAVENOUS O-15 LABELED WATER FOR CEREBRAL BLOOD FLOW. SC Jones, JH Greenberg, R Dann, GD Robinson, Jr, M Kushner, A Alavi and M Reivich. University of Pennsylvania, Philadelphia, PA.

The purpose of this work was the development of a new technique for the determination of LCBF using the continuous, intravenous infusion of O-15 H2O and PET imaging. Eight normal human subjects were studied. During a 20-30 min infusion, multiple arterial blood samples were withdrawn for PaCO2 and O-15 concentration measurement. PET imaging commenced 8-12 minutes after the infusion was started. CBF was determined by using the equilibrium model or, when appropriate, a non-equilibrium CBF model which permitted the arterial O-15 concentration to change with time. In contrast to the equilibrium model, our model uses the actual arterial time course as the input function. Whole brain CBF was determined with an average brain-blood partition coefficient of 0.96 ml/g. Corrections were made for tissue heterogeneity and for the loss of counts from the whole brain region of interest (ROI). Regional CBF values were generated by selecting ROI's in predominantly gray or white matter areas using an atlas overlay system and actual brain-blood partition coefficients of 0.88 and 1.05 ml/g for white and gray matter, respectively. The mean whole brain CBF for 9 measurements in 8 subjects was 57 ml/min/100g (SD 11) corrected to a normal PaCO2 of 40 mmHg. In comparison to techniques employing O-15 CO2 inhalation, the advantages of the continuous infusion technique are low radiation dose to the lung and ease of tracer administration in patients who will not tolerate inhalation. In addition, PET instruments with low count rate capabilities can be used. The new, non-equilibrium CBF model permits arterial curve changes with time and enables imaging to be started before equilibrium.

QUANTITATIVE ASSESSMENT OF ABSOLUTE CBF VALUES MEASURED BY POSITRON COMPUTED TOMOGRAPHY(PCT) AND O-15 WATER. SC Huang, JG Frazee, JC Mazziotta, RE Carson, ME Phelps, UCLA School of Medicine, Los Angeles, California

CBF measurements in man using PCT and O-15 water have been shown to be comparable to literature values. Absolute quantitation of the technique still needs verification. We have used a monkey model to compare directly the CBF values from PCT and O-15 water with those determined by the quantitative microsphere technique. PCT and microsphere studies were performed simultaneously. Two or three separate studies were done on each animal at different CBF values (manipulated by $PaCO_2$ changes) and with microspheres of different labels. The PCT scanning level was marked. The animal was later sacrificed and the marked cross-section removed. Microspheres in removed tissue were counted and quantitated for true CBF. PCT CBF was calculated by the integrated projection technique developed at UCLA (J CBF 2:99-108, 1982). The hemispheric and whole slice average CBF so obtained were compared with those by the microsphere technique. Results of 6 studies over a CBF range of 0.4 to 2.2 ml/min/g show the following relationship

$$(\text{PCT CBF})=0.85(\text{TRUE CBF})-0.13(\text{TRUE CBF})^2$$

The nonlinearity is believed to be due to finite permeability of water through blood brain barrier(BBB); a slope of less than unity at low flow is due to partial volume effect. Both effects can be corrected and are less in human studies. It is concluded that variations in PCT CBF reflect true CBF changes but values may need to be adjusted for partial volume effect and for BBB permeability limitations to improve their accuracy.

THE MEASUREMENT OF SEQUENTIAL CHANGES IN CEREBRAL BLOOD FLOW AND OXYGEN METABOLISM BY POSITRON COMPUTED TOMOGRAPHY WITH CONTINUOUS INHALATION OF OXYGEN-15 LABELED GASES. S. Tanada, Y. Yonekura, M. Senda, K. Nishimura, N. Tamaki, H. Saji, T. Fujita, A. Kobayashi, W. Taki, M. Ishikawa, Y. Yonekawa, H. Handa, J. Konishi, and K. Torizuka, Kyoto Univ. School of Medicine, Kyoto, Japan.

The use of continuous inhalation of oxygen-15 labeled gases is a widely accepted method to measure regional cerebral blood flow (CBF) and oxygen metabolism (CMRO2) with positron computed tomography (PCT). The purpose of this study is to evaluate the feasibility to measure sequential changes in CBF and CMRO2 by PCT.

The functional images of CBF, oxygen extraction fraction (OEF), and CMRO2 were obtained using continuous inhalation of oxygen-15 labeled carbon dioxide and oxygen. The effects of spinal drainage in CBF and CMRO2 were studied in patients with hydrocephalus following subarachnoid hemorrhage due to the rupture of intracranial aneurysm. Following the measurement in control state, 20 ml of cerebrospinal fluid (CSF) were withdrawn gradually through lumbar puncture, and sequential PCT scans were performed. CBF and CMRO2 were markedly depressed in the case with hydrocephalus. The drainage of CSF significantly improved OEF and CMRO2, whereas CBF remained depressed. In patients with chronic cerebrovascular disease, the changes in CBF were studied with inhalation of 5% carbon dioxide (CO2). CO2 loading demonstrated the increase in CBF, while poor regional increase was observed in "moyamoya" disease, which permitted the assessment of vascular response to the elevation of plasma CO2.

Our preliminary work indicated the potential usefulness of sequential PCT to study the changes in CBF and CMRO2 with various interventions.

1:30–3:00 **Room 212A**

ONCOLOGY III: TOMOGRAPHIC TUMOR IMAGING

Moderator: Albert A. Driedger, M.D., Ph.D.
Comoderator: Frank H. DeLand, M.D.

ASSESSMENT OF TUMOR BLOOD FLOW USING C-11 BUTANOL. W.H. Knapp, F. Helus, K. Layer, F. Oberdorfer, H. Ostertag, H.-J. Sinn. German Cancer Research Center, Heidelberg, FRG.

This study was undertaken to evaluate C-11 butanol as a possible radioagent for flow quantitation in human neoplasia.

100-120 mCi of no-carrier added C-11-n-butanol were obtained in 1.0 ml solution, the radiochemical puritiy was > 99 %.

In the dog, only 3 % of decay-corrected activity was released from the organism within 20 min. Following injection, 80 % of the label was cleared from the blood within less than 1 min. HPLC analysis did not reveal any metabolites after a 1 min incubation time of the radiotracer with blood or when C-11 butanol was injected into the femoral vein of the rabbit and samples were taken from the left atrium. Single-pass extraction fraction in tumor (VX 2) and muscle was 100 %. Tumor : muscle uptake of C-11 butanol was correlated (r = 0.86) with the retention of I-121 microspheres (N = 10; 5 tumor lines). A close correlation (r = 0.96) was found when uptake data in 17 tumor transplants (3 lines) were compared with Xe-133 washout rates. Differences between two consecutive uptake measurements - one after i.v. and one after intra-aortic tracer injection - did not exceed 10 % (12 rats).

High diffusion capacity, lack of intravascular and intrapulmonary metabolism and appreciable retention in tissue make C-11 butanol an appropriate radiotracer for non-invasive monitoring of tumor blood flow.

POSITRON IMAGING FEASIBILITY STUDIES: SHORT TERM UPTAKE OF THYMIDINE IN NORMAL AND NEOPLASTIC TISSUES. A.F. Shields, M.M. Graham, and S.M. Larson. Fred Hutchinson Cancer Research Ctr., University of Washington, Seattle, WA. and N.I.H., Bethesda, MD.

The uptake of labeled thymidine (TdR) as measured by labelling index has provided useful experimental and clinical data regarding tumor cell cycle. This approach is limited by the requirement for repeated tissue sampling, but could potentially be extended to in vivo measurements using C-11 TdR and positron emission tomography (PET). Since TdR is rapidly cleared from the circulation, there is concern that the distribution in vivo might reflect blood flow and not cellular metabolism. Therefore, uptake of H-3 TdR was studied in AKR mice, both normal and with spontaneous lymphoma, and in organs and tumors of dogs with spontaneous tumors. Uptake was compared to relative blood flow as measured by the distribution of C-14 iodoantipyrine. Metabolic H-3 water was removed by air drying the samples before oxidizing them for counting. The initial distribution of thymidine in normal mice, measured 20 seconds after injection, correlated with relative perfusion measurements. However, between one and sixty minutes after injection there was no correlation of TdR uptake with perfusion in any of the systems studied. This indicates that the distribution more than one minute after injection is primarily dependent on subsequent redistribution and/or metabolism of TdR, rather than the initial distribution by blood flow. The time acitvity curve of TdR content in normal mouse organs demonstrated that organs with high rates of proliferation retain all the labeled TdR initially taken up. Organs with low rates of proliferation lost their label in a nearly exponential wash out. These studies provide further evidence of the feasibility of using C-11 TdR for PET and provide the experimental basis for developing kinetic models of Tdr metabolism necessary to interpret PET studies.

EXPERIMENTAL AND CLINICAL STUDY OF CANCER DIAGNOSIS WITH (F-18) FDG USING POSITRON EMISSION TOMOGRAPHY. H. Fukuda, T. Matsuzawa, M. Ito, Y. Abe, S. Yoshioka and K. Yamada. The Research Institute for Tuberculosis and Cancer, Tohoku University, Sendai, Japan.

The purpose of this study was to evaluate the validity of cancer diagnosis with (F-18) FDG. Tissue distribution studies and positron imaging studies were made using rat and rabbit tumor system, and it was found that (F-18) FDG was a good tracer for cancer detection. The advantages for cancer detection were as follows: (a) The tumor uptake was very high and increased with time. Whereas, clearance from blood was rapid. (b) Intrahepatic tumors can be positively delineated, because of rapid clearance from normal liver. (c) The uptake of inflammatory tissue was relatively lower than that of tumor and the uptake level did not increase during the study period.

Based on these experimental results, we studied the feasibility of this diagnostic technic in 7 cases of liver and pancreatic cancers. After injection of 4-10 mCi of (F-18) FDG, serial scanning for every 5 min was performed by positron emission tomography. There were increased accumulation of the radioactivity in either liver or pancreatic cancers with a rapid clearance of the activity form normal liver. By 40-60 min after injection, positive image of tumors were obtained. In a case who was irradiated to a part of tumor, there was a decrease of the activity in agreed with the irradiated area.

From these experimental and clinical studies, we concluded that the cancer diagnostic technic with (F-18) FDG can be useful for the location of tumors and evaluation of tumor viability. Especially, liver tumors were most promising to be examined.

GALLIUM-68 ETHYLENEDIAMINE TETRAACETIC ACID (EDTA) IMAGING OF BRAIN TUMORS BY POSITRON TOMOGRAPHY. D.F. Wong, Y. Inoue, S. Rosenbloom, M. Wharam, B. Carson, H.N. Wagner, Jr. The Johns Hopkins Medical Institutions, Baltimore, MD.

While non contrast CT demonstrates the effects of brain tumors, such as regions surrounding the tumors with low CT numbers, contrast is often required to show the tumor itself. Unfortunately, contrast may cause seizures in 9-15% of patients with brain metastases (AJR 140:787, 1983). Contrast enters the tumor region because of absence of the blood-brain barrier (BBB). Chelates have been used in planar nuclear imaging to study BBB integrity, but have

not been used widely in positron tomography. We carried out positron tomography (PET) with Ga-68 EDTA in 22 patients with suspected or proven brain tumors. In 13/22, the lesions were detected equally well by contrast CT and PET. In 3/22 the lesions were more clearly visualized with PET than contrast CT. In 1 case, there was a more extensive abnormality on PET than on contrast CT. In 2 postoperative patients, the presence of tumor was detected by contrast CT and PET, but interference from surgical clips obscured the CT but not the PET images.

Indications for positron tomography with Ga-68 EDTA include allergy to contrast media, history of seizures with contrast media, or interfering opacities such as surgical clips or calcifications. An important characteristic of Ga-68 EDTA is that it is easily eluted from a long lived Ge-68 generator. Furthermore, Ga-68 EDTA can be used to quantify BBB integrity with the appropriate modelling, e.g. as in steroid therapy.

DETERMINATION OF REGIONAL BLOOD-TISSUE TRANSFER CONSTANTS AND INITIAL (PLASMA) VOLUME IN BRAIN AND BRAIN TUMORS USING ^{68}Ga-EDTA AND DYNAMIC POSITRON EMISSION TOMOGRAPHY. R.G. Blasberg, D.C. Wright, C.S. Patlak, R.A. Brooks, R.E. Carson, D.R. Groothuis and G. Di Chiro. NIH, Bethesda, MD.

Beagle dogs with Avian Sarcoma Virus induced brain tumors were studied under pentobarbital anesthesia at 8 to 10 wks of age when they demonstrated contrast enhancing lesions on CT scans of 1.5 cm or greater diameter. Four to 6 mCi of ^{68}Ga-EDTA in saline was intravenously infused over 3 min, arterial blood rapidly sampled, and serial 30 sec scans obtained on the Neuro-PET. The scanning period and interval between blood sampling was gradually increased after 5-6 min; 15 min scans were obtained from 30 min until the end of the experiments (2 to 4 hrs). Fifteen min prior to the end of the experiments, 1 mCi of ^{14}C-α-aminoisobutyric acid (AIB) was intravenously injected, arterial blood sampled, the animal killed with intravenous KCl, and the brain rapidly frozen for later processing of histology and quantitative autoradiography. Regions of interest could be outlined on the basis of histology image overlays and directly compared with the ^{14}C-AIB autoradiographic images. Assuming a simple two compartment model, the following values were obtained for ^{68}Ga-EDTA distribution by nonlinear least-squares fit of the data: initial/vascular volume (V_v), influx (K_1), efflux (k_2):

	V_v ml g^{-1}	K_1 ml g^{-1} min^{-1}	k_2 min^{-1}
Tumor	0.039	0.0017	0.0049
Brain	0.032	0.00014	0

These preliminary results demonstrate a significant blood-tumor barrier in these experimental animals and suggest that similar studies could be performed in patients with brain tumors in order to individualize their chemotherapy.

SPECT AND PLANAR IMAGE DETECTION OF HOT LESIONS IN A CHEST PHANTOM USING GA-67 AND TC-99M. J Floch, N Alazraki, W Wooten. Department of Nuclear Medicine, VA Medical Center Salt Lake City, UT and University of Utah School of Medicine

The aim of this study is to define Ga-67 and Tc-99m lesion detectability using SPECT and planar imaging and to identify the effects of specific variables. A chest phantom was designed with lungs, sternum, and spine; varying sized and shaped lesions (1.5cm x 1.0cm to 2.2cm x 1-8cm) were imaged with varying lesion to background activity ratios (3.7:1 to 30:1), placed in different positions in the phantom.

Lesion to background ratios, lesion size, number of lesions, Ga-67 imaging energy peaks (184KeV-20%; 184KeV-20%, 300KeV-15%; 94Kev-20%, 184KeV-20%, 300KeV-15%), and SPECT reconstruction factors including, 180° vs 360° reconstructions and attenuation corrections were varied.

Results showed (1) Reconstructions from data acquired with three windows for gallium 67 were least satisfactory; 184 KeV alone or 184 and 300 KeV acquisitions were approximately equal. (2) With 10:1 lesion to background Ga-67, 1.5cm lesions were seen on transaxial reconstructed images, but not on 500k, dual peak planar images. Lesions 2.2cm in diameter were seen equally well on planar and SPECT for 10:1 ratios. (3) Lesion length: a 2.2cm diameter tube with Ga-67 at 3.7 to 1 lesion to background was seen on SPECT if the tube length was $\geq$ 2cm, but not at 1cm. (4) Attenuation corrections did not improve images. (5) 180° reconstructions improved detectability of 1.5 x 1cm simulated mediastinal lesions not seen with 360° reconstructions for 10:1 activity ratios. However, choice of the 180° was critical. (6) Spine and sternum phantoms within the thorax were well visualized with activity ratios of only 3.7:1. Experiments with Tc-99m showed much improved images compared with Ga-67. Smaller lesions were seen with lower activity.

1:30-3:00 **Room 212B**

BONE/JOINT II

Moderator: Leonard Rosenthall, M.D.
Comoderator: Ernest K.J. Pauwels, M.D.

STRESS INJURIES OF THE PARS INTERARTICULARIS: RADIOLOGIC CLASSIFICATION AND INDICATIONS FOR RADIONUCLIDE IMAGING. R. Pennell, A.H. Maurer, and A. Bonakdarpour. Temple University Health Sciences Center, Philadelphia, PA.

Lumbar spine radiographs and radionuclide images were compared and correlated with clinical histories of 20 atheletes with low back pain. Radiographs were classified as: normal (Type 0); showing a healing stress fracture (an irregular lucent line) with sclerosis (Type I); as an evolving or healed stress injury with either sclerosis, narrowing, or demineralization (Type II); and as a chronic fracture showing a large lucency with well-defined margins classically referred to as spondylolysis (Type III). Patients were grouped clinically on the basis of their pain: acute onset (Group A, n=7), acute superimposed on chronic (Group B, n=9), and chronic pain without an acute event (Group C, n=4). Radiographic abnormalities were present in 95% (19/20) of the patients and radionuclide studies were positive in 60% (12/20). Scintigraphy was positive most often with Type I pars abnormalities (77%, 10/13) and negative most often with Type III abnormalities (91%, 11/12). Of all positive scintigraphy 12/14 (86%) were in pts in Groups A and B (acute symptoms). Our findings support theories that radiographic pars abnormalities exist which correspond to stages in the healing of stress induced fractures. With acute symptoms radionuclide imaging need not be obtained if a Type I radiographic abnormality is seen. Radionuclide imaging is indicated with either Type 0, II or III radiographs to confirm or rule out recent stress injury.

PROSPECTIVE EVALUATION OF FEMORAL HEAD VIABILITY FOLLOWING FEMORAL NECK FRACTURE. B. Binkert, S.A. Kroop, J.V. Nepola, A.S. Grantham and P.O. Alderson. Columbia University, New York, N.Y.

The bone scans of 33 patients (pts) with recent subcapital fractures (fx) of the femur were evaluated prospectively to determine their value in predicting femoral head viability. Each of the 33 pts (11 men, 22 women, age range 30-92) had a pre-operative bone scan within 72 hrs of the fx (23 pts within 24 hrs). Anterior and posterior planar views of both hips and pinhole views (50% of pts) were obtained 2 hrs after administration of Tc-99m HDP. The femoral head was classified as perfused if it showed the same activity as the opposite normal side or if it showed only slightly decreased activity. Femoral heads showing absent activity were classified as nonperfused. Overall, 20 of the 33 pts showed a photopenic femoral head on the side of the fx. Only 2 pts showed increased activity at the site of the fx. Internal fixation of the fx was performed in 23 pts, 12 of whom had one or more follow-up scans ($\bar{x}$ follow-up time = 2.8 $\pm$ 3.3 months). Five of these 12 pts showed absent femoral head activity on their initial scan, but 2 showed later reperfusion. The other 7 pts showed good perfusion initially, with only 1 later showing decreased femoral head activity. The other 10 pts (7 of whom had absent femoral head activity) had immediate resection of the femoral head and insertion of a Cathcart prosthesis. The results suggest that femoral head activity seen on a bone scan in the immediate post-fx period is not always a reliable indicator of femoral head viability. Decreased femoral head activity may reflect, in part, com-

promised perfusion secondary to post-traumatic edema, with or without anatomic disruption of the blood supply.

SIMULTANEOUS Tc-99M SKELETAL AND IN-111 HIP ARTHROGRAPHIC SCINTIMAGING COMPLEMENTING CONTRAST RADIOGRAPHY. H.N. Wellman, B.G. Uri, P. Stiner, B.H. Mock and W. Capello, Indiana University School of Medicine, Indianapolis, IN

Prosthetic hip replacement has become a frequent procedure with femoral component (FC) loosening occuring frequently at a rate of 24% at 7 yrs post arthroplasty. Pain may occur from a variety of causes and identification of loosening as the cause is critical. Experience with radiographic contrast arthrography (XA) alone has often resulted in equivocal studies because of confusion caused by the radio-opaque glue-bone interface and adjacent radiolucency of the FC. Radionuclide arthrography (RA) with Tc-99m Sulfur Colloid (SC) has been previously shown to improve the efficiency of FC loosening determination. However, with extravasation or other confusing patterns of tracer distribution more precise localization relative to skeletal structure is required with RA. Simultaneous use of RA using In-111 (IN) chloride (0.2 mCi) injected with contrast at XA superimposed on prior injected Tc-99m MDP (20 mCi) skeletal imaging (SI) has considerably improved interpretation and complemented XA, correlated with surgery.

Fifty RA and XA patients have been studied; 18 with SC alone, 7 with SC and IN in the joint space simultaneously and 25 with IN RA and SI. Simultaneous joint injection RA with IN and SC demonstrated exactly the same pattern with no translocation of IN. Thirty patients had surgery with 20 loose FC verified; all loose by RA but only 16 by XA plus 2 false positives. Also simultaneous SI has shown unreliable criteria for FC loosening. Thus, addition of simultaneous RA and SI for FC evaluation is a valuable adjunct in 20% of patients in the performance of arthrography.

In-111 WBC IMAGING IN MUSCULOSKELETAL SEPSIS. L. Thompson, T.J. Ouzounian, M.M. Webber, H.C. Amstutz. UCLA School of Medicine, Los Angeles, CA.

This study evaluated the accuracy and utility of the In-111 labeled WBC imaging in a series of patients who were suspected of having musculoskeletal sepsis.

The labeling of the WBCs was patterned after the method described by Goodwin, in which the WBCs are labeled with In-111 oxine in plasma. The WBCs from 100 ml of blood are separated and incubated with In-111 oxine complex, and then 500 uCi. of the labeled cells are reinjected into the patient. Images of the areas in question are obtained at 24 hrs. In some instances, 48 hour images were also obtained. Images were interpreted using consistent criteria.

Forty imaging procedures were done on 39 patients. These included 39 total joint protheses, and 17 other images to evaluate possible osteomyelitis, septic arthritis or deep abscesses. Of these studies, 15 were positive, and 41 negative. The findings were then correlated with operative culture and pathology in 21, aspiration cultures and gram stains in 14, and with clinical findings in the remaining 21. This correlation showed 41 true negatives, 12 true positives, 1 false negative, and 2 false positives. The sensitivity was 92.9% and the specificity was 95.2%. The false negative occurred in a patient on chronic suppressive antibiotic therapy for an infected total hip replacement. The false positive images occurred in a patient with active rheumatoid arthritis and in a patient imaged one month post operative placement of the prosthesis. These images were very useful in several septic patients who had many possible sites of infection.

We conclude that In-111 imaging is an accurate and useful non-invasive method of evaluating musculoskeletal sepsis.

COMPLICATING OSTEOMYELITIS IMAGED WITH Tc-99m MDP, In-111 GRANULOCYTES, AND Ga-67 CITRATE. D.S. Schauwecker, H.M. Park, B.H. Mock, R.W. Burt, C.B. Kernick, A.C. Ruoff III, H.J. Sinn, and H.N. Wellman. Richard L. Roudebush VAMC, Indiana University School of Medicine, Indianapolis, IN.

Gallium-67 and 3-phase bone scan (3P) studies, though very sensitive, are not very specific in evaluating suspected osteomyelitis (OM) which is superimposed upon other diseases that cause increased bone turnover (IBT). We compared In-111 acetylacetone labeled granulocytes (In-111 GRAN) with 3P in 57 such patients; 29 of these patients had Ga-67 studies as well. In-111 GRAN had a sensitivity of 100% in acute OM, 62% in chronic OM, and a specificity of 96%.

Gallium-67 ruled out OM when the study was normal; it diagnosed OM when the relative uptake of Ga-67 exceeded the uptake of Tc-99m MDP, or when the skeletal distribution of Ga-67 was different from that of the Tc-99m MDP. Unfortunately, these criteria were met in only 28% of the subjects. The simple approach of increased Ga-67 activity meant OM gave a sensitivity of 100%, but an unacceptable specificity of 38%.

Chronic cellulitis or long-standing decubiti were seldom detected by In-111 GRAN. Clinically obvious soft tissue infections or cellulitis were seen with In-111 GRAN 27% of the time, and 17% of the time with Ga-67.

In conclusion, when added to 3P, In-111 GRAN provided more useful information than did Ga-67. A combination of all 3 studies did not significantly increase the diagnostic yield. Performing In-111 GRAN without 3P in patients with IBT is not recommended since the 3P provides anatomic information that aids in the differentiation of OM from soft tissue infections.

SCINTIGRAPHY OF INFECTED TOTAL HIP ARTHROPLASTY (THA): A CANINE MODEL. K.D. Merkel, M.L. Brown, R.H. Fitzgerald, M.K. Dewanjee, Mayo Clinic and Foundation, Rochester, MN.

Differentiating low-grade sepsis from aseptic loosening of an orthopedic prosthesis is difficult. This study was designed to compare the ability of Tc-99m-HMDP, Ga-67, and In-111 leukocytes (WBC) to differentiate low-grade sepsis from aseptic THA component loosening in a canine model. A canine THA was implanted in 14 dogs. Six dogs were given infected femoral components by injecting 10^5 colony-forming units of Staphylococcus aureus into the femoral canal 60 to 90 seconds prior to cementing. Four dogs had an aseptic loose femoral component, and four dogs had an aseptic tight femoral component (control). At six months all dogs were evaluated with x-ray, lab, scintigraphy, and tissue quantitation of each tracer. Diagnosis was confirmed by histology and quantitative microbiology. White blood cell counts and differentials were normal in all dogs, and in only one out of six infected dogs was the sedimentation rate abnormal. X-rays were interpreted as possible infection in five dogs and probable infection in only one dog. In-111 WBC scans were more accurate than sequential Tc-Ga scans (sensitivity 94% vs 61%, specificity 86% vs 71%, accuracy 90% vs 67%). Quantitative counting of gamma camera data and tissue samples demonstrated significantly ($P < .01$) higher accumulation of In-111 WBC about the infected than the loose or control component. No significant difference was demonstrated between the loose and septic components with Tc-HMDP or Ga.

These results correlate well and confirm our clinical data that In-111 WBC scanning is accurate and useful in the workup of the painful orthopedic prosthesis.

3:30–5:00 **Room 217A**

CARDIOVASCULAR VIII: THALLIUM-201 IMAGING IN CORONARY ARTERY DISEASE

Moderator: Daniel S. Berman, M.D.
Comoderator: George A. Beller, M.D.

SINGLE PHOTON RB-82 IMAGING OF REMOTE MYOCARDIAL INFARCTION. J.W. Ryan, P.V. Harper, L. Resnekov, and V.Stark. The University of Chicago, Chicago, IL.

Rb-82, a short-lived (t 1/2 = 75 sec) positron emitting tracer which accumulates in the myocardium, is available from a long lived (t 1/2 = 25d) Sr-82 generator. Using a Pho-IV gamma camera and a rotating tungsten collimator, we

have previously demonstrated the feasibility of single photon imaging of the myocardium with Rb-82 in subjects without myocardial defects on Tl-201 scans. To evaluate myocardial lesion detection with this technique we selected 10 patients with documented remote (>3 months) myocardial infarctions (MI) and imaged them at rest with both Tl-201 and Rb-82. After injection of 1.2 mCi Tl-201, 3 views (Ant, LAO 40, LAO 70) were obtained with a portable camera (LEM-Siemens). Subsequently, 2 views were chosen for Rb-82 imaging using 40 mCi i.v. per view. Images were accumulated from 2-7 minutes and compared to the Tl-201 images. In general, contrast was good with Rb-82 and interference from liver activity was minimal. In 1 patient the Tl-201 and Rb-82 images were normal. In 4 patients with inferior wall MI, the lesion site was abnormal in 4 with Tl-201 and in 3 with Rb-82. Both studies showed decreased activity at the site of the lesion in 5 patients with an MI in the LAD distribution. Although lesion detection was similar with both tracers, the defects in some cases were more visible with Rb-82 than Tl-201 and vice versa.

Single photon imaging with Rb-82 provided lesion detection comparable with Tl-201 imaging in these patients with remote MI. Rb-82 imaging should prove especially useful in clinical situations such as acute MI in which rapid sequential myocardial perfusion imaging is desirable.

PREVALENCE OF HIGH RISK TL-201 SCINTIGRAPHIC FINDINGS IN PATIENTS WITH CORONARY ARTERY DISEASE: RELATION TO CORONARY ANATOMY AND ECG STRESS TEST FINDINGS. J.M. Ryan, T.W. Nygaard, R.S. Gibson, J.A. Gascho, D.D. Watson, G.A. Beller, University of Virginia, Charlottesville, Virginia.

The prevalence of a high risk exercise (Ex) Tl-201 (Tl) scintigram (scint) was determined in 295 consecutive patients (pts) with angiographic (angio) (>50% stenosis) coronary artery disease (CAD) and correlated with extent of CAD and Ex stress test findings. A high risk scint by quantitative criteria was defined as either: 1) a typical left main (LM) CAD pattern showing $\geq$25% homogenous disease in Tl activity in septal and posterolateral walls; 2) a multivessel disease (MVD) pattern showing abnormal Tl uptake and/or washout in multiple vascular scan segments; 3) increased lung Tl uptake. The typical LMCAD pattern was observed in 6 of 43 pts (14%) with LMCAD compared to 2% of 53 pts with 3VD (p=0.03), 3% of 99 pts with 2VD (p=0.02) and 2% of 100 pts with 1VD (p=0.01). The MVD scint pattern was seen in 67% of pts with LMCAD compared to 49% (p=0.05) in 3VD pts, 41% (p=0.004) in 2VD pts and 24% (p=<0.0001) in 1VD pts. Prevalence of abnormal lung Tl was comparable in LMCAD (42%), 3VD (38%) and 2VD (34%) pts, but greater than observed in 1VD pts (26%; p=0.05). High risk ECG stress test was defined as 2 or more of: 1) >2.0 mm of ST +; 2) $\geq$1.0 mm ST + persisting >5 min post-Ex; 3) ST + at $\leq$5 METS; 4) $\geq$10 mm Hg + in Ex blood pressure. A high risk ECG stress test was observed in 58% of LMCAD pts compared to 32% of 3VD pts (p=0.009), 31% of 2VD pts (p=0.003) and 16% of 1VD pts (p<0.0001). Eighty-six % of LMCAD and 70% of 2 and 3VD pts had either a high risk Ex scint or stress test. Thus, Ex Tl-201 scint appears useful in identifying high risk CAD pts.

PROGNOSTIC IMPLICATIONS OF NORMAL EXERCISE THALLIUM-201 IMAGES. J. Wahl, A-H Hakki, A.S. Iskandrian, H. Kay. Hahnemann University Hospital. Philadelphia, PA.

The usefulness of exercise-thallium-201 imaging (ETI) in the evaluation of patients (pts) with suspected coronary heart disease (CHD) is well established. A more far-reaching use of the method is, however, in risk stratification. The purpose of this study was to determine the prognosis of pts with normal ETI results. The study group consisted of 432 pts (218 men and 214 women with a mean age of 51 years) who underwent ETI for suspected CHD. Of those, 305 (71%) had typical or atypical angina pectoris and 65% achieved $\geq$85% of maximum predicted heart rate. The exercise ECG was positive in 65 pts (15%), inconclusive in 153 (35%) and negative in 214 (50%). At a mean follow-up of 13.5 mos (range 4 to 44), 6 pts had cardiac events: 1 had fatal myocardial infarction (MI) and 5 had non-fatal MI's, (one pt with non-fatal MI had spasm by coronary angiography). Two other pts had coronary artery bypass grafting. Of the 6 pts with events, none had positive exercise ECG's, 2 had typical angina, 2 had atypical angina, and 2 had non-anginal chest pain.

Conclusions: (1) normal ETI results identify pts at a very low risk for future cardiac events (death: 0.2%, MI: 1.2%) which is comparable to that reported in pts with chest pain and angiographically normal coronary angiograms, (2) pts with positive exercise ECG's but normal ETI results have good prognosis, none of the 65 pts in this study had cardiac events, and, (3) ETI is a far better prognostic indicator than exercise ECG, because of the high incidence of inconclusive exercise ECG results (35%) and the good prognosis in pts with positive results.

PROGNOSTIC SIGNIFICANCE OF NORMAL QUANTITATIVE TL-201 STRESS SCINTIGRAPHY IN RELATION TO PRETEST LIKELIHOOD OF CORONARY ARTERY DISEASE. D.J. Russo, D. Russo, J. Clements, F. Wackers. University of Vermont, Burlington, Vermont.

Beller, et al have reported an excellent prognosis and low cardiac event rate in patients(pts) with chest pain and normal quantitative Tl-201 scintigraphy(SC). Such result would not be unexpected if the population under study had a predominance of pts with low pre-Tl-201 likelihood(L) of significant coronary artery disease(CAD). Hence, we undertook telephone follow-up in pts with chest pain syndrome and normal quantitative Tl-201 exercise SC, and related outcome to pretest L of CAD. Pretest L was determined by serial L analysis on the basis of: symptoms, age, sex, and exercise ECG. All pts had Tl-201 SC immediately post exercise and 2 hrs later. After interpolative background correction, circumferential count and washout profiles were generated. All pts had unequivocally normal studies. Of a total of 96 pts studied in 1981-82, 20 pts were lost to follow-up. Of the remaining 76 pts, 45 were males and 31 females. The pretest L of CAD had an inverted Gaussian distribution: thirty-four pts(47%) had $\leq$33% L of CAD, 3 pts (5%) had 33-66% L of CAD, and 35 pts(48%) had $\geq$66% L of CAD. Mean follow-up was 22$\pm$3 months. No deaths occurred. Two pts(3%)(with pretest L of 54% and 94%) had myocardial infarctions, 8 and 22 months respectively after Tl-201 stress SC. One pt underwent percutaneous transluminal coronary angioplasty(PTCA) 16 months after Tl-201 stress SC. Thus: 1) our findings confirm excellent prognostic significance of normal quantitative Tl-201 stress scintigraphy; 2) cardiac events were rare and non-fatal. 3) Events occurred in pts with moderate to high L of CAD in concordance with Bayesian theorem.

TL-201 SCINTIGRAPHY IN ASSESSING THE HEMODYNAMIC SIGNIFICANCE OF ISOLATED CORONARY ARTERY STENOSES. V. Kalff, M.J. Kelly, A. Soward, R.W. Harper, P.J. Currie, Y.L. Lim, A. Pitt. Nuclear Medicine and Cardiology Services, Alfred Hospital, Melbourne , Australia.

This study tests the hypothesis that the results of stress TL-201 scans (TL201) are related to the transstenotic pressure gradient (GRAD) of coronary stenoses independent of the % luminal diameter narrowing (%NAR) seen at angiography. The 22 study patients (mean age 46 years, range 30-62, 2 female) had no prior myocardial infarction. Each underwent a symptom limited erect bicycle Tl201 off antianginal therapy, shortly before percutaneous transluminal coronary angioplasty (PTCA) for isolated left anterior descending coronary artery stenosis. The %NAR, GRAD (mmHG) at PTCA and severity of TL-201 defects (scaled 0-4) were independently evaluated and results compared. The GRAD (mean$\pm$SD) is tabulated in relation to positive (+) or negative (-) TL201, and %NAR.

	$\leq$70 %NAR	71-89 %NAR	$\geq$90 %NAR
GRAD of +TL201	67$\pm$10 (N=4)	62$\pm$16 (N=7)	72$\pm$11 (N=4)
GRAD of -TL201	25$\pm$22 (N=4)	45$\pm$9 (N=3)	- (N=0)

In the 18 patients with <90 %NAR, the GRAD was higher (P<.001) in those with +TL201 (64$\pm$15) than those with -TL201 (33$\pm$20) but their %NAR did not differ significantly (72$\pm$14% vs 66$\pm$19%; P=NS). At multiple regression analysis the severity of TL201 defect (p<.001) was a strong and %NAR (P<.05) a weak independent predictor for GRAD.

TL201 adds valid information on the hemodynamic significance of a stenosis independent of %NAR. This may of most value when %NAR is <90% and the clinical significance of the coronary stenosis is uncertain.

THE REVERSE REDISTRIBUTION PHENOMENON WITH Tl-201: CORONARY ANGIOGRAPHIC AND CLINICAL CORRELATION. E.B. Silberstein, and D.F. DeVries. University of Cincinnati Medical Center and The Jewish Hospital, Cincinnati, OH.

Poor perfusion with Tl-201 in a myocardial segment at rest with apparently normal distribution immediately post-exercise, (reverse redistribution, RR) has been correlated with a high probability of coronary artery disease (CAD) in two previous studies of 20 and of 5 patients. In 785 consecutive Tl-201 exercise studies over a 15 month period we re-examined the clinical and coronary angiographic correlates of this finding.

RR was read on 38 studies (5%) and of these, 20 patients had coronary angiograms. Of these 20, 9 (5 male, 4 female) had coronary arteries with < 50% stenosis but three of these 9 had other diseases involving the heart (idiopathic cardiomyopathy, 2; familial Mediterranean fever). Six of these false positives with RR had no defect immediately post stress, while three also had perfusion defects post stress which improved. Of the 11 true positives with abnormal angiography and RR, 4 had only RR while 7 had RR plus other post stress defects. Contrary to prior reports, in only 7 of the 11 was the vessel supplying the area of RR the least obstructed coronary artery.

RR therefore had a positive predictive value for C.A.D. 11/20 = 55%, also contrary to prior reports. For all heart disease the predictive value rises to 14/20 = 70%.

3:30–5:00 **Room 216BC**

COMPUTERS AND DATA ANALYSIS III: TOMOGRAPHY

Moderator: Peter D. Esser, Ph.D.
Comoderator: Ernest V. Garcia, Ph.D.

IMAGE RECONSTRUCTION ALGORITHM FOR A HEXAGONAL BAR POSITRON CAMERA. A. Guvenis and G. Muehllehner, Hospital of the University of Pennsylvania, Philadelphia, PA

A positron camera consisting of 6 position-sensitive continuous detectors presents unique requirements for the reconstruction algorithm. In particular, spatial nonlinearities in the detectors must be removed in software, the large but sparsely populated data matrix must be reduced in size, and the gaps in the data at the intersection of the detectors must be compensated for. These problems have been investigated and an appropriate algorithm for this system has been implemented and tested.

In order to map spatial nonlinearities, a circular lead ring with ninety evenly spaced slits is placed in the aperture with a line source positioned at the center of the ring. Since the slits define the positions on the detectors which can be reached by gamma rays from the line source, nonlinearities between the recorded and actual position can be determined. The lead ring is rotated four times by 1-degree increments to obtain a total of 360 measured positions. These measured values are used to generate a look-up table for each detector to remove the nonlinearities.

At the intersection of the detectors, small gaps result in a 4-degree gap in the angular sampling. While these gaps could be avoided with a simple rotation of the ring, a totally stationary ring makes gated cardiac imaging easier. These data gaps produce artifacts if a filtered backprojection algorithm is used. While interpolation across the gaps reduces the artifacts, it appears that iterative algorithms are more suitable for the particular detector geometry employed.

The algorithm has been tested with both simulated and real data.

A GENERALIZED DECONVOLUTION ALGORITHM FOR IMAGE RECONSTRUCTION IN POSITRON EMISSION TOMOGRAPHY WITH TIME-OF-FLIGHT INFORMATION (TOFPET). C.-T. Chen and C.E. Metz. The University of Chicago, Chicago, IL.

Positron emission tomographic systems capable of time-of-flight measurements open new avenues for image reconstruction. Three algorithms have been proposed previously: the most-likely position method (MLP), the confidence weighting method (CW) and the estimated posterior-density weighting method (EPDW). While MLP suffers from poorer noise properties, both CW and EPDW require substantially more computer processing time. Mathematically, the TOFPET image data at any projection angle represents a 2D image blurred by different TOF and detector spatial resolutions in two perpendicular directions. The integration of TOFPET images over all angles produces a preprocessed 2D image which is the convolution of the true image and a rotationally symmetric point spread function (PSF). Hence the tomographic reconstruction problem for TOFPET can be viewed as nothing more than a 2D image processing task to compensate for a known PSF. A new algorithm based on a generalized iterative deconvolution method and its equivalent filters ("Metz filters") developed earlier for conventional nuclear medicine image processing is proposed for this purpose. The algorithm can be carried out in a single step by an equivalent filter in the frequency domain; therefore, much of the computation time necessary for CW and EPDW is avoided. Results from computer simulation studies show that this new approach provides excellent resolution enhancement at low frequencies, good noise suppression at high frequencies, a reduction of Gibbs' phenomenon due to sharp filter cutoff, and better quantitative measurements than other methods.

COMPARISON OF PARAMETER ESTIMATION TECHNIQUES FOR THE QUANTITATION OF LOCAL CEREBRAL BLOOD FLOW BY SERIAL POSITRON COMPUTED TOMOGRAPHY. R.A. Koeppe, J.E. Holden, Medical Physics Department, University of Wisconsin, Madison, WI

Local cerebral blood flow (lCBF) can be quantitated from positron computed tomographic (PCT) data by several general methods. Those using serial PCT scans allow the simultaneous estimation of both lCBF and λ, the tissue:blood partition coefficient. This paper reports a comparison of three estimation techniques for use with serial PCT data, each of which is based on the orginal Kety-Schmidt equation:

$$C_t(t) = f\, C_a(t) * e^{-(f/\lambda)t}$$

where C_t and C_a are indicator concentrations in cerebral tissue and arterial blood, and f is the flow/volume. Two of the methods (Refs. 1 and 2) involve multiplying measured data by two weighting functions $w_1(t)$ and $w_2(t)$. The method of Ref. 1 offers direct calculation of parameters, while the method of Ref. 2 calculates a "lookup table" for matching measured data to model predictions. The third method, developed in our laboratory, is a rapid least-squares search scheme that minimizes the mean squared discrepancy between model predictions and measured data.

Theoretical studies of noise properties and other errors were carried out under a variety of simulated conditions by varying total scan duration, indicator half-life and administration protocol (arterial input shape), flow rate, and temporal resolution of the PCT data. Images of lCBF and λ were calculated for each method using both phantom and human subject data acquired on an ECAT-II tomograph. Errors can differ by as much as a factor of 2-3 between methods, each having its own unique advantages and disadvantages.

1. Huang SC, et al., J Cereb Blood Flow Metabol 2:99, 1982.
2. Alpert NM, et al., J Nucl Med 24:P33, 1983.

DISTANCE WEIGHTING FOR IMPROVED TOMOGRAPHIC RECONSTRUCTIONS. D.J. Nowak and R.L. Eisner, General Electric Medical Systems Group, Milwaukee, WI and Emory University, School of Medicine, Atlanta, GA.

An improved method for the reconstruction of emission computed axial tomography images has been developed. The method is a modification of filtered back-projection, where the back projected values are weighted to reflect the loss of information, with distance from the camera, which is inherent in gamma camera imaging. This information loss is a result of: loss of spatial resolution with distance, attenuation, and scatter. The weighting scheme can best be described by considering the contributions of any two opposing views to the reconstruction image pixels. The

weight applied to the projections of one view is set to equal the relative amount of the original activity that was initially received in that projection, assuming a uniform attenuating medium. This yields a weighting value which is a function of distance into the image with a value of one for pixels "near the camera", a value of .5 at the image center, and a value of zero on the opposite side.

Tomographic reconstructions produced with this method show improved spatial resolution when compared to conventional 360° reconstructions. The improvement is in the tangential direction, where simulations have indicated a FWHM improvement of 1 to 1.5 millimeters. The resolution in the radial direction is essentially the same for both methods. Visual inspection of the reconstructed images show improved resolution and contrast.

ADVANCED INTERPRETIVE LANGUAGE FOR IMAGING PROTOCOLS. J.A. Cooper, C.W.J. Schiepers, H.M. Dansky, and B.R. Line. Albany Medical Center, Albany, NY.

The production of new image processing protocols is primarily limited by software development. Protocols written by menu selection or with compiled languages are inflexible and difficult to change. We have designed an interpretive language to control FORTRAN-77 coded modules to simplify protocol development, but retain the speed of compiled languages. The software system takes advantage of 32-bit virtual memory hardware and is designed to provide a multi-user environment for imaging research and clinical analysis. The stack based threaded interpreter supports scalars, text strings, curves, regions-of-interest and images of varying sizes and types (byte, integer, real). Functions for acquisition, arithmetic manipulation, image processing and display operate independently of datatype. Type interconversion, memory allocation, error checking, and database management are transparent to the user. The language's block structure syntax is easily learned yet powerful and flexible. It supports complex nested control structures including recursion and facilitates protocol construction through the combination of lower level procedures. For example, protocols for optimized count dependent Fourier filtering, phase-amplitude analysis, and quantitative ventilation-perfusion imaging were implemented in less than one day. This high level language for image processing has proven to be a powerful tool for developing image processing protocols by the programmer and non-programmer alike.

THE CONSEQUENCES OF MULTIPLEXING AND LIMITED VIEW ANGLE IN CODED-APERTURE IMAGING. W.E. Smith, H.H. Barrett, R.G. Paxman. Radiology Dept., Arizona Health Sciences Center, Tucson, AZ.

Coded-aperture imaging (CAI) is a method for reconstructing distributions of radionuclide tracers that offers advantages over ECT and PET; namely, many views can be taken simultaneously without detector motion, and large numbers of photons are utilized since collimators are not required. However, because of this type of data acquisition, the coded image suffers from multiplexing; i.e., more than one object point may be mapped to each detector in the coded image.

To investigate the dependence of the reconstruction on multiplexing, we reconstruct a simulated two-dimensional circular object from multiplexed one-dimensional coded-image data, then perform the reconstruction from un-multiplexed data. Each of these reconstructions are produced both from noise-free and noisy simulated data.

To investigate the dependence on view angle, we reconstruct two simulated three-dimensional objects; a spherical phantom, and a series of point-like objects arranged nearly in a plane. Each of these reconstructions are from multiplexed two-dimensional coded-image data, first using two orthogonal views, and then a single viewing direction.

The two-dimensional reconstructions demonstrate that, in the noise-free case, the multiplexing of the data does not seriously affect the reconstruction quality and that in the noisy-data case, the multiplexing helps, due to the fact that more photons are collected. Also, for point-like objects confined to a near-planar region of space, we show that restricted views can give satisfactory results, but that, for a large, three-dimensional object, a more complete viewing geometry is required.

3:30–5:00 **Room 214BC**

RADIOPHARMACEUTICAL CHEMISTRY IV: MONOCLONAL ANTIBODIES

Moderator: David R. Elmaleh, Ph.D.
Comoderator: Mathew L. Thakur, Ph.D.

OPTIMIZATION OF AN ANTIBREAST CARCINOMA MONOCLONAL ANTIBODY AS A TUMOR IMAGING AGENT. M.R. Zalutsky, D. Colcher, W.D. Kaplan, J. Schlom, and D. Kufe. Harvard Medical School, Boston, MA and The National Cancer Institute, Bethesda, MD.

We have previously reported that monoclonal antibody B6.2 and its fragments labeled with I-125 selectively localizes in human breast tumor (bt) xenografts in nude mice. Herein we compare I-125 B6.2 and its fragments with regard to (a) in vitro binding to bt extracts and (b) blood clearance. Antibody B6.2 and fragments were labeled using iodogen and then incubated with cell extracts of a human bt metastasis to the liver (Met.173), MCF-7 bt line, and normal human liver. Scatchard analysis of the data revealed that I-125-B6.2 and its fragments bound to both breast tumors with affinity constants of the order of $10^9 M^{-1}$; no specific binding to normal liver was observed. The affinity constant for both divalent fragments was higher than that observed for the monovalent Fab´ fragment. Serial sampling of blood from tumor bearing mice indicated that the blood clearance of $F(ab')_2$ was more rapid than IgG and that Fab´ cleared considerably faster still. A comparison of the biodistribution at 0.1 and 5 µg protein per mouse suggests that with 1 gm tumors, lower doses do not necessarily result in better tumor-to-tissue ratios. When the blood clearance of I-125-B6.2 was compared to that of a non-specific IgG (MOPC), a much faster clearance of I-125 activity, significantly greater than that resultant from uptake in the tumor, was observed. Accelerated blood clearance may be due to selective catabolism of the specific antibody. When I-125 labeled B6.2 was injected into mice bearing breast and melanoma tumors, the thyroid uptake of I-125 activity was 2-3 times greater in the bt mice. We conclude that catabolism may be an important factor in determining the optimal radiolabel for immunoscintigraphy.

A NOVEL APPROACH FOR TESTING THE IMMUNOINTEGRITY OF RADIOLABELED ANTIBODIES. W. Chanachai, W. Wolf and J. Shani, Radiopharmacy Program, Univ. Southern California, Los Angeles, CA, and R.A. Reisfeld, N.M. Varki and L.E. Walker, Scripps Clinic and Rsch. Found., La Jolla, CA

A key element in evaluating whether a labeled antibody (LAB) is suitable for in vivo studies is its immunological binding to the antigen against which it was prepared. The standard Enzyme-Linked Immunosorbent Assay (ELISA) measures the total amount of immunocompetent antibody present, irrespective of the fact that it may (or may not) be labeled. However, if coupling or labeling results in a loss of immunocompetence, then an ELISA test will not give an accurate estimation of the immunocompetent LAB's. However, LABs can be used to measure directly the % of the immunological binding ability they retain. Multiwell plates were coated with lung adenocarcinoma (UCLA P3) cells to yield concentrations of 10^4 to 10^5 cells/well. A known activity of In-113m-DTPA-IgG (<1% free In-113m) was placed in a well, the unbound material was washed off 3 times following 30 minutes incubation, and each well was excised and counted. Surface-active agents such as Tween affect the binding of the LAB to the antigen, and should not be used. Studies with In-113m labeled DTPA-IgG2a antibodies documented the heterogenicity of the LAB population: a standard ELISA test gave an 85% value for immunointegrity, but only 28-30% when using this new test. As imaging can only be performed through binding of the immunocompetent radiolabeled antibodies, such a direct test is a more

reliable method for evaluating the binding capacity of radiolabeled antibodies as potential imaging agents.

VARIABLES INFLUENCING THE ATTACHMENT OF BIFUNCTIONAL CHELATES TO ANTIBODIES. O.A. Gansow, R.W. Atcher and D.C. Link. Radiation Oncology Branch, National Cancer Institute, Bethesda, MD.

The parameters affecting the attachment of bifunctional chelates to proteins have been investigated. H-3 DTPA dianhydride was synthesized and used to determine the effect of pH of the reaction mixture and concentration of the reactants on the final number of chelates attached to the protein. The tritiated chelate enables one to unambiguously ascertain this information without resorting to indirect measurement techniques which are subject to error due to adventitious binding of metals to protein.

Bovine immunoglobulins (IgG) were used as the model protein. All aqueous reagents were treated with Chelex 100 resin to remove any divalent or trivalent cations. All organic reagents were dried to remove any water.

In order to assess the effect of pH, a chelate to antibody ratio of 100:1 and a protein concentration of 5 mg/ml were used. The protein was dissolved in a series of buffers from pH 4.0 to 10.0. The binding was a maximum at a pH of 8.0 resulting in the attachment of 1.2 chelates per antibody.

In order to assess the effect of concentration, the pH was maintained at 8.0 throughout the reaction and the chelate to antibody ratio was varied from 1:1 to 1000:1. Further tests with monoclonal antibodies showed loss of specificity at ratios exceeding 150:1 and loss of viability at ratios exceeding 300:1 in in vitro tests.

Finally, the concentration of the antibody was varied from 0.1 mg/ml to 20 mg/ml while keeping the pH at 8.0 and the chelate to antibody ratio at 100:1. The number of chelates per antibody is 0.4 above a concentration of 2.5 mg/ml.

COUPLING ANTIBODY WITH DTPA...AN ALTERNATIVE TO THE CYCLIC ANHYDRIDE. A. Najafi, R. Childs and D.J. Hnatowich. University of Texas Medical Branch, Galveston, TX, and University of Massachusetts Medical Center, Worcester, MA.

We have previously shown that the bicyclic anhydride of DTPA may be used to attach this chelator to several proteins, including IgG antibody, rapidly and efficiently and that the coupled proteins may be labeled with In-111. As an alternative to the cyclic anhydride, we have now investigated the N-hydroxysuccinimide pentaester of DTPA for this purpose. The ester was prepared by reacting the imide with the cyclic anhydride and, like the cyclic anhydride, the ester is stable to storage at room temperature in moisture-free environments. The conditions under which IgG may be coupled with the ester were compared to that of the anhydride. Whereas maximum coupling with the anhydride is achieved in 20 seconds, about 10 minutes is required at room temperature with the ester, although the rate of coupling is increased at 37°C. The effect on coupling efficiency of pH, protein concentration, and molar ratios is quantitatively different than that observed earlier with the anhydride although the trends are similar. Under optimum conditions, coupling efficiency with the ester is 90 ± 5% (pH=7.0) vs. 80 ± 5% (pH=8.4) for the anhydride. Antibody coupled with the ester showed a greater degree of dimer and polymer formation under identical coupling conditions and significantly greater instability during serum incubations.

A NEW APPROACH TO BIFUNCTIONAL CHELATE ATTACHMENT TO ANTIBODIES. T.S.T. Wang, J.M Rosen, R. Smith, R.A. Fawwaz, S. Ferrone, P.O. Alderson. Columbia University, N.Y., NY., and New York Medical College, Valhalla, NY.

One potential problem with the synthesis of bifunctional chelates (BC) of antibodies (Abs) is inactivation of the Ab by attachment of the chelate (C) at or near the antigen (Ag) binding site. The most common method of synthesizing BC depends on attachment of a C (e.g., DTPA) to a free amino group on the Ab molecule. However, the Ab may be inactivated if this amino group is too near the Ag binding site. We examined an alternative method, with attachment of a C, desferrioxamine-B(DF), to free carboxyl groups of Ab molecules. BC of a monoclonal Ab to a melanoma-associated Ag were prepared using DF, and labeled with In-111. DF-Ab was prepared by mixing Ab, DF, and 1-ethyl-3-(3-dimethylaminopropyl) carbodiimide at pH 4.75. BC of the same Ab also were prepared, using DTPA, by the cyclic anhydride method (DTPA-Ab). Good radiolabeling yields were achieved with both DF-Ab and DTPA-Ab. The reactivity of DF-Ab and DTPA-Ab with melanoma Ag was tested in vitro. Binding of the Ab to melanoma cells and to control (lymphoma) cells was assayed. DF-Ab and DTPA-Ab demonstrated significant cell binding (61.5 and 38.2% respectively, at appropriate dilutions)when tested with melanoma cells. Neither Ab bound significantly to control cells (6.9 and 3.3% respectively). These experiments demonstrate that BC of Abs can be successfully prepared by binding C to free carboxyl groups on Abs. The DF-Ab so produced demonstrates significant reactivity with its Ag. With some Abs, as with the above anti-melanoma Ab, this method of BC preparation may result in less loss of antigenic reactivity than occurs with conventional methods.

PREPARATION OF Ga-67 LABELED MONOCLONAL ANTIBODIES USING DEFEROXAMINE AS A BIFUNCTIONAL CHELATING AGENT: K.Endo, T.Furukawa, Y.Ohmomo, H.Sakahara, H.Ohta, T.Nakashima, K.Okada, O.Yoshida, A.Yokoyama and K.Torizuka, Kyoto University, Kyoto, Japan.

Ga-67 labeled monoclonal IgG or $F(ab')_2$ fragments against α-fetoprotein and β-subunit of human choriogonadotropin (HCG), were prepared using Deferoxamine (DFO) as a bifunctional chelating agent. DFO, a well-known iron chelating agent, was conjugated with monoclonal antibodies (Ab) by a glutaraldehyde two step method and the effect of conjugation on the Ab activities was examined by RIA and Scatchard plot analysis. In both monoclonal Ab preparations, the conjugation reaction was favored as the pH increased. However, Ab-binding activities decreased as the molecular ratios of DFO to Ab increased. Preserved Ab activities were observed when Ab contained DFO per Ab molecule less than 2.1. At a ratio of over 3.3 DFO molecules per Ab, the maximal binding capacity rather than the affinity constant decreased. The inter-molecular cross linkage seemed to be responsible for the deactivation of binding activities. The obtained DFO-Ab conjugates, were then easily labeled with high efficiency and reproducibility and Ga-67 DFO-Ab complexes were highly stable both in vitro and in vivo. Thus, biodistribution of Ga-67 labeled $F(ab')_2$ fragments of monoclonal Ab to HCG β-subunit was attempted in nude mice transplanted with HCG-producing human teratocarcinoma. Tumor could be visualized, in spite of relatively high background imaging of liver, kidney and spleen.

In summary, the use of DFO as a bifunctional chelating agent provided good evidence for its applicability to labeling monoclonal Ab with almost full retention of Ab activities. Further, availability of Ga-68 will make Ga-68 DFO-monoclonal Ab a very useful tool for positron tomography imaging of various tumors.

3:30–5:00 **Room 217B**

NEUROLOGY IV: CLINICAL

Moderator: David E. Kuhl, M.D.
Comoderator: John Mazziotta, M.D., Ph.D.

PET MEASUREMENTS OF CEREBRAL METABOLISM CORRECTED FOR CSF CONTRIBUTIONS. J. Chawluk, A. Alavi, R. Dann, M.J. Kushner, H. Hurtig, R.A. Zimmerman, and M. Reivich. Hospital of the University of Pennsylvania, Philadelphia PA.

Thirty-three subjects have been studied with PET and anatomic imaging (proton-NMR and/or CT) in order to determine the effect of cerebral atrophy on calculations of metabolic rates. Subgroups of neurologic disease investigated include stroke, brain tumor, epilepsy, psychosis, and dementia. Anatomic images were digitized through a Vidicon camera and analyzed volumetrically. Relative

areas for ventricles, sulci, and brain tissue were calculated. Preliminary analysis suggests that ventricular volumes as determined by NMR and CT are similar, while sulcal volumes are larger on NMR scans. Metabolic rates (18F-FDG) were calculated before and after correction for CSF spaces, with initial focus upon dementia and normal aging. Correction for atrophy led to a greater increase (%) in global metabolic rates in demented individuals (18.2±5.3) compared to elderly controls (8.3±3.0, $p<.05$). A trend towards significantly lower glucose metabolism in demented subjects before CSF correction was not seen following correction for atrophy. Our data suggest that volumetric analysis of NMR images may more accurately reflect the degree of cerebral atrophy, since NMR does not suffer from beam hardening artifact due to bone-parenchyma juxtapositions. Furthermore, appropriate correction for CSF spaces should be employed if current resolution PET scanners are to accurately measure residual brain tissue metabolism in various pathological states.

ANTERIOR-POSTERIOR AND LATERAL HEMISPHERIC ALTERATIONS IN CORTICAL GLUCOSE UTILIZATION IN ALZHEIMER'S DISEASE. R. P. Friedland, T. F. Budinger, W. J. Jagust, Y. Yano, R. H. Huesman, B. Knittel, E. Koss and B.A. Ober. VA Medical Center, Martinez, CA, Univ. of California, Davis and Donner Laboratory, Univ. of California, Berkeley, CA.

The anatomical and chemical features of Alzheimer's disease (AD) are not distributed evenly throughout the brain. However, the nature of this focality has not been well established in vivo. Dynamic studies using the Donner 280-Crystal Positron Tomograph with (F-18)2-fluorodeoxyglucose were performed in 17 subjects meeting current research criteria for AD, and in 7 healthy age-matched control subjects. Glucose metabolic rates in the temporal-parietal cortex are 27% lower in AD than in controls. Ratios of activity density reveal consistently lower metabolic rates in temporal-parietal than frontal cortex in the AD group, while healthy aged subjects have equal metabolic rates in the two areas. Similar findings have been reported by other laboratories.
A major finding is a striking lateral asymmetry of cortical metabolism in AD which does not favor either hemisphere. (The asymmetry is 13% in the AD group, 3% in controls, $p < .005$.) This has not been previously reported in AD.
The consistency with which anterior-posterior metabolic differences are found in AD suggests that the focality of the metabolic changes may be used to develop a noninvasive diagnostic test for the disorder. The metabolic asymmetry in AD may be compared to the clinical and pathological asymmetry found in Creutzfeldt-Jakob disease, and may represent an additional link between AD and the subacute spongiform encephalopathies.

PET IMAGING OF DOPAMINE RECEPTORS IN MPTP-INDUCED PARKINSONISM. S.M. Larson, G. Di Chiro, R.S. Burns, R.F. Dannals* I.J. Kopin, R.A. Brooks, R.M. Kessler, R.F. Wayner, W.C. Eckelman, R.A. Margolin, H. Pakkenbergt, M.V. Green, D.F. Wong*, and H. N. Wagner, Jr.* NIH Bethesda and JHMI*, Baltimore; Md., and Hvidovre Hospital, Denmarkt

MPTP(N-methyl-4-phenyl-1,2,3,6-tetrahydropyridine) induces parkinsonism in animals and man (PNAS 80:4546, 1983) by selectively destroying dopaminergic neurons in the pars compacta of the substantia nigra. The postsynaptic neurons (and presumably the dopamine receptors) are intact. We have imaged dopamine receptors in a patient with MPTP induced parkinsonism, using ^{11}CMS (3-N[^{11}C] methylspiperone; Science 221:1264, 1983). Seven and 9 mCi's, respectively, were injected at one week intervals while the patient was first off, and then on, L-dopa. As measured by NeuroPET (NIH), putamen to cerebellum concentration ratios rose progressively to 5.5:1, by 90 min. after injection. At this time the concentration of ^{11}CMS was 10 picomole/cc (off L-dopa), and 14 picomole/cc (on L-dopa). The Duvoisin scale was used to assess the severity of the patient's parkinsonism immediately prior and at the end of PET imaging. On both occasions, despite the small mass amount of ^{11}CMS injected, (1.1 g/kg), a transient worsening of symptoms was seen. The effect of L-Dopa was almost completely reversed by the ^{11}CMS. In contrast, off L-Dopa the patients severe basal state was worsened only slightly. The PET scans suggested that dopamine receptors are not reduced in MPTP-induced parkinsonism. The findings were consistent with the hypotheses that PET may identify patients who will benefit from L-Dopa, and that expression of parkinsonian symptoms reflects desaturation of dopamine receptors in striatum.

BRAIN METABOLISM AND MEMORY IN AGE DIFFERENTIATED HEALTHY ADULTS. W.H. Riege, E.J. Metter, D.E. Kuhl and M.E. Phelps. Sepulveda VA Medical Center and UCLA School of Medicine, Los Angeles, CA.

The [F-18]-fluorodeoxyglucose (FDG) scan method with positron emission tomography was used to determine age differences in factors underlying both the performances on 18 multivariate memory tests and the rates of cerebral glucose utilization in 9 left and 9 right hemispheric regions of 23 healthy adults in the age range of 27-78 years. Young persons below age 42 had higher scores than middle-aged (age 48-65 yrs) or old (age 66-78 yrs) persons on two of seven factors, reflecting memory for sequences of words or events together with metabolic indices of Broca's (and its mirror region) and Thalamic areas. Reliable correlations (critical $r = 0.48$, $p<0.02$) indicated that persons with high Superior Frontal and low Caudate-Thalamic metabolic measures were the same who performed well in tests of memory for sentences, story, designs, and complex patterns; while metabolic indices of Occipital and Posterior Temporal regions were correlated with the decision criteria adopted in testing. The mean metabolic ratio ($b = -0.033$, $F = 5.47$, $p<0.03$) and those of bilateral Broca's regions ($b = -0.002$, $F = 13.65$, $p< 0.001$) significantly declined with age. The functional interrelation of frontal-subcortical metabolic ratios with memory processing was more prominent in younger persons under study and implicates decreasing thalamo-frontal interaction with age.

PET WITH F-18 FLUORODEOXYGLUCOSE MEASURES OF LOCAL BRAIN ACTIVITY AND MEMORY IN SCHIZOPHRENIA AND IN DEPRESSION. W.H. Riege, E.J. Metter, D.E. Kuhl, M.E. Phelps and A. Kling. Sepulveda VA Medical Center and UCLA School of Medicine, Los Angeles, CA.

Positron emission tomography with [F-18] fluorodeoxyglucose (FDG) scan has provided non-invasive measures of regional cerebral glucose utilization which are directly related with levels of functional activity in regions of the brain. The FDG technique was applied to the study of brain activity thought to be impaired in 6 chronic schizophrenics (SCH) and 6 depressed (D) patients in comparison with 6 healthy age-matched controls (C). Local cerebral metabolic rates of glucose utilization (LCMRglc were determined for 8 regions in both left and right hemispheres and were expressed in reference to a person's mean CMRglc. Multivariate comparisons of the 16 measures showed no significant differences between the 3 groups; follow-up step-down analyses and t-tests failed to specify any regional or global LCMRglc reliable to separate patients from controls. They also did not differ in any of 18 multidimensional tests of memory and decision, except for lower delayed verbal recall in D patients. When both SCH and D were classified into those with CT large and those with CT small ventricles, there were no multivariate differences. Only parietal LCMRglc separated large from small ventricle patients ($F(1,7) = 6.12$, $p<0.042$), but finding no multivariate significance makes this result questionable. The ventricular grouping of SCH alone may reveal a marginal difference in global CMRglc ($t(4) = 2.58$, $p<0.06$, given a larger patient sample. In contrast to recent reports, indices to brain activity in schizophrenic and depressed patients do not seem to be abnormal.

SINGLE-PHOTON TOMOGRAPHIC DETERMINATION OF REGIONAL CEREBRAL BLOOD FLOW IN PSYCHIATRIC DISORDERS. M.D. Devous, Sr., A.J. Rush, M.A. Schlesser, J. Debus, J.D. Raese, H.H. Chehabi, F.J. Bonte. University of Texas Health Science Center, Dallas, TX.

Regional cerebral blood flow (rCBF) was measured by single-photon emission computed tomography (SPECT) of 133-Xe washout in 29 normal volunteers, 22 unipolar endogenous depressives (UPE), 9 unipolar nonendogenous

depressives (UPNE), 13 bipolar depressed patients (BPD), and 14 schizophrenic patients (SCHZ). RCBF was measured 2 and 6 cm above and parallel to the cantho-meatal line and quantitated in 14 gray matter regions. Most subjects were drug-free for 4-14 days. Diagnoses were made by experienced clinicians employing the Research Diagnostic Criteria, the Hamilton Rating Scale, and the dexamethasone suppression test. SCHZ were rated with the Brief Psychiatric Rating Scale. UPE had reduced flow compared to normals in the right parietal and temporal lobes and a nonsignificant trend toward left temporal flow reductions. UPNE were not different from normal or other patient groups. BPD had significant flow elevations in the left hemisphere relative to normal, and in both hemispheres relative to UPE. SCHZ were not significantly different from normal or other patient groups. Anterior-posterior flow shifts were evaluated by subtracting parietal or temporal flows from frontal flows. SCHZ demonstrated a greater posterior shift (lower relative frontal lobe flow) in comparison to both UPE and UPNE. The most significant regional flow abnormalities were observed as frontal flow reductions in individual SCHZ, although these were not significant in the whole group in comparison to normal.

3:30–5:00 **Room 212B**

PEDIATRICS

Moderator: John R. Sty, M.D.
Comoderator: Margaret A. Gainey, M.D.

URETERAL PERISTALSIS IN PEDIATRIC UROLOGY. W.Müller-Schauenburg, K.Anger, U.Feine,*A.Flach,*P.Reifferscheid,and U.Hofmann* Nuklearmedizinische Abtlg.u.*Kinderchirurgische Abtlg. der Universität Tübingen, Tübingen, FRG.

The review is based upon more than 300 pediatric studies from 6 years. Ureteral motility has been assessed in routine renography with I-123-hippuran and Tc-99m-DTPA. Normal ureters were studied with Tc-99m-MDP as by-product to bone scans. In a few cases the radioisotope was injected or infused into the renal pelvis via a Sober loop or a catheter.

Ureteral motility information is compressed,similar to the M-mode in sonography, by a space time matrix approach, which was introduced by Müller-Schauenburg in 1978.

The clinical applications focussed upon vesico-ureteral reflux, megureter motility, and ureteral stenosis.

Concerning vesico-ureteral reflux, the method revealed the clinical and diagnostic interference of retroperistalsis and reflux:
(i) Retroperistalsis supports the backflow mechanism.
(ii) Retroperistalsis may be a symptom of a refluxive ureter, even if there is no actual reflux documented.
(iii) Discrepancies between direct and indirect tests for reflux are explained partly by the occurrence of retroperistaltic transport of prevesical urine during indirect testing, simulating vesico-ureteral valve dysfunction.

Concerning megaureters, the preoperative motility is known to be of prognostic value.

Early ureteral stenosis may be judged from peristaltic frequency,either in the basic study or after frusemide.

The method became reliable ,when the absence of motility could be distinguished from the absence of information on motility,due to a low isotope input into the ureter. In conclusion, the method is now available as routine tool.

DETERMINATION OF REGIONAL ESOPHAGEAL TRANSIT IN CHILDREN BY MEANS OF KRYPTON-81m. A.Piepsz,H.R.Ham,B.Georges,M.H.Delaet, S.Cadranel. Depts Radioisotopes and Pediatrics, St Peter Hospital, Free University of Brussels.

Radionuclide methods using Tc-99m have been developed in the last few years for the assessment of the esophageal transit. The method is physiologic, easy to perform and giving thus interesting informations concerning the severity of the disease as well as the effect of the applied treatment. In children, however, one is limited by radiation protection considerations, and the results are often of poor quality due to the low count rate. Furthermore,the risk of external contamination and the impossibility of repeating the test constitute significant disadvantages, particularly in young children. These problems are completely avoided by using Krypton-81m diluted in a glucose solution. For each swallowing about 8 mCi of Kr-81m are administered. Sixty one-second frames are recorded and several parameters of regional transit can be extracted in a few minutes, using time activity curves and parametric images. The test is very sensitive in detecting minor regional transit alterations. The reproducibility of the test is good and phenomenons like intercurrent gastro-esophageal reflux or asynergic peristaltic waves can easily be detected. The test has been applied to 52 children, aged 1 week to 19 years, and provided helpful informations concerning the localization and the importance of transit abnormalities in caustic and peptic esophagitis, postoperative cases (atresia or anti-reflux plasty) and in patients with neuromuscular disorders.

COUNT-BASED METHOD TO CALCULATE RIGHT VENTRICULAR VOLUMES IN CHILDREN; IN VITRO AND CLINICAL VALIDATION. P. Guiteras, M.E. deSouza, M. Green, J.M. Ash, D. Gilday, P. Olley. The Hospital for Sick Children, Toronto, Ont.

A rapid method for obtaining scintigraphic right ventricular volumes was developed and validated against cineangiography in 36 children, 10 with normal right ventricles (RV) and 26 with volume (VO) or pressure overload. Using a phantom, we validated the estimate of depth and the effect of different attenuation coefficients on volumes (V). End diastolic (EDV) and end systolic volumes (ESV) were calculated by dividing background corrected count rates by the count rate per millilitre of a reference blood sample. Attenuation corrected volume was given by $V \div e^{-ud}$, where u=linear attenuation coefficient and d=depth of the phantom or RV centre. Phantom volumes were accurately predicted (r=0.99, $p < .001$) but only attenuation coefficients between 0.11 cm^{-1} and 0.13 cm^{-1} yielded slopes close to 1.

In-vivo data was therefore analyzed using $u=0.11\ cm^{-1}$ with RV counts corrected with either RV or LV background. Closest agreement between scintigraphic and angiographic volumes was obtained using RV background (r=.91, $p < .001$, SEE 13 mls), although EDV's larger than 100 mls were substantially underestimated. The method was less accurate in VO particularly for ESV. The use of a larger attenuation coefficient ($0.15\ cm^{-1}$) improved the estimate of EDV's, but reduced the accuracy of ESV's in children with either large or small ventricles and those with small body surface.

Our conclusion is that the optimum volume estimates require using an absorption coefficient of $.11\ cm^{-1}$ for children with a body surface area less than .95 m^2, and $.15\ cm^{-1}$ in larger children.

EFFECTIVE IMAGE FILTRATION OF PEDIATRIC SINGLE PHOTON EMISSION TOMOGRAMS. D.L. Gilday, M.D. Green, R. Puntillo, J.M. Ash. The Hospital for Sick Children, Toronto, Ont.

Single Photon Emission Computed Tomography (SPECT) in children suffers from relatively poor photon statistics due to the lower radiopharmaceutical dose when compared with adults. Consequently, we have made a major effort to improve the resultant tomographic images.

We compared the effect that different enhancements had on the basic reconstruction. The baseline study was a reconstruction with an internal filter appropriate to the planar image's photon density. The first enhancement was to three dimensionally filter planar images prior to reconstructing with an internal "high resolution" filter. The second was to apply three dimensional filter to the images which were reconstructed with an internal "high resolution" filter. The filtration and reconstruction were performed on both MDS-A^2, A^3 and GE Star computers.

The results showed that planar images which were of poor photon flux produced much better reconstructions when pre-filtered, whereas the difference was not nearly so dramatic with high photon flux studies.

Therefore, we recommend routine pre-reconstruction three dimensional filtering on all SPECT studies, especially those of poor photon flux. In fact in some very low photon flux 24 hour CSF, Thallium and Gallium studies, it was only possible to interpret those images when pre-filtered first.

GROWTH PLATE CLOSURE: APEX VIEW ON BONE SCAN.
R. Howman-Giles., M. Trochei., K. Yeates.
Royal Alexandra Hospital for Children ,SYDNEY. AUSTRALIA.

Angular deformities of the extremities in children following premature closure of the growth plate are well known. The deformities depend on the position of an osseus bridge which forms between the epiphysis and metaphysis. Several surgical procedures including resection of the osseus bridge have been described ,however delineation of the site of fusion is difficult to define. The commonest site of growth plate arrest is the distal femoral or proximal tibial growth plate. A new technique using the bone scan has been developed which accurately defines the area and position of these osseus bridges. Two hours after injection of technetium 99m methylene diphosphonate apex views of the affected distal femoral growth plate were performed. The knee was flexed into its smallest angle. Using a pinhole collimator the gamma camera was angled to face the affected growth plate end on. The image was collected onto computer and analysed by: (i) regions of interest over segments of the growth plate to calculate the relative area of total growth plate affected: (ii) generating histograms: (iii) thresholding or performing isocontours to accentuate abnormal areas. The growth plate is normally uniformly increased when compared to the normal shaft of the bone. Fusion across the plate appears as an area of diminished uptake. The apex view gives a unique functional map of the growth plate such that abnormal areas are displayed, and the site, size and position of osseus fusion obtained. The technique has the potential for determining the metabolic activity of the growth plate before and after surgery. Serial studies will allow assessment of regeneration of the plate and reformation of new osseus bridges.

BRAIN PERTECHNETATE SPECT IN PERINATAL ASPHYXIA.
G. Sfakianakis, R. Curless, R. Goldberg, L. Clarke, C. Saw, E. Sfakianaki, F. Bloom, C. Bauer, A. Serafini.
University of Miami/Jackson Memorial Hospital, Miami, FL.

Single photon emission computed tomography of the brain was performed in 6 patients with perinatal asphyxia aged 8-26 days. A single-head (LFOV) commercial SPECT system (Picker) was used and data were acquired 2-3 hr after an IV injection of 1-2 mCi Tc-99m-pertechnetate (360° rotation, 60 views, 64 x 64 matrix, 50K cts/view). Reconstruction in three planes was performed using MDS software (Hanning medium resolution filter, with or without attenuation correction using Sorenson's technique). For each clinical study, a ring type phantom source was used to identify the level of reconstruction noise in the tomographic planes.

Abnormalities were found in all patients studied, 3 central (moderate intensity), 2 peripheral (1 severe, 1 moderate) and 1 diffuse (mild intensity). Despite use of oral perchlorate (50 mg) in one patient the choroid plexus was visible. Since attenuation correction tended to amplify noise, the clinical studies were interpreted both with and without this correction. All 3 patients with central lesions were found abnormal on early (1-4 mo) neurologic follow-up examination, whereas the others were normal. No correlation was found between SPECT and 24 hr blood levels of CPK, ammonia, base excess, or the Apgar scores. CT scans were reported abnormal (3 diffuse, 1 peripheral, 1 central and 1 questionable). Planar scintigrams obtained immediately after SPECT were normal (2), questionable (2) and abnormal (2). Follow-up SPECT brain scintigrams in two of the patients showed partial resolution.

SPECT of the brain appears promising in perinatal asphyxia but long term correlation with patient development is necessary.

3:30-5:00 **Room 212A**

GASTROENTEROLOGY III: LOWER GI

Moderator: Michael G. Velchik, M.D.
Comoderator: James H. Thrall, M.D.

GASTRIC EMPTYING OF SOLIDS. WHEN SHOULD WE SAMPLE?
G. Sfakianakis, G. Spoliansky, J. Cassady, J. Barkin, A. Serafini. University of Miami, Miami, FL

Gastric emptying of solids has been studied for 20 normal volunteers using Tc-99m-sulfur-colloid labeled chicken liver (1) or eggs (2). Residual gastric activity measured in 15 min intervals for 2½ hrs was used to calculate gastric emptying. The procedure was proposed and is used to examine patients for suspected abnormal emptying. This approach however ties up one gamma camera and one technologist for a period of 2½-3 hrs. Furthermore to classify any value more than 1SD below the mean as abnormal (1) includes 16% of normals as abnormally low (false positives).

In order to find the pattern of abnormalities and the best time to study patients we analyzed the results of 54 studies performed in patients with a variety of clinical problems. Gastric emptying was measured in 30 min intervals for 2½ hrs after a standard meal of 2 scrambled eggs labeled with 1 mCi of Tc-99m-sulfur-colloid, 2 slices of bread and 300 ml of juice. To choose the points important to observe we studied the distribution of values at each time-point to determine when there is the greatest variability from the reported normal. When there is delayed emptying the 2½ hr observation is the best discriminator and when there is accelerated emptying the 60 min observation is the best discriminator. In our group of patients the 150 min observation had no correlation with the age of the patients. It is possible that sampling at a later time could be more discriminatory. We propose sampling at 0, 60, and 150 min time as the most informative and cost effective approach to study the solid gastric emptying. The 2SD rather than 1SD below and above the mean should be used as the level to separate normal from abnormal results. (1) Clin Nucl Med 7:215-221, 1982, (2) J Nucl Med 23:p21, 1982.

GASTROINTESTINAL TRANSIT OF PHARMACEUTICAL PREPARATIONS.
J.G. Hardy, S.S. Davis, and C.G. Wilson. Queen's Medical Centre, Nottingham, England.

Attempts to improve drug delivery have resulted in a range of a sustained-release products for oral administration. A comprehensive study has been undertaken of the factors influencing the gastrointestinal transit of such preparations.

The transits of solutions, tablets and osmotic devices have been compared with those of pellets. The systems were radiolabeled with either technetium-99m or indium (In-111 or In-113m) and administered to groups of healthy volunteers. The effects of particle size and density, and the presence of food in the stomach, on gastric emptying and transit rates through the small intestine have been monitored using a gamma camera.

The results are summarized in tabular form.

Systems	Number of Subjects	Mean Times (minutes) Gastric Emptying	Transit Through Small Intestine
solution/pellets	10	18/99	244/204
tablet/pellets	6	164/79	188/227
osmotic device/pellets (with 1500 kJ meal)	6*	183/119	191/188
osmotic device/pellets (with 3600 kJ meal)	6*	>600/285	- /202
pellets (0.94 Mgm^{-3}) /pellets (1.96 Mgm^{-3})	4	380/300	(* same subjects)

Gastric residence was greatly influenced by the presence of food and the nature of the preparations. Transit time through the small intestine was independent of the size, shape or density of the material.

THE SCINTIGRAPHIC DETERMINATION OF SMALL INTESTINAL TRANSIT TIME IN PATIENTS WITH IRRITABLE BOWEL SYNDROME.
A.R. Marano, V.J. Caride, R.V. Shah, E.K. Prokop, F.J. Troncale, R.W. Mc Callum. Hospital of St. Raphael and Yale University, New Haven, CT.

Diffuse disturbance in gastrointestinal motility may be present in patients with irritable bowel syndrome (IBS). To further investigate small intestinal motility in IBS patients small intestinal transit time (SITT) was determined and related to the symptom status. 11 female patients with IBS (mean age 29 years) were divided into

those whose predominate symptom was diarrhea (N=6), and those with only constipation (N=5). All subjects ingested an isosmotic solution of lactulose (10 gm in 150cc of water) labeled with 99m-Tc-DTPA (Sn). The patient was studied supine under a 15 inch gamma camera with data collected at 1 frame per minute for 180 minutes or until activity appeared in the ascending colon. Regions of interest were selected over the cecum and ascending colon. The time of first appearance of radioactivity in the region of the cecum was taken as the small intestinal transit time. SITT in the 5 normal females was 98.7 ± 13 min (mean ± SEM). SITT in the IBS patients with diarrhea, 67.3 ± 7 min was significantly faster ($p < 0.08$). SITT in the constipated IBS patients, 126 ± 12 min, was slower than normals and significantly different from diarrhea patients ($p < 0.001$). These studies show that IBS patients with diarrhea have significantly faster SITT than normals while constipated IBS patients have significantly slower SITT than the diarrhea subgroup. Further, this study emphasizes the need to study the various symptomatic subgroups of IBS patients independently and indicates a possible role for abnormal SITT in the pathogenesis of IBS.

COMPARISON OF THREE TESTS FOR ESTIMATING GASTROENTERAL PROTEIN LOSS. D. Glaubitt, M. Marx, and H. Weller. Department of Nuclear Medicine, Academic Teaching Hospital, Krefeld, Federal Republic of Germany.

A decisive step in the diagnosis of exudative gastroenteropathy which shows a pathologically increased transfer of plasma proteins into the stomach or intestine is the measurement of fecal radioactivity after intravenous administration of radionuclide-labeled large organic compounds or of small inorganic compounds attaching themselves to plasma proteins within the patient.

In 24 patients (12 men and women each) aged 40 to 66 years, the gastroenteral protein loss was estimated after intravenous injection of Cr-51 chloride, Cr-51 human serum albumin, or Fe-59 iron dextran. Each test lasted 6 days. There was an interval of 2 weeks between 2 tests. The feces were collected completely within the test period for determination of radioactivity. External probe counting over liver, spleen, right kidney, and thyroid was performed daily up to 10 days.

The results obtained with Cr-51 chloride presented the largest range whereas the test with Fe-59 iron dextran exhibited both the smallest deviation from the mean value and the lowest normal range. During the tests for gastroenteral protein loss external probe counting demonstrated no distinct tendency to a more rapid radionuclide loss from liver, spleen, and kidney in the patients suffering from exudative gastroenteropathy when compared with healthy subjects.

In conclusion, the most suitable test to estimate gastroenteral protein loss is the Fe-59 iron dextran test although Fe-59 iron dextran is not available commercially and causes a higher radiation burden than the other tests do. In second place, the Cr-51 chloride test should be used, the radiopharmaceutical of which is less expensive and has no significant disadvantage in comparison with Cr-51 human serum albumin.

CHROMIUM-51-EDTA AND TECHNETIUM-99m-DTPA EXCRETION FOR ASSESSMENT OF SMALL BOWEL CROHN'S DISEASE. C. O'Morain, L. R. Chervu, D.M. Milstein, and K.M. Das. Albert Einstein College of Medicine, Bronx, NY.

Cr-51-EDTA is excreted in urine in healthy control subjects to the extent of 2% as shown by our group and others. Patients with Crohn's disease localized in the small bowel had shown a significantly higher urinary excretion (n=18; 3.5 ± 1.2%, mean ± S.D., $P < 0.05$) with no overlap with control values (n=15; 1.3 ± 0.4%). Tc-99m-DTPA is similar structurally and has similar clearance characteristics as Cr-51-EDTA when administered intravenously. Tc-99m-DTPA would also have the potential to localize the diseased bowel area by imaging, and it is far more readily available. Previous reports of the i.v. administration of Tc-99m-DTPA to patients with inflammatory bowel disease have not demonstrated its ability to localize diseased bowel.

In the present study, 4 patients with radiologically documented Crohn's disease were given 100 uCi of Cr-51-EDTA and 5 mCi of Tc-99m-DTPA together orally in 10ml of water, and urine was collected during the following 24 hr period. Sequential imaging of the stomach and the GI tract was done with a LFOV gamma camera at 10 min intervals until the activity cleared the small bowel. The images failed to show any localization of the activity in any disease process and no extraintestinal accumulation site was observed scintigraphically. Mean 24 hr urinary excretion for Tc-99m-DTPA was 4.8 ± 2.6% comparable to that of Cr-51-EDTA in these patients. This study suggests that a comparable oral dose of Tc-99m-DTPA could be substituted for Cr-51-EDTA as a far more readily available agent for documenting small bowel Crohn's disease by quantitative assessment of its urinary excretion.

111-Indium Labelled Autologous Leucocytes in Diagnosis of Inflammatory Bowel Disease. J.H.Wandall,C.-J.Edeling,J.Trap-Jensen,J.O.Lund,O.Bonnevie, H.Haxholdt,H.C.Jensen,P.Matzen,P.S.Myschetsky,A.M.Nielsen, &S.S.Poulsen. Dept.Medicine B, Dept.Clinical Physiology & Radiology, Fredriksberg Hospital and Inst.Anatomy B, University of Copenhagen, Denmark.

111-Indium labelled leucocytes have been used to visualize inflammatory lesions in ulcerative colitis (CU) and in Crohn's disease (CD).The aim of this study was to compare findings by scintigraphy, radiology and endoscopy. Material: Twelwe patients with CU and 15 patients with CD were studied. All patients were non-febrile. Two patients recieved prednisolone 5 mg/daily, 8 sulphasalazine. Methods: Autologous leucocytes were labelled with 111-In-Oxine and given i.v. Scintigrams were obtained 3 and 24 hrs. p.i. Double contrast x-ray studies were done of the colon and small intestine after 2 and 14 days respectively. Colonoscopy with biopsy was done after 4 days. Results: Active lesions were found in 24 of 27 patients. Scintigrams 24 hrs.p.i. did not give any additional information compared with scintigrams 3 hrs.p.i. Intraluminal activity masked the location and extension of lesions after 24 hrs. Excretion in the stool was 2.4-25.8% of administred activity. Compared with scientigraphy a corresponding extension and location was found by colonoscopy. In 4 patients x-ray of the colon was normal but scintigraphy and colonoscopy showed active inflammation. Conclusion: Scintigraphy after injection of 111-In labelled leucocytes is a atraumatic method for visualization of inflammatory lesions in UC and CD. Furthermore, it appears to be more sensitive than conventional x-ray studies.

FRIDAY, JUNE 8, 1984

10:30–12:00 **Room 217A**

CARDIOVASCULAR IX: TOMOGRAPHIC THALLIUM-201 IMAGING

Moderator: Jamshid Maddahi, M.D.
Comoderator: Robert Eisner, Ph.D.

QUANTIFICATION OF THE EXTENT AND SEVERITY OF MYOCARDIAL ISCHEMIA IN SINGLE-VESSEL DISEASE USING STRESS-REDISTRIBUTION THALLIUM-201 SINGLE-PHOTON EMISSION COMPUTERIZED TOMOGRAPHY. F Prigent, J Maddahi, E Garcia, K Van Train, J Friedman, J Bietendorf, HJC Swan, A Waxman, D Berman. Cedars-Sinai Medical Center, Los Angeles, CA

Single-vessel coronary artery (CA) disease (SVD) is not uniformly benign: long-term prognosis is likely to be related to the extent (E) and severity (S) of myocardial ischemia (isch). To assess the ability of stress thallium-201 (Tl) single photon emission computerized tomography (SPECT) to quantify E and S of isch, we studied 15 patients (pts) without myocardial infarction who had SVD (8 LAD, 4 RCA, and 3 LCX). SPECT cuts were analyzed using maximum count circumferential profiles (CPs) which were compared with previously established normal (nl) limits derived from 20 nl pts. E of isch was defined as the % of the CP points falling below nl, S and depth (D) of ischemia respectively expressed the total and the mean % by

which the abnormal points fell below normal limits. Although all pts had SVD, the range of E, S and D of isch was wide (0 to 48% and 0 to 38% and 0 to 20% respectively). CA scores (CS) were derived using a 15-point system accounting for the distribution of the diseased CA, location, and degree of stenosis, and collateral supply. CS varied from 1.2 to 8. E and S significantly correlated with CS (r=.74, p=.001, and r=.78, p=.000, respectively). The 6 pts with a D ≥ .1 had 75% CA stenosis whereas 5 of the 9 pts with D < .1 had only 50-75% stenosis. Thus, 1) pts with SVD have highly differing degrees of isch; 2) E, S and D scores from Tl SPECT correlate favorably with the angiographic extent and severity of disease; 3) SPECT offers potential for quantification of the magnitude of isch and may become a useful, noninvasive prognostic indicator.

NONINVASIVE QUANTITATIVE ASSESSMENT OF PACING INDUCED ISCHEMIA IN CORONARY ARTERY DISEASE PATIENTS USING SPECT IMAGING WITH THALLIUM-201. D.A. Summerville, J.F. Polak, B.L. Holman, B.E. Jaski, and R.W. Nesto. Brigham and Women's Hospital and Harvard Medical School, Boston, MA.

We have investigated the use of a quantification algorithm which measures total myocardial mass using thallium-201 and single photon emission computed tomography (SPECT). Myocardial and lung uptake ratios were determined from the early and redistribution scintigrams of twelve coronary artery disease patients who had received intraventricular thallium-201 during pacing induced ischemia. The Iowa heart phantom placed in an Alderson chest phantom were imaged tomographically for the obtained range in target-to-background ratios. Tomographic acquisitions were made over 180°: 30° RAO to 60° LPO for 64 projections. All reconstructions were made using attenuation compensation. Transverse tomographic slices were formatted into oblique data sets. The slices perpendicular to the left ventricular long axis (typically 16 to 19, .62 cm thick) were processed by a previously described algorithm† which estimates volumes above certain threshold count values in contiguous slices and then sums according to Simpson's rule. Calibration curves for different target-to-background values and different threshold values were obtained. In the phantom, changes in the refillable chambers were accurately quantifiable. When applied to six patient studies, estimates of the change in myocardial mass correlated with the amount of ischemia (elevation in left ventricular EDP, r = .93). We conclude that SPECT can be used to make accurate estimates of myocardial mass using such algorithms if care is taken to adjust for individual variations in the uptake of thallium-201.

† J Nucl Med 1983;24:P19

VALUE OF QUANTITATIVE STRESS THALLIUM-201 EMISSION CT FOR LOCALIZATION OF CORONARY ARTERY DISEASE: COMPARISON WITH QUALITATIVE ANALYSIS. N. Tamaki, Y. Yonekura, S. Kodama, M. Senda, K. Minato, R. Nohara, H. Kambara, C. Kawai, and K. Torizuka. Kyoto University Medical School, Kyoto Japan.

We previously reported the value of segmental analysis of stress thallium emission computed tomography (ECT) for localization of coronary artery disease (CAD). This study was undertaken to evaluate whether quantitative analysis (QNT) may further improve the diagnostic accuracy over the visual qualitative analysis (QLT). The gamma camera was rotated over 180°, collecting 32 views (30 sec each). Stress and 2.5hr delayed ECT images were evaluated in 83 cases who underwent coronary arteriography. The initial uptake and % washout were assessed by circumferential profiles of the three short-axis sections and one middle RAO long-axis section. Those with initial uptake or washout profiles below the mean minus 2SD of the 10 normals in more than 20° contiguous regions were considered abnormal. Among 61 cases with CAD, QNT showed abnormality in 60 cases (98%), while QLT showed in 57 (93%). The specificity was both 91%. The sensitivity for detecting diseased vessels was:

	1VD	2VD	3VD	RCA	LAD	LCX	overall
QNT	24/24	37/38	44/54	37/40	44/49	23/27	105/116(91%)
QLT	22/24	34/38	36/54	35/40	41/49	16/27*	92/116(79%)*

VD:vessel disease; *p<0.05

The specificity of QNT (RCA:86%, LAD:88%, LCX:91%) were not significantly different from those of QLT (86%, 91%, 98%). Besides, QNT detected diseased vessels with mild stenosis (51-75%) more often (86%) than QLT (68%).

In conclusion, both QLT and QNT of stress ECT showed high accuracy for diagnosing CAD. QNT is valuable for evaluating multivessel disease and detecting mild stenosis.

FALSE-POSITIVE PERFUSION DEFECTS AND IMAGE DISTORTIONS OF 180 DEGREE ACQUIRED THALLIUM-201 MYOCARDIAL SPECT IMAGES WITH AND WITHOUT ATTENUATION CORRECTION. R.T.Go, W.J. MacIntyre, T.S. Houser, C. Piez, J.K. O'Donnell, D.Feiglin, C. Napoli. Cleveland Clinic Foundation, Cleveland, Ohio.

Initial preliminary phantom and isolated clinical case studies have shown artifactual false-positive perfusion defects and image distortion with 180° acquired images. The present study was performed to verify if previous findings were reproducible with other imaging systems and reconstruction as well as to determine the effect on short-axis orientation. In addition, the effect of attenuation corrections of the two techniques on normal and abnormally perfused myocardium was evaluated. Normal patients and patients with myocardial ischemia and infarction diagnosed on 360° acquired images were confirmed by coronary angiography and reprocessed for the 180-360° comparison. Each patient was processed twice, first with data from 0° (ANT) to 180° (POS) then with data acquired from 45° (LAO) to 225° (RPO). Reconstructions were displayed and reinterpreted blindly without knowledge of the patient's diagnosis. The present study confirmed that 180° acquired images produce significant false-positive defects and image distortion in patients with normally perfused myocardium. The false defects were accentuated by the attenuation correction program. The 180° acquired data also produced prominent streaking artifacts which were not seen on the 360° acquired images. Although the contrast resolution of the 180° acquired images was better compared to the 360°, the display of ischemic redistribution pattern was more accurate on the 360°. This study reiterates our previous preliminary conclusion that despite the advantages of time and contrast, the reconstruction of 180° acquired data is not sufficiently reliable for 201-myocardial SPECT imaging.

CLINICAL EVALUATION OF THALLIUM-201 SPECT WITH CARDIAC SHORT AXIS DISPLAY. J.K. O'Donnell, R.T. Go, C.K. Keyser, J. Hollman, D.A. Underwood, D.H. Feiglin, W.J. MacIntyre, B. Sufka. Cleveland Clinic Foundation, Cleveland, Ohio.

Application of transaxial emission tomography (SPECT) to Tl-201 myocardial perfusion imaging has reduced the difficulties inherent in planar imaging. However, SPECT reconstruction along the body axis still poses problems in orien tation and interpretation of tangential slices. An alternate technique with SPECT reconstruction orthogonal to the long axis of the heart should allow more accurate comparison of uniform slices. In order to establish the validity of such a technique, we have obtained 433 SPECT stress perfusion studies using cardiac short axis reconstruction and display. 64 images of raw data were acquired over a 360 degree transaxial rotation. A computer reconstruction program then provided a base-to-apex image series orthogonal to the cardiac long axis with simultaneous display of corresponding segments of myocardium at stress and redistribution. Angiographic (AN) correlation was obtained within 6 mos. of SPECT in 140 cases. Our technique showed a sensitivity of .97 and specificity of .88 for this group if AN >70% stenosis is considered to be positive (sensitivity .92 and specificity .86 if AN >50% stenosis was considered). We also found that cardiac short axis SPECT provided very good delineation of the involved area of abnormal myocardium as sequential slices were reviewed. 12 patients had repeat studies within 6 months and confirmed the excellent reproducibility of the technique. We conclude that cardiac short axis SPECT is an accurate technique that allows comparison of exactly corresponding myocardial segments at stress and redistribution. It also more precisely defines the total area of myocardium that is abnormal.

DETERMINATION OF LEFT VENTRICULAR MASS IN MAN USING SINGLE PHOTON EMISSION COMPUTED TOMOGRAPHY. CL Wolfe, DE Jansen, JR Corbett, JT Willerson, K Lipscomb, G Redish, N Filipchuk, G Gabliani, and SE Lewis, University of Texas Health Science Center, Dallas, TX.

The measurement of viable left ventricular (LV) mass may have

important prognostic significance in patients with ischemic heart disease or hypertrophic heart disease. To test the hypothesis that single photon emission computed tomography (SPECT) could accurately determine LV mass in man, we compared SPECT measurements of LV mass to LV mass determined by cineangiography in 12 patients with normal coronary arteries and normal LV function. Repeat SPECT determinations of LV mass were carried out in 5 patients. Each patient was injected with 2 to 2.4 mCi of thallium (Tl)-201 in the resting state. Projection images (64x64) containing a minimum of 80,000 counts were acquired at 6-degree intervals over 180-degrees using a rotating gamma camera. Transverse sections were reconstructed by filtered backprojection. The boundary of LV uptake of Tl-201 in each transverse section was defined using a simple three-dimensional threshold detector. The total number of voxels demonstrating LV Tl-201 uptake was multiplied by the voxel volume and the specific gravity of myocardium (1.05g/cc). Cath determinations of LV mass were made from end diastolic frames of a biplane left ventriculogram using the method of Kennedy, et al. There was good correlation between LV mass determined by SPECT and by cineangiography. Mean cath LV mass was 207.8±45.4g (S.D.). Mean SPECT LV mass was 207.4±43.3 g. Linear regression analysis revealed the following relationship: SPECT LV mass = 0.78 x Cath LV mass +45.8 (r=0.82, root mean square deviation from regression = 25.1). The SPECT values of LV mass varied an average of 10.4±4.6 (S.D.) % in the 5 patients where two determinations were made. We conclude that SPECT of Tl-201 can accurately measure left ventricular mass in man.

10:30-12:00 **Room 216BC**

COMPUTERS AND DATA ANALYSIS IV: GENERAL

Moderator: Robert E. Zimmerman, MSEE
Comoderator: Ronald R. Price, Ph.D.

ESTIMATION OF PROBABILITY OF CORONARY DISEASE BY QUANTITATIVE THALLIUM SCINTIGRAPHY. J.H.C. Reiber, M.L.Simoons, W.Wijns, Thoraxcenter, Erasmus University Rotterdam, Netherlands

Various methods for visual interpretation(VI) and quantitative analysis of early (E) and late (L) postexercise myocardial Tl-201 scintigrams (3 static views) were compared in 60 patients with coronary artery disease (CAD) and in 25 without CAD. Visual reading was done by 4 independent experienced observers. Computer processing of background subtracted E and L images provided E, L and washout (W) circumferential (circ.) profiles from 60 radii. Normal ranges for E, L and W profiles were determined by 10th and 90th percentiles from 15 normal subjects. Three methods for quantitation of profile abnormalities were compared with the aid of ROC-curves: 1) areas between profiles in a given patient and the normal ranges; 2) difference of these areas from E and L profiles and 3) area between washout profile in a given patient and normal washout range.

Area measurements from E scintigrams improved detection of abnormalities (sensitivity (sens.)=88%) in comparison with VI (sens.=75%) at a level of specificity of 64%. Measurement of area differences between E and L scintigrams (sens.=80%) were superior to VI (sens.=65%) at level of specificity of 88%. Computation of segmental Tl-washout did not enhance the detection of CAD, nor the detection of multivessel disease.

Quantitative analysis of the Tl-profiles provides an objective measure for the degree and extent of abnormal Tl-distribution. In each individual patient, area and area difference values can be expressed as probability figures for presence of CAD on basis of likelihood ratio curves, which is useful in diagnostic decision making.

FUNCTIONAL IMAGING OF KINETIC PARAMETERS FROM THE TIME DEPENDENT LINEAR RESPONSE FUNCTION BY DYNAMIC SCINTIGRAPHY. P.Stritzke, J.Knop, R.P. Spielmann, R.Montz, C.Schneider. Department of Nuclear Medicine, University Hospital Hamburg-Eppendorf.

A new method is proposed to determine the locally differing time dependent linear response function h(r,t) of a radioactive tracer injected into a patients blood pool B(t) by mathematical analysis of a dynamic scintigraphic study A(r,t). Transit times, uptake rates and clearance rates of different tracers are calculated from the linear response function at every matrix point by one computer program. The parameters are presented in functional images on a standard computer display. Thus the whole information from a dynamic study can be condensed within a few images. The integral equation A=h+B +c(r)*B (+ means convolution, c(r)*B(t)=nontarget activity) derived from tracer theory is deconvoluted by mathematical methods, which are unsensitive against noise contamination of the input data. The numerical technique is successfully applied in Iodide-123-Hippuran and Tc-99m-DMSA kidney studies, in Tc-99m-MDP and -DPD bone studies, in Tl-201 myocardial studies and in Iodide-123 thyroid studies. Because the regional blood pool- or nontarget activity is calculated and subtracted, the kinetic parameters are considered to be free from nontarget contributions in all dynamic scintigraphic studies. Examples are demonstrated and the usefulness for clinical application is discussed.

A NON-EQUILIBRIUM TECHNIQUE FOR THE MEASUREMENT OF REGIONAL CEREBRAL BLOOD FLOW BY POSITRON TOMOGRAPHY. J.H. Greenberg, S.C. Jones and M. Reivich. University of Pennsylvania School of Medicine, Philadelphia, PA.

Equilibrium imaging, which uses a static image generated by the balance between physical decay, blood flow and delivery rate is in use in a number of laboratories to measure regional cerebral blood flow by positron emission tomography. We have developed a modification of this technique that does not necessitate that a equilibrium condition be present during the scanning period. In addition, for the same dose administered to the subject, more counts are obtained in the image utilizing this non-equilibrium technique (NET) than by the conventional equilibrium technique. The basis of NET is the solution of the conservation of mass equation for O-15 labelled water. Instead of assuming that the arterial concentration of O-15 remains constant after a certain period of time, no assumption is made about its time course. This has two main advantages. Firstly, in some subjects an equilibrium cannot be achieved over the period of the scan due either with the O-15 delivery system or with the subject. Secondly, the removal of the constraint of a constant arterial concentration curve allows tomographic scanning to begin at the time of the start of the 15-O CO_2 inhalation (or 15-O H_2O infusion). This leads to 60-70% more counts for the same inhalation time and in addition produces a more linear brain concentration:flow relationship. Thus, the signal to noise ratio is improved approximately 40% over the equilibrium technique for the equivalent radiation dose to the subject.

DETERMINATION OF EFFICACY OF NUCLEAR MEDICINE PROCEDURES. E.L.Saenger, C.R.Buncher, B. Specker, R.A. McDevitt. Committee on Efficacy, SNM and University of Cincinnati Medical Center, Cincinnati, Ohio

Nuclear medicine, a high technology field, is evaluated as to its usefulness. This paper describes the SNM study of 2023 patients comparing two methods evaluating efficacy for lung scanning (LS). Only the referring physicians determined the probabilities of the most important (MI) and most likely (ML) diagnoses and management before and after lung scanning.

A logistic regression model was developed for probability of a signout diagnosis of PE. Equal patient groups tested the validity of the regression equations for the probability of PE as MI or ML. The models developed on Group I (G-I) and used on Group II (G-II) gave similar results. This shows that LS classifies PE and NOT PE categories (bar graphs 4a&b,5a&b) where PE was considered both MI and ML.

Entropy minimax pattern detection (EMPD) attempts prediction of signout diagnosis and management from prior

patient attributes. In 2023 cases, attributes alone could not eliminate the use of LS for all patients.

Comparing the two methods (Table XI), the predictive values, sensitivity and specificity of each method are similar. EMPD predicts on a relatively small percent (40% before LS, 71% post LS) while the logistic equation predicts on 100% of the cases. An advantage of EMPD is that it does not require estimates of prior probability. However, LR, uses this estimate, thus incorporating intuitive knowledge not evaluated by EMPD.

These methods are unique in showing that LS can direct the referring physician toward or away from anticoagulant therapy based on findings of the lung scan.

FACTORS AFFECTING ESTIMATION OF THE RATE CONSTANTS OF THE FLUORODEOXYGLUCOSE (FDG) MODEL FROM POSITRON EMISSION TOMOGRAPHY (PET) DATA. R.E. Carson, J.C. Mazziotta, S.-C. Huang. National Institutes of Health, Bethesda, MD; UCLA School of Medicine, Los Angeles, CA.

A study has been performed of the factors affecting the statistical estimation of the rate constants of the FDG model from sequential PET scan data. The conditions under study are the effect of total data collection time and scan sampling rate on the accuracy of the estimates, the influence of vascular space in the tissue region-of-interest on the rate constants, the mathematical form of the fitting equation, the weighting of samples according to the total counts per scan (observation noise), and the intercorrelation of the parameter estimates. Plasma radioactivity samples and tomographic time-activity curves collected from four normal volunteers on the NeuroECAT tomograph were used to assess these factors. For typical input functions and average rate constants, near optimal estimation of the rate constants requires a total data collection period of at least 40, 90, 115, and 150 minutes for k_1-k_4. Fits of 48 tissue curves to the FDG model were compared to fits which included a fifth parameter representing vascular volume. In one third of the cases, the fifth parameter produced a significant improvement in the fit ($p<.05$), with vascular space estimated at 3 to 7% for gray matter and 2 to 3% for white matter regions. The original rate constants changed: k_1 from .082 to .057, k_2 from .155 to .063, k_3 from .076 to .052, and no change in k_4. This study concludes that the accuracy and precision of FDG rate constant estimates are critically affected by the data collection protocol and the parameter estimation procedure.

VALIDATION OF A KINETIC MODEL FOR RECEPTOR-MEDIATED UPTAKE OF Tc-99m-GALACTOSYL-NEOGLYCOALBUMIN (Tc-NGA). D.R. Vera, K.A. Krohn, E.S. Woodle, P.O. Scheibe, R.C. Stadalnik. University of California, Davis Medical Ctr., Sacramento, CA

Tc-NGA is a receptor-binding radiopharmaceutical which localizes specifically to the liver. The rate of uptake depends upon: 1) Tc-NGA-receptor affinity, k_b, 2) molar dose, $L_e(0)$, and 3) hepatic blood flow, Q. We have proposed a kinetic model which describes hepatic uptake in terms of measurable physiochemical quantities: Q, k_b, R, V_e, V_h (systemic and liver blood volumes), and V_r (liver plasma volume).

Model States (mole)	
L_e	NGA in systemic blood
L_h	NGA in hepatic blood
R	receptor in liver
C	R-NGA complex in liver
P	metabolic product

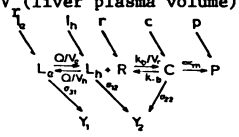

Observer Y_1 and Y_2, which hold the time-activity data, are coupled to the states via σs. Initial conditions l_e, l_h, r, c, and p sum to $L_e(0)$, and represent the values of each state at the start of the simulation (2 mins).

Computer simulations were compared to kinetic data (ROIs: precordium and liver, 420 data pts) resulting from injection into pigs (n=12) of Tc-NGAs of differing k_b (0.6, 1.2, 1.8 x 10^5 $M^{-1}sec^{-1}$). Each pig was studied twice using different molar doses (0.5 - 10. x 10^{-8}mole). Measurements of V_e (Tc-RBCs) and Q (indocyanine green extraction) were obtained during each study. Weights of excised livers were used to calculate V_h and r. With exception of the low-dose, low-affinity studies, all data was fit to within a reduced chi-square of 3 by adjustment of l_e, l_h, c, α_m and the σs.

We conclude that this model is a valid description of a receptor-binding process, however competition by endogenous ligand may prevent its use at low molar doses of low-k_b NGA.

10:30-12:00 **Room 214BC**

RADIOPHARMACEUTICAL CHEMISTRY V: SHORT-LIVED

Moderator: Joanna S. Fowler, Ph.D.
Comoderator: Robert F. Dannals, Ph.D.

A COMPARISON OF [^{18}F]SPIROPERIDOL, [^{18}F]BENPERIDOL AND [^{18}F]HALOPERIDOL KINETICS IN BABOON BRAIN. C.D. Arnett, C.-Y. Shiue, A.P. Wolf, J.S. Fowler and J. Logan. Brookhaven National Laboratory, Upton, NY

Neuroleptic receptor ligands, spiroperidol, benperidol and haloperidol were labeled with fluorine-18 by a nucleophilic aromatic substitution reaction of p-nitrobenzonitrile with $^{18}F^-$ to produce p-[^{18}F]fluorobenzonitrile which was converted to p-[^{18}F]fluoro-γ-chlorobutyrophenone and then alkylated with the appropriate amine to give [^{18}F]spiroperidol ([^{18}F]SP), [^{18}F]benperidol ([^{18}F]BEN), or [^{18}F]haloperidol ([^{18}F]HAL). Specific activity ranged from 3 to 6 Ci/μmol. Anesthetized baboons were injected with 6-17 mCi of [^{18}F]-labeled tracer. Kinetic curves (striatum and cerebellum) were obtained from PETT scans up to 4 hr with each drug; [^{18}F]SP was studied to 8 hr. [^{18}F]SP and [^{18}F]BEN exhibited similar kinetics in striatum, with radioactivity concentrations plateauing by 30 min after injection and remaining constant for the remainder of the study. These two compounds cleared rapidly from the cerebellum. [^{18}F]HAL showed a much different kinetic pattern in the striatum. Although it reached a higher striatal concentration (~ 0.07% per ml vs. ~ 0.02% per ml for [^{18}F]SP or [^{18}F]BEN), a peak occurred at 30 min after injection, followed by a decline almost as rapid as that in the cerebellum. Plasma analyses for [^{18}F]SP showed > 90% unchanged drug up to 5 min and ~ 30% metabolites at 20 min after injection. Pretreatment with (+)-butaclamol abolished the selective distribution of [^{18}F]SP to the striatum in the four animals studied. Both [^{18}F]SP and [^{18}F]BEN may be suitable for PETT studies of neuroleptic receptors, but the in vivo kinetics of these compounds are markedly different from their in vitro receptor binding kinetics.

RADIOSYNTHESIS OF AN OPIATE RECEPTOR-BINDING RADIOTRACER FOR POSITRON EMISSION TOMOGRAPHY: [C-11 METHYL]-METHYL-4-[N-(1-OXOPROPYL)-N-PHENYLAMINO]-4-PIPERIDINE CARBOXYLATE (C-11 4-CARBOMETHOXYFENTANYL) R.F. Dannals, H.T. Ravert, J.J. Frost, A.A. Wilson, H.D. Burns, and H.N. Wagner, Jr. The Johns Hopkins Medical Institutions, Baltimore, MD

The development of high affinity, high specific activity tritium-labeled neurotransmitter receptor ligands has made it possible to determine the spatial distribution and relative regional concentration of several neuroreceptors by means of in vivo receptor labeling techniques in animals. This development made possible the biochemical identification of opiate receptors by autoradiographic visualization in experimental animals. The quantitation and localization of opiate receptors in man using non-invasive methods, such as positron emission tomography, could provide a means of obtaining information about a variety of receptor-linked neuropsychiatric diseases as well as normal brain mechanisms regulating pain and emotions. As part of a continuing program to identify and radiolabel high affinity, highly specific ligands for the opiate receptor, we have selected two derivatives of fentanyl, a well-known analgesic, as candidates for radiolabeling: R-31,833 (4-carbomethoxy-fentanyl) and R-34,995 (lofentanil).

Carbon-11 labeled R-31,833 was synthesized by the methylation of the appropriate carboxylate with C-11 methyl iodide in dimethylformamide at room temperature and purified by high performance liquid chromatography. The average synthesis time from end-of-bombardment (E.O.B.) was 30 minutes. The average specific activity was determined by ultraviolet spectroscopy to be 890 mCi/μmole end-of-synthesis (approx. 2500 mCi/μmole E.O.B.).

SYNTHESIS OF 3-(C-11-METHYL)-NIFEDIPINE, A POTENT Ca^{++} CHANNEL ANTAGONIST, FOR POSITRON EMISSION TOMOGRAPHY. A.A. Wilson, H.D. Burns, R.F. Dannals, H.T. Ravert, S.E. Zemyan, S.H. Snyder, and H.N. Wagner, Jr. The Johns Hopkins Medical Institutions, Baltimore, MD.

Nifedipine is a potent calcium channel blocker with therapeutic utility in cardiac disease. We report here the synthesis of C-11 nifedipine labeled at the methyl ester position.

Model reactions showed that 5-methoxycarbonyl-2,6-dimethyl-4-(o-nitrophenyl)-1,4-dihydropyridine-3-carboxylic acid (1) could be methylated with CH_3I in DMF containing tetrabutylammonium hydroxide (TBAH) to produce nifedipine. Yields were essentially quantitative after 7 mins at 25°C. C-11 CO_2, produced by a biomedical cyclotron, was chemically transformed into C-11 CH_3I and reacted with (1) in DMF containing TBAH. C-11 labeled nifedipine was isolated by preparative HPLC and the chemical and radiochemical purities were determined by analytical HPLC. Two hundred mCi of C-11 nifedipine (99% radiochemically pure) with specific activity (at end-of-synthesis) of up to 1400 mCi/μmole could be obtained in 25 mins from end-of-bombardment. Radiochemical yields (from C-11 CH_3I) were 70-80%.

Large quantities of C-11 labeled nifedipine, of high specific activity, can routinely be prepared from C-11 CO_2. We are currently conducting biodistribution studies of this material to evaluate its usefulness as an imaging/diagnostic tool.

FLUORINATION OF AROMATIC COMPOUNDS BY CLEAVAGE OF ARYL-TIN BONDS WITH F-18 F_2 AND CH_3COOF. M.J. Adam, B.F. Abeysekera, T.J. Ruth, S.Jivan and B.D. Pate. TRIUMF and the University of British Columbia, Vancouver, B.C.

Direct fluorination of aromatic nuclei is difficult since the reaction is usually accompanied by unselective, partial, or total replacement of hydrogen. By attaching the tri-n-butyltin moiety to one position of the ring one can achieve an enhanced reactivity and site selectivity toward electrophilic fluorination. The intent of this study was to demonstrate the utility of the fluorodestannylation reaction for fluorine labelling of aromatic compounds and to compare F_2 and acetyl hypofluorite as the fluorinating agents. Thus, eight stannylated aromatic compounds (1-8) were synthesized

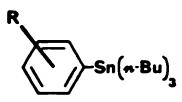

1, R=3,4-OMe 5, R=o-Me
2, R=p-OMe 6, R=H
3, R=p-Me 7, R=p-Cl
4, R=m-Me 8, R=p-F

via lithium halogen exchange of the bromo precursor and subsequent transmetallation using tri-n-butyltin chloride. The stannylated substrates were treated with F-18 F_2 at -78°C and CH_3COOF at room temperature. Both reagents gave good yields of labelled aryl fluorides. Overall, acetyl hypofluorite gave more consistent yields (~70%), while F_2 gave more variable yields (54-95%).

This method is currently being extended to label more complex systems such as L-Dopa with F-18 for brain studies with positron emission tomography. We have successfully stannylated Dopa on the ring and fluorination studies of this substrate are underway.

ENZYMATIC SYNTHESIS OF (N-13) OR (C-11) CARBAMYL PHOSPHATE AND THEIR USE FOR LABELING METABOLITES OF THE UREA CYCLE AND THE PYRIMIDINE NUCLEOTIDE PATHWAY. A.S. Gelbard, D.S. Kaseman, K.C. Rosenspire, R.E. Reiman, A.J.L. Cooper and A. Meister. Memorial Sloan-Kettering Cancer Center and Cornell University Medical College, New York, NY.

Carbamyl phosphate (CP) serves as a precursor for the synthesis of metabolites of the urea cycle and the de novo pyrimidine nucleotide pathway. CP is enzymatically formed from ATP, NH_4^+ and HCO_3^- by carbamyl phosphate synthetase (CPS). By utilizing CPS purified from E. coli and by adding (N-13) ammonia or (C-11) carbon dioxide to the reaction mixture we have incorporated either label into CP, as demonstrated by cation exchange HPLC analyses. Co-immobilization of CPS with either ornithine transcarbamylase or aspartate transcarbamylase onto CNBr-activated Sepharose resulted in the synthesis of L-(ω-N-13) citrulline or L-(carbamyl-N-13) carbamyl aspartate, respectively. Carbamyl L-(N-13) aspartate has also been synthesized from L-(N-13) aspartate and CP using immobilized aspartate transcarbamylase. In this case labeled aspartate was prepared by passage of (N-13) ammonia through columns containing immobilized glutamate dehydrogenase and glutamate-oxaloacetate transaminase.

Tissue distribution studies were carried out in melanoma-bearing mice. Five minutes after retro-orbital venous injection of (N-13) CP, tumor uptake of label was observed. Concentration of activity from CP was 2-3 times higher in heart but 30% lower in liver and 80% lower in pancreas when compared with (N-13) leucine and methionine.

This study illustrates the feasibility of labeling metabolites in different molecular positions with N-13 or C-11 by use of immobilized multi-enzyme systems.

METABOLIC FATE OF THE CARBOXYL-CARBON OF VALINE. K.A. Lathrop, R.D. Bartlett, P.F. Faulhaber and P.V. Harper. The University of Chicago, Chicago, IL.

Although several C-11-carboxyl-labeled amino acids show promise for clinical use, few detailed biokinetic studies have been reported. Such information is necessary for the calculation of comprehensive radiation absorbed doses and may reveal additional clinical uses. We have collected data in mice at intervals between 1 and 90 m after i.v. injection of D,L-, L-, or D-valine for 22 whole organs or tissue samples and for CO2 and urinary excretion. The enantiomers were cleanly separated by HPLC, but studies with the D,L- mixture were also done as additional assurance of purity for the separation (i.e., (D+L)/2=D,L). Elimination of C-11 from L-valine is restricted to the ~25% of injected activity (IA) observed as exhaled CO2, the production of which appears completed in ~15 m, the exhalation in ~100 m. The remaining 75% IA is available for incorporation directly into proteins or into coenzyme-A after deamination to 2-oxoisovalerate. The ~25% IA from D-valine that appears to be retained in the body probably is not converted to L-valine since virtually no CO2 is recovered. The pancreatic content of ~8% of retained activity (RA) for both L- and D-valine at 90 m suggests similar localization mechanisms for the activity remaining in the body after excretion is ended. A similar correspondence of RA is seen in most other organs, the notable exceptions being the ~2 to 3 times higher %RA in blood and muscle for D-valine and in small intestine for L-valine. Studies such as this offer the possibility for quantitation of isolated metabolic processes, in this case production of CO2 from 2-oxoisovalerate formed by deamination, and for separating metabolized from non-metabolized localization of C-11 when the D-amino acid can be shown to remain undegraded.

10:30-12:00 **Room 212B**

HEMATOLOGY II: PLATELETS

Moderator: David C. Price, M.D.
Comoderator: Sally J. DeNardo, M.D.

EVALUATION OF MATHEMATICAL MODELS TO ASSESS PLATELET KINETICS. M.G.Lötter, A. du P.Heyns, E.Snyman, P.N.Badenhorst and P.C. Minnaar. UOFS, Bloemfontein, South Africa.

Various mathematical methods (MM) have been proposed for analysis of platelet survival curves (SC) and the estimation of mean platelet survival time (PT). We compared 8 different MM for estimation PT, and a variance shape factor (S) for assessment of the shape of the survival curve, in various clinical situations. SC in 15 normal subjects and 39 patients were analized with the following MM: Linear (L), exponential (E), Multiple hit (H), Dornhorst (D), Meuleman (M), alpha order (A) and polynomial (P). The SC was fitted to the MM and PT was calculated by the ratio of the y-intercept and initial slope. In the case of the D and M models, the potential senescent survival time was firstly assumed to be 10d and secondly estimated during the fitting procedure. S was formulated on the basis of a comparison of the "goodness

of fit" of the other MM with the L and E models. All calculations were performed using a computer program developed for the MDS A² imaging system. The MM were assessed by evaluating "goodness of fit" of the models to the data by calculating the standard deviation (SD) of SC data points around the regression curve for each model. The value of SD for the L and E models were significantly larger than for the other MM indicating that these models are not suitable for calculation of PT. There was not a significant difference between the values of SD, PT and S for the MM excluding the L and E models. Poor correlation between S and number of "hits" (H model) was obtained (r=0.55). Good correlation between S and PT (r=0.87) as well as between S and alpha (r=0.92) (A model) was obtained. The value of S is therefore a good indicator of PS shape. We conclude that all the MM except the L and E models are equally for estimation of PT in a wide spectrum of clinical situations.

QUANTITATIVE KINETICS OF In-111 AUTOLOGOUS (In-AP) AND HOMOLOGOUS (Cr-HP) PLATELETS IN IMMUNE THROMBOCYTOPENIC PURPURA (ITP). M.G.Lötter, A.du P.Heyns, P.N.BAdenhorst and P.C.Minnaar. UOFS, Bloemfontein, South Africa.

Contrary to the accepted view, we have found that platelet turnover is not always increased in ITP if the mean platelet survival time (PS) is measured with In-AP. We investigated the possible cause of the discrepancy by comparing kinetics of In-AP with those of Cr-HP in 10 patients with ITP. PS was estimated with the multiple hit model. The equilibrium and final in vivo distribution of In-AP was quantitated with the geometrical mean method. The patients could be divided into either those with splenic or diffuse RES platelet destruction:

Pattern		Equilibrium In-AP activity(%)		Final In-AP activity(%)	
		Spleen	Liver	Spleen	Liver
Splenic	5	32.8±9.0	15.8±6.7	50.7±13.6	19.4±7.1
RES	5	21.4±8.6	42.6±4.4	22.1± 9.1	42.5±3.6
Normal	12	31.1±6.1	9.6±1.2	35.6± 9.7	28.7±8.3

PS and turnover of In-AP and Cr-HP was as follows:

	In-AP		Cr-HP	
C	Lifespan (h)	Turnover (pl/µl/h)	Lifespan (h)	Turnover (pl/µl/h)
Splenic	46.5±50.4	3230±1961	18.2±10.6	6810±3497
RES	19.5±15.9	568±339	15.4±163	1248±1223

It is concluded that in ITP platelet survival of In-AP is significantly ($p<.05$) longer than that of Cr-HP. Platelet turnover measured with In-AP is only normal in patients with mainly splenic platelet sequestration. Results with Cr-HP give a false impression of PS. It seems that in ITP those patients with severe disease also have a platelet production defect.

KINETICS AND BIODISTRIBUTION OF IN-111 PLATELETS IN PATIENTS WITH BONE MARROW TRANSPLANTS, REFRACTORY TO PLATELET TRANSFUSIONS. C. Civelek, H. Braine, U. Scheffel, H. Drew, A. Koester, N. LaFrance, W. Kasecamp, H. Wagner, Jr. The Johns Hopkins Medical Institutions, Baltimore, MD.

The kinetics and biodistribution of HLA identical In-111 labeled platelets was studied in 10 leukemic patients with bone marrow transplants refractory to HLA matched platelet transfusions. Platelet survival time was short ($\bar{x} \pm SEM$ = 1.64 ± 0.83 days). The mean recovery (extrapolated to zero time) was 29.9%, ranging from 14.2 to 63.0%.

The deposition of the In-111 platelets in the liver and spleen was quantified by the geometric mean method using anterior and posterior imaging. In 3 patients liver uptake was significantly increased. The highest hepatic accumulation of In-111 occurred 2 hrs after injection ($\bar{x}$= 76 ± 6% dose (SEM); at 48 hrs 62% of the dose remained in the liver. In 7 patients the spleen was the organ with the highest labeled platelet deposition. The splenic uptake of In-111 platelets in this group correlated with the spleen size (r=+0.95). At 30 min after injection 75±6% of the dose was found in the spleen. Splenic activity decreased to 62% after 48 hrs. At the same time, In-111 liver accumulation increased from 14 to 31%. This finding suggests that In-111 may be released from the spleen and subsequently sequestered by the liver. Two patients with high splenic uptake underwent splenectomy after the In-111 platelet study. Both benefited from splenectomy in terms of platelet survival after transfusion.

Our results suggest that, in some patients with bone marrow transplants refractory to platelet transfusion, the spleen is the primary site of platelet sequestration, while in others it is primarily the liver.

EVALUATION OF I-123 AND In-111 LABELED ANTI-PLATELET MONOCLONAL ANTIBODY FOR THE SCINTIGRAPHIC LOCALIZATION OF IN VIVO THROMBI. S.C. Srivastava, G.E. Meinken,*Z.H. Oster, P. Som, *B. Coller, *H.L. Atkins, *L.E. Scudder, L.F. Mausner, K. Yamamoto, and A.B. Brill, Brookhaven National Laboratory, Upton, NY and *State University of New York, Stony Brook, NY.

Development of a method to selectively label platelets in whole blood in vitro or in vivo is a highly desirable goal. We have investigated the labeling with I-123, I-131, and In-111 of an IgG_1 monoclonal antibody, 7E3 (MAb) that specifically inhibits the interaction of dog platelets with fibrinogen-coated beads and blocks ADP-induced aggregation of dog platelets. The MAb, typically 100 µg, was radioiodinated using the chloramine T method. Following a G-25 or P-6 column purification, labeling yields of ~70% were achieved (2 I/MAb). The MAb-DTPA conjugate was labeled with In-111 in >80% yields with a specific activity of 10-30 µCi/µg (~0.1 In/MAb). Retention of inhibiting activity in the fibrinogen-coated bead assay was excellent for both I-123 and In-111 labeled 7E3. In dogs, the blood pool activity persisted for up to 24 hr and some urinary excretion (In-111) and deiodination (I-123) were observed in vivo. When In-111-MAb was incubated with whole blood (0.13 µg/ml) and the mixture then clotted with thrombin (1u/ml), 68% of the radioactivity remained with the clot despite repeated washing. Preliminary in vivo data in dogs suggest that the label becomes localized at the site of vascular injury and/or thrombus formation. We conclude that radiolabeled monoclonal anti-platelet antibodies may show promise for imaging vascular lesions and thrombi.

PLATELET LABELING IN PLASMA MADE SIMPLE AND EFFICIENT: PREPARATION AND EVALUATION. M. L. Thakur, S. McKenney, C. H. Park, M. S. Philp*, T. Bruggman*, and G. Werre*. Thomas Jefferson University, Philadelphia PA., and Mediphysics*, California.

Over the past few years the use of In-111 platelets (In-111-P) has continued to grow rapidly. The lack of efficient labeling in plasma have made the preparation procedures complex resulting into almost indivisualized methods which have used a variety of salt balance media, anticoagulants, and centrifugal forces, and thereby made the comparison of results from different laboratories impossible. We have developed a kit method for preparing In-111-P in plasma that restricts these parameters, uses 2 ug of dry Mercaptopyridine-N-oxide (Merc) or its Na-salt and a weak chelate of In-111 either in solution at pH 6-6.5 or in a dry form. Eighty to 95% labeling efficiency is achieved in 20 minutes incubation at an ambient temperature. Seventy percent radioactivity is incorporated within two minutes, 90% of which is bound to cytoplasmic components. The aggregability of In-111-P remains practically unchanged. In a canine model, In-111-P thus prepared, had 65% recovery and 7.5 days survival.

Two - 50 ug of oxine or tropolone employed under identical conditions produced only 4%-28% and 7%-10% labeling efficiency. Similarly, with 2 ug Merc, labeling efficiency using Ga-67, Tc-99m, Tl-201, and I-131 was only 7.5%, 6.8%, 13.8%, and 5.8% respectively.

This new approach provides investigators a simple, efficient and uniform method for preparing viable In-111-P in plasma.

IN VIVO CROSSMATCHING WITH TC-99m-RBC's AND IN-111-OXINE-RBC's. C.S. Marcus, B.A. Myhre, M.C. Angulo, R.D. Salk, and C.E. Essex. Harbor-U.C.L.A. Med. Cntr., Torrance, Calif.

In vitro crossmatching techniques are often inadequate for patients who have received multiple prior transfusions. These patients usually have multiple antibodies to minor blood groups, not all of which are necessarily important in vivo. It becomes increasingly difficult to

obtain appropriate units for transfusion, and often units are used with hopes that a minor group antibody will not be significantly active in vivo. If a transfusion reaction occurs, the unit is stopped. We have developed and successfully tested a method whereby 1.5 to 3cc of potential donor RBC's are labeled with 25-50 μCi of Tc-99m using the BNL kits. After injection, samples are drawn at 10, 20, 60, and 120 minutes and the RBC survival is measured. If it is desirable to test 2 units simultaneously, we use 400 μCi Tc-99m to label an RBC aliquot of one unit and 25 μCi In-111-oxine to label the other; both labeled aliquots are injected together. The method is simple and reliable. In addition to assessing compatibility, we may also estimate the % viability of transfused, compatible RBC's by starting with 400 μCi of Tc-99m and multiplying % survival at 24 hours by 1.2. For 24 hr. survival measurements of In-111-oxine-RBC's, 25 μCi is adequate and no multiplication factor is necessary. We have performed 13 in vivo crossmatches, 4 of which were double, in 6 patients. One documented mild transfusion reaction occurred. There were no false positive or false negative results.

10:30-12:00 **Room 212A**

GASTROENTEROLOGY IV: HEPATIC STUDIES

Moderator: Kenneth A. McKusick, M.D.
Comoderator: Zachary D. Grossman, M.D.

DIAGNOSTIC YIELD OF BLOOD FLOW AND BLOOD POOL STUDIES OF THE LIVER. M. Azar, H.D. Royal, J.A. Parker, G.M. Kolodny. Departments of Radiology, Beth Israel Hospital and Harvard Medical School, Boston, MA.

The accuracy of Tc-99m RBC studies of the liver to diagnose cavernous hemangiomas has been previously reported. We have reviewed 82 of these studies performed in the last four years to determine the prevalence of this benign lesion when it is suspected. Studies were performed in patients with focal solid abnormalities of the liver if the patient had no known primary or if there were no definitive clinical or laboratory findings to support the diagnosis of metastatic disease.

Blood flow, immediate blood pool and one hour delayed blood pool images were obtained in all patients. The combination of decreased or normal blood flow and markedly increased blood pool is pathognomonic for patients having cavernous hemangiomas. Seventeen percent (14/82) of patients were found to have cavernous hemangiomas of the liver. The remaining patients had metastatic disease (38), abscess (6), hepatomas (6), and miscellaneous diagnosis (11). All patients diagnosed as having cavernous hemangioma have been followed for at least one year. Seven of the remaining patients were lost to medical follow-up. In our series no false positive or false negative results have been obtained; however, false negative cases are anticipated for small or thrombosed hemangiomas.

RBC liver studies should be encouraged since 1) the diagnostic yield is high; 2) it is the diagnostic procedure of choice; 3) biopsy of these lesions can be catastrophic; 4) therapy and prognosis is greatly altered if the liver lesions are proven to be benign.

CLINICAL EVALUATION OF ANGIOTENSIN II PERFUSED Tc-99m RBC IMAGING ON HEPATOMA AFTER TRANSCATHETER ARTERIAL EMBOLIZATION THERAPY. M.Kudo,M.Hirasa,Y.Ibuki,H.Takakuwa,K. Fujimi,S.Ueda,S.Tomita,H.Komori,A.Todo,Y.Kitaura,T.Higa and K.Ikekubo. Kobe General Hospital,Kobe,Japan and K.Torizuka. Kyoto University, School of Medicine, Kyoto, Japan.

Transcatheter arterial embolization therapy(TAE) has been the main treatment for hepatoma recently in Japan because it is as effective as surgical therapy. But only one therapy of TAE is not sufficient because it will soon get a recanalization or collateral blood flow. So it is important to repeat TAE when the tumor recovers the high vascularity. However, it is very difficult to know exactly when it does. On the other hand, Angiotensin II (AT-II) is known to decrease the blood flow in normal liver tissue and increase the blood flow in hepatoma relatively much by circulatory autoregulation. This investigation was undertaken to evaluate if AT-II perfused Tc-99m RBC imaging is useful as a monitering procedure of hepatoma after TAE.

Ten AT-II perfused Tc-99m RBC imagings were obtained out of 7 patients with hepatoma after TAE therapy. The efficacy of Tc-99m RBC imaging in estimating the vascularity of hepatoma was evaluated by comparison with a hepatic angiogram which was performed a few days later.

The blood flow images of tumors on Tc-99m RBC imaging were undoubtedly enhanced with AT-II in comparison with conventional Tc-99m RBC imaging. In 9 out of 10 images, of which 6 were hypervascular and 4 were hypovascular with a hepatic angiogram, the vascularity was correctly estimated with Tc-99m RBC imaging(90%).

In conclusion, enhanced Tc-99m RBC imaging with AT-II is very useful to judge the recurrence of hepatoma after TAE non-invasively and easily, and then we may definitely decide when to repeat TAE therapy.

USE OF Tc-99m-GALACTOSYL-NEOGLYCOALBUMIN (TC-NGA) TO DETERMINE HEPATIC BLOOD FLOW. R.C. Stadalnik, D.R. Vera, E.S. Woodle, D.P. Hutak, R.E. Ward, K.A. Krohn, University of California, Davis Medical Center, Sacramento, California

Tc-NGA is a new liver radiopharmaceutical which binds to a hepatocyte-specific membrane receptor. Three characteristics of Tc-NGA can be exploited in the measurement of hepatic blood flow (HBF): 1) ability to alter the affinity of Tc-NGA for its receptor by changing the galactose: albumin ratio; 2) ability to achieve a high specific activity with Tc-99m labeling; and 3) ability to administer a high molar dose of Tc-NGA without physiologic side effects. In addition, kinetic modeling of Tc-NGA dynamic data can provide estimates of hepatic receptor concentration.

In experimental studies in young pigs, HBF was determined using two techniques: 1) kinetic modeling of dynamic data using moderate affinity, low specific activity Tc-NGA (Group A, n=12); and 2) clearance (CL) technique using high affinity, high specific activity Tc-NGA (Group B, n=4). In both groups, HBF was determined simultaneously by continuous infusion of indocyanine green (CI-ICG) with hepatic vein sampling.

Regression analysis of HBF measurements obtained with the Tc-NGA kinetic modeling technique and the CI-ICG technique (Group A) revealed good correlation between the two techniques (r=0.802, p=0.02). Similarly, HBF determination by the clearance technique (Group B) provided highly accurate measurements when compared to the CI-ICG technique. Hepatic blood flow measurements by the clearance technique (CL-NGA) fell within one standard deviation of the error associated with each CI-ICG HBF measurement (all CI-ICG standard deviations were less than 10%).

Tc-99m-GALACTOSYL-NEOGLYCOALBUMIN (TC-NGA) LIVER IMAGING: POTENTIAL APPLICATION IN LIVER TRANSPLANTATION. E.S. Woodle, D.R. Vera, R.E. Ward, D.P. Hutak, and R.C. Stadalnik, University of California, Davis Medical Center, Sacramento, CA.

Tc-NGA is a hepatocyte receptor-specific imaging agent whose uptake by the liver has been shown to be dependent upon blood flow and receptor concentration. The combination of anatomic and physiologic information obtained with Tc-NGA may provide a new tool for studying hepatic function in liver transplant recipients.

To evaluate the potential role of Tc-NGA in liver transplant recipients, studies were performed in four groups of pigs: controls (n=18); common bile duct (CBD) ligation (n=8); orthotopic liver transplant (n=9); and acute hepatic artery ligation (n=1). Serial studies performed in two animals with CBD ligation demonstrated normal imaging anatomy with minor changes in the hepatic time-activity curves when compared to control studies. Studies in liver-transplanted animals showed significant changes in the hepatic time-activity curves during acute rejection and in preservation-related ischemic injury. Tc-NGA also demonstrated focal areas of hepatic infarction in a hepatic allograft within 24 hours of transplantation. The hepatic artery ligation study showed massive changes in the hepatic time-activity curve within two hours after ligation, with a dif-

fuse decrease in hepatic activity.

These results indicate that: (1) extrahepatic biliary tract obstruction causes only minor changes in Tc-NGA uptake; (2) Tc-NGA uptake by the liver is very sensitive to acute hepatic ischemia; (3) Tc-NGA may indicate the presence of preservation damage in the early postoperative period; and (4) Tc-NGA hepatic time-activity curves demonstrate significant changes during acute rejection.

A NEW NON-INVASIVE METHOD OF EVALUATING PORTAL-SYSTEMIC SHUNTING BY COMPUTER QUANTITATION OF HEPATIC AND PULMONARY ACTIVITY AFTER RECTAL DELIVERY OF Xe-133. L.S. Witanowski, A. Samin, C. Ritter-Hrncirik, F.D. Thomas, J.G. McAfee, K. Koizumi, L. Tupper and Z. Grossman. The Upstate Medical Center, SUNY, Syracuse, NY.

While portal blood flow and portal-systemic shunting have been previously studied with Xe-133, lack of computer quantitation and invasive isotope delivery into the portal circulation have severely limited the procedure's value. However, our method of rectal delivery of Xe-133 solubilized in water is non-invasive; furthermore, computer quantitation of hepatic and pulmonary activity, and hepatic/pulmonary activity ratios, correlate with portal blood flow and portal-systemic shunting.

3-4 mCi of Xe-133 in 10-15 cc of H_2O was delivered per rectum through a Foley catheter into each of 4 anesthetized normal mongrel dogs. A dynamic study of hepatic and pulmonary activity was acquired over 17 mins. at 1 frame per 10 seconds. Time vs. activity curves (normalized for organ area) were generated over the liver and lungs. In normal dogs, the area under hepatic Xe-133 time/activity curves was approximately twice that of lung curves.

Shunts were created surgically between the portal vein and the inferior vena cava in 4 anesthetized dogs. Shunting was controlled by a variable constrictor on the portal vein and shunt flow quantitated by flow meter. The ratios of the integrated areas under liver and lung activity curves were inversely proportional to the degree of portal-systemic shunting, as expected.

This non-invasive technique appears promising for study of portal-systemic shunting in patients with portal hypertension.

THE HEPATIC-ARTERIAL/PORTAL-VENOUS SCINTIANGIOGRAM IN ALCOHOLIC HEPATITIS. C. Stewart, I. Sakimura, M.E. Siegel, H. Harley, and K. Lee. Rancho Los Amigos Hospital - USC School of Medicine, Downey, Ca.

This study was designed to identify abnormalities in the hepatic-arterial/portal-venous scintiangiogram (SA) in alcoholic hepatitis (AH).

SA's were performed in 35 patients with acute alcoholic hepatitis (AAH), 8; acute alcoholic hepatitis superimposed on cirrhosis (A/C), 14; and cirrhosis (C), 13. Posterior flows were done with a bolus of 10 mCi Tc-99m sulfur colloid with computer time-activity curves over the liver and left kidney. Curves were analyzed for per cent of hepatic arterial (HA) and portal venous contribution using the slope ratio method. Hepatic arterialization was estimated from the angle of the HA component of the curve.

Reversal of the relative contribution of the hepatic and portal components of total flow were seen in all groups. Although quite severe in AH, the degree of reversal could not be used to differentiate among the groups.

The average HA angle in AAH was 48.3 ± 8.1, in A/C 41.5± 10.6, and in C 30.4 ± 12.1. In reviewing the data of only those in the acute clinical phase of AH and not the recovery phase (1 AAH, 3 A/C) and those without other causes of alteration in hepatic arterialization(1 hepatoma, 1 portal-caval shunt, 6 renal failure), the average HA angle in AAH was 50.1 ± 6.6, 45.4 ± 8.2 in A/C, and 23.2 ± 4.2 in C. In 6 with renal failure (2 C, 2 AAH, 2 A/C) the HA angle was 52.7 ± 5.7.

In all cases cirrhosis could be differentiated from both A/C (P=.05) and AAH (P<.01) using the HA angle. In absence of renal failure, portal shunt, or hepatoma, P was <.01 in both comparisons.

10:30–12:00 Room 217B

PULMONARY II

Moderator: Zvi H. Oster, M.D.
Comoderator: A. Bertrand Brill, M.D.

A RAPID METHOD FOR ASSESSING VENTILATION POST-PERFUSION: THE USE OF Tc-99m DTPA AEROSOL AND COMPUTER SUBTRACTION. A.D. Waxman, L. Ramanna, D. Brown, D. Chapman, M.B. Brachman, D.E. Tanasescu, D.S. Berman, and P. Julien. Cedars-Sinai Medical Center, Los Angeles, CA.

Aerosol ventilation studies currently require considerable cooperation on the part of the patient and may result in lengthy study periods or potentially high doses of radiation. This report validates an aerosol method which minimizes patients study time and attempts to keep radiation exposure to a minimum.

Seventeen patients underwent a control pre-perfusion Tc-99m DTPA aerosol multi-view study prior to a 2 mCi Tc-99m MAA multi-view perfusion study. The patient was then placed in an "optimum position" to maximize a visual abnormality seen on perfusion. Nebulized Tc-99m DTPA at two times the original concentration for the pre-perfusion aerosol was again inhaled. Images were obtained on film for two minutes and on computer in one minute frame increments for two minutes. The "perfusion" image consisted of counts from the Tc-99m MAA and Tc-99m DTPA pre-perfusion aerosol. This image was used as a "mask" and subtracted from the post-perfusion aerosol image. The resultant image represented the post-perfusion aerosol counts only.

With the patient acting as his own control all 17 patients demonstrated no significant differences between the pre-perfusion image and the post-perfusion computer subtracted image.

We conclude that post-perfusion aerosol imaging equivalent to pre-perfusion may be obtained using as little as one minute of imaging time. An entire study can be performed in 5-6 minutes or less allowing for all of the advantages of post-perfusion ventilation imaging while not sacrificing the quality of a pre-perfusion test.

INFLUENCE OF POSTURE AND POSITIVE END-TIDAL EXPIRATORY PRESSURE (PEEP) ON CLEARANCE OF Tc99m-DTPA FROM THE LUNGS. GR Mason, J. Maublant, K. Sietsema, RM Effros and I. Mena, Harbor-UCLA Med. Ctr., Torrance, CA.

The clearance of Tc99m-DTPA aerosols from the lung has been used to detect and quantitate alterations in the permeability of the pulmonary epithelium. Clearance of the radionuclide is accelerated by both chronic and acute injuries to the lung and by smoking. Several laboratories have reported that Tc99m-DTPA clearance from upper lobes exceeded that from lower lobes in upright subjects. To investigate this phenomenon further we studied subjects with simultaneous anterior and posterior cameras in upright and supine positions. In the upright position, clearance from both the anterior and posterior upper regions of interest (ROI's) exceeded the lower regions (-1.64 ±.42 S.D. vs. -0.75 ± .41, anterior, $p < .05$, $n = 6$), -1.04 ± .23 vs. - 0.50 ± .36, posterior . All units = %/min. This difference was not observed in the supine subjects. Clearance from the anterior chest exceeded that from the posterior chest in the supine subjects (-1.28 ± .45 vs. -0.05 ± 1.08) and a small increase in radio-activity was observed in at least one ROI of 5 of 6 subjects from the posterior camera. An increase in activity is likely to be secondary to labeling of blood pool, which would have greatest affect where pulmonary blood volume is largest. Computer processing of the entire lung without observer bias in ROI placement showed similar effects of posture over non-peripheral ROI's. Five subjects breathed on PEEP to cause airspace distention, causing clearance to double. Both dependency and airspace distention appear to influence clearance of aerosolized DTPA, the latter may occur by stretching of epithelial pores.

IMPROVED DIAGNOSTIC ACCURACY OF LUNG PERFUSION IMAGING USING Tc-99m MAA SPECT. J.K. O'Donnell, J.A. Golish, R.T.

Go, B. Risius, R.A. Graor, W.J. MacIntyre, D.H. Feiglin. Cleveland Clinic Foundation, Cleveland, Ohio.

The addition of emission tomography (SPECT) to pulmonary perfusion imaging should improve diagnostic accuracy by detecting perfusion defects otherwise masked by superimposition of normal lung activity and by reducing problems with interpretation of defects that result from overlying soft tissue or pleural effusions. In order to examine the contribution of SPECT in the scintigraphic evaluation for pulmonary embolus (PE), we have obtained both planar and SPECT studies in 94 cases of suspected PE. All studies employed 3-4 mCi of Tc-99m MAA and standard six-view planar image acquisition. SPECT raw data of 64 images were then acquired over a 360 degree transaxial rotation with subsequent computer reconstruction. Xe-133 ventilation studies were performed when clinically indicated and tolerated by the patient. For 19 studies angiographic (AN) correlation was obtained within 24 hours. In 16/19 planar and SPECT both gave a high probability of PE but SPECT gave better segmental localization and showed better agreement with the number of defects seen at AN. In 3 indeterminate planar scans, 2 were low probability with SPECT and had negative AN. The third, a patient with Wegener's vasculitis, remained indeterminate with SPECT and had negative AN. Five patients with PE had repeat planar/SPECT/AN studies to evaluate response to treatment. SPECT correlated better with AN findings in each case.

We conclude that SPECT perfusion imaging provides better anatomic accuracy for defects representing PE and is the non-invasive technique of choice for documenting response to therapy.

KRYPTON 81M VENTILATION/PERFUSION RATIOS ($\dot{V}/\dot{Q}$) MEASURED IN LATERAL DECUBITUS IN PULMONARY EMBOLISM (P.E.). M.Meignan, L. Cinotti, A. Harf, L. Oliveira, G. Simonneau. Department of nuclear medicine and I.C.U, Hôpital Henri Mondor, Créteil 94010, France.

In normal subjects lateral decubitus induces in both dependent (lower) and non dependent lung (upper), major changes in perfusion, ventilation and $\dot{V}/\dot{Q}$ ratios which can be studied with the short life radioisotope Krypton 81m. Regional $\dot{V}/\dot{Q}$ are computed from ventilation and perfusion scans, successively obtained with a gamma camera linked to a computer by continuous inhalation or infusion of this gas during tidal breathing. They were displayed as a color coded functional image.To assess the effect of posture on $\dot{V}/\dot{Q}$ in P.E. and other diseases which decrease the regional perfusion, 32 patients with unilateral lung diseases were studied in supine posture and both lateral decubitus : 8 with proved P.E., (3 out of them having radiological opacity matching the perfusion defect), 9 with bullous emphysema, 6 with bronchogenic carcinoma, 9 with acute bacterial pneumonia. $\dot{V}/\dot{Q}$ were computed in the region of the perfusion defect. In P.E. the mean $\dot{V}/\dot{Q}$ was high (1.92 ± 0.6 SD), and did not change whatever the posture. Conversely major changes of $\dot{V}/\dot{Q}$ were induced with postural changes in bullous emphysema and lung carcinoma whatever the $\dot{V}/\dot{Q}$ in patient supine. In pneumonia low $\dot{V}/\dot{Q}$ were observed in supine posture (.73 ± .2). They decreased significantly when the pneumonia was dependent (.53 ± .2 $p < 0.02$) and increased in the controlateral decubitus (1.07 ± .3, $p < 0.001$). Since posture has no or little effect on regional $\dot{V}/\dot{Q}$ in P.E., it can be used to discriminate P.E., even in the case of radiological opacity, from other unilateral disease inducing perfusion defect.

MEASUREMENT OF REGIONAL PULMONARY BLOOD VOLUME IN PATIENTS WITH INCREASED PULMONARY BLOOD FLOW OR PULMONARY ARTERIAL HYPERTENSION. P. Wollmer, A. Rozcovek, C.G. Rhodes, R.M. Allan, and A. Maseri. MRC Cyclotron Unit, Hammersmith Hospital, London, U.K.

The effects of chronic increase in pulmonary blood flow and chronic pulmonary hypertension on regional pulmonary blood volume was measured in two groups of patients. One group of patients had intracardiac, left-to-right shunts without appreciable pulmonary hypertension, and the other consisted of patients with Eisenmenger's syndrome or primary pulmonary hypertension, i.e. patients with normal or reduced blood flow and severe pulmonary hypertension. A technique based on positron tomography (Rhodes et al, J Comput Assist Tomogr 5:783, 1981) was used to measure lung density (by transmission scanning) and regional pulmonary blood volume (after inhalation of ^{11}CO).

The distribution of pulmonary blood volume was more uniform in patients with chronic increase in pulmonary blood flow than in normal subjects. There were also indications of an absolute increase in intrapulmonary blood volume by about 15 %. In patients with chronic pulmonary arterial hypertension, the distribution of pulmonary blood volume was also abnormally uniform. There was, however, no indication that overall intrapulmonary blood volume was substantially different from normal subjects.

The abnormally uniform distribution of pulmonary blood volume can be explained by recruitment and/or dilatation of vascular beds. Intrapulmonary blood volume appears to be increased in patients with intracardiac, left-to-right shunts. With the development of pulmonary hypertension, intrapulmonary blood volume falls, which may be explained by reactive changes in the vasculature and/or obliteration of capillaries.

CLINICAL COMPARISON OF A NEW Tc-99m DTPA DELIVERY SYSTEM WITH Kr-81m. J.P. Finn, M.J. Myers, K.M. Nair, J.P. Lavender. Departments of Diagnostic Radiology and Medical Physics, Hammersmith Hospital, London, England.

Satisfactory agents for ventilation imaging are not widely available. Access to Kr-81m is limited and image quality with Xe-133 is poor, so attention is being focussed on radioaerosols as possible alternatives. The authors assessed the diagnostic value of a new Tc-99m DTPA aerosol delivery system*. Forty patients were studied, most with suspected pulmonary embolism. The protocol involved FEV_1 measurement, six minutes aerosol inhalation immediately followed by steady-state Kr-81m imaging and, 60 minutes later, by Tc-99m MAA perfusion imaging. The efficiency of the system was 2%.

Twenty-one patients had no central airways deposition of aerosol, 14 had 'spotty' images which were correctly interpretable and five had airways deposition sufficient to be misleading. The overall sensitivity of the test relative to Kr-81m was 75% and the specificity 84% (100% and 94% respectively among non-smokers). Airways deposition was significantly more frequent in smokers than in non-smokers and in patients whose FEV_1 was less than 50% predicted.

We conclude that the system provides accurate clinical information in non-smokers but is of less value in smokers. It should prove a practical alternative to Xe-133.

*SynteVent, Synaco Inc., Palo Alto, California.

1:30-3:00 **Room 217A**

CARDIOVASCULAR X: MYOCARDIAL PERFUSION

Moderator: Thomas F. Budinger, M.D., Ph.D.
Comoderator: Ernest G. DePuey, M.D.

MEASUREMENT OF REGIONAL MYOCARDIAL PERFUSION WITH XENON-133. T.D. Ruddy, T. Yasuda, M.M. Barlai-Kovach, M.A. Nedelman, R.M. Moore, N.M. Alpert, J.A. Correia, C.A. Boucher, H.W. Strauss. Massachusetts General Hospital, Boston, MA.

This study reports the validation of a method of measuring regional myocardial perfusion (RMP) following left atrial (LA) injection of Xe-133. This approach also allows measurement of both global and regional left ventricular (LV) function (by recording data in a gated first pass mode during the transit of the tracer through the chamber) as well as the RMP of both left and right ventricles (during the subsequent myocardial phase).

Sequential images were obtained using a single crystal gamma camera, following LA injection of Xe-133, in 8 dogs during rest, pharmacologic hyperemia and after coronary

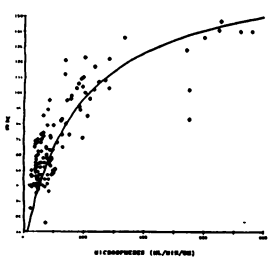

ligation. Values of RMP, computed by generating a functional image of clearance rates according to a monoexponential model, were compared with flow (F) determined by microspheres (fig). The data were best described by the regression equation, RMP=(185)F/(F+185); (r=0.97, F=0.0001), suggesting that blood:tissue Xe equilibration is not instantaneous at high F.

This approach may be useful in the assessment of RMP and LV function in post-operative cardiac patients with LA lines and in the catheterization laboratory via LV catheter injection.

MAXIMIZING MYOCARDIAL PERFUSION WITH COMBINED DIPYRIDAMOLE AND PHENYLEPHRINE. K.P. Lyons, J. Lyons, J. Eugene, S. McColgan, V. Gelezunas, and L. Swan. Veterans Administration Medical Center, Long Beach, CA.

Intravenous dipyridamole (DP), a potent coronary vasodilator, has been used as a pharmacological exercise substitute for Thallium scintigraphy. Increased coronary artery flow occurs in animals. Humans with severe coronary disease have been imaged with Thallium using this technique. However, in both animals and man, the systemic blood pressure decreases especially at higher dosages. Myocardial perfusion (MP) is dependent on delivery pressure as well as the diameter of the coronary artery. We therefore maintained blood pressure by infusion of phenylephrine (PE) during maximal coronary artery dilatation from DP. Seven anesthetized, mongrel, open chest dogs weighing 20-25 kgs were infused with DP alone, 0.075 mg/kg/min for 10 minutes. MP was measured in a highly localized small volume (0.5 cm^3) of myocardium using a silicon avalanche radiation detector to record the washout of a 2-5 mCi bolus of xenon in saline using the Kety-Schmidt formula. Polyethylene tubing (O.D. 0.03 inches) was directed into the proximal LAD using a brass canula introduced through the carotid artery. In 5 other dogs, 0.1 mg of PE was added to the DP.

DP alone caused only a minor elevation of MP (15%) while the blood pressure decreased. In contrast with PE, the pressure was maintained and MP more than doubled. With continued infusion, both pressure and MP fell.

In conclusion, elevation of MP by a coronary dilator DP can be enhanced when combined with a vasopressor (PE) and may be better for pharmacological stimulation of MP for Thallium imaging. Prolonged administration of DP may decrease rather than increase MP even during infusion of phenylephrine.

EFFECTS OF ANOXIA AND ISCHEMIA ON THALLIUM EXCHANGE IN RABBIT MYOCARDIUM. J. Krivokapich, C.R. Watanabe, and K.I. Shine. UCLA Center for the Health Sciences, Los Angeles, CA

The isolated, arterially perfused rabbit interventricular septum was used to study the effects of anoxia and ischemia on thallium (Tl-201) exchange. Anoxia or ischemia was introduced for periods of 20, 40, or 60 minutes during either uptake or washout of Tl-201. These interventions were followed by a reperfusion period. Effluent samples were collected during washout experiments. Anoxia lasting 20, 40, or 60 minutes during uptake resulted in a decrease in net Tl-201 uptake, which was promptly reversed upon reoxygenation. Effluent washout curves demonstrated that an increased efflux of Tl-201 occurred during 20 and 40 minutes of anoxia. Surprisingly, comparison of the Tl loss due to anoxia during uptake with the loss of Tl during washout was consistent with an increased influx of Tl-201 during the first 40 minutes of anoxia. Between 40 and 60 minutes of anoxia, the increased efflux of Tl-201 was reversed and the increase in Tl-201 influx was absent. Total ischemia for 20, 40, or 60 minutes during uptake was followed by continued accumulation of Tl-201 in 8 of 9 septa. Total ischemia during washout was followed by an immediate rapid washout of Tl-201 before a new steady-state was achieved. In conclusion, these results represent important differences from those reported previously using K-42. Anoxia did not increase the influx of K-42 as we observed with Tl-201. Also, 60 minutes of ischemia did not result in progressive loss of Tl-201 as previously noted for K-42. This implies there are different sensitivities and/or mechanisms for Tl as compared to K uptake.

MYOCARDIAL PERFUSION BY DYNAMIC POSITRON EMISSION TOMOGRAPHY (PET) USING O-15-WATER. T.F. Budinger, R.H. Huesman, B.L. Knittel, J.A. Twitchell, K.M. Brennan, Y. Yano, Donner Lab., Univ. of California, Berkeley, CA

Water labeled with O-15 (2.0 m half-life) can be used as a diffusible tracer to quantitate regional myocardial perfusion using PET and bolus injections (i.v.). This is the first report of the validation of a dynamic PET method wherein both the input and residue functions are discerned simultaneously without using arterial sampling. These studies underpin noninvasive myocardial perfusion studies with an inert diffusible tracer in which variability in physiological extraction with altered flows or ischemic conditions is not a concern as with Rb-82 and N-13 ammonia.

A 7 s bolus venous injection of O-15 (up to 20mCi) was done simultaneously with left atrial infusion of microspheres in all 4 thoracotomized dogs. O-15 was produced by the N-14(d,n)O-15 reaction at the 88-inch cyclotron.

The input function is measured from the activity in a region of interest (ROI) over the left ventricular blood pool from sequential PET images (2.5 s intervals for 60 s; 10 s for 80 s; 20 s for 160 s totalling 5 min). The O-15 water residue function is determined from the ROI over the myocardium as determined from a Rb-82 PET study. These two data sets are used to calculate rate constants in a two-compartment model which lumps the capillary and myocite membrane transport. This model is equivalent to the basic diffusible tracer equation for variable input. The rate constant k is related to flow via a partition coefficient of 0.91 and the tissue density of 1.05g/cc.

In 9 studies with 4 dogs under normal and dipyridamole-induced high flow studies we found an excellent correlation (r=0.8) between PET water perfusion results and flow determined from the microsphere reference organ technique.

MEASUREMENTS OF MYOCARDIAL FLOW VS. EXTRACTION OF RUBIDIUM UNDER VARYING PHYSIOLOGICAL CONDITIONS T.F. Budinger, Y. Yano, B.R. Moyer, J.A. Twitchell, K.M. Brennan, R.H. Huesman. Donner Laboratory, University of California, Berkeley, CA

The relationship between myocardial rubidium extraction (E) and flow (F) are well described by the single capillary model E = [1-exp(-PS/F)] with a permeability surface product PS = 0.87 cc/min/gm (Physiologist 26:31, 1983). Some effects of alkalosis and acidosis have been reported (JNM 24:907, 1983). Here we investigate the effects of dipyridamole, norepinephrine-atropine, exsanguination, pacing, ouabain and calcium on extraction using Rb-82 PET and Rb-86 acute studies with microspheres in dogs. Thoracotomies were performed for left atrial microsphere infusion. Anesthesia was by N_2O and methoxyflurane. The degree of exsanguination, drug levels administered and pacing rates were sufficient to produce flow modifications. Extraction was calculated by dividing FE from Rb observations by F from microsphere data.

These results of extraction vs. flow do not show a significant dependence on the method used for flow modification. There was less than a 20% change in FE after an infusion of 0.04 mg/kg ouabain over 5 minutes in 3 replicate studies each on 4 dogs. An important finding not previously explained in flow vs. extraction studies is the occurence of extraction values greater than 1.0 which is possible only if the distribution opportunities of small cations are greater than that of microspheres. This is equivalent to the well known hematocrit effect in small channels.

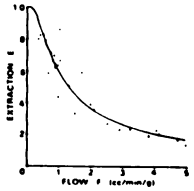

INFARCT SIZE AFTER REPERFUSION BY SIMULTANEOUS INTRACORONARY In-111-MONOCLONAL ANTIMYOSIN AND Tc-99mPYROPHOSPHATE; COMPARISON BY GAMMA SCINTIGRAPHY. B.A. Khaw, H.K. Gold, R. Moore, J.T. Fallon, T.

Yasuda, R.C. Leinbach, H.W. Strauss and E. Haber. Mass General Hospital, Boston, MA.

To determine if Tc-99m labeled pyrophosphate (PYP) and In-111 labeled antimyosin (AM) identify similar zones of acute myocardial infarction (MI), their distribution was determined in 7 dogs, and the results compared to a triphenyl tetrazolium chloride (TTC) measurement of the MI. Seven anesthetized open chest dogs had a 3 hr LAD occlusion. After 15 min of reperfusion, a mixture of 4mCi of Tc-99m PYP and 2mCi In-111 AM was administered into the LAD via the coronary artery catheter. The dogs were killed 45 min later; the hearts sliced into 0.5cm sections parallel to the atrioventricular groove and then stained with TTC. The 0.5 cm slices were imaged with a gamma camera equipped with a medium energy collimator at 140 KeV for Tc-99m and 260KeV for In-111. The Tc-99m and In-111 images of the slices were normalized to the pixel with highest intensity and the area of radioactivity planimetered. Ratios of pixel density of PYP to In-111 AM (P/A) were compared. In 6 dogs with small to moderate TTC infarcts (No. pixels SD=1131±445), P/A=1.97±0.36 (mean±SD), whereas P/A=0.78 only in a dog with a large infarct(No. pixels=2159). TTC stained MIs were almost identical to AM delineated MIs but were smaller than PYP delineated areas of damage. These results indicated that in large infarcts, the AM delineated infarct is approximately equal to PYP infarct. But in small to medium size infarcts where a large zone of severely compromised but reversibly injured myocardium may exist, PYP delineated area of MI is approximately twice that shown by AM. Comparison of these 2 zones of myocardial compromise may provide important information for delineation of severely but reversibly effected myocardium.

1:30-3:00 **Room 216BC**

INSTRUMENTATION IV: SPECT

Moderator: William L. Rogers, Ph.D.
Comoderator: James C. Carlson, M.S.

THE ESTIMATION OF SPECT STATISTICAL RELIABILITY. R.J. Jaszczak, K.L. Greer, C.E. Floyd, C.C. Harris, and R.E. Coleman. Duke University Medical Center, Durham, NC.

To provide a quantitative understanding for the interdependence of radiopharmaceutical uptake, detector efficiency, and reconstruction parameters on SPECT statistical accuracy, a unified approach to estimating %rms noise has been developed. The procedure consists of the following steps: 1) Determine an acceptable geometric model for the organ system including radionuclide concentration Q_s. 2) Select desired transverse and axial resolutions. 3) Select an acceptable imaging time T_{scan}. 4) Compute the total number N_t of expected gamma photons in slice using:

$$N_t = \pi \cdot R_s \cdot R_{eff} \cdot L_{slice} \cdot Q_s \cdot \varepsilon \cdot T_{scan} \cdot A_{body}$$

where ε is the detection efficiency, R_s is the physical source radius, R_{eff} is the reduced source radius resulting from self-absorption, L_{slice} is the slice thickness, and A_{body} is the attenuation factor of surrounding body tissue. 5) Compute the %rms noise using an equation that includes the effects of spatial filtering and attenuation compensation. Two cylindrical phantoms (10 cm dia.) containing concentrations of Tc-99m (Q_s=0.5 and 1.0 μCi/cc) were sequentially placed in a water-filled cylinder (20 cm dia.), and scanned (T_{scan}=1175 sec.) with a SPECT system. Values of N_t equal to 120 (117) and 236 (238) kcnts were obtained using the mathematical model (phantom data). Using a generalized Hann filter (f_c=3.1 cycle/cm) values of %rms noise equal to 21 and 15% were mathematically computed for the two concentrations, compared with measured values of 25 and 13%. These results indicate that the mathematical model is useful in 1) evaluating SPECT performance, 2) selecting SPECT imaging parameters, and 3) predicting the utility of proposed SPECT pharmaceuticals.

ACCURACY OF ROTATIONAL TOMOGRAPHY FOR PREDICTING ABSOLUTE T1-201 CONCENTRATIONS. E Garcia, D Chapman, J Areeda, K Van Train, J Maddahi, D Berman, A Waxman. Cedars-Sinai Medical Center, Los Angeles, CA

Standard filtered back-projection (FBP) reconstruction of Tl-201 myocardial tomograms does not accurately reflect the actual regional distribution of radioactivity. This limitation is partly due to the lack of corrections for photon scattering and attenuation as well as the dependence of recovered counts on object size. Thus we have implemented post-processing methodology to correct for these phenomena. This methodology was tested on a phantom consisting of 16 square vials (40x35x100 mm) arranged in a 4x4 matrix and submerged in a cylindrical water bath of 22cm diameter. Each vial was filled with a relative Tl-201 concentration of 1, 2, 3 or 4 (where 1=.4 μCi/ml). FBP tomograms were obtained using an asymmetric 20% energy window placed at 81 keV. Scatter correction was performed by subtracting from the FBP tomogram a fraction (.56) of a scatter tomogram obtained using a 20% window placed at 65 keV. Each voxel of the scatter corrected tomogram was then corrected for the mean attenuation from all projections using a constant attenuation coefficient of .18/cm. Results: Recovered Tl-201 mean (and standard deviation) concentrations:

Actual	1	2	3	4
Uncorrected	.39(.05)	.66(.05)	.93(.19)	1.13(.24)
Corrected	1.12(.46)	2.18(.4)	3.14(.16)	4.25(.25)

Thus, the implementation of this correction methodology resulted in major improvement in tomographic estimates of varying Tl-201 concentrations in this phantom model. These findings support the hypothesis that, with the incorporation of variable attenuation coefficients, tomography may ultimately provide accurate myocardial Tl-201 absolute concentrations.

MOTION DETECTION AND CORRECTION IN Tl-201 SPECT IMAGING: A SIMPLE, PRACTICAL METHOD. J Friedman, E Garcia, D Berman, J Bietendorf, F Prigent, K Van Train, A Waxman, J Maddahi. Cedars-Sinai Medical Center, Los Angeles, CA

Since Tl-201 SPECT imaging requires that pts remain in an awkward position for a prolonged time, pt motion (M) is a potentially serious source of artifactual defects on tomographic (tomo) reconstructions. Thus we developed a simple method for detection and correction of M from SPECT images. A Co-57 point source is placed on the lower anterior chest, an area remaining in the camera's field of view throughout imaging, and is imaged concurrently with Tl. In the absence of M, this point source inscribes a straight line on planar summation of the 32 projections over 180°. Movement is detected by deviation from this line. The number of pixels (P) of M is used to shift images so that the resultant images of the point source are linear. The method was tested in 48 consecutive patients undergoing Tl tomo. Uncorrected and corrected images were reconstructed, and long- and short-axis tomo cuts were quantitatively analyzed using circumferential profiles (CPs) of maximum counts with comparison to lower limits of normal. Extent (E) of abnormality was expressed as the % of CP points falling below normal. M was detected in 8/48 pts (17%) and was 2 P in 3 and 1 P in 5 pts. E was less following correction in 7/8 pts, with a mean decrease of 71% with 2 PM and 44% with 1 PM. Visual change in tomo after correction was dramatic with 2 PM and subtle with 1 PM. The E and location of tomo abnormality after correction more closely resembled subsequent planar imaging than did the uncorrected reconstructions. We conclude: 1) pt M is a common problem in SPECT Tl images; 2) when > 1 pixel, M results in major tomographic artifacts; and 3) the method described provides a simple, practical approach for detection and correction of M.

A STUDY OF ANGER CAMERA SENSITIVITY AND LINEARITY AS A FUNCTION OF SPATIAL ORIENTATION. R.E. Malmin, J.A. Bieszk, E. G. Hawman, Siemens Gammasonics, Inc., Des Plaines, IL.

As part of an ECT quality assurance program, we have investigated the effect of Anger camera orientation on system linearity, sensitivity, and pulse height stability. Data have been acquired from two Siemens ZLC 7500 cameras using 2" photomultiplier tubes from two different vendors. Each PMT is individually shielded with mu-metal.

Point source sensitivity and position stability were studied using 1 mm Co-57 point sources mounted within tantalum well-collimators fixed onto the crystal facing. Measured variations in sensitivity as a function of rotation were 0.35% RMS and 1.2% peak-peak. Centroid position variations were 0.27 mm RMS and 1.0 mm peak-peak. The observed sensitivity variations increased markedly (≈x4) if the cam-

era was not shielded from backscatter. The position variation, however, was only weakly affected (≈x1.15). Pulse height stability and flood uniformity variations with orientation were studied by fixing a Co-57 flood source to the collimator and acquiring 20 million count flood images. Images corresponding to the average energy signal at each pixel (Z-map) were simultaneously recorded. The variation in regional flood count density, analyzed over 1" x 1" regions of interest, was comparable to that found in the point source experiments. Regional and global Z-map data varied approximately sinusoidally with angle - 0.6% (RMS) and 1.7% (peak-peak). Direct measurement of the pulse height spectra versus angle yielded similar results.

These data imply that variations of camera sensitivity and linearity during gantry rotation are small and relatively uniform over the detector area. Recent simulations in this laboratory indicate that ECT reconstructions are insensitive to such variations.

COMPARISON OF PLANAR IMAGES AND SPECT WITH BAYESEAN PREPROCESSING FOR THE DEMONSTRATION OF FACIAL ANATOMY AND CRANIOMANDIBULAR DISORDERS. L.T. Kircos, D.A. Ortendahl, R.S. Hattner, D. Faulkner, R.L. Taylor. University of California, San Francisco, CA.

Craniomandiublar disorders involving the facial anatomy may be difficult to demonstrate in planar images. Although bone scanning is generally more sensitive than radiography, facial bone anatomy is complex and focal areas of increased or decreased radiotracer may become obscured by overlapping structures in planar images. Thus SPECT appears ideally suited to examination of the facial skeleton.

A series of patients with craniomandibular disorders of unknown origin were imaged using 20 mCi Tc-99m MDP. Planar and SPECT (Siemens 7500 ZLC Orbiter) images were obtained four hours after injection. The SPECT images were reconstructed with a filtered back-projection algorithim. In order to improve image contrast and resolution in SPECT images, the rotation views were pre-processed with a Bayesean deblurring algorithim which has previously been shown to offer improved contrast and resolution in planar images. SPECT images using the pre-processed rotation views were obtained and compared to the SPECT images without pre-processing and the planar images.

TMJ arthropathy involving either the glenoid fossa or the mandibular condyle, orthopedic changes involving the mandible or maxilla, localized dental pathosis, as well as changes in structures peripheral to the facial skeleton were identified. Bayesean pre-processed SPECT depicted the facial skeleton more clearly as well as providing a more obvious demonstration of the bony changes associated with craniomandibular disorders than either planar images or SPECT without pre-processing.

MONTE CARLO EVALUATION OF COMPTON SCATTER COMPENSATION BY DECONVOLUTION IN SPECT. C.E. Floyd, R.J. Jaszczak, C.C. Harris, R.E. Coleman. Duke University Medical Center, Durham, NC.

This study evaluates a deconvolution algorithm which compensates for Compton scattering in SPECT images. Using Monte Carlo methods, the scattered and non-scattered components of a SPECT image are simulated thus allowing a comparison of scatter compensated results with direct non-scatter results. This technique is crucial for evaluating compensation algorithms since scattered photons are not distinguished from non-scattered photons experimentally. Compton scatter is modeled as a convolution of the non-scattered projection with an exponential function. Deconvolution of the total (scatter + non-scatter) data yields the compensated true data:

$$D = FT^{-1}\left[\frac{FT(T)}{FT(\delta(x) + \alpha \exp(-\beta|x|))}\right]$$

where D is the direct non-scatter data, T is the total data, FT is the Fourier Transform operator, α and β are parameters, and δ is the Dirac delta functional. Fitting the exponential to the simulated scatter component of a line source in a water filled phantom 11 cm in radius yields α= 0.023 and β=0.46 cm^{-1}. The quality of the compensation is shown by comparing the ratio of total to direct counts (= 1.39 on-axis, 1.32 off-axis), with the ratio of compensated to direct counts (=1.04 on-axis, 0.99 off-axis). The true line shape was well reproduced both on and off axis. These results show that for the test geometry considered, deconvolution of an exponential function can significantly reduce the effect of Compton scattering in quantitative SPECT imaging.

1:30–3:00 **Room 212B**

ENDOCRINE II

Moderator: James C. Sisson, M.D.
Comoderator: I. Ross McDougall, M.D.

RADIOIODIDE IMAGING OF PERTECHNETATE "HOT" SOLITARY THYROID NODULES. C.N. Chapman, J.J. Sziklas, R.P. Spencer, B.F. Bower, R.J. Rosenberg. Univ. Connecticut Health Center, Farmington, CT, and Hartford Hospital, Hartford, CT.

In 5,100 consecutive patients having pertechnetate thyroid images, 96 were noted to have solitary "hot" nodules (1.9%). Each was reimaged (by 2 months) with I-123 sodium iodide (I-131 in 1 case). In 84 of the 96 cases (88%), the nodules were also "hot" on the radioiodide images. Seven of these cases were biopsied; all were follicular adenomas. In 9 cases, the solitary radiotechnetium "hot" nodules were not delineated on the radioiodide images; hence, 8% of the cases had areas that would not have been noted if radioiodide was the sole imaging agent. Of the 9 "non-delineated" nodules, 3 were biopsied. One was reported as being normal (? adequate tissue removed), one was a follicular adenoma, and one was a follicular adenoma with a focus of metastatic tumor from an undetermined site (there were other metastases in the lungs and mediastinum). Hence, the 3 biopsied areas showed benign thyroid tissue (with one metastatic site). In 3 cases (4%) the pertechnetate "hot" nodule was "cold" on the radioiodide study. Two of these were biopsied. One was a follicular carcinoma, while the second was a follicular adenoma with pleomorphic Hurthle cells. We conclude that, in this series, 88% of the "hot" pertechnetate thyroid solitary nodules were also "hot" to radioiodide; all those biopsied were nonmalignant. In 8% of the cases, the pertechnetate "hot" areas were not delineated on the radioiodide images. Biopsies in this group showed nonmalignant lesions (although one had a metastatic area). In 3 cases with pertechnetate "hot", but radioiodide cold areas, 2 were biopsied and showed malignant or premalignant elements.

EVALUATION OF RADIONUCLIDE SCINTIGRAPHY, ECHOGRAPHY, AND SERUM THYROGLOBULIN IN THE DIAGNOSIS OF THYROID NODULES. K. Ikekubo, H. Tochio, T. Hamasaki, H. Yamaguchi, Y. Saiki, H. Ito, T. Higa, M. Hirasa, M. Kudo, T. Ishihara, and N. Waseda. Kobe General Hospital, Kobe, Japan ; M. Senda, T. Mori, and K. Torizuka. Kyoto University, School of Medicine, Kyoto, Japan.

For the purpose of rapid and precise diagnosis of thyroid nodules, thyroid imagings with both Tc-99m and Tl-201 were performed in 152 untreated patients with thyroid nodules. Among them, 86 patients were evaluated by ultrasound study. Serum thyroglobulin (Tg) levels were also determined in 69 patients.

The final diagnosis of nodules was confirmed by the histological findings. Of the 152 patients, 81 patients (53 %) had carcinoma.

Scintigraphic patterns obtained with Tc-99m, and Tl-201 were classified into eight types (I-VIII). Abnormal thyroid images were found in 90 % of 152 patients. Tl-201 images clearly revealed enormous intrathoracic tumor invasion in 6 carcinomas and 2 adenomas. Of 29 patients with regional lymph-node metastases,69 % showed positive scans with Tl-201 at these sites. The presence and extent of lesions were diagnosed in 99 % of 86 patients with scintiscans and ultrasonography.

Serum Tg was elevated in 71 %. However, there was no significant relationship between Tg levels and scintigraphic patterns.

We conclude that radionuclide scintigraphy in combination with echography provides improved sensitivity and specificity in detecting the presence and extent of tumor

lesions, and is a convenient and useful screening method for the diagnosis of thyroid tumors.

ACUTE AND LONG-TERM EFFECTS OF RADIOIODINE THERAPY ON SERUM LEVELS OF CALCITONIN. A.Franke and K.Oeff. Department of Nuclear Medicine, Klinikum Steglitz, Free University of Berlin, Berlin, F.R.Germany.

The purpose of this study is to establish data on the radiosensitivity of thyroid C cells and medullary carcinoma of the thyroid (MCT) as reflected by the alterations in serum concentrations of calcitonin (Ct) after radioiodine therapy.

Serum levels of Ct were measured by radioimmunoassay in 1437 patients subjected to diagnostic and therapeutic procedures for thyroid diseases. The effect of low dose and of high dose radioiodine therapy (RLO, RHI) was studied in158 patients with hyperthyroidism and in 84 patients with thyroid cancer, respectively.

RLO and RHI were followed by significant alterations in the distribution of Ct values. RLO decreased the occurrence of high values. RHI was followed by the absence of high concentrations and a substantial reduction in normal levels. The effect of RLO was confirmed in 47 patients by comparing their individual levels before and 8 weeks after RLO, the means ±SD being 24.3 ±8.3 and 12.6±5.7 pmol/l, respectively ($p<0.001$). In 30 patients followed up for late onset hypothyroidism who had been treated by RLO 10-25 years ago, the concentrations of Ct were almost normal (mean ± SD 16.6 ± 5.7 pmol/l). To monitor the acute effects of radioiodine therapy, sequential serum levels of Ct were measured in 12 hyperthyroid patients before up to 3 days after RLO as well as in 1 patient with MCT before up to 8 weeks after RHI. A short-lived increase in serum levels of Ct was observed up to 3 days after RLO. However, due to the wide variation in individual Ct levels, the significance of the differences between basal and destruction-induced Ct levels could not be proved. In the patient with residual MCT a short-lived increase in the serum concentration of Ct was observed 24 hours after RHI, followed by a gradual decline within 8 weeks.

Radioiodine therapy in patients with hyperthyroidism and radioiodine ablation in patients with thyroid cancer significantly decrease serum levels of Ct, indicating an impairment of thyroid C cell function. In contrast, radioiodine therapy might be of benefit in the treatment of patients with MCT, if residual disease is confined to the area near the thyroid remnant. The destruction-induced, short-lived increase in serum levels of Ct within 3 days after RLO cannot be easily detected due to 1. the very low levels of circulating Ct in hyperthyroid patients, 2. the short half-life of Ct (12 min), and 3. the considerable overlap in individual levels of Ct.

^{131}I-METAIODOBENZYLGUANIDINE TREATMENT OF MALIGNANT PHEOCHROMOCYTOMAS. J. Sisson, B. Shapiro, J. Glowniak, W. Beierwaltes, T. Mangner, D. Wieland, J. Carey, N. Petry, J. Copp, P. Eyre. University of Michigan, Ann Arbor, MI.

When ^{131}I-metaiodobenzylguanidine (^{131}I-MIBG) concentrates in malignant pheochromocytomas, therapeutic radiation can be delivered from within these tumors. Ten patients have now received 1-5 therapies (97-215 mCi/therapy, up to 628 mCi total) for malignant pheochromocytomas.

Results in the first 5 patients gave encouragement (J Nucl Med, in press): 2 had subjective (disappearance of clinical features of disease) and objective (reduction of catecholamine excretion by more than 50%, and of tumor size by more than 70%) benefits. One responding patient developed a new tumor on scintigraphy; a fifth treatment caused regression of the new abnormality and preserved the attained benefits. The other 3 patients have shown little or no response despite additional (third) treatments in 2.

Three of the next 5 patients have responded beneficially to ^{131}I-MIBG. One (208 mCi) and two (197 & 169 mCi) doses in separate patients resulted in: disappearance of symptoms and a diminution of catecholamine excretion (by more than 50% in one and to almost normal levels in the other); but the boney sites made changes in volume of tumors difficult to measure. In an asymptomatic patient, 130 mCi reduced her catecholamine excretion by 33%, but volumes of her liver tumors remain unchanged as yet. One patient had no change after two doses (207 & 167 mCi), and one patient's disease progressed unabated after 186 mCi.

In addition to uptake and retention of ^{131}I-MIBG by tumors, other factors must also determine responses. Moderate leukopenia in two patients has been the only adverse effect. We conclude that ^{131}I-MIBG offers hope to patients with heretofore resistant malignant pheochromocytomas.

ADRENAL IMAGING WITH TECHNETIUM-99m-LABELLED LOW DENSITY LIPOPROTEINS. J.L. Isaacsohn, A.M. Lees, R.S. Lees, M. Barlai-Kovach, and H.W. Strauss. New England Deaconess and Massachusetts General Hospitals and Massachusetts Institute of Technology, Boston and Cambridge, MA.

Plasma low density lipoproteins (LDL) are a major source of cholesterol for adrenal cortical steroid hormone synthesis. To test whether LDL labelled with Tc-99m could be used to assess adrenal cortical function, we prepared Tc-99m-LDL by dithionite reduction of TcO_4^- in the presence of LDL. About 80% of the Tc-LDL bonds were covalent. Purified Tc-99m-LDL was injected intravenously into 16 rabbits (4 to 8mCi/rabbit). External imaging was carried out 16 to 18 hrs later, at which time the adrenals were visualized clearly; the animals were sacrificed, the organs dissected out, weighed, and counted. The biodistribution demonstrated that 0.81 ± 0.19% of the injected radioactivity was taken up per gm of whole adrenal gland. This compared with an uptake of 0.19 ± 0.02% per gm by liver, 0.22 ± 0.04% per gm by spleen, and 0.11 ± 0.02% per gm by kidney. To verify that we were indeed imaging the adrenals, additional rabbits were tested with dexamethasone. First they were injected with Tc-99m-LDL; 18 hrs later the adrenals were again well visualized. Then the rabbits were given dexamethasone for 5 days to suppress adrenal cortical function. The adequacy of suppression was monitored by serum cortisol measurements. When Tc-99m-LDL was injected again, the adrenals could not be seen 18 hrs later. Counts of the adrenals from the suppressed rabbits were at background levels. These data indicate that Tc-99m-LDL is a useful radiopharmaceutical for evaluating adrenal cortical function.

1:30-3:00 **Room 217B**

NEUROLOGY V: NEURORECEPTORS

Moderator: Henry N. Wagner, Jr., M.D.
Comoderator: Thomas C. Hill, M.D.

KINETIC MEASUREMENTS ARE NECESSARY FOR DESCRIPTION OF BRAIN RECEPTORS WITH PET. Mintun MA and Raichle ME. Washington University School of Medicine, St. Louis, MO

Following injection of radiolabeled spiperone a brain PET image demonstrates a distribution of tracer similar to the known distribution of dopamine receptors. However, the usefulness of a single PET image to quantitate receptor density can be limited by the effect of local blood flow (CBF), brain permeabilty (P), forward receptor rate constant (k1), and the reverse receptor rate constant (k-1). Using a 3-compartment model that we have described and successfully employed to interpret brain receptor kinetics with PET (Ann Neurol, Mar. 1984), we simulated the effect of changes in the above variables on the image contrast (IC) between receptor-containing tissue (T), and receptor-free tissue like cerebellum (C), expressing this contrast as (T-C)/C. The blood activity curve and initial values for the variables were taken from our in vivo PET work in baboons using 18-F-spiperone. The model shows IC increases directly with time, not reaching 90% of maximum until over 3 hours. Thus, the timing of a single PET scan is critical for reproducible results. The sensitivity of IC is seen below:

Time	Initial	% IC change with +50% change in:			
(min)	IC	CBF	P	k1	k-1
30	0.56	5.6	18.6	38.1	-6.0
60	1.50	2.2	7.3	37.1	-12.2
120	2.71	0.8	2.5	40.2	-22.8

While the effect of changes in CBF are very small, changes in P , k1 and k-1 at 60 minutes, and k1 and k-1 at 120 minutes result in substantial changes in the observed IC. Until more is known about the behavior of these variables reliable description of brain receptors requires dynamic PET data from sequential images, analyzed by an appropriate mathematical model.

IN VIVO KINETICS OF [H-3]SPIPERONE IN RAT BRAIN. D.C. Chugani, J.R. Barrio, S.C. Huang, and M.E. Phelps. UCLA School of Medicine, Los Angeles, CA.

The quantitative measurement of neuroreceptors with PET and high affinity ligands requires an understanding of those critical variables determining in vivo ligand deposition. We have performed kinetic studies of various rat brain regions following bolus intravenous administration of [H-3]spiperone ([H-3]SP; 250 μCi/kg, 20 μg/kg) in order to understand differences we have found between in vivo and in vitro autoradiographic labeling of rat brain sections. Arterial blood samples were collected, and 50 λ aliquots of

plasma were counted. The rats were sacrificed at various times after injection, and the brains were rapidly removed. Striatum, frontal cortex, hippocampus and cerebellum were dissected, homogenized in 10 volumes ethanol and counted. Plasma and brain tritium content were corrected for metabolism to reflect only [H-3]SP. Kinetic curves for brain regions were fitted to a 3-comparment model: plasma ligand ⇌ free and nonspecifically bound ligand in brain ⇌ specifically bound ligand in brain. These curves show that [H-3]SP continues to accumulate in striatum up to 3 hr after injection, whereas, its concentration declines after 30 min in frontal cortex. Spiperone binds primarily to dopaminergic receptors in striatum and to serotonergic receptors in frontal cortex with similar affinity for both receptor types. Although the receptor concentration in frontal cortex is approximately half of that in striatum, the cortical receptors are restricted for the most part to lamina IV resulting in local receptor concentrations similar to those in striatum. These results suggest that we must look for variables other than receptor number and affinity to explain the differences between [H-3]SP kinetics in striatum and in frontal cortex.

THE EFFECTS OF AGE ON DOPAMINE RECEPTORS MEASURED BY POSITRON TOMOGRAPHY IN THE LIVING HUMAN BRAIN. D.F. Wong, H.N. Wagner, Jr., R.F. Dannals, J.J. Frost, H.V. Ravert, J.M. Links, M.F. Folstein, B.A. Jensen, M.J. Kuhar, J.T. Toung. The Johns Hopkins Medical Institutions, Baltimore, MD.

C-11 n- methylspiperone has been used to measure dopamine (D2) receptors in the caudate and putamen of 30 normal persons. In vitro studies in rodent brain revealed a high affinity for dopamine (D2) receptors and five fold less for serotonin (S2) receptors. In vivo drug competition studies in rodents demonstrated that 90% of striatal binding is to dopamine receptors. In the frontal cortex, the majority of receptor binding is to serotonin receptors.

Thirty normal volunteers aged 19 to 73 years were screened for normality by medical, neurological and neuropsychological examinations. Positron tomography was performed serially for 2 hours after injection. In 10 subjects there was good agreement between activity in arterial samples and that in venous samples from a heated hand.

Binding in the dopamine rich caudate and putamen progressively increased while binding in the dopamine poor cerebellum decreased. The dopamine receptor density was estimated by the ratio of the caudate-to-cerebellar mean counts/pixel (Ca/Cb) and putamen-to-cerebellar mean counts/pixel (Pu/Cb). The ratios (Ca/Cb, Pu/Cb) increased linearly with time ($r>0.95$) for each subject. There was a decrease (Ca/Cb) with age (0.8%/yr) that could be approximated with a linear fit: ($Ca/Cb = -.02 \text{ age} + 3.92$, $r=.6$). For the 21 males alone, the decrease was (1.1%/yr, $r=.7$, $p<.01$), while for the 9 females there was no significant decrease with age. Similar findings were noted in the putamen. This decline in dopamine receptor density with age has been reported in rodent and human autopsy studies, but never before in the living human brain.

MEASUREMENT IN VIVO OF DOPAMINE RECEPTOR DENSITY I: EFFECT OF ENDOGENOUS DOPAMINE ON SPIROPERIDOL BINDING. O.T. DeJesus, G.J.C. VanMoffaert, A.M. Friedman, and R. J. Dinerstein.
THE UNIVERSITY OF CHICAGO, CHICAGO, IL 60637 AND ARGONNE NATIONAL LABORATORY, ARGONNE, IL 60439

Non-invasive localization of brain dopamine (DA) receptors has been achieved by us and others using gamma emitting derivatives of the DA antagonist spiroperidol (SP). To accurately characterize this localization, we have previously described an equilibrium binding model involving SP and DA for a single DA receptor (Ann. Neuro. in press).

It is the purpose of this study to establish experimentally the significance of endogenous DA on the ability of SP to bind a group of DA receptors. Several mice were administered different doses of SP. To one group of mice L-dopa was given with peripheral decarboxylase inhibitor, RO-4-4602, in order to elevate brain DA levels while a separate group served as control. ^{3}H-SP binding and DA levels were measured in each brain sample.

The results are as follows:

Spiroperidol Dose, ug/kg	Decrease In in vivo ^{3}H-SP Specific binding as % of control	L-Dopa mediated Increase In Striatal [DA] as % of control
60	25 ± 5	185 ± 12
100	41 ± 13	168 ± 22
265	54 ± 17	222 ± 3

These results reflect a significant competition between DA and SP for caudate DA binding sites. (Supported by NIH grant NS 16835 and DOE. Div. of Biomedical Research).

MEASUREMENT IN VIVO OF DOPAMINE RECEPTOR DENSITY II: EFFECT OF D-AMPHETAMINE ON SPIROPERIDOL BINDING. A.M. Friedman, O.T. DeJesus, W. Woolverton, and R.J. Dinerstein. THE UNIVERSITY OF CHICAGO, CHICAGO, IL 60637 AND ARGONNE NATIONAL LABORATORY CHICAGO, IL 60439

In our continuing studies to measure dopamine (DA) receptors in vivo using the DA antagonist bromospiroperidol (BrSP) and positron emission tomography (PET), we have examined the effect of d-amphetamine (d-AMP) on BrSP distribution in primate brain. Using the University of Chicago PETT VI scanner, ^{76}Br-BrSP was found to localize in the caudate and putamen of anesthesized rhesus monkeys. The maximum level of this drug in these regions was reached at 100 minutes post-injection and remained constant for the next 200 minutes. Levels in the cerebellum, on the other hand, decline steadily after an hour post-injection. This is consistant with the presence of high level of DA receptors in the basal ganglia and low levels in the cerebellum. Preliminary studies showed that the administration of d-AMP (0.5 mg/kg i.v.) resulted in a small but statistically significant decrease in caudate ^{76}Br-BrSP levels. Since d-AMP is known to release DA in the caudate, these findings are consistent with the competition of released DA for BrSP binding at caudate DA binding sites. (Work supported by the DOE, Division of Biomedical Research, NIH grant NS-16835 and the Brain Research Foundation affiliated with the University of Chicago).

IMAGING OPIATE RECEPTORS WITH POSITRON EMISSION TOMOGRAPHY. J.J. Frost, R.F. Dannals, H.T. Ravert, A.A. Wilson, D.F. Wong, J.M. Links, H.D. Burns, M.J. Kuhar, S.H. Snyder, and H.N. Wagner, Jr. The Johns Hopkins Medical Institutions, Baltimore, MD.

Opiate receptors exist in the mammalian brain and are thought to mediate the diverse pharmacological actions of the opiates, such as analgesia, euphoria, and sedation. The 4-carbomethoxy derivatives of fentanyl, such as lofentanil and R31833 (4-carbomethoxyfentanyl) bind to the opiate receptor with high affinity. C-11 R31833 was synthesized by reacting C-11 methyl iodide with the appropriate carboxylate. Male ICR mice were injected intravenously with C-11 R31833 (5 µg/kg), killed 30 minutes later, and the brains rapidly dissected. The thalami, striata, and cerebral cortex are rich in opiate receptors, but the cerebellum contains a very low concentration of opiate receptors. The thalamus/cerebellum and striatum/cerebellum activity ratios, calculated per mg of wet tissue, were 4.1 and 5.2, respectively. Coinjection of 5 mg/kg naloxone reduced the ratios to 1.1, which indicates that the preferential localization of C-11 R31833 in the thalami and striata is due to binding to opiate receptors. A 22 kg anesthetized male baboon was imaged using the NeuroECAT after injection of 18.9 mCi of C-11 R31833 (0.50 µg/kg, specific activity 616 Ci/mmole at time of injection). From 15-70 minutes after injection preferential accumulation of activity could be seen in the thalami, caudate nuclei, and cerebral cortex and, conversely, low activity was demonstrated in the cerebellum. At one hour postinjection the maximum measured caudate/cerebellum activity ratio per pixel was 2.9. For the NeuroECAT the recovery coefficient for the baboon caudate is ca. 0.2-0.3, and therefore the actual caudate/cerebellum ratio is ca. 10-15.

1:30-3:00 Room 212A

ONCOLOGY IV: TUMOR-LOCALIZING AGENTS

Moderator: William D. Kaplan, M.D.
Comoderator: Victor R. McCready, M.D.

SCINTIGRAPHIC STUDIES OF F(ab')2 IN HUMAN TUMOR XENOGRAFTS IN MICE. A. Alavi, J. Powe, D. Herlyn, M. Velchik, H. Koprowski University of Pennsylvania School of Medicine and Wistar Institute, Philadelphia, PA

F(ab')2 fragments of a large number of anti-tumor monoclonal antibodies were examined for their potential use in radioimmunodetection. Mice bearing 30-150 mg human tumor grafts received 15 uCi of I-131 F(ab')2 and organ distribution studies were performed 2 and 4 days later. Some mice were imaged daily after the injection of 100 uCi of labelled fragments. Non-specific I-125 F(ab')2 was used as a control. Antibody affinities and the number of antigenic sites per cell were determined by Scatchard analysis of the in vitro binding of antibody to the tumor cell lines grafted. Specific localization of 2 colorectal, 1 lung and 1 breast monoclonal antibody was easily demonstrated in mice bearing the appropriate tumors while mice bearing unrelated tumors showed no localization. Good images were obtained from the second day onwards. However, it was more difficult to obtain good images of melanoma grafts using 6 different anti-melanoma antibodies. Although tumor to blood ratios of radiotracer as high as 34:1 were obtained, the total amount of radioactivity within the melanoma grafts was always considerably lower than in the other tumor types examined (0.8% of injected dose per gm compared to 1.4%). For tumor grafts with greater than 10^6 antigenic sites per cell, antibodies with affinities as low as $1.8X10^8$ 1/mole successfully localized in vivo. When only 10^5-10^6 sites per cell were available, antibodies with affinities of at least 10^9 1/mole were required to yield good biodistribution results and even then imaging was difficult. No significant localization was seen for antibodies with affinities lower than 10^8 1/mole or less than 10^5 antigenic sites per cell.

VISUALIZATION OF A HUMAN MAMMARY TUMOR IN NUDE MICE WITH IN-111 LABELED MONOCLONAL ANTIBODY B.A. Khaw, H.W. Strauss, J. Cooney, T. Edgington, H. R. Soule. Massachusetts General Hospital, Boston, MA, and Scripps Clinic, La Jolla, CA.

A monoclonal antibody designated 103D2, specific for a tumor associated 126 kilodalton phosphoglycoprotein antigen from human mammary carcinoma (HMC) was used to determine the feasibility of tumor detection and visualization in nude mice. 103D2 was precoupled to DTPA and labeled with In-111 by the transchelation method. The labeled 103D2 (200μCi /20μg) was injected intravenously via the tail veins into nude mice hosting a HMC BT-20(n=8). The mice were imaged at 1 hr, and every 24 hr thereafter for up to 6 days with a pinhole collimator. Four animals were killed at 48 hr and 4 at 7 days, and biodistribution determined by gamma counting of various organs. To define the specificity of distribution of the antibody, 8 additional tumor bearing animals were studied: 4 with a different In-111 labeled IgG (MOPC-21-myeloma IgG_1) and 4 with injection of ionic In-111. Localization of the In-111 labeled 103D2 was 14.72±2.25% injected dose per gram of the tumor (D/g) at 48 hr, whereas In-111 labeled MOPC-21 was 5.78±1.08 D/g and ionic In-111 was 3.8±0.81% D/g. Tumor localization at 7 days after iv administration of In-111 labeled 103D2 was observed to be 21.97±4.44% D/g. Tumors were visualized with In-111 labeled 103D2 as early as 1-2 hr after iv injection but by 24 hr, unequivocal delineation of the tumors was observed in all animals, with the best tumor delineation at 2 to 4 days. Tumor visualization with In-111 labeled 103D2 was also possible even when the tumors were inplanted in the upper abdominal region over the liver and spleen. In summary, monoclonal antibody specific to a HMC associated 126 kd phosphoglycoprotein antigen can be used to visualize human mammary tumors hosted in nude mice by gamma scintigraphy.

I-123-INSULIN: A NEW MARKER FOR HEPATOMA. J.C. Sodoyez, F. Sodoyez-Goffaux, Ch. Fallais, and P. Bourgeois, University of Liege, Liege, Institut des Radioéléments, Fleurus and J. Bracops Hospital, Brussels, Belgium.

Previous studies have demonstrated that carrier-free I-123-Tyr A14 insulin was taken up by the liver (by a saturable mechanism) and by the kidneys (by a non saturable mechanism). Autoradiographs of rat liver after injection of I-125-insulin showed that binding specifically occurred at the plasma membrane of the hepatocytes. I-123-Insulin binding to the hepatocyte plasma membrane appeared mediated by specific receptors. Indeed it was blocked by antibodies to the insulin receptors and by an excess of native insulin. Furthermore insulin derivatives with low biological potency (proinsulin and desoctapeptide insulin) did not inhibit I-123-insulin binding to the hepatocytes. I-123-Insulin (1.3 mCi) was I.V. injected into a patient in whom the right liver lobe was normal (normal uptake of Tc-99m-colloid sulfur) but the left liver lobe was occupied by a voluminous hepatoma (no uptake of Tc-99m-colloid sulfur). Liver blood supply was also studied by Tc-99m-pyrophosphate-labeled red cells. Computer analysis of the data revealed that compared to the normal liver lobe, binding of I-123-insulin to the hepatoma was more precocious (vascularization through the hepatic artery and not the portal vein), more intense and more prolonged (half-lives were 6 min in the normal liver and 14 min in the hepatoma). These results are consistent with characteristics of hepatoma cells in culture in which high insulin binding capacity contrasts with a markedly decreased insulin degrading activity. It is concluded that I-123-insulin may be used as a specific marker of hepatoma in man.

MEASURING FUNCTIONING HEPATOCYTES USING TC-99m GALACTOSYL-NEOGLYCOALBUMIN (TC-NGA)
R.C. Stadalnik, D.R. Vera, R.E. Quadro, K.A. Krohn, P.O. Scheibe, and L.F. O'Grady. University of California, Davis Medical Center, Sacramento, California.

Tc-NGA is a synthetic ligand which binds only to hepatic binding protein (HBP), a receptor found only in the liver. It exhibits the properties of high tissue specificity, affinity-dependent uptake, and dose-dependent uptake. Tc-NGA provides an opportunity to study the functioning hepatocyte. We evaluated the usefulness of this technique in patients with hepatitis (3), and hepatoma (4). After intravenous administration of 5 mCi Tc-NGA, dynamic images were acquired for 30 minutes followed by static views. Estimates of HBP concentrations were obtained by kinetic analysis of blood and liver time-activity curves.

Kinetic estimates (reduced chi-squares < 3.0) of HBP correlated well with the clinical course and histology. For example, a patient with hepatoma whose calculated receptor population (functioning hepatocytes) was $3.0 \pm 0.9 \times 10^{-7}$ mole, which is the normal range, is doing well undergoing chemotherapy. Liver biopsy demonstrated normal liver tissue except for the hepatoma. Another patient with hepatoma who had a severely depressed receptor population, $1.2 \pm 0.2 \times 10^{-8}$ mole, expired one week after the study. Liver biopsy demonstrated practically no normal tissue.

Thus, by means of a complementary receptor radiopharmaceutical and mathematical model, one should be able to quantitatively follow hepatocyte function and predict response to a therapeutic regimen.

PREDICTION OF RESPONSE TO PREOPERATIVE RADIOTHERAPY IN SOFT TISSUE TUMORS BY THALLIUM AND PYROPHOSPHATE SCANNING. K. Nishizawa, P. Okunieff, M. Barlai-Kovach, D. Elmaleh, K.A. McKusick and H.W. Strauss, H.D. Suit. Massachusetts General Hospital, Boston, MA.

To determine if local perfusion or extent of necrosis in soft tissue tumors could be used to predict response to radiotherapy, a prospective study was performed in patients with malignant soft tissue tumors (all greater than grade 2 stage IIb). Fourteen patients were scanned after injection of 2 mCi of 201-Thallium (Tl) and after 20 mCi 99mTc pyrophosphate (PYP). The response of the tumor, expressed as a 30% or greater decrease in tumor mass, was compared to the local intensity of tracer concentration (tumor/background T/BG).

There was a positive correlation in T/BG between Tl and PYP ($r=0.72$, $p<0.01$). The relationship of T/BG and tumor response to radiotherapy was:

T/BG	1	2	3	4
T1	*	* * *	o o	o
	**	***		oo
PYP	* * **	o o *		o
	**	* * o o		

*=Response; o=No Response

A decrease of >30% of tumor mass was observed in 9 patients with a mean T1 T/BG of 1.59±0.31 and a PYP of 1.55±0.57.

Tumors with poor perfusion and limited necrosis had significant volume reductions to radiotherapy, while those with greater perfusion and more extensive necrosis did not.

These results suggest that either thallium or pyrophosphate can be used to predict a decrease in volume of tumor from preoperative radiotherapy in patients with soft tissue tumors.

SCINTIGRAPHIC IMAGING OF NEUROBLASTOMA WITH I-131-META-IODOBENZYLGUANIDINE (I-131- MIBG)
U. Feine, J. Treuner*, W. Müller-Schauenburg, D. Niethammer, J. Meinke, E. Eibach, R. Dopfer*, Th. Klingebiel*St. Grumbach., Nuklearmed. Abteilung, Pädiatrisch-Haematologische Abteilung*Universität Tübingen, F. R. Germany

I-131MIBG is commonly used for the scintigraphic localisation of phaeochromocytoma. We present data with indicate that the neuroblastoma may show a similar or even higher accumulation of I-131-MIBG.

4 children were examined quantitatively by 8" crystal dual head whole body scanner interfaced to a computer. Scans were performed 4 h, to 21 d p. i. of 1-4 MBq (25-100 µCi) I-131-MIBG. 3 of the 4 children aged 2 month to 2.8 years had large tumor masses in the abdomen or diffuse infiltration of the enlarged liver and high catecholamine levels in 24 h urine samples. They showed high tumor uptake of the tracer already in the 4 h scans. The uptake level correlated well with the catecholamin excretion. The biological half live was in all 3 cases about 4 days. In the following days contrast between tumor and non tumor tissues became excellent. The 4. child was clinicaly free of tumor 1 year after cytostatic treatment and had normal catecholamin levels. The MIBG-scans did not show any tumor uptake but the myocardium and the salivary glands shows pronounced tracer uptake according to the results of NAKAJO et al.

In conclusion: MIBG may not be only a diagnostic-tracer für neuroblastoma but may perhaps permit therapy.

1:30-3:00 **Room 214BC**

RENAL, ELECTROLYTE, HYPERTENSION II

Moderator: M. Donald Blaufox, M.D., Ph.D.
Comoderator: Eva V. Dubovsky, M.D., Ph.D.

INVESTIGATION OF CHANGE OF RENAL FUNCTION FOLLOWING PERCUTANEOUS NEPHROLITHOTOMY. R.G. Schiff, L.M. Levy, M. Eshghi, G.M. Moskowitz, A. Smith. Long Island Jewish-Hillside Medical Center, New Hyde Park, New York 11042

The percutaneous removal of renal calculi is a relatively new technique which may significantly decrease the morbidity due to calculous disease of the upper urinary tract. Over two hundred such procedures have been performed in our institution over the last two years. We have designed a prospective study of fifty patients with non-obstructing calculi referred for percutaneous nephrolithotomy in order to determine if there is any functional change of the kidney secondary to the operation itself. Each patient is studied using a standard Tc99m DTPA renogram and computer assisted analysis both before and four to six weeks after surgery. In order to make the selection of regions of interest (ROIs) as reproducible as possible, the ROI of the entire kidney is selected on a frame early in the study, and later frames are used to outline the collecting system. Using subtractive techniques, the contribution of the cortex of the side to be operated upon to total cortical function is derived from the previously defined regions. Renogram curves are drawn for the entire kidney as well as renal cortex. The analysis post-operatively is performed using the same ROIs generated on the pre-operatuve study. To date, we have studied twenty patients pre-operatively and followed up seven. A small but consistent decrease in renal function is seen post-operatively in both the entire kidney and cortex. A statistical analysis of the study group will be performed after further follow up and data processing of more patients.

UPTAKE OF INDIUM-111 LABELLED PLATELETS BY NORMAL, NEPHROTIC AND TRANSPLANTED KIDNEYS. G. Desir, R. Lange, E. Smith, M. Bia, M. Flye, M. Kashgarian, A. Canganelli, M. Ezekowitz Yale University School of Medicine, New Haven, CT.

To determine the role of platelets in the genesis of renal transplant (T) rejection, we studied 3 groups of adult patients. Group I, n=8, had normal renal function (Cr =1±0.1 mg%, Mean±SD). Group II, n=9, had nephrotic syndrome (Cr=2.4±1). Group III, n=7, consisted of 5 cadaveric (C) and 2 living related donor (LRD) T. In Group II, 1 patient had received a T 4 years prior to study. Group I and II received 448±101 µCi and Group III 236±51 µCi of Indium-111. In Groups I and II the first image was obtained 18±6 hrs after injection. In Group III the first was obtained 6±2 hr after injection and 1-3 times/day thereafter for a maximum of 7 days. Renal biopsies were obtained in all patients in Group III during imaging (n=5) or within 2 - 5 days of the last image. One patient was studied twice. In Group III, 5 patients received prednisone and azothiaprine and 2 prednisone and cyclosporine. Platelet uptake index (PUI) was calculated as the ratio of uptake over the T against a reference area. Rejection was diagnosed by biopsy.

In Groups I and II platelet uptake was seen only in the T patient. In Group III the PUI was 1.54±.13 in the rejecting T (n=5), 1.42±.2 in the non-rejecting T (n=3), 1.62 in a LRD non-rejecting T and 1.31 (n=2) in C non-rejecting T. In the four patients studied within 5 days of T the PUI was elevated at 1.47±.1.

We conclude that 1)platelets do not accumulate in normal or nephrotic native kidneys, 2)significant uptake occurs in the first week after C and LRD whether or not rejection is present, and 3)uptake in non-rejecting kidneys cannot be ascribed to perfusion induced endothelial injury since it was present in LRD transplants.

TC-99M GLUCOHEPTONATE (GHA) RENAL UPTAKE: INFLUENCE OF BIOCHEMICAL AND PHYSIOLOGIC FACTORS. H.B. Lee and M.D. Blaufox. Albert Einstein College of Medicine/Montefiore Medical Center, Bronx, NY.

Tc-99m-GHA is widely used for renal imaging but little is known about its handling by the kidney. Simultaneous single injection clearances of Tc-99m-GHA and I-125 Iothalamate were performed on 60 Sprague-Dawley female rats divided among six groups: I Control; II Dehydrated; III Mannitol infusion; IV Probenecid: V Alkaline urine (sodium bicarbonate); and VI Acid urine (ammonium chloride). Plasma concentration and urine excretion were followed during 80 minutes post injection. The livers and kidneys were removed and counted 120 minutes post injection.

Total clearance of GHA was lower than Iothalamate in controls (0.90 ± 0.24 S.D. ml/min/100gr vs 1.47 ± 0.18, $p < 0.005$) but clearance of the protein free supernate was higher (1.67 ± 0.28 p=N.S.) raising a possibility of degree of tubular secretion. Unlike Tc-99m-Dimercaptosuccinic acid (DMSA) acidification of the urine appeared to have no effect on the amount of GHA in the urine (66.1 ± 6.35% Inj. dose vs 67.19 ± 6.05 p=n.s.) and hepatic uptake was minimal in all groups averaging less than 1%. Kidney uptake of GHA was 11.16 ± 1.53 (% Inj. dose) in controls This varied slightly among groups but was markedly reduced by Probenecid blockade (4.08 ± 1.75, $p < 0.0005$). It appears that liver uptake of GHA is minimal, the non-protein bound fraction is freely filtered and its clearance correlates significantly with the GFR. Importantly renal accumulation of GHA is blocked by probenecid suggesting that it is actively concentrated in the proximal tubule by the enzyme system involved in PAH and Hippuran transport. It thus appears

that measurement of renal function with GHA represents a different aspect of function than DMSA.

RADIONUCLIDE MEASUREMENT OF RENAL FUNCTION: A COMPARISON OF METHODS. E.J. Fine, J. Gorkin, N. Bank, K. Saleemi and M.D. Blaufox; Albert Einstein College of Medicine/ Montefiore Medical Center, Bronx, NY

Numerous methods have been devised to measure effective renal plasma flow (ERPF) using I-131 labeled orthoiodohippurate (OIH). Few data are available to determine which is the most accurate and clinically useful. We compared 5 methods (29 examinations, 20 patients). 300 μCi of OIH in 5 ml normal saline was first imaged on a gamma camera interfaced to a 64x64 computer matrix and then injected intravenously. Duplicate 10μl aliquots of the dose were used for standards. 15 second images were obtained on the gamma camera for 30 min. At 20 and 45 min., 5ml blood specimens were obtained. Method I; Specimens were centrifuged and 1 ml plasma from each was measured to obtain ERPF= -dose x slope/intercept. Method II: The 45 min. plasma sample alone was used to obtain ERPF= $-51.1+8.21x-0.019x^2$ where x=dose/45 min. plasma activity/liter.

Gamma camera renal uptake between 1 and 2 min after injection was used to obtain individual kidney and total ERPF choosing 3 different background (bg) regions of interest. Method III: bg regions between the upper poles; Method IV: between the lower poles; Method V: Crescent shaped regions lateral to each kidney.

All Methods were compared against Method I which was previously validated with standard PAH clearances. The r obtained by each technic was statistically significant ($p < 0.05$): II vs I, r=.974; III vs I = .918; IV vs I, r=.893; V vs I, r=.892. The lowest SEE was obtained with Method II which requires 1 blood sample. III has the lowest SEE among those without a blood sample. These data may help in selecting the optimum nuclear medicine method for measuring renal function.

MEASUREMENT OF GLOMERULAR FILTRATION RATE USING TECHNETIUM-99m-DTPA AND THE GAMMA CAMERA: A COMPARISON OF METHODS. C.D. Russell, P.G. Bischoff, F. Kontzen, K.L. Rowell, M.V. Yester, L.K. Lloyd, W.N. Tauxe, E.V. Dubovsky. University of Alabama Hospitals and Birmingham V.A. Medical Center, Birmingham, Alabama.

A variety of methods has been proposed to estimate glomerular filtration rate (GFR) from renal uptake of Tc-99m-DTPA using a gamma camera. To compare alternative methods, we have calculated GFR in several different ways from measurements in 33 patients, and compared the results with an independent GFR measurement based on 8-point plasma clearance of Yb-169-DTPA. The best agreement was obtained using an algorithm that has not been described previously. This was a modification of that used by Assailly et al. (1) and by Brodkey et al. (2), in which correction was made for overlap of kidneys by liver and spleen. The correlation coefficient was 0.958 and the residual standard deviation was 12.1 ml/min. This method required a single 20-min blood sample as well as the camera data. The best method not requiring a blood sample was significantly less accurate, with correlation coefficient 0.866 and residual standard deviation 21.1 ml/min. The accuracy of these methods was comparable to that reported for creatinine clearance, the most commonly used estimate of GFR in current clinical practice.

(1) J Nucl Med 18:684-691, 1977
(2) Invest Urol 14:417-420, 1977

RADIONUCLIDE SCINTIGRAPHY OF BACTERIAL NEPHRITIS. J.J. Conway, S.C. Weiss, A. Shkolnik, R. Yogev, C. Firlit, and E.S. Traisman. The Children's Memorial Hospital, Chicago, IL.

Pyelonephritis is a leading cause of renal failure and is expected to cost as much as three billion dollars in 1984. The diagnosis of urinary tract infection is usually not difficult. However, localization of the infection within the renal parenchyma as opposed to the collecting system is much more difficult. Flank pain, fever, bacteiuria and evidence of parenchymal involvement by intravenous urography may be absent or unrecognized particularly in the infant. Ultrasound and Nuclear Medicine are advocated as better methods to define parenchymal involvement. Such definition is important in the consideration of treatment since parenchymal involvement of the kidney carries a much more ominous potential outcome than infection restricted to within the collecting system.

38 children with a clinical diagnosis of urinary tract infection were studied. 26 of the patients demonstrated abnormal renal parenchymal findings with Gallium-67 Citrate or Tc-99m Glucoheptonate scintigraphy. Intravenous urography was notably ineffective with only 5 of the 20 interpreted as abnormal due to parenchymal disease or decreased function. 11 were entirely normal while only 5 demonstrated scars or hydronephrosis. Only 10 of 17 patients demonstrated vesicoureteral reflux on x-ray or nuclear cystography. Ultrasound depicted 6 of 20 patients as having parenchymal abnormalities. Seven were normal. Nonspecific findings such as dilitation of the renal pelvis or renal enlargement was noted in 11 of the 20 patients. Radionuclide Scintigraphy is the most efficacious modality to detect acute bacterial nephritis.